Institut für Organische und Makromolekulare Chemie

Universität Bremen

Synthesis and photocatalytic properties of new water-soluble phthalocyanines and related compounds

DISSERTATION

Zur Erlangung des Doktorgrades der Naturwissenschaften
- Dr. rer. Nat. -

vorgelegt dem Promotionsausschuß
des Fachbereichs 2 (Biologie/Chemie)
der Universität Bremen

von

Łukasz Łapok

Bremen 2006

1. Gutachter: Prof. Dr. D. Wöhrle

2. Gutachter: Prof. Dr. D. Gabel

Vorgelegt: im August 2006

Öffentliches Kolloquium: September 2006

Table of Contents

Acknowledgement

Foremost, I would like to express my particular gratitude to my supervisor Professor Dieter Wöhrle for giving me an opportunity to do this Ph.D., for all his support, advices and countless discussions over the last three years. Professor Dieter Wöhrle was the first person who introduced me to this fascinating and rewarding field of phthalocyanine chemistry. I would like to thank him for his enormous kindness, patience and for being for me such a wise mentor.

In the three years I have worked on this dissertation, I have been most fortunate to be offered the intelligence, inspiration and support of so many people. Thus, special thanks are due to all my colleagues form the "AG Wöhrle", who were engaged in establishing a nice and friendly atmosphere. Thus, I would like to thank Olga, Aneta, Carolin, Esther, Wilfrid, Thorsten, Brita, Olaf, Rudiger, Oliver, Robert, Günther, Andreas, Natasha, Serguey, and Hiromi. However, two people deserve special mention that is Oliver Bratels and Robert Gerdes. Both Oliver and Robert supervised me in the beginning of my work in the "AG Wöhrle" and assisted me with the photocatalytic measurements. They contributed to that work also by sharing they capacious knowledge and joining me so often in interpretation of the results.

I am especially indebted to Angela Wendt. I will never forget her help, support, patience and all these kind words she always had for me, although maybe not always I really deserved them.

I greatly acknowledge Dr. Thomas Dülcks who introduced me to the ESI-MS technique and often provided help with mass spectra interpretation. Without his assistance, extensive knowledge and stimulating discussions the chapter entitled "Electrospray Ionization Mass Spectrometry of Diverse Water Soluble Photosensitizers" could have never been realised.

I am grateful to Professor T. Torres from the Universidad Autonoma de Madrid who gave me an opportunity to join his group. I owe a special thanks to Dr. Christian Claessens who assisted me during the time I spent in his group as well as introduced me to the SubPc subject and gave me many valuable hints as for the synthesis.

My second scientific visit took me to Switzerland (EPFL). Thus, I am indebted to Prof. Dr. M. Graetzel for inviting me to his group and giving an opportunity to do challenging researches concerning new phthalocyanines useful as photosensitizers in solar cells.

I thank my friend Krzysztof Kaczmarek for all the help concerning computer-related hassles.

I would like to thank also Professor F. P. Montforts who some years ago recommended me as a PhD candidate to Professor D. Wöhrle.

My special thanks are due to Prof. W. –D. Stohrer for financial support.

The financial support of this research by the European Community (The Phthalocyanine European Project, contract HPRN-CT-2000-00020) is greatly acknowledged as well.

Last, but not least, I thank my family and friends for their invaluable support and constant encouragement.

This work is dedicated to my grandmother

Abstract

Almost 100 years of research on phthalocyanines and related compounds have produced an abundance of data on the synthesis and photophysical properties of miscellaneous derivatives of these compounds. Today literally thousands of diverse phthalocyanines have been reported in the chemical literature. The chemistry of phthalocyanines has been undergoing a renaissance because of their applications in materials science, liquid crystals, Langmuir-Blodgett films, electrochromic devices, gas sensors, non-linear optical devices, catalytic processes and pigments production, among others. Moreover, they are an important industrial commodity- thousands of tons of phthalocyanines are produced annually.

The main focus of this work was the synthesis of differently charged (negatively, positively and zwitterions) compounds, potentially applicable as photocatalysts (chapter 2). In order to induce water solubility, different functional groups have been added to the macrocycle framework, *i.e.* salts of sulfonic groups and quaternary aromatic amines. The following macrocycles were investigated: a) metal-free, silicon and germanium phthalocyanines, b) oxophosphorus(V) and hydroxysilicon(IV) triazatetrabenzcorroles, c) subphthalocyanines, d) metal-free and zinc porphyrins. Synthesis of these compounds was undertaken purposely, *i.e.* to find possibly stable and efficient photosensitizers in the photocatalytic photo-oxidation reactions.

Chapter 3 shows how electrospray mass spectrometry was utilized to support the analysis of water-soluble dyes. ESI-MS proved to be excellent analytical tool, superior to NMR, for the scrutiny of charged water-soluble photosensitizers since aggregation and strong intermolecular interactions characteristic for zwitterions do not hinder obtaining of good mass spectra. Moreover, for the first time in our laboratory, ESI-MS has been successfully implemented for characterization of sulfophthalocyanines.

The characterization of photosensitizers obtained during this work is supplemented with UV-Vis spectroscopy (chapter 4). The emphasis was mainly on the aggregation phenomena in water solution since singlet oxygen generation requires that the photosensitizer be in the monomeric state, otherwise in aggregates dissipation of the energy of the excited state readily takes place. Thus, UV-Vis spectra were recorded in

the absence and upon addition of appropriate detergent. In this way the extent of the aggregation process can be estimated.

Part of this work was devoted to studies towards photocatalytic properties of phthalocyanines and related compounds. Tetrapyrrolic dyes were used to activate oxygen to rapidly convert 2-mercaptoethanol and phenol, two severe pollutants present in the environment, to nonhazardous products, using three inexhaustible natural resources: oxygen (present in the air), photons (from sunlight), water (as environmentally friendly solvent). The results included within this dissertation are part of ongoing worldwide investigation dedicated to new possibly economic green approach for the treatment of hazardous organic contaminations in wastewater. Chapter 5 presents results concerning photocatalytic activity of different photosensitizers obtained during these investigations. The efficiency of sensitised photo-oxidation of 2-mercaptoethanol (and in some cases photo-oxidation of phenol) was studied in water solution at high pH, in the presence or absence of detergent. Since all investigated photosensitizers have charged functionalities, immobilization on ion exchanger was possible. Thus, the activity of sensitizers dissolved in a solution was compared with the reactivity of polymer-bound dyes. Heterogeneous photocatalysis can be an excellent remedy to the long-standing problem of sensitizer recovery and reuse, especially on an industrial scale. During the photo-oxidation process the photosensitizer may oxidatively decompose. A good photosensitizer has to be stable enough to ensure longevity of the photocatalytic system. Therefore, the degradation of each photosensitizer was measured with the aid of UV-Vis spectroscopy. So far, chemists in their work have involved single photosensitizer, this means that only small fraction of the solar spectrum is exploited. The fraction of light collected by the sensitizer must be increased to improve efficiency of the catalytic system. In order to overcome this obstacle it was proposed to utilize panchromatically absorbing system, consisted of several dyes, absorbing at different wavelengths, which would be capable of collecting considerably fraction of light resulting in enhancement of the photocatalytic activity. It has been demonstrated that the multi-component system is superior to the photocatalytic system that consists of single photosensitizer in terms of efficiency of photo-oxidation reaction.

Publications, Conferences & Collaborations

D. Wöhrle, O. Suvorova, R. Gerdes, O. Bartels, Ł. Łapok, N. Baziakina, S. Makarov, A. Słodek, “Efficient oxidation and photooxidation of sulfur compounds and phenols by immobilized phthalocyanines”, Process of Petrochemistry and Oil Refining, 3, 30-46 (2002).

D. Wöhrle, O. Suvorova, R. Gerdes, O. Bartels, Ł. Łapok, N. Baziakina, S. Makarov, A. Słodek, “Efficient Oxidations and Photooxidations with Molecular Oxygen using Metal Phthalocyanines as Catalysts and Photocatalysts“, J. Porphyrins Phthalocyanines, 8, 1020-1041 (2004).

M. Kaneko, H. Ueno, S. Masuda, K. Suzuki, H. Okimi, M. Hoshino, Ł. Łapok, D. Wöhrle, “Mechanism of photoinduced electron transfer from water soluble phthalocyanines and porphyrin to viologens interacting electrostatically”, J. Porphyrins Phthalocyanines, in press.

Ł. Łapok, D. Wöhrle, “Synthesis, Characterization and Photocatalytic Activity of Water-Soluble Metal-free, Silicon and Germanium Phthalocyanines. Photooxidation of 2-Mercaptoethanol to Environmentally Nonhazardous Compounds.”, in preparation.

Ł. Łapok, D. Wöhrle, “Photooxidation of 2-Mercaptoethanol and Phenol by Water-Soluble Oxophosphorus(V) Triazatetrabenzcorroles and Porphyrins.”, in preparation.

Ł. Łapok and D. Wöhrle, Ch. G. Claessens, T. Torres, “Synthesis of Novel Water-Soluble Subphthalocyanines.”, in preparation.

P. G. Jones, P. Kuś, Ł. Łapok, „2-[Bis(4-methoxyphenyl)methyl]benzyl chloroacetate.” Acta Cryst. 2005, E61, o827-o828.

Second Annual Meeting, Universidad Autonoma de Madrid (Spain), 15 March 2002: oral presentation.
Midterm Review Meeting, Katholieke Universiteit Nijmegen (The Netherlands), 17 June 2002: oral presentation.

Third Annual Meeting, Universität Bremen (Gremany), 14-15 February 2003: oral presentation.
Fourth Annual Meeting, University of East Anglia (United Kingdom), 3-4 October 2003: oral presentation.
Seminar on Material Sciences, Universität Bremen (Germany), February 2004: oral presentation.

Professor Tomás Torres and Dr Christian G. Claessens, Departamento de Quimica Orgánica (C-I), Facultad de Ciencias, Universidad Autónoma de Madrid, Cantoblanco, 28049 Madrid, Spain. I spent two months at UAM working at new water-soluble subphthalocyanines potentially useful as photocatalysts in the photo-oxidation reactions of severe pollutants present in the environment to nonhazardous products. This project was part of ongoing research dedicated to the photocatalytic properties of phthalocyanines and related compounds, like subphthalocyanines, porphyrins and triazatetrabenzcorroles.

Prof. Dr. M. Graetzel, Laboratory for Photonics and Interfaces, Institute of Physical Chemistry, Swiss Federal Institute of Technology, CH-1015, Lausanne, Switzerland. I was invited by Prof. M. Graetzel to design and prepare new ruthenium phthalocyanines with amino group at 1,4 position. Such compounds are expected to be an efficient near IR sensitizer for photovoltaic injection cells on nanocrystalline TiO_2 films. I had a three weeks stint in the group of Professor M. Graetzel.

Professor Masao Kaneko, Faculty of Science, Ibaraki University, 2-1-1 Bunkyo, Mito, 310-8512 Japan. Within the confines of collaboration with Prof. Masao Kaneko I was responsible for synthesis of differently charged phthalocyanines and porphyrins. Quenching of singlet photoexcited state was investigated. It was confirmed that the quenching takes place and that mechanism is mostly a statistic one.

Abbreviations

AcCN	Acetonitrile
CTAC	Cetyltrimethylammonium chloride
DCI	Direct chemical ionisation
DMF	Dimethyl formamide
DMSO	Dimethylsulphoxide
EI	Electron ionisation
ESI-MS	Electrospray mass spectrometry
HOMO	Highest occupied molecular orbital
HPLC	High performance liquid chromatography
ISC	Intersystem crossing
LUMO	Lowest unoccupied molecular orbital
MALDI	Matrix Assisted Laser Desorption Ionization
MPc	Metal containing phthalocyanine
NMR	Nuclear magnetic resonance
$^1O_2$	Singlet oxygen
$^3O_2$	Triplet oxygen
PcH_2	Metal-free phthalocyanine
PDT	Photodynamic tumor therapy
Po	Porphyrin
RR_i	Initial reaction rate [$mlO_2 \cdot min^{-1}$]
SDS	Sodium dodecylsulfate
Sen	Sensibilizator
$Sens^{1*}$	Exited singlet state sensitizer
$Sens^{3*}$	Exited triplet state sensitizer
SOMO	Single occupied molecular orbital
SubPc	Subphthalocyanine
tbc	Triazatetrabenzcorrole
TON	Turnover number [min^{-1}]
UV-Vis	Ultravilett and visible spectral range

List of structures

Table 1: List of structures.

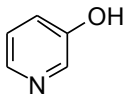

1

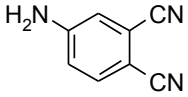

5

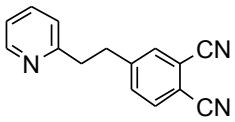

9

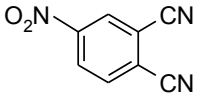

2

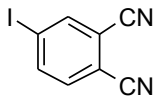

6

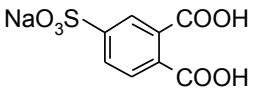

19

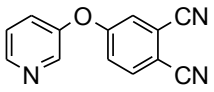

3

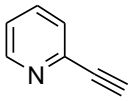

7

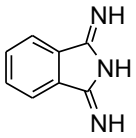

21

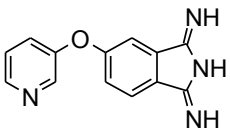

4

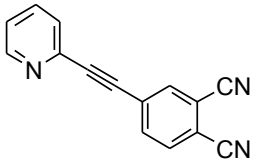

8

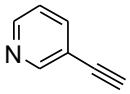

33

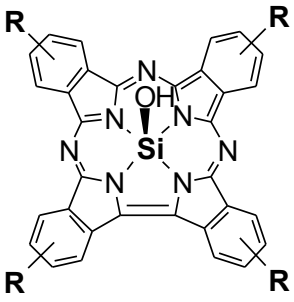

R = SO_3Na

23

Si(tbc)TS

Table 2: List of structures.

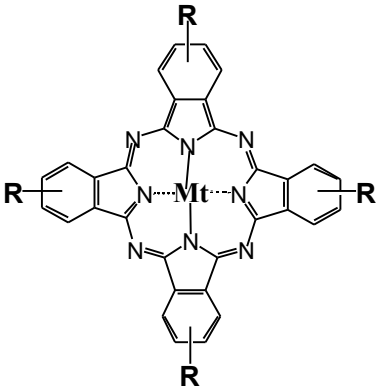

R^1 = H

R^2 = SO_2Cl

R^3 = SO_3^-

R^4 = 

R^5 = 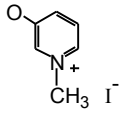

R^6 = 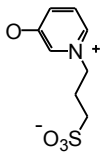

Compound	Mt	R	Abbreviation
10	2H	R^4	
11	2H	R^5	**H_2PcOPM**
12	2H	R^6	**H_2PcOPPS**
13	$Si(OH)_2$	R^4	
14	$Si(OH)_2$	R^5	**SiPcOPM**
15	$Si(OH)_2$	R^6	**SiPcOPPS**
16	$Ge(OH)_2$	R^4	
17	$Ge(OH)_2$	R^5	**GePcOPM**
18	$Ge(OH)_2$	R^6	**GePcOPPS**
20	2H	R^3	**H_2PcTS**
22	$Si(OH)_2$	R^1	**SiPc**
24	$Si(OH)_2$	R^2	**SiPc(SO_2Cl)$_4$**
25	$Si(OH)_2$	R^3	**SiPcTS**
26	$Ge(OH)_2$	R^1	**GePc**
27	$Ge(OH)_2$	R^2	**GePc(SO_2Cl)$_4$**
28	$Ge(OH)_2$	R^3	**GePcTS**
53	Zn	R^3	**ZnPcTS**
54	Al(OH)	R^3	**AlPcTS**
55	Ga(OH)	R^3	**GaPcTS**

Table 3: List of structures.

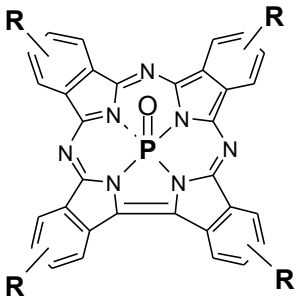

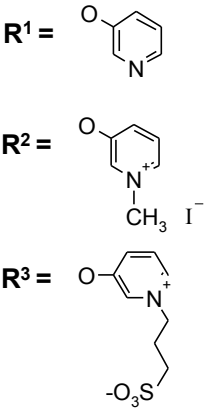

Compound	R	Abbreviation
29	R^1	
30	R^2	**PO(tbc)OPM**
31	R^2	**PO(tbc)OPPS**

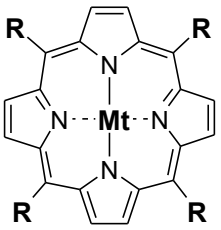

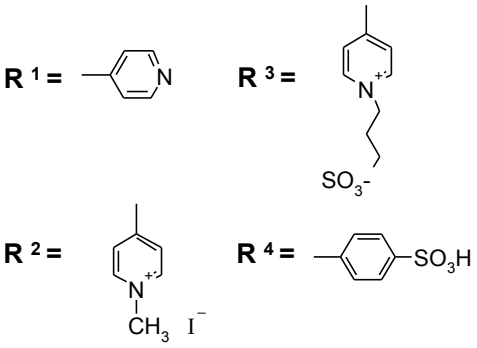

Compound	Mt	R	Abbreviation
45	2H	R^1	
46	2H	R^2	**H_2PoOPM**
47	2H	R^3	**H_2PoOPPS**
48	Zn	R^1	
49	Zn	R^2	**ZnPoOPM**
50	Zn	R^3	**ZnPoOPPS**
51	2H	R^4	**H_2PoTS**
52	Zn	R^4	**ZnPoTS**

Table 4: List of structures.

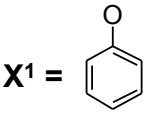

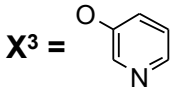

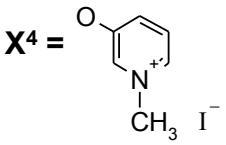

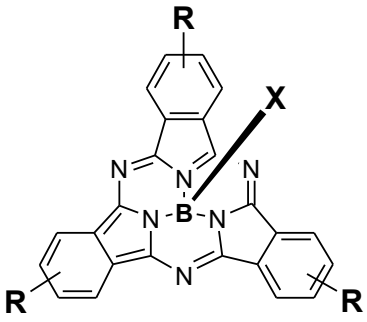

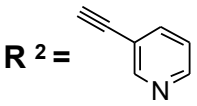

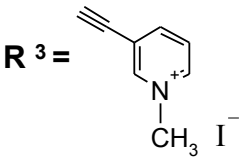

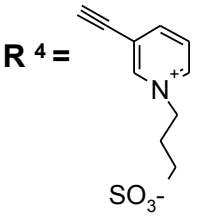

Compound	X	R
32	X^1	R^1
34a	X^1	R^2
34b	X^1	R^1, R^2, R^2
34c	X^1	R^1, R^1, R^2
35	X^1	R^3
36	X^1	R^4
37a	X^1	R^5
37b	X^1	R^1, R^5, R^5
37c	X^1	R^1, R^1, R^5
38	X^1	R^6
39	X^1	R^7
40	X^1	R^8
41	X^1	R^9
42	X^2	R^{10}
43	X^3	R^{10}
44	X^4	R^{10}

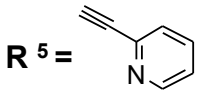

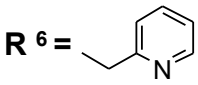

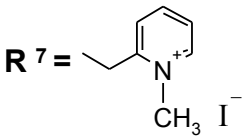

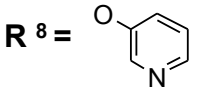

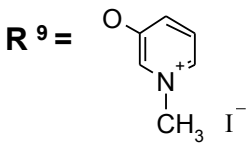

1. Introduction

1.1Aims of this study and scientific approach

The present study was part of ongoing research dedicated to the photocatalytic properties of phthalocyanine derivatives and related compounds, like subphthalocyanines, porphyrins and triazatetrabenzcorroles. Of special interest were possibly stable and efficient new photocatalysts useful in the photo-oxidation reactions of severe pollutants present in the environment to nonhazardous products. Besides, of interest were multicomponent systems absorbing at different wavelengths of ultraviolet and visible irradiation – so called panchromatically absorbing systems. Therefore, one of the main objectives of this study was the synthesis of new tetrapyrrolic macrocycles. A particular focus was placed on water-soluble photosensitizers that could be useful for the reactions conducted in aqueous solution.

Therefore, at the beginning of this work, after extensive survey of the literature available on the photocatalytic properties of phthalocyanines, the synthesis of a set of differently charged, water-soluble compounds was designed. The following tetrapyrrolic macrocycles were intended:

- metal-free, silicon and germanium phthalocyanines,
- oxophosphorus(V) triazatetrabenzcorroles,
- subphthalocyanines,
- metal-free and zinc porphyrins.

A very strong aggregation may effectively hamper photocatalytic process by dissipation of the energy of the excited state of the photosensitizer. Hence, the UV-Vis spectra of investigated compounds were recorded both in micellar and non-micellar solution to establish the aggregation tendency for each photosensitizer.

The photocatalytic activities of the individual compounds were measured volumetrically by oxygen consumption over time using specially designed equipment. Two substrates were chosen to test the photocatalytic properties, *i.e.* 2-mercaptoethanol and phenol.

1.2Phthalocyanines

1.2.1 Introduction

The unglamorous and serendipitous discovery of phthalocyanines (Fig. 1.1.), as a by-product in an industrial preparation of ortho-disubstituted benzene derivatives, took place almost century ago. In 1907 Braun and Tcherniac reported a dark insoluble by-product during the preparation of 2-cyanobenzamide [1]. Later in 1927 de Diesbach and von der Weid discovered an exceptionally stable blue compound prepared during the reaction of 1,2-dibromobenzene with copper cyanide in refluxing pyridine [2].

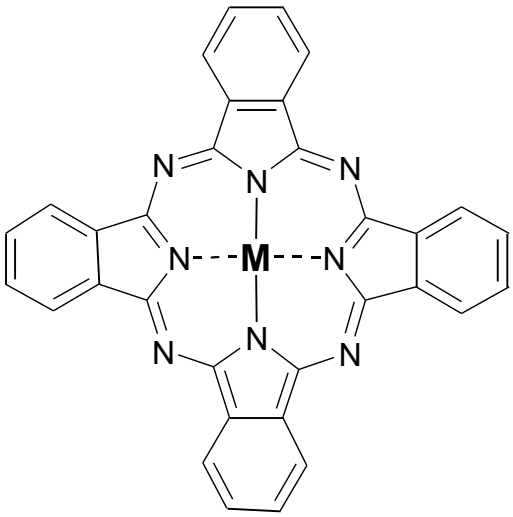

Figure 1.1. Structure of unsubstituted metallophthalocyanine (MPc).

The story of phthalocyanines began in 1928 at the Grangemouth plant of Scottish Dye Ltd. during the industrial preparation of phthalimide from phthalic anhydride. As described by McKeawn in his excellent review on phthalocyanine synthesis, the glass-lined reaction vessel containing phthalic anhydride had cracked, exposing the outer steel casing to the reaction resulting in the formation of a blue-green material. A sample of this novel coloured substance was handed over to young Prof. Reginal P. Linstead who, as the first one, elucidated and described the correct structure

of phthalocyanine and the synthesis of some of its metal derivatives [3-8]. Phthalocyanine is a highly symmetrical, flat, 18 π-electron aromatic macrocycle that consists of four iminoisoindoline units. To some exent Pc macrocycle closely resembles the naturally occurring porphyrin ring system. Although, it has to be pointed out that, unlike porphyrins, phthalocyanines do not occur in the nature and are not involved in the biochemical processes; they are completely synthetic organic compounds. The main difference between the phthalocyanine macrocycle, also called tetrabenzotetraazaporphyrin, and porphyrins system is the nitrogen atoms at each of the four *meso* positions instead of carbon bridges as well as the presence of the four benzo subunits.

The name "phthalocyanine" was created by Linstead. It stems from the combination of two prefixes, *i.e.* "phthal", to emphasise the association with various phthalic acid derivatives, and the Greek "cyanine" (blue).

Initially, phthalocyanines were of interest as pigments. Industrial production of phthalocyanine dyes is based upon the procedure worked out by Max Wyler at the Imperial Chemical Industries research centre. This involves heating of easily available phthalic anhydride in a melt of urea, in the presence of metal salt, and suitable catalyst (e.g. ammonium molybdate). Water-soluble dyes based on sulfonated phthalocyanines were discovered in 1950s and successfully used for permanent textile coloration. Today, duet to their utilitarian properties, thousands of tons of phthalocyanines are produced worldwide annually, to satisfy the demand for blue and green dyes.

However, real academic interest in phthalocyanines chemistry had come many decades after Linstead`s pioneering work. Today, literally thousands of different phthalocyanine derivatives exist in the literature with a variety of metals and substituents. Apart from many interesting properties, they are able to form stable chelate compounds with nearly every metal of the periodic system [9,10].

1.2.2 Synthesis

The various 1,2-disubstituted benzene precursors have been employed successfully for phthalocyanine synthesis, i.e. phthalonitriles, isoindolines, phthalimides, phthalic acid and anhydride derivatives, 1,2-dibromobenzenes and 2-cyanobenzamides (Fig. 1.2.) [11]. Depending on the precursor, nature of the substituents

and metal to be inserted into the macrocycle, wide range of reaction conditions - temperature, solvent, choice of base and catalyst - have been utilized.

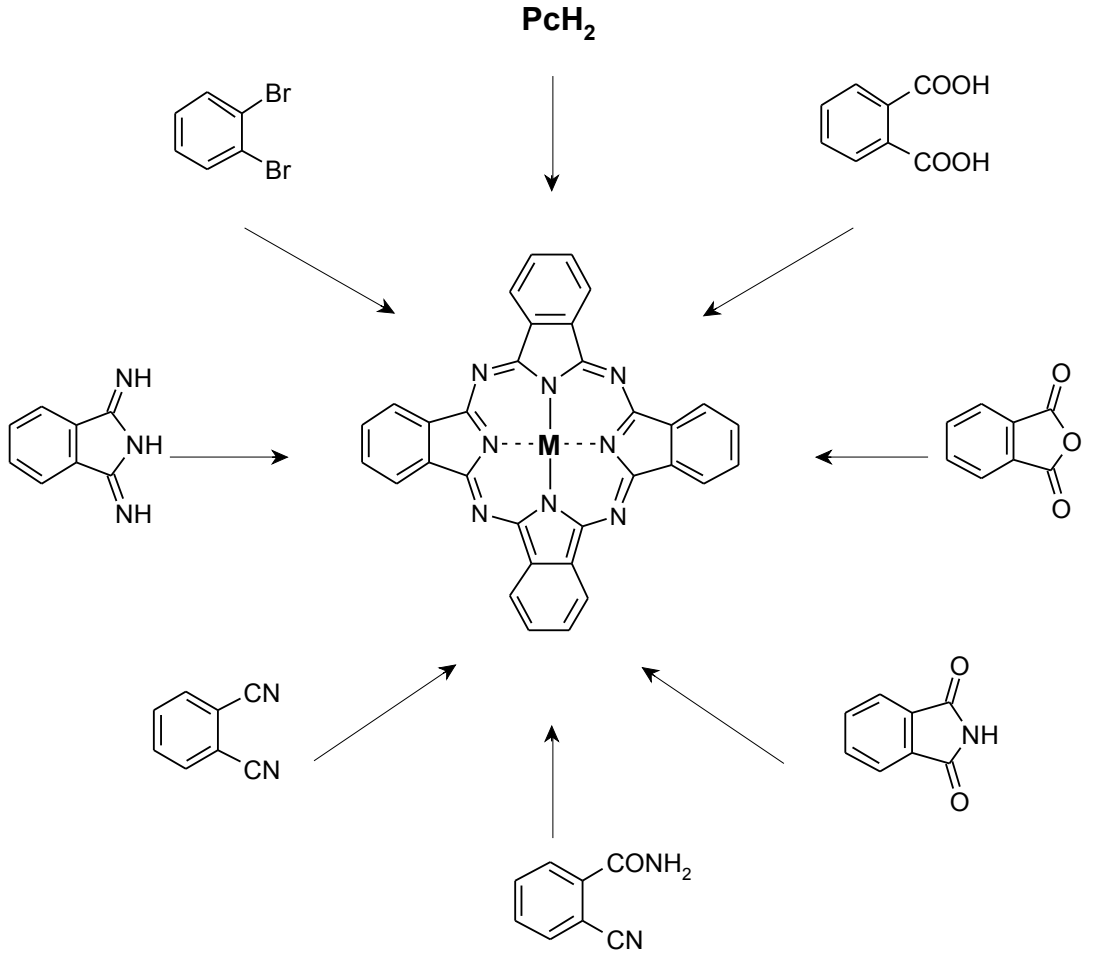

Figure 1.2. The synthesis of metal-containing phthalocyanines

A fairly mild, clean and direct method for metal-free phthalocyanine (PcH_2) synthesis involves heating of phthalonitrile with a base (DBU, DBN or NH_3) in a solvent (e.g. 1-pentanol) or use of basic solvent *N,N*-dimethylaminoethanol (DMAE). Of particular interest and value is the method in which lithium, sodium or magnesium alkoxides are used in primary alcohols (usually *n*- or *iso*-pentan-1-ol) for the cyclotetramerisation. The metal ions are easily removed to give PcH_2 by acidic or aqueous work-up.

Another approach involves reducing agent (usually inexpensive hydroquinone) that is melted together with phthalonitrile. The cyclotetramerisation of 1,3-diiminoisoindoline is usually performed in a refluxing DMAE.

A direct and in some cases convenient method for metal containing phthalocyanine (MPc) synthesis is heating of phthalonitrile with a metal or metal salt. However, it is not suitable for substituents with low thermal stability, as it requires high temperatures. Moreover, the cyclotetramerisation of phthalonitrile with metal salt can be achieved in a solvent. Of particular use are some high boiling solvents such as quinoline, DMF, 1-chloronaphthalene, DMAE. In a modification to this method, the use of organic "super-bases" DBU and DBN in conjunction with a metal salt and a solvent gives good results in many cases.

Phthalimide, phthalic anhydride and phthalic acid have been applied successfully for MPc synthesis. Of special interest is phthalic anhydride as a precursor, as most commercial processes are based upon this compound. Such reactions are commonly carried out in melted urea, which serves as a convenient source of nitrogen (ammonia). In addition to the appropriate metal salt, ammonium molybdate is usually added as a catalyst. Nitrobenzene has been used in some cases as a solvent. It is accepted that phthalic acid is converted to phthalimide via phthalic anhydride under the reaction conditions.

Diiminoisoindoline, prepared from the reaction of phthalonitrile and ammonia in the presence of catalytic amount of sodium methoxide, proved to be an excellent precursor for metal-containing phthalocyanines. It has been widely used for silicon and germanium phthalocyanine preparation.

It is common to obtain some copper(II) phthalocyanine directly from 1,2-dibromobenzene. This reaction involves heating the dibromide with CuCN in a solvent, usually DMF or quinoline.

Historically, the eldest method for phthalocyanine synthesis is the reaction of 2-cyanobenzamide in the presence of metal or metal salt in a bulk reaction or in a solution. However, this method is limited to very few cases and has not received much attention in daily lab practice.

The complexation of metal-free phthalocyanine is usually a clean and efficient reaction.

Additionally, subphthalocyanines can undergo ring expansion reaction to yield unsymmetrical phthalocyanines.

Nearly every metal from the periodic system can replace two hydrogen atoms in the centre of the macrocycle. Moreover, the axial substituents can be attached to many metals. Additionally, multinuclear structures can be formed either through metal or through peripheral substituents. And finally, there are sixteen positions on the periphery

that can be replaced by many substituents. Taking in to account all these facts, today it is possible to prepare bespoken phthalocyanine derivatives with highly tailored properties (*e.g.* Q-band position, solubility, light absorption, self-assembling, *etc.*).

There are two excellent reviews on phthalocyanines preparation; one by Leznoff et al. [10] and the other, actually the most up-to-date, by Neil B. McKeown [9]. Phthalocyanine and related compounds synthesis has been rapidly developing field with yearly appearing new achievements and publications.

1.2.3 The mechanism of phthalocyanine formation

Although many studies have been dedicated to the explanation of the mechanism of phthalocyanine formation, still the exact and unambiguous course of the reaction remains unclear. However, some intermediates isolated by many chemists give certain insight into the plausible mechanism [9,10].

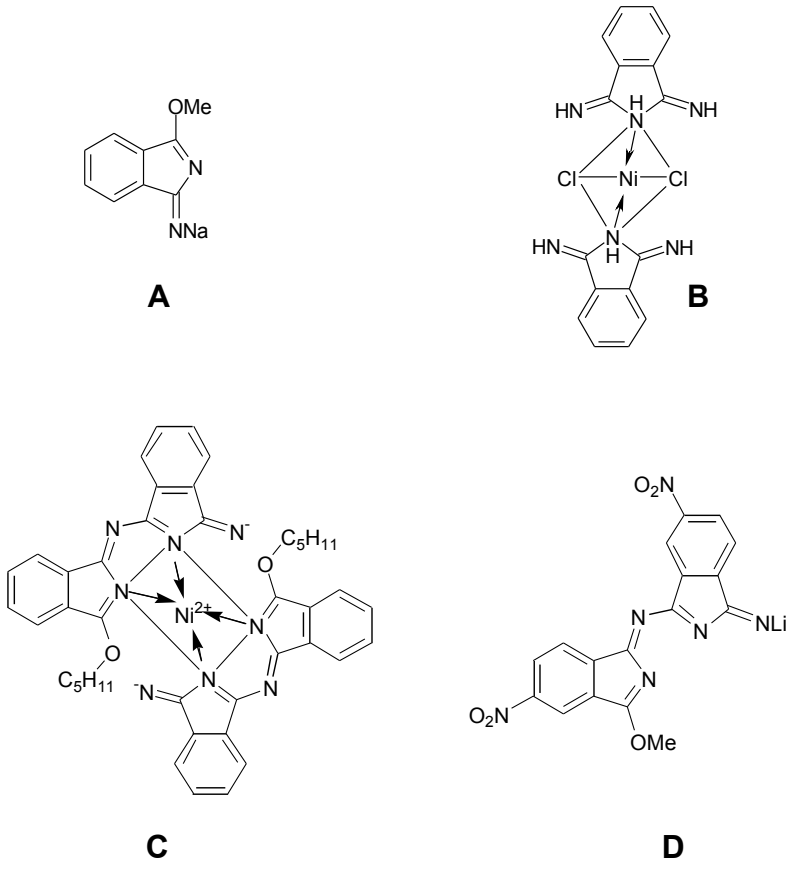

Figure 1.3. Some intermediates isolated during metallophthalocyanine synthesis.

First of all, Brodkin et al. [12] isolated a sodium derivative of methoxyiminoisoindolenine **A** as an intermediate. Later Hurley et al. [13] characterised two nickel complexes **B** and **C** able to form nickel phthalocyanine. And finally, dimeric lithium salt **D** was isolated by Oliver at al. [14] and shown to condense to tetranitrophthalocyanine (Fig. 1.3.).

An important piece of chemical information gives the reaction of 4-*t*-butylphthalonitrile with powdered zinc. The reaction leads to single isomer of a tetrasubstituted compound, namely, zinc 2,9,17,24-tetra-*t*-butylphthalocyanine [15]. The intermediacy of charged and radical anion species are postulated to explain the exclusive formation of one isomer (Fig. 1.4).

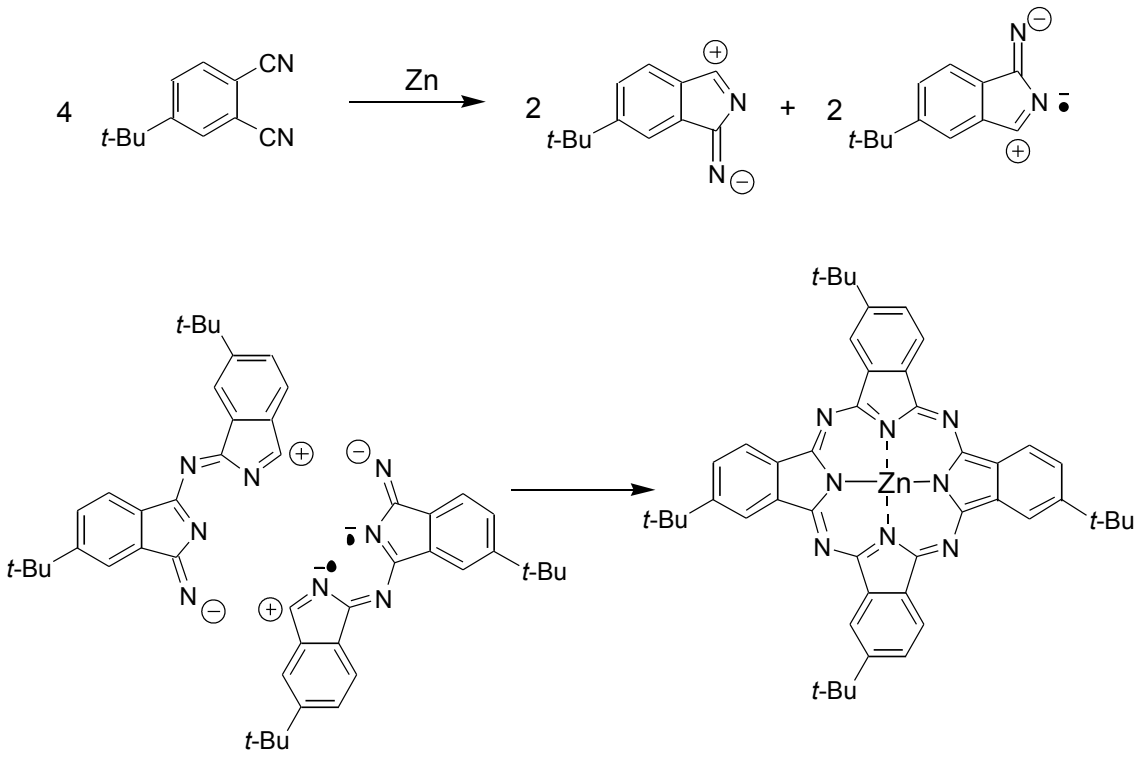

Figure 1.4. Intermediates postulated in the formation of zinc 2, 9, 17, 24-tetra-*t*-butylphthalocyanine.

An attempt to put all these facts together leads to the following mechanism of the cyclotetramerisation of phthalonitrile and diiminoisoindoline (Fig. 1.5). The protonated form of iminoisoindoline anions **E** and **F** was isolated [12,16,17]. The former structure is formed in methanol or ethanol whereas higher alcohols favour the formation of **F**. However, coexistence of both forms in equilibrium can not be ruled out.

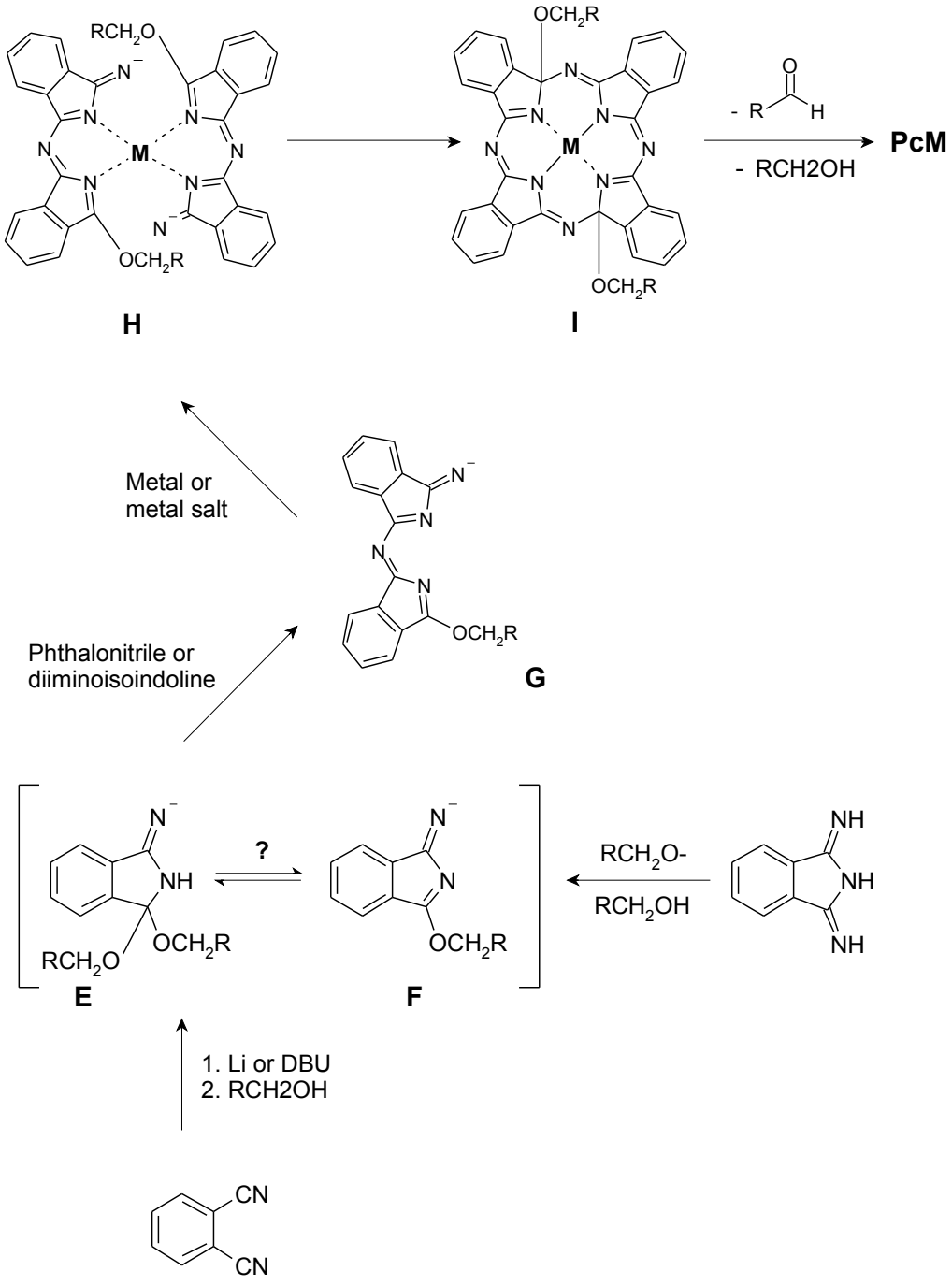

Figure 1.5. Mechanism of phthalocyanine formation (based on [9]).

The reaction of 4-nitrophthalonitrile and lithium methoxide in methanol at 116 °C gave an intermediate **G** [14]. The reaction of $NiCl_2$ with diiminoisoindoline in pentanol gave structure **H**. Hence, conclusion can be drawn that a metal ion template effect plays an important role in the formation of some phthalocyanines [13]. Later studies shown that heating an intermediate **H** obtained in the Ni^{2+} assisted cyclotetramerisation of 3,5-di-*t*-

butylphthalonitrile in pentanol leads to concomitant pentanol and pentanal liberation [13]. Ring closure followed by aromatisation most probably proceeds via complex **I**, which has been isolated as well [18]. For the lithium alkoxide mediated cyclotetramerisation of phthalonitrile a template effect is unlikely, rather the sequential addition of two molecules of phthalonitrile onto intermediate **G** takes place. The presence of aldehyde as a by-product indicates the role of the alkoxide ion as both nucleophile and reducing agent [19]. The alkoxide anion can be formed both by the addition of alkali metal (lithium, sodium) or by the action of the strong organic base (DBU, DBN or NH_3).

In general, the mechanism of phthalocyanine formation can be regarded as a stepwise polymerisation of the appropriate precursor (or more reactive intermediate) followed by coordination of the central metal ion and ring closure yielding the macrocycle molecule. An interaction of two factors seems to be the driving force for the Pc macrocycle formation. First of all the template effect of the central metal ion and the resulting stabilization this complex causes. Secondly, ring closure is driven by the thermodynamic stabilization and the aromaticity involved in the cyclotetramerization.

1.2.4 Optical properties

The main and most characteristic feature of the absorption spectra of phthalocyanines is the presence of two very intensive bands; one in the visible region called the Q-band and a weaker band in the UV region called B or the Soret band (Fig.1.6). Due to their 18 π-electron conjugated chromophore system, phthalocyanines possess high extinction coefficient of approximately 10^5 $M^{-1}cm^{-1}$ [10,20].

Metallation of the phthalocyanine, with a metal that maintains the planarity of the molecule increases the symmetry from the D_{2h} of H_2Pc to the D_{4h} of MPc. However, the symmetry drops to C_{4v} for metals that do not fit exactly inside the ring cavity. Hence, the absorption spectra of metal containing phthalocyanines are composed of two very intense bands Q-band and a B-band (called also Soret band). The Q-band represent absorption of light and consequently excitation of electrons from the highest occupied molecular orbital (HOMO), namely the a_{1u} (π), to the lowest unoccupied molecular orbital (LUMO), namely the e_g (π*). Furthermore, the transition from a_{2u} to e_g results in the B-band formation (Fig. 1.7).

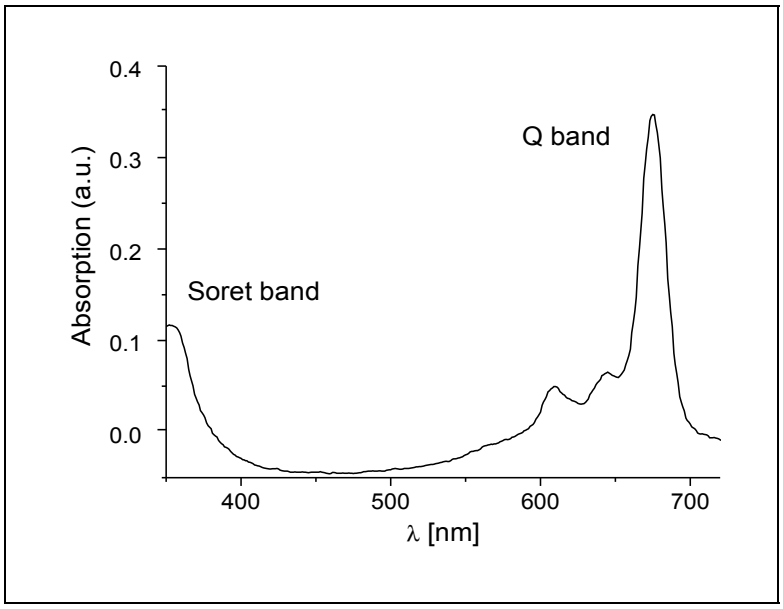

Figure 1.6. Absorption spectrum of germanium phthalocyanine GePcOPM **17** in water (pH 13, 0,1 M SDS). The very intensive absorption peak is the Q-band and a weaker peak is the Soret band.

Interestingly, for metal-free phthalocyanine the Q-band splits into a doublet. The splitting of the Q-band observed for metal-free phthalocyanine arises from lower symmetry (D_{2h}) in comparison with planar metallophthalocyanine (D_{4h}). Consequently, the LUMO orbital loses degeneracy giving rise to Q_x and Q_y states. It was found that the oscillator strength of the Q band of the metallophthalocyanine is about twice that of the metal-free absorbance band [10,20].

Position, appearance and intensity of bands depend on peripheral substitution, metallation, solvent as well as aggregation of the molecules.

Dimmerization of symmetrically substituted phthalocyanines gives rise to pronounced spectral changes that extend from band broadening, to a blue shift of the Q and B bands as well as to an observed splitting of the Q band and sometimes of the B band (Fig. 1.8). The extend of the spectral effect on dimmerization depends on the closeness of approach of the rings, the overlap position, the tilt angle that the rings adopt, the bulkiness of the peripheral substituents and the extinction coefficient of the electronic bands involved. Aggregation is also solvent dependent.

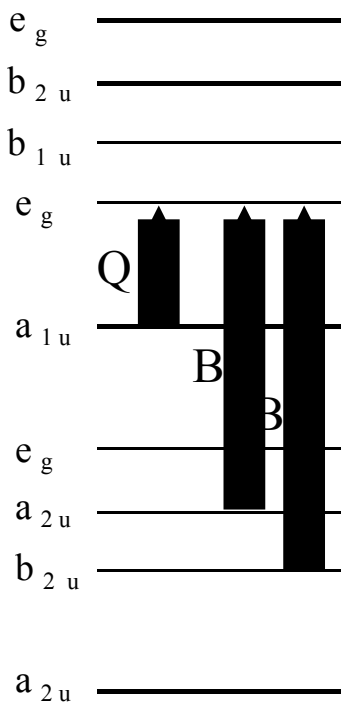

Figure 1.7. Origin of absorption and orbitals involved in Q and B band transitions for phthalocyanine.

The result of two adjacent D_{4h} metallophthalocyanines interaction is appearance of four degenerate states. Those four degenerate states arise from ^1E_u excited states splitting. Transitions are formally allowed only to the upper pairs of states. Transitions to the lower energy pairs of states are symmetry forbidden. Hence, the spectral properties manifested following dimmerization will include blue shift of the Q band and B band. For metal-free phthalocyanines, the Q_x, Q_y, B_x, and B_y components will couple to give pairs of Q_x^+/Q_x^-, etc., thus, the degeneracy is lifted. It is only the upper states being accessible optically. This is the reason that the Q and B band splitting of the aggregated metal-free phthalocyanine is lost [10,20].

Redox reactions of metallophthalocyanines are dominated by the appearance of beautifully coloured solutions, with spectacular changes in hue as the reaction is carried to completion. Redox chemistry may involve both ring and central metal. Reduction of the central metal usually leads to a Q-band shift without significant change in intensity.

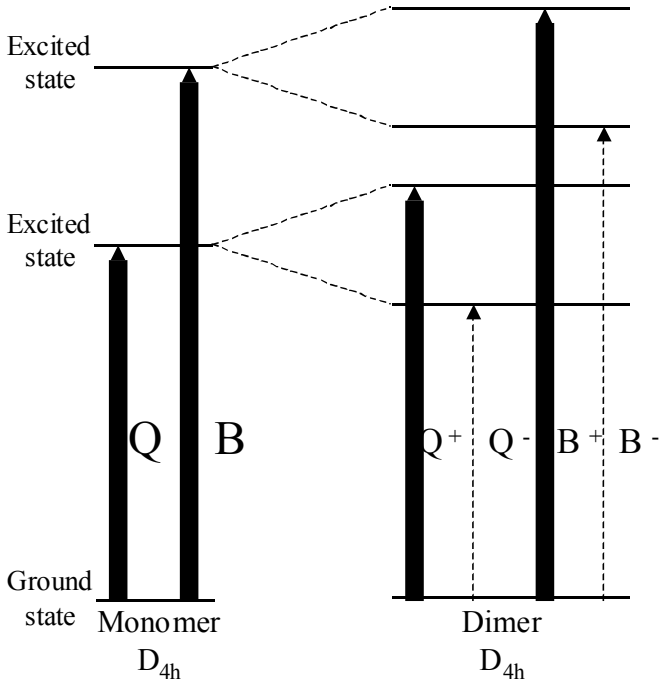

Figure 1.8. Interaction of two coplanar D_{4h} metallophthalocyanine rings (full and dashed arrows indicate allowed and forbidden transitions, respectively).

Unlike metal, reduction of the phthalocyanine ring manifests with the formation of new bands between 500 and 600 nm and absorption of the original bands, characteristic for MPc^{2-}, are significantly weaker. The phthalocyanine unit is able to gain up to four electrons and hence formation of MPc^{6-} takes place. Oxidation occurs through removal of one or two electrons from the HOMO. Intensity is lost and a new broad band formation between 700 and 800 nm and another at 500 nm is observed. By making use of spectroelectrochemistry it can be judge whether redox process occurs on the metal or on the Pc unit [10].

1.2.5 Applications

The list of phthalocyanine applications is immensely long. Listed below is merely a selection of the most commonly cited examples.

- Owing to beautiful colour, usually blue or green, considerable chemical and photochemical stability, phthalocyanines are used worldwide as a dyestuffs. They are an important industrial commodity- in 1987 output of 45 000 tons was noted. Phthalocyanines are widely used in inks (ballpoint pens, printing inks etc.),

colouring for plastics and metal surfaces as well as dyestuff for jeans and other clothing. Interestingly, copper phthalocyanine was certified as a food dyestuff in Germany and for colouring contact lenses in the United States [10].

- Photodynamic therapy (PDT) uses a combination of a photosensitizing drug (dye) and light in the presence of molecular oxygen to obtain a therapeutic effect that depends on selective cell injury. PDT has been developed as an alternative to conventional treatments such as radiotherapy and chemotherapy. The photosensitizer is harmless unless it is activated by light. Light can be therefore selectively focused on the tumour through an optical fibre, followed by the photosensitizer activation and cell destruction afforded in a predetermined area. Among the second-generation photosensitizers developed for PDT, the phthalocyanines have received particular attention due to their high molar absorption coefficient (ε ca. 10^5 $M^{-1}*cm^{-1}$) in the red part of the spectrum (640- 710 nm), which allows increased tissue penetration of the activating light. Low toxicity of phthalocyanines makes them promising for PDT application. Both lipophilic and water-soluble phthalocyanines have been considered as candidates for PDT [21-23].
- Due to the narrow bandwidth, excellent thermal, chemical as well as photochemical stability and compatibility with semiconductor diode lasers, phthalocyanines have been successfully applied as a laser-optical recording media. They are particularly attractive candidates for applications in long-term optical data storage (i.e. write-once, read many times (WORM) discs) [24].
- The phenomena of electrochromism relays on the reversible colour change of the material upon application of an electric field. Many phthalocyanines are famous for they electrochromic properties. Films of dyes can be switched over many colours what make them useful for display devices construction [25].
- Besides, phthalocyanines find uses in the petroleum industry as catalysts in sulfur compounds oxidation (Merox process) [26-30]. Especially, the cobalt complex is produced on a large scale by UOP for the catalytic oxidation of mercaptans in petroleum distillates.
- Metallophthalocyanines have several potential technological applications, including energy conversion [31-33], liquid crystal displays [34-36], gas sensing [10,37] and electrocatalysis in fuel cells [38-39]. Moreover, metallophthalocyanines are widely used as photoconductors in the printer and photocopier industry [40-41] as well as non-linera optical devices [42-44].

1.3Subphthalocyanines

1.3.1 Introduction

The unintentional discovery of subphthalocyanines (SubPcs) was made in 1972 by Ossko and Meller [45]. An attempt to synthesize boron containing phthalocyanines via condensation reaction of boron trichloride in chloronaphthalene at 200°C did not give the expected cyclotetramerization product. Unexpectedly, a pink coloured product with unusual UV-visible spectrum was isolated of which structure was determined two years later by Kietaibl using X-ray crystallography [46].

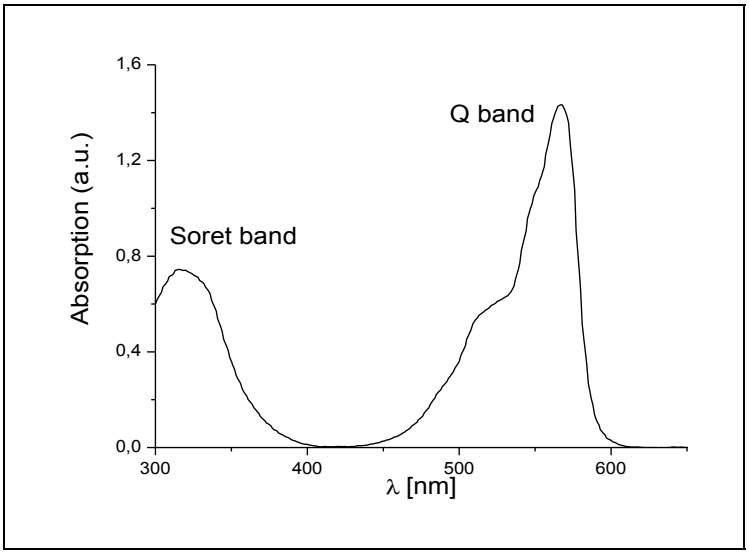

Figure 1.9. UV-Vis absorption spectrum of triiodosubphthalocyanine **32** in CH_2Cl_2.

Subphthalocyanines – regarded as lower homologues of phthalocyanines- are composed of three iminoisoindoline units N-fused around a boron core. Subphthalocyanines possess a delocalized 14-π-electron system and therefore are aromatic compounds, although they present nonplanar cone-shaped structure with axial substituent attached to boron and placed in the opposite direction of the open bowl.

Two intense bands, at 565nm (Q band) and 305nm (Soret band), dominate the UV-visible spectrum of SubPcs respectively (Fig.1.9). Additionally, a shoulder at around 520nm is also observed and most probably associated to a vibronic transition. The position of these bands can be slightly shifted towards red or towards blue by

introduction of electron-donating or electron-attracting substituents, respectively. SubPcs show very large absorption coefficients, bright, intense colour and non-linear optical behaviour [47,48].

1.3.2 Synthesis

Generally, SubPcs are synthesized by cyclotrimerization reaction of phhtalonitrile precursors in the presence of a boron derivative (typically a boron trihalides, BX_3) (Fig.1.10). Boron trichloride is by far the most commonly used reagent for SubPcs synthesis [47].

Considering the fact that SubPcs synthesis proceeds at very harsh conditions– presence of Lewis acid and usually very high temperature- only very few phthalonitrile derivatives have been successfully employed as starting materials. Thus, phthalonitriles with following substituents are compatible with BCl_3: methyl [48], *tert*-butyl [48], pentyl [48], nitro [48], iodo [48], chloro [49], fluoro [50], thioethers [51], sulfones [52] and crown ether [53].

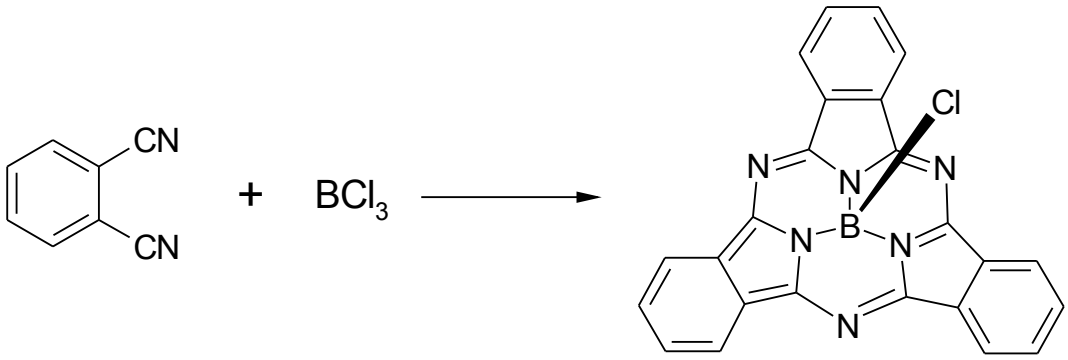

Figure 1.10. Preparation of unsubstituted subphthalocyanine.

The axial substitution in SubPcs derivatives has provided another successful way for modifying the molecule structure. Bromo- and chloroSubPcs were reacted with a wide range of oxygen nucleophiles to give rise to axially substituted SubPcs. The axial substitution reaction on SubPcs was performed with: alcohols, phenols, carboxylic acids, trialkylsilanols, trialkylchlorosilanes, carbon nucleophile (phenyl lithium) as well as axial exchange with OH group is also well known [47,48,50,54].

The peripheral reactivity of SubPcs has not been explored thoroughly enough. In fact the only available and compatible with SubPcs is palladium catalysed cross-coupling of alkynes with iodide substituted SubPcs [55].

1.3.3 Properties

Subphthalocyanines have received much attention over the last years due to their interesting chemical and photophysical properties. The ring expansion reaction of SubPcs is one of the most promising synthetic approaches for obtaining unsymmetrically substituted Pcs of A_3B type, otherwise unattainable [52,56,57,58]. Due to the properties of their excited states, singlet oxygen formation (with high quantum yields ranging from 0.23 to 0.74) and lack of aggregates in solution, SubPcs are interesting candidates for use in photosensitization processes. Furthermore, SubPcs can be organized at the supramolecular level in liquid crystals [59] and Langmuir-Blodget films [60]. SubPcs are molecules that show high second-order non-linear responses as a consequence of their octupolar character; hence their NLO properties have been studied intensively [61,62].

1.4Triazatetrabenzcorroles

1.4.1 Introduction

Triazatetrabenzcorroles are contracted phthalocyanines in that they are missing one *meso*-nitrogen atom but still retain the aromatic framework of the basic phthalocyanine macrocycle. Furthermore, they can be regarded as reduced phthalocyanines as hypothetical metal-free triazatetrabenzcorroles would have –3 charge, unlike –2 charged phthalocyanine free-base.

In 1981, Gouterman *et al.* [63] described an attempt to synthesize phosphorus (III) phthalocyanine, "PcP^{III}". The authors pointed out that the so-called "PcP^{III}" obtained showed a very unusual, sharp Soret band at 442 nm, in contrast to the broad Soret band at ca, 330 nm observed usually for phthalocyanines. Moreover, the "PcP^{III}" exhibited an unusual mass spectrum with intensive peak at 545.4 Da corresponding to $[PH_2Pc]^+$. Later, in the review on the preparation and spectral properties of metalloid

porphyrins and phthalocyanines [64], the same authors reported that the [(*t*-Bu)$_4$PcP^{III}] obtained also displays unusual electronic and mass spectra as those found for "PcP^{III}". In 1986, Fujiki *et al.* [65] ascertained for the first time that previously reported phthalocyanine containing lower valent state metalloid Ge(II), produced by reducing PcGeCl$_2$ with NaBH$_4$, was in fact hydroxygermanium(IV) triazatetrabenzcorrole; a phthalocyanine-like tetrapyrrole macrocycle. In the same publication three other triazatetrabenzcorroles containing Si(IV), Al(III) and Ga(III) were obtained by the same method and their UV-Vis spectra were reported to exhibit the same pattern. At the same time it became clear that the Gouterman´s "PcP^{III}" is compound closely related in terms of structure to that described by Fujiki. The UV-Vis spectrum of "PcP^{III}" closely resembled that observed for hydroxygermanium(IV) triazatetrabenzcorrole.
In 1997, during ongoing studies dedicated to phthalocyanine dimers with direct Si-Si bond Hanack *et al*. [66] noticed that the reaction of 4,5-dipentyldiiminoisoindoline with Si$_2$Cl$_6$ produced no dimer. Unexpectedly, a deep green compound was isolated which displayed a very sharp absorption at 448nm with intensity nearly twice that of the Q band. Thus, a new example of triazatetrabenzcorrole was found the structure of which was fully corroborated.
Finally, in 1998 an extensive publication by Hanack *et al.* [67] appeared. The publication dealt with the reaction of PBr$_3$ with metal-free phthalocyanines. The product obtained was characterized as the oxophosphorus(V) triazatetrabenzcorrole.

1.4.2 Synthesis

The mechanism for the formation of triazatetrabenzcorroles macrocycles remains obscure. However, it has been proved that the reaction proceeds via reduction of the corresponding phthalocyanine with reagents such as NaBH$_4$, H$_2$Se, Si$_2$Cl$_6$ or PBr$_3$ [65]. In this way a *meso*-nitrogen is extruded from the parent phthalocyanine precursor and ring-contraction reaction takes place.

The oxophosphorus(V) triazatetrabenzcorrole can be obtained in the reaction of PBr$_3$ with the metal-free phthalocyanines in pyridine (Fig. 1.11).

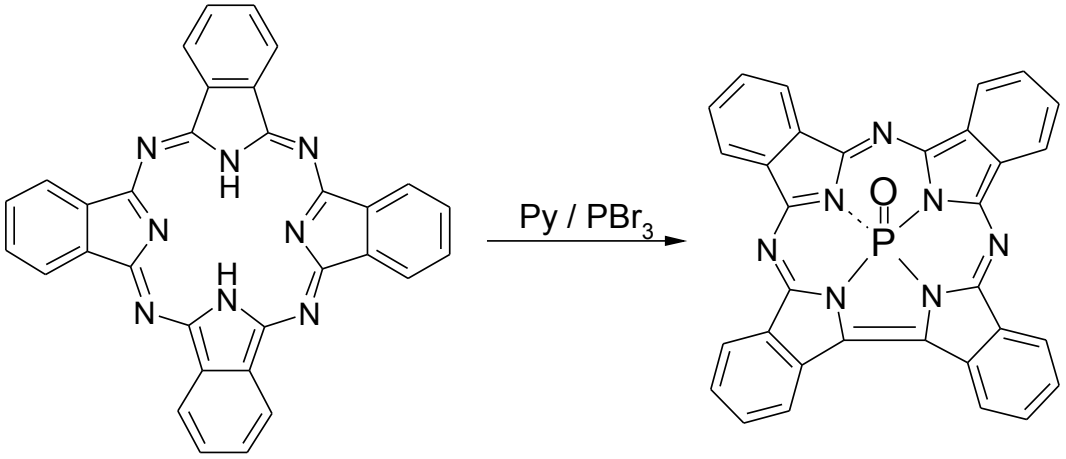

Figure 1.11. Reaction of metal-free phthalocyanine with PBr_3 in pyridine.

The reaction proceeds in any solvent but pyridine [63]. It is supposed that the very reactive intermediate is first formed by association of PBr_3 and pyridine (Fig.1.12):

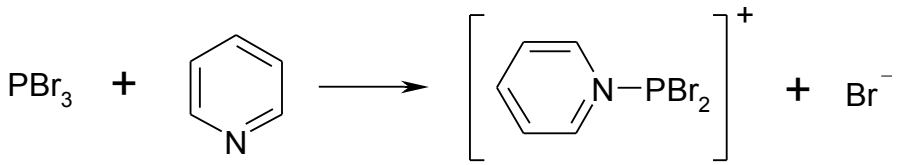

Figure 1.12 Intermediate formed between PBr_3 and pyridine.

Hanack *et al.* [67] postulated that phosphorus phthalocyanine must be formed initially in the reaction and then reduced by the excess of PBr_3 to the corresponding triazatetrabenzcorrole. This was ascertained by conducting an experiment in which phosphorus(V) containing phthalocyanine, namely [$P(OH)_2$*t*-Bu_4Pc](OH), was treated with PBr_3 in pyridine, whereupon oxophosphorus(V) triazatetrabenzcorrole PO[*t*-Bu_4(tbc)] was isolated as the only product.

Recently, Fox and Goldberg [68] reported the synthesis of new series of highly soluble phosphorus(V) triazatetrabenzcorroles prepared via the ring-contraction of $(BuO)_8PcH_2$ and $(BuO)_8Cl_8PcH_2$. They have shown that subtle modification in the conditions of the synthesis and purification of these compounds determines the phosphorus coordination number and identity of the axial ligands.

1.4.3 Optical properties

The most characteristic feature of the UV-Vis spectrum of PO(tbc) is a very sharp Soret band at ca. 442 nm of an intensity almost twice that of the Q band (Fig. 1.13). Comparing to phthalocyanines the Q band and Soret band of triazatetrabenzcorroles are markedly blue and red shifted, respectively.

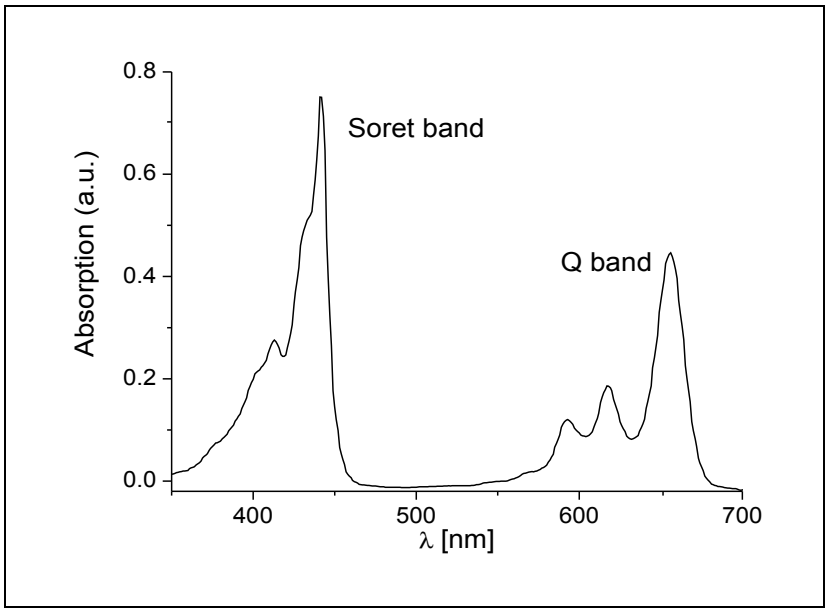

Figure 1.13 Typical UV-Vis spectra of oxophosphorus(V) triazatetrabenzcorrole PO(tbc). Absorption maxima: 441 nm (Soret band) and 656 nm (Q band).

The unusual spectrum was attributed to the porphyrin-like four orbital electronic transitions a_{1u} (π), a_{2u} ($3p_z$) → e_g (π^*), where a_{1u} (first HOMO) and a_{2u} (second HOMO) are nearly degenerated [63]. Gouterman suggested that in PO(tbc) a new filled orbital a_{2u} ($3p_z$) is introduced into Fermi energy region, where $3p_z$ is an orbital on phosphorus. In this way a porphyrin type Soret band appears. In contrast to analogous porphyrins derivatives, PO(tbc) shows strong fluorescence [63].

1.5Porphyrins

1.5.1 Synthesis

During this work a focus was on synthesis of *meso*-tetrapyridylporphyrins, which as *meso*-tetraphenylporphyrins can be synthesized by the classical method worked out by Rothemund. The method is a condensation between pyrrole and benzaldehyde derivatives (Fig 1.14).

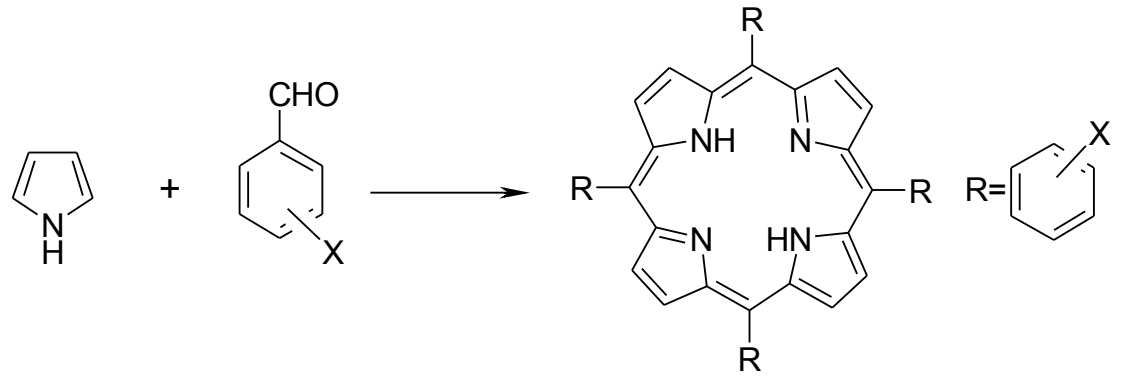

Figure 1.14. Synthesis of *meso*-tetraphenylporphyrin derivatives.

Fairly often the reaction is performed in propionic acid as a solvent what may considerably improve the yield of the reaction. This synthesis rout is a convenient way to prepare tetranitrophenylporphyrin, tetra(pentafluorophenyl)porphyrin, tetratolylporphyrin as well as tetra(4-pyridyl)porphyrin [69].

1.5.2 Optical properties

The absorption spectrum of regular metalloporphyrin consists of several bands, Q, B, N, L and M bands. The Q-band is in fact two bands observed in the visible region between 500-600 nm. The lower energy band, known as "a " band, is the lowest excited state Q (0,0). The higher energy band, known as a "b" band, is the origin Q (1,0) (Fig. 1.15). The Q-band has a molar extinction coefficient in the range of 10^4 mol^{-1} dm^3 cm^{-1}. The B band, called the Soret band, is an immensely intense band observed in the region 380-400 nm. The B (0,0) band is attributed to the second excited singlet state and has a high molar extinction coefficient in the range of 10^5 mol^{-1} dm^3 cm^{-1} (Fig. 1.15). The N, L, and M bands are located in the ultraviolet region

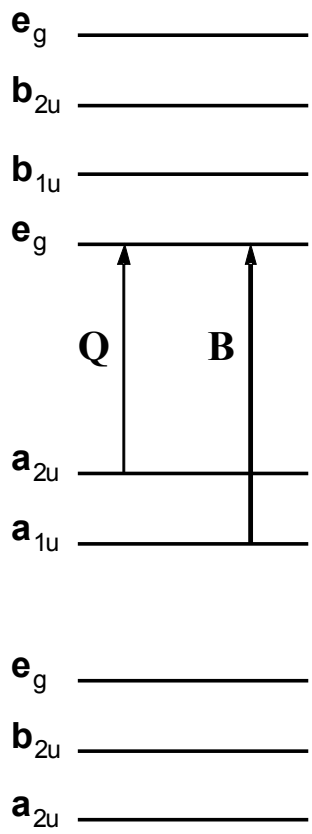

Figure 1.15. Origin of absorption and orbitals involved in Q and B band transitions for porphyrin molecule.

In the metal-free porphyrin, presence of two protons in the cavity of molecule leads to a reduction of the overall symmetry as it does for phthalocyanines. A consequence of it is a split of the Q-band from two bands to four bands. The Q (0,0) splits into Q_x (0,0) and Q_y (0,0) [20,69].

1.6 The nature of electronically excited states

1.6.1 Unimolecular deactivation

An electronically excited state of a molecule is formed by absorption of a photon promoting an electron from the highest occupied molecular orbital (HOMO) to the

lowest unoccupied molecular orbital (LUMO). The HOMO-LUMO promotion of an electron is the lowest possible energy transition that occurs between the frontier orbitals of a molecule. The concept of an energy absorption, and consequently excitation, is clearly described by the **Jablonski diagram** (Fig.1.16).

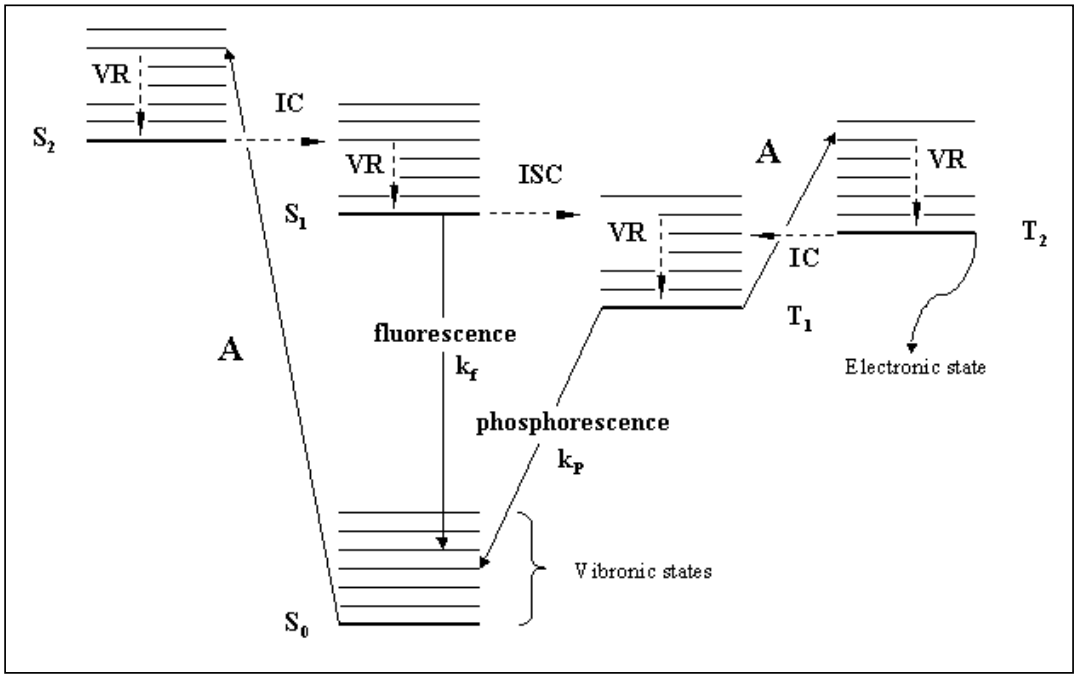

Figure 1.16. Jablonski diagram. Absorption (A) and emission processes are indicated by straight arrows (fluorescence, phosphorescence), radiationless processes by dashed arrows (IC – internal conversion, ISC – intersystem crossing, VR – vibrational relaxation).

It demonstrates the various electronic states of a molecule that are grouped according to multiplicity, including vibrational and rotational sublevels. This diagram visualises photophysical processes that allow an electronically excited molecule to dissipate its energy by non-radiative and by radiative deactivation phenomena [70-73]. Thus, absorption of a photon of sufficient energy by an organic molecule results in promotion of one bonding or non-bonding electron to a first (S_1) or second (S_2) excited singlet state, depending on the photon energy. **Internal conversion (IC)** is non-radiative transition between two isoenergetic electronic states of equal multiplicity, *e.g.* $S_2 \rightarrow S_1$ (10^{-13}-10^{-12} s), $S_1 \rightarrow S_0$ (10^{-12}-10^{-6} s), $T_2 \rightarrow T_1$. Internal conversion competes with fluorescence. Relaxation of vibrationally excited (**vibrational relaxation, VR**) levels occurs very fast (10^{-13}-10^{-12} s) and leads to the occupation of the lowest vibrational state

of S_1 or T_1. Hence, according to **Kasha´s rule**, fluorescence almost invariably occurs from S_1 state, and phosphorescence from T_1 [71]. Emissions from higher states are rare. Since IC for $S_x \rightarrow S_1$ proceeds much faster than radiative decay ($k_{IC} > k_f$), usually no fluorescence is observed from higher vibronic states. In contrast, k_f is greater than k_{IC} for the $S_1 \rightarrow S_0$ transition and fluorescence is usually observed. **Fluorescence** is a spontaneous spin-allowed emission of radiation within vibronic states of the same multiplicity, usually from the thermally relaxed S_1 to S_0. The vibrational structure of the fluorescence band is a mirror image of the longest wavelength band in absorption spectrum, shifted to longer wavelengths. The difference between the position of the band maxima in absorption and fluorescence spectra is called **Stokes shift**. The lifetime for fluorescence is rather short, usually around 10^{-8} s [70]. The change of multiplicity by **intersystem crossing (ISC)** is spin-forbidden. However, it may occur as a consequence of spin-orbit coupling. **Spin-orbit coupling** is a process by which an electron flips its spin and leads to an S → T or T → S transitions by ISC [71]. Either paramagnetic compounds or heavy atoms enhance spin-orbit coupling. ISC is non-radiative transition between two vibronic states of different multiplicity, *e.i.* $S_1 \rightarrow T_1$ (10^{-11} - 10^{-6} s), $T_1 \rightarrow S_0$ (10^{-7} - 10 s) [70]. Again, vibrational, non-radiative relaxation of the T_1 competes with radiative process, called phosphorescence. The energy gap order for ISC is $T_1 \rightarrow S_0 > S_1 \rightarrow T_1$, and the corresponding rate constant are in opposite order. Hence, phosphorescence is shifted bathochromically relative to fluorescence emission [71]. Typical singlet energies $E(S_1)$ are in the range from 180 to 500 kJ mol^{-1} and triplet energies $E(T_1)$ are between 125 and 360 kJ mol^{-1} [70]. **Phosphorescence** is the spin-forbidden emission of radiation between vibronic states of different multiplicity, i.e. from $T_1 \rightarrow S_0$. The phosphorescence spectrum is a mirror image of the phosphorescence excitation spectrum ($S_0 \rightarrow T_1$). Since the T_1 state always lies below the S_1 state, phosphorescence is shifted bathochromically relative to fluorescence. The lifetimes of phosphorescence are fairly long (from 10^{-4} to 10^2 s) [70].

In conclusion, the following rough estimations of rate constants may be given. For internal conversion for instance $k_{IC} \approx 10^{12}$-10^{14} s^{-1} for $S_n \rightarrow S_1$ and $k_{IC} < 10^8$ s^{-1} for $S_1 \rightarrow S_0$ were found. For intersystem crossing typical values are $k_{ST} \approx 10^6$-10^{11} s^{-1} for $S_1 \rightarrow T_1$ and $k_{TS} \approx 10^4$-10^{-1} s^{-1} for $T_1 \rightarrow S_0$. It has been reported that ISC for carbonyl compounds is particularly fast, whereas for biradicals T_1 and S_0 are very nearly degenerated; hence k_{TS} tends to be high, often in the range 10^6- 10^8 [72].

1.6.2 Bimolecular deactivation

Deactivation of an excited state occurs by a photochemical or a photophysical process, either monomolecularly or bimolecularly. The monomolecular pathway such as emission or radiationless deactivation was described previously. The bimolecular deactivation mechanism involves the transfer of excited energy from one molecule to another. In general these processes are referred to as **quenching** if suppression of luminescence takes place. If it is not the deactivation that is of principal interest during a bimolecular process but rather the excitation of the acceptor molecule, the process is described as **sensitization** [71]. The bimolecular deactivation may occur in one of three ways:

- Energy transfer $^{*}D + A \rightarrow D + {}^{*}A$
- Excimer/exciplexs formation $^{1}M^{*} + M \rightarrow {}^{1}(MM)^{*}$
- Electron transfer $^{*}D + A \rightarrow D^{\bullet+} + A^{\bullet-}$

1.6.2.1 Energy transfer

Energy transfer is the photophysical process in which an excited molecule (D^{*}) is deactivated to a lower-lying state by transferring energy to a second molecule (A), which is thereby raised to a higher energy state. Energy transfer may occur via different mechanisms that are collected and briefly described below:

- **Radiative energy transfer**, frequently described as "trivial" mechanism, occurs via two steps and does not involve direct interaction of donor end acceptor. The energy emitted by excited donor is trapped by acceptor:

$$D^{*} \rightarrow D + h\nu$$
$$A + h\nu \rightarrow A^{*}$$

- **Nonradiative energy transfer** is a single step process. It requires the transitions $D^{*} \rightarrow D$ and $A \rightarrow A^{*}$ to be isoenergetic as well as coupled by a suitable donor-acceptor interaction:

$$D^{*} + A \rightarrow D + A^{*}$$

- **Förster mechanism** is based on classical dipol-dipol interactions. This excitation transfer occurs between molecular entities separated by distance considerably exceeding the sum of their van der Waals radii. Interaction is significant at distances up to the order of 10 nm, which is large but less than the range of radiative energy transfer. Förster mechanism is in fact the interaction of the transition moments of the excitation A → A* and deactivation D* → D. Energy transfer are fully allowed only if there is no change in spin in either component. Thus $^1D^* + {}^1A \rightarrow {}^1D + {}^1A^*$ and $^1D^* + {}^3A \rightarrow {}^1D + {}^3A^*$ are allowed. The lifetime of the excited donor plays important role, as the probability of energy transfer is proportional to this lifetime. Also the spectral overlap of the emission spectrum of donor and absorption spectrum of acceptor enhances efficiency of energy transfer.

- **Dexter mechanism** is also referred to as electron exchange excitation transfer. It requires that the excitation energies should be in the order $E(D\text{-}D^*) \geq E(A\text{-}A^*)$; the second requirement is an overlap of wavefunctions of the donor and acceptor. Figure 1.17 shows that the two electron transfers are simultaneous and no recognizable ions are formed as intermediate. Both donor and acceptor remain neutral species throughout the electron exchange. This double electron exchange requires the spatial overlap of the orbitals so that the D* and A must be in very close contact. For Dexter excitation transfer the spin conservation rules are obeyed. It is the dominant mechanism in triplet-triplet energy transfer.

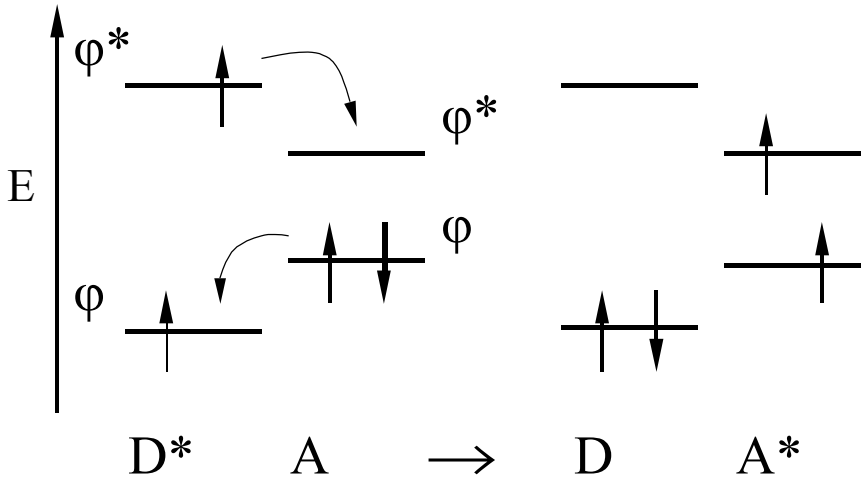

Figure 1.17. The Dexter mechanism of energy transfer. The HOMO and LUMO of the acceptor must fall between the HOMO and LUMO of the donor.

A special case of energy transfer is process dubbed as **triplet-triplet annihilation** (abr. **TTA**) [72]. This energy transfer occurs between two molecules in their excited states; most frequently between two triplet states due to their long lifetimes. According to Wigner spin conservation rule the following triplet-triplet annihilation processes are allowed:

$$^3D^* + {}^3A^* \rightarrow {}^1D + {}^1A^{**}$$
$$^3D^* + {}^3A^* \rightarrow {}^1D + {}^3A^{**}$$
$$^3D^* + {}^3A^* \rightarrow {}^1D + {}^5A^{**}$$

The double asterisk denotes higher excited states. However, the acceptor molecule will undergo internal conversion and finally reach the lowest singlet, triplet or quintet excited state. If the $^1A^*$ molecule is fluorescent, triplet-triplet annihilation produces **delayed fluorescence**. This phenomenon is known as **P-type delayed fluorescence**, since for the first time was studied for pyrene. On the other hand, $^3A^*$ molecule after thermal activation via reverse ISC may reach singlet excited state. This process gives rise to **E-type delayed fluorescence**. This phenomenon was first studied for eosin. The first process is of special importance as it can be utilized for synthetically useful method of singlet oxygen generation [72]:

$$\text{Sens} + h\nu \rightarrow {}^1\text{Sens}^* \rightarrow {}^3\text{Sens}^*$$
$$^3\text{Sens}^* + {}^3O_2 \rightarrow \text{Sens} + {}^1O_2$$

Strongly absorbing dyes such as Rose Bengal, methylene blue, porphyrins or phthalocyanines are usually used as photosensitizers.

1.6.2.2 Quenching of excited states via exciplex or excimer

The bimolecular deactivation of an excited state is often referred to as **quenching**, and the compound that causes this process is the **quencher**. In this process usually bimolecular entity (association of two identical or different species) is formed, with or without electron transfer. The bimolecular entity is formed after collision of a

molecule in an excited state with a molecule in the ground state. Such collisions based deactivation processes are subject to the **Wigner spin conservation rule** according to which the total spin must not change during a reaction [71]. If the two interacting components are identical an **excimer** (*exci*ted di*mer;* **MM***) is formed. If they are different, an **exciplex** (*exci*ted com*plex*, **MQ***) is formed (Fig.1.18). Excimers and exciplexes are supposed to be stabilized both by energy transfer and charge transfer.

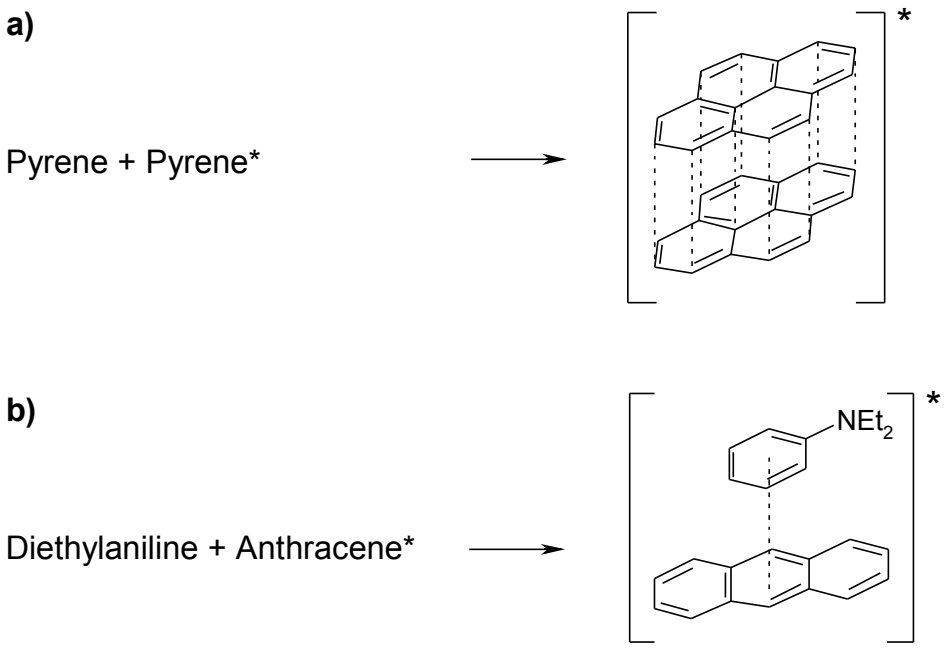

Figure 1.18. Examples of excimer a) and exciplex b) with their hypothetical structures.

The formation of an excimer (exciplexs) can be explained on the base of the frontier orbital theory. The interaction between the lower SOMO and higher SOMO of the excited molecule with the HOMO and LUMO of the ground state molecule results in an excimer (exciplexs) formation. The interactions are strong, and formation of complex is fast as the corresponding orbitals are usually close in energy (Fig. 1.19).

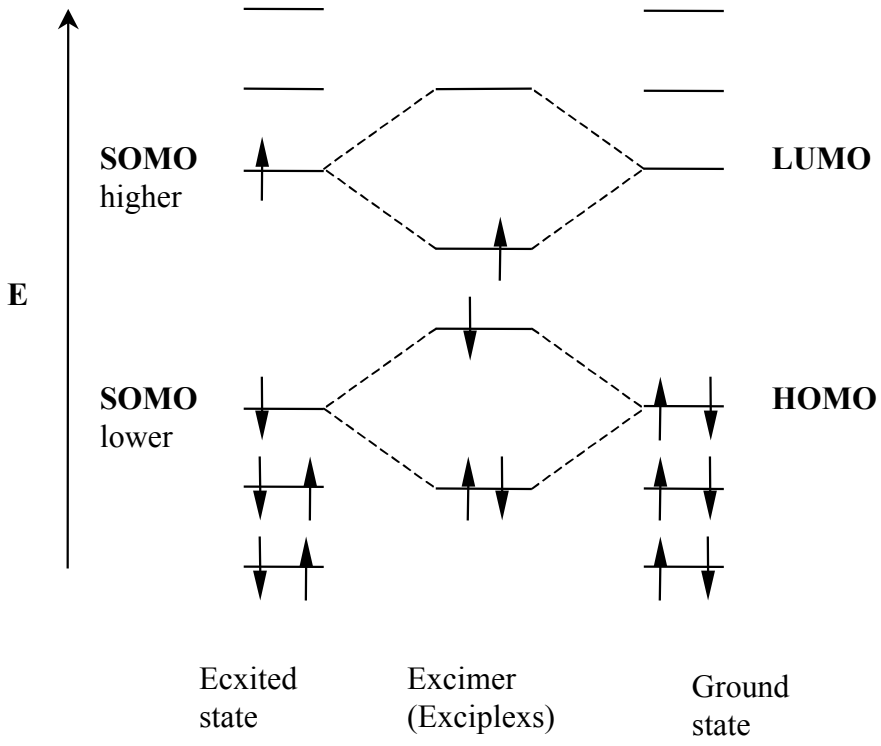

Figure 1.19. MO scheme of excimer formation.

The fluorescence of exciplex exhibits a bathochromic shift, and is known to diminish in intensity with increasing polarity of the solvent, and vanishes in highly polar solvents.

Apart from excimer or exciplexs, **encounter complex** ($M^{*}\cdots Q$) can be formed. In encounter complex the components are separated by widely varying distances and have more random orientations. An encounter complex may evolve into exciplexs or competing electron transfer within the encounter complex take place, followed by dissociation into solvated radical ion pairs in a doublet state:

$$^{1}M^{*} + {}^{1}Q \rightarrow ({}^{1}M^{*}\cdots {}^{1}Q) \rightarrow {}^{1}({}^{2}M^{-}\cdots {}^{2}Q^{+})$$

1.6.2.3 Electron transfer

In **photochemical electron transfer** (abr. **PET**) two neutral molecules D* and A form an ion pair. If one of them is electronically excited it will be deactivated after the ion pair recombination and return to the neutral ground state and the overall process can be described as quenching.

$$D^* + A \rightarrow D^{\bullet+} + A^{\bullet-} \rightarrow D + A + h\nu$$
$$D + A^* \rightarrow D^{\bullet+} + A^{\bullet-} \rightarrow D + A + h\nu$$

The molecule always possesses a lower ionization potential and a higher electron affinity in its excited state than in its ground state. In this connection it is of great importance that in the excited state a molecule can be a better oxidant and as well as a better reductant than in the ground state. Hence, electron transfer either from an excited donor D^* to an acceptor in the ground state A, or from D to A^* is possible and an exciplexs $^1(A^{\bullet-}D^{\bullet+})$ is formed. Then a radical ion pair decays to the reactants by **back electron transfer** (Fig. 1.20).

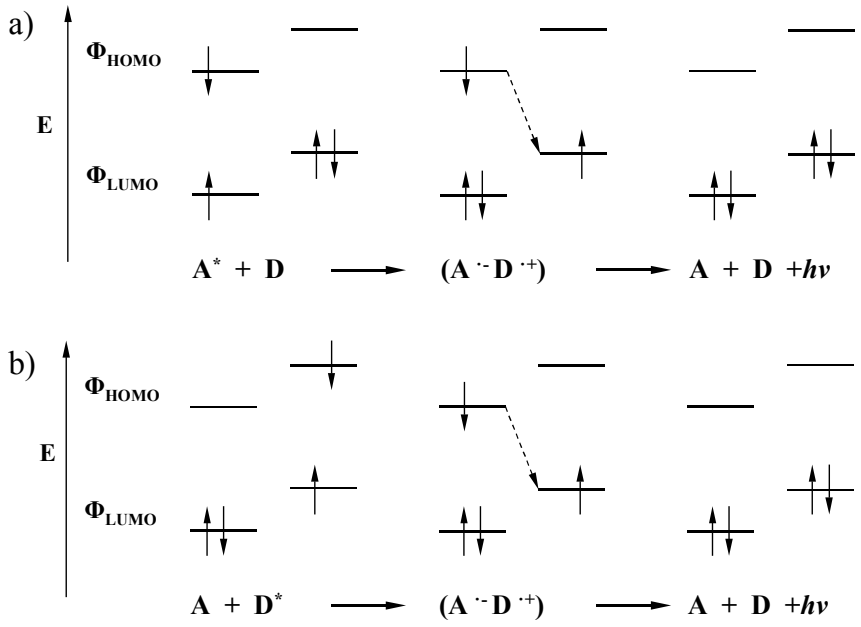

Figure 1.20. Exciplexs formation by charge transfer a) from the donor to the excited acceptor and b) from the excited donor to the acceptor.

The overall process can be characterized as an electron transfer quenching. However, it should be pointed out that fast secondary reactions may lead to product formation and in that instance the process becomes a photoinduced electron transfer reaction, and this can be utilized synthetically.

The photoinduced electron transfer in a three-component system, *i.e.* donor/photosensitizer/acceptor, has received much attention as an artificial system mimicking the photosynthesis [43,45]. The reaction mechanism is classified into two types: oxidative and reductive quenching, (Fig. 1.21).

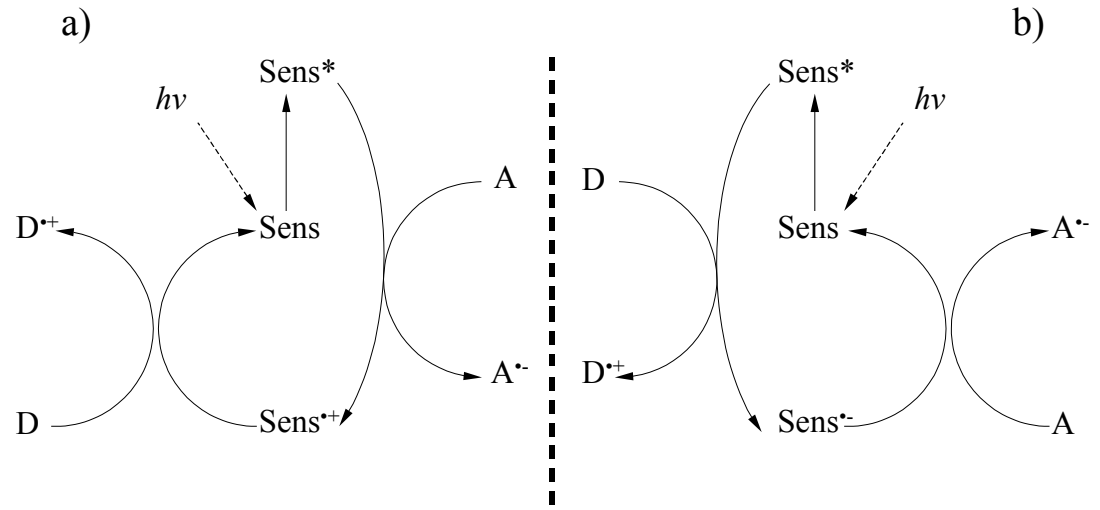

Figure 1.21. Oxidative a) and reductive b) quenching in photoinduced electron transfer.

Whether the reaction proceeds via oxidation or reduction depends on the structure and redox potential of the sensitizer [73]. Following conditions have to be fulfilled for the oxidative quenching:

$E(Sens^{\bullet+}/Sens^{*}) < E(A/A^{\bullet-})$
$E(D^{\bullet+}/D) < E(Sens^{\bullet+}/Sens)$

and for the reductive quenching:

$E(D^{\bullet+}/D) < E(Sens^{*}/Sens^{\bullet-})$
$E(Sens/Sens^{\bullet-}) < E(A/A^{\bullet-})$

Widely used photosensitizers for these kinds of experiments are: porphyrin derivatives, in particular zinc tetrakis(4-methylpyridyl)porphyrin (reductive quenching) and zinc tetraphenylporphyrin tetrasulfonate (oxidative quenching), phthalocyanines as well as tris(bipyridyl)ruthenium complex. Very suitable electron donors are NADH, EDTA, TEA or RSH. By far the most commonly used electron carrier is methyl viologen MV^{2+} [73].

1.6.3 Kinetics of photophysical processes

The number of defined events, which occurs per photon absorbed by the system, is referred to as **quantum yield (Φ)**. Quantum yield usually ranges from 0 to 1, although, Φ´s of the order of 10-100 have been reported for photoinitiated chain reactions.

$$\Phi = \frac{\text{Number of molecules of product formed}}{\text{Number of photons absorbed}} \qquad 0 \leq \Phi \geq 1$$

The basic assumption in photochemical kinetic states that monomolecular deactivation processes follow the first-order rate law [71,72]. The $\mathbf{k_i}$´s are first-order rate constants of the individual events, *e.g.* fluorescence rate constant ($\mathbf{k_f}$), internal conversion rate constant ($\mathbf{k_{IC}}$), intersystem crossing rate constant ($\mathbf{k_{ST}}$, $\mathbf{k_{TS}}$). Considering the above assumption, the **total rate constant of disappearance ($\mathbf{k_d}$)** of the singlet state (S_1), as well as any other state, of the reaction is equal to the sum of the rate constants of the individual events that are involved in deactivation process. Accordingly, the **average lifetime (τ)** of the excited state is the reciprocal of the total rate constant, and particularly **excited singlet state lifetime (τ_s)** can be derived.

$$k_d = k_f + k_{IC} + k_{ST} + \ldots$$

$$\tau = \frac{1}{\sum_i k_i}$$

$$\tau_S = \frac{1}{k_f + k_{IC} + k_{ST}}$$

The presence of quencher changes the rate of disappearance of S_1, and requires addition of the term $k_q[Q]$ to the rate expression, where $\mathbf{k_q}$ is the **quenching rate constants**, hence:

$$\tau_S^Q = \frac{1}{k_f + k_{IC} + k_{ST} + k_q[Q]}$$

The magnitude of the quenching constant k_q can be obtained experimentally from the Stern-Volmer plot (Fig. 1.22). The **Stern-Volmer equation** states that the emission quantum yield is a linear function of the concentration of the quencher, and can be derived from the fluorescence quantum yield in the absence of a quencher Φ_f and Φ_f^Q in its presence:

Figure 1.22. Example of Stern-Volmer plot.

Nonlinear Stern-Volmer plot indicates that the quenching mechanism is complicated and, in many instances, is accompanied by competing photochemical reactions.
Another important parameter is the **efficiency of S→T intersystem crossing (η_{ST})**:

$$\eta_{ST} = \frac{k_{ST}}{k_f + k_{IC} + k_{ST}} = k_{ST}\tau_S$$

If the T_1 state is deactivated only by first-order processes such as phosphorescence and ISC with rate constants $\mathbf{k_P}$ and k_{ST}, **the quantum yield of phosphorescence ($\mathbf{\Phi_P}$)** is given by following equation:

$$\Phi_P = \frac{k_P}{(k_{TS} + k_P)} \frac{k_{ST}}{(k_{IC} + k_{ST} + k_f)}$$

Knowing that the lifetime of the excited state is the reciprocal of the total rate constant the **triplet lifetime (τ_P)** can be derived and written according to equation:

$$\tau_P = \frac{1}{k_{ST} + k_P}$$

Analogously, expression for the **efficiency of the T→S intersystem crossing (η_{TS})**, which populates the singlet ground state S_0 and competes with phosphorescence, may be given:

$$\eta_{TS} = \eta_{ST} \frac{k_{TS}}{(k_P + k_{TS})} = \eta_{ST} k_{TS} \tau_T$$

The kinetic equations for quantum yields, efficiencies, lifetimes and rate constants for any of the events that takes place in the molecule system during excitation and deactivation are well-known and describe in the chemical literature [71,73]. Moreover, all this parameters are experimentally available. All this spectroscopic data can be collected in a Jablonski diagram that is extremely useful in discussing photochemistry of investigated molecule [72].

1.7 Singlet oxygen

1.7.1 Introduction

Singlet oxygen ($^1O_2$, $^1\Delta_g$) was first observed in 1924 and then defined as a more reactive form of oxygen. The main method of production of $^1O_2$ is by photosensitization reaction. In 1931, Hans Kautsky at Heidelberg University first proposed that $^1O_2$ might be a reaction intermediate in dye-sensitized photo-oxygenation. Following this suggestion, many studies have showed that $^1O_2$ is an important intermediate species in the detrimental oxidation of biomolecules. It has been demonstrated now that $^1O_2$ can react with many kinds of biological molecules such as DNA, proteins and lipids. Since oxygen is ubiquitous and efficiently quenches electronically excited states, $^1O_2$ is likely

to be formed following irradiation in countless situations and involved in various chemical and biological processes as well as in several disease processes. Therefore, a better understanding of its chemical and physical nature is important [73,74]. This chapter will discuss the properties, generation, reactions, quenching and detection of $^1O_2$.

1.7.2 Electronic structure and lifetime of singlet oxygen

On the basis of molecular orbital theory the electronic structure of molecular oxygen can be easily explained. The lowest electronic state of oxygen is a triplet ground state ($^3O_2$, $^3\Sigma_g^-$) with two unpaired electrons distributed in the highest occupied orbitals (Fig.1.23). This triplet character is responsible for the paramagnetism and diradical-like properties of ground state molecular oxygen. More importantly, this triplet electronic configuration only permits reactions involving one-electron steps. Thus, despite the exothermicity of oxygenation reactions, a spin barrier prevents $^3O_2$ from reacting indiscriminately with the plethora of singlet ground-state organic compounds surrounding it [75,76].

Rearrangement of the electron spins within these two degenerate orbitals results in two possible singlet excited states. The $^1\Delta_g$ state has energy only 94.2 kJ mol^{-1} above that of the ground state; both electrons are paired in a single orbital, leaving the other vacant (Fig.1.24). This state might be expected to undergo two-electron reactions. The higher singlet state ($^1\Sigma_g^+$), lying 62.7 kJ yet higher, comes from the spin pairing electrons in different orbitals and might be expected to undergo one-electron free-radical reactions. Because there are no unpaired electrons, neither $^1\Delta_g$ form nor $^1\Sigma_g^+$ are radicals. In both forms of $^1O_2$, the spin restriction is removed so that the oxidizing ability is greatly increased [75,76].

The $^1\Sigma g^+$ state has a much shorter lifetime than $^1\Delta g$ state because $^1\Sigma g^+$ is more reactive than the $^1\Delta_g$ form. It decays to $^1\Delta_g$ state before chemical reactions can occur. O_2 ($^1\Delta_g$) is the lower energy species that reacts chemically as $^1O_2$. The excitation energy is 0.98 eV (94.2 kJ mole^{-1}) and the radiative decay lifetime is 45 minutes at very low gas pressures. However, collisions with other molecules induce much shorter lifetime, e.g. 14 minutes in oxygen gas at 760 torr. For the higher energy excited state O_2 ($^1\Sigma g^+$) the excitation energy is 1.63 eV (156.9 kJ mole^{-1}) and the decay lifetime is 7 seconds in the gas phase [75,76].

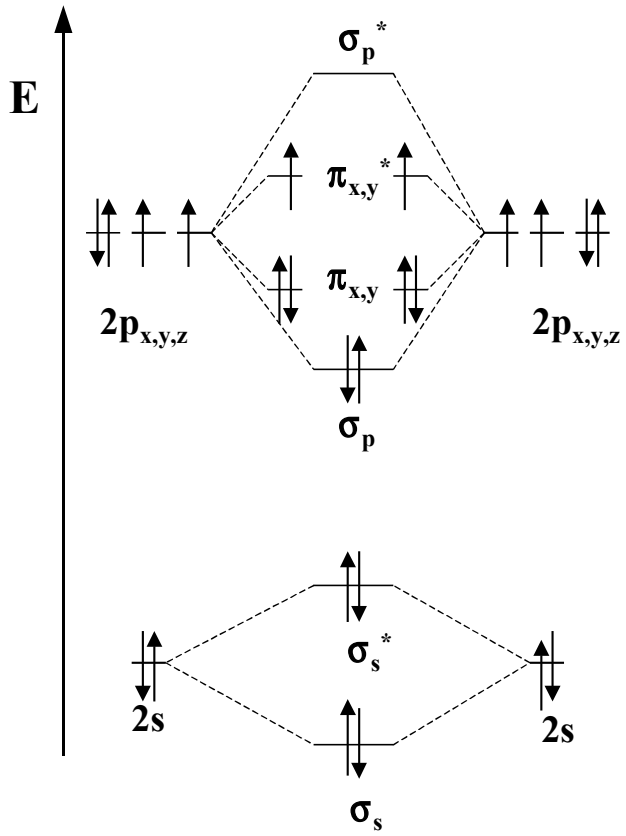

Figure 1.23. Molecular orbital diagram of an oxygen molecule in the triplet ground state ($^3O_2$).

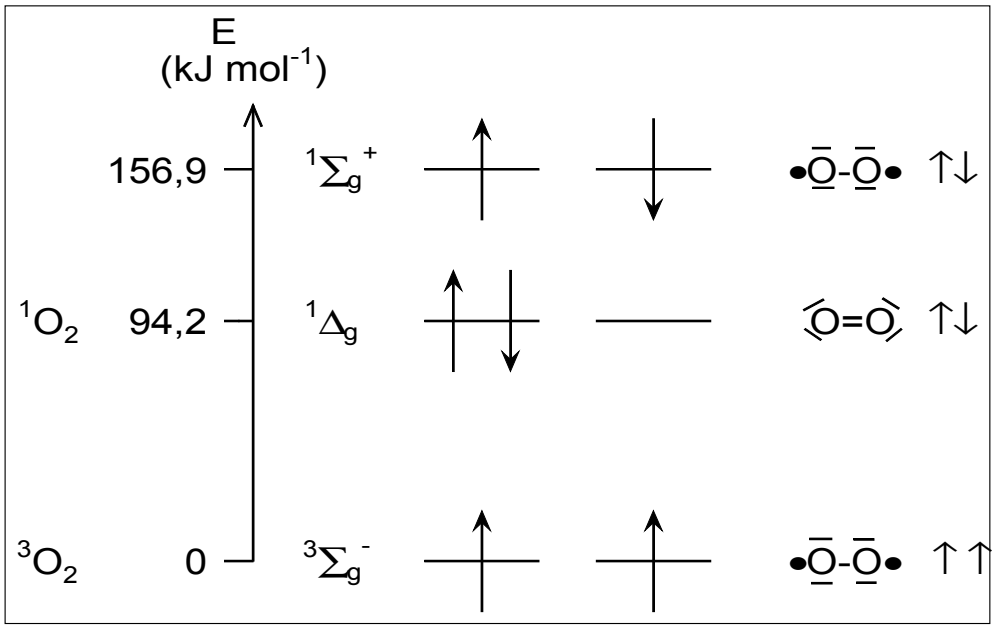

Figure 1.24. The three electronic states of molecular oxygen, *i.e.* one triplet ($^3\Sigma_g^-$) and two singlet states ($^1\Delta_g$, $^1\Sigma_g^+$), and the energy of their HOMO orbitals.

The lifetime of $^1O_2$ depends immensely on the nature of the solvent; as a rule deuterated solvents give rise to longer lifetimes (Table 1.1).

Table 1.1 Lifetimes of singlet oxygen in various solvents [75].

Solvent	**t [μs]**	**Solvent**	**t [μs]**
H_2O	3,3-7,4	D_2O	55-120
CH_3OH	10	CD_3OD	227
C_6H_6	25-32	C_6D_6	550-790
$(CH_3)_2CO$	34-65	$(CD_3)_2CO$	588-837
CCl_4	26000-31000	C_6F_6	25000

Because the reactions that concern us during this work are generally carried out in solution, it is longer-lived $^1\Delta_g$ state that is involved as the active oxygen species. We shall, henceforth, refer to this longer-lived species as singlet oxygen.

1.7.3 Reactions of singlet oxygen

$^1O_2$ reacts with the plethora of organic compounds including olefins, dienes, sulphides, aromatics, hetero-aromatics, terpenes, steroids, fatty acids, flavones, tetracyclines, vitamins, amino acids, proteins, nucleic acids, blood and bile pigments, and synthetic polymers. Most of the reactions fall into three general classes [73].

- Alder-ene reaction (Schenk reaction)

The ene-reaction is a general type of reaction that is essentially a hydrogen abstraction and oxygen addition. In this reaction, oxygen adds to the alkyl substituted olefins to form allylic hydroperoxides with a migration of the double bond, (Fig.1.25):

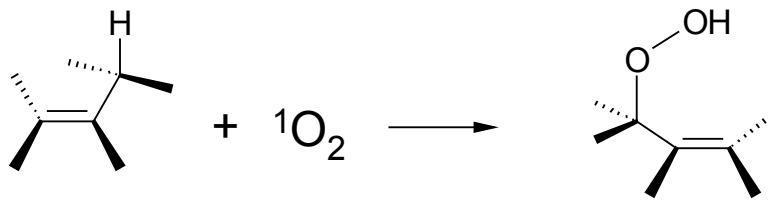

Figure 1.25. Schenk reaction - formation of allylic hydroperoxide.

The resulting allylic hydroperoxides can be easily converted into α,β-unsaturated carbonyl compounds and allyl alcohols. A variety of mechanisms have been proposed to explain the products observed in this reaction. They involve either a six-centered transition state typical of the classical ene reaction, peroxide or a biradical intermediate. While the involvement of peroxide intermediate is consistent with the experimental observations, the classical ene mechanism is favoured by most authors. Involvement of radical intermediates has been ruled out on the basis of various evidences. The question of the mechanism of this reaction has been the subject of much heated debate over the past decade [76]. An example of industrially important Schenk reaction is β-citronellol photo-oxidation to (-)-rose oxide (Fig.1.26).

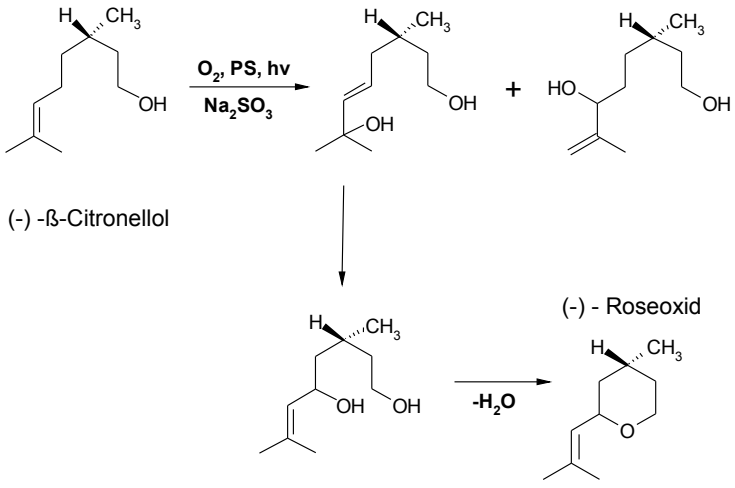

Figure 1.26. (-)-Rose oxide synthesis as an example of Schenk reaction.

- Diels-Alder Reaction

With acceptors such as *cis* dienes or aromatic hydrocarbons, $^1O_2$ can react as a good dienophile. This reaction is similar to the well-known Diels-Alder reaction. The initially formed endoperoxides may undergo fragmentation back to reactants or rearrange to products through the homolytic fission of the oxygen-oxygen bond, (Fig.1.27).

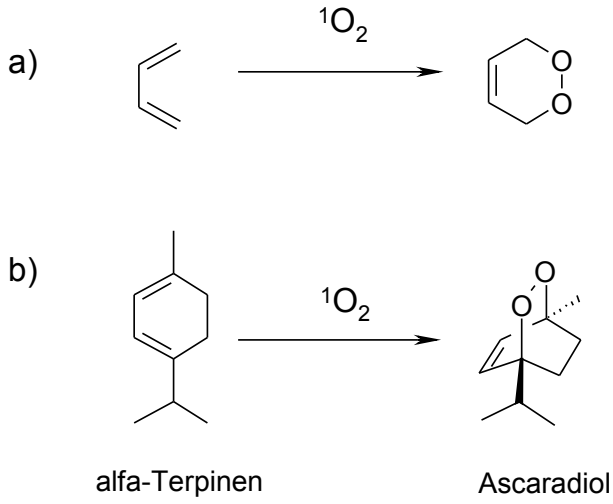

Figure 1.27. An example of endoperoxide formation in [4+2] cycloaddition.

The products of these reactions are energy-rich and their thermal decomposition reactions are chemiluminescent. The endoperoxides of naphthalenes and anthracenes generally restore the parent compound plus $^1O_2$.

Singlet oxygen can also react with electron rich systems, in which carbon-carbon double bonds have adjacent electron donating atoms (nitrogen, sulfur). In these reactions, an oxetane type adduct is formed. These dioxetanes may be unstable and decompose to give carbonyl compounds. Decomposition of dioxetane is sometimes accompanied by chemiluminescence (Fig.1.28).

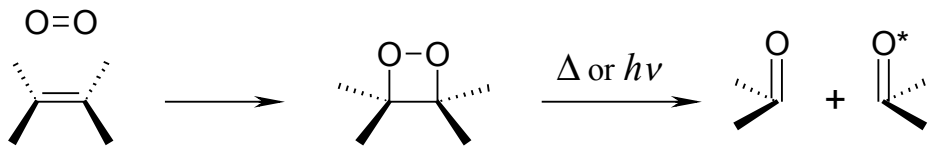

Figure 1.28. Dioxetane formation in a [2+2] cycloaddition.

- Oxygenation is another common reaction as exemplified by (Fig.1.29):

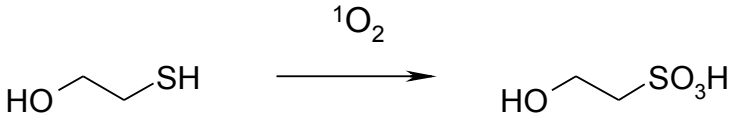

Figure 1.29. Photo-oxidation of 2-mercaptoethanol.

A variety of factors control all singlet oxygen reactions. Singlet oxygen is mildly electrophylic and the rate of reaction within a homologous series of compounds is generally inversely proportional to their ionization potential. Solvent has only minimal effect on the rate of reaction; changes in rate are commonly due to solvent effects on the lifetime of singlet oxygen. Because of the low activation energy for singlet oxygen processes (0.5-8 kcal), little if any temperature effect on the rate of reaction is observed. Regarding the mode of reaction, electron-rich olefins as well as sterically hindered alkenes tend to prefer dioxetane formation, though two modes often compete. Finally, the direction of singlet oxygen attack is predominantly, if not exclusively, from the less hindered side of the molecule [76].

1.7.4 Sensitization - singlet oxygen source

An impressive variety of physical and chemical sources of $^1O_2$ are now available for laboratory scale purposes. These include photosensitization, oxidation of H_2O_2, decomposition of phosphite ozonides and endoperoxides, and microwave discharge. Photosensitization is clearly the most convenient technique available for generating $^1O_2$ and, by far, the most commonly used, since it is applicable to a large spectrum of reaction temperatures, solvents and sensitizers (including those, which are polymer or resin based). **Photosensitization** refers to a light-activated process that requires the presence of a light-absorbing substance, the photosensitizer, that initiates a physical, chemical, or biological process in a non-absorbing substrate [77].

Photooxygenation is an example of photosensitized process; during this light induced process incorporation of molecular oxygen into a molecular entity takes place. In general, there are three common mechanisms [77]:

- Type I: the reaction of triplet molecular oxygen ($^3O_2$) with radicals formed photochemically.
- Type II: the reaction of photochemically produced singlet molecular oxygen ($^1O_2$) with molecular entities to give rise to oxygen containing molecular entities.
- Type III: the third mechanism proceeds by electron transfer to produce the superoxide radical anion ($O_2^{-\bullet}$) as the reactive species [77].

In the case of Type I and Type III the sensitizer triplet ($Sens^3$), formed via intersystem crossing of the exited singlet state sensitizer ($Sens^{1*}$), interacts directly with a molecule of substrate. This interaction can lead down either of two different pathways. The first one is hydrogen atom abstraction, which initiates free radical autoxidative process (it is so called "Type I") [76].

Type I

$$Sens^1 + h\nu \rightarrow Sens^{1*} \rightarrow Sens^{3*}$$

$$Sens^{3*} + RH \rightarrow {}^{\bullet}SensH + R^{\bullet}$$

$$R^{\bullet} + {}^3O_2 \rightarrow ROO^{\bullet}$$

$$ROO^{\bullet} + {}^{\bullet}SensH \rightarrow ROOH + Sens$$

$$ROO^{\bullet} + RH \rightarrow ROOH + R^{\bullet}$$

Alternatively, electron transfer from substrate to excited sensitizer may occur, in which case the oxygenation products result from the coupling of the substrate cation radical with superoxide anion radical (so called "Type III") [76].

Type III

$$Sens^{3*} + R \rightarrow Sens^{-\bullet} + R^{+\bullet}$$

$$Sens^{-\bullet} + {}^3O_2 \rightarrow Sens + O_2^{-\bullet}$$

$$Sens^{3*} + {}^3O_2 \rightarrow Sens^{+\bullet} + O_2^{-\bullet}$$

$$Sens^{+\bullet} + R \rightarrow Sens + R^{+\bullet}$$

$$R^{+\bullet} + O_2^{-\bullet} \rightarrow Oxygenation$$

Irrespective of whether the mechanism of oxygenation is a photoinitiated autooxidation or an electron transfer photo-oxidation, only ground state molecular oxygen ($^3O_2$) is involved [76].

The Type II, on the other hand, is characterized by initial interaction between the sensitizer triplet and a molecule of oxygen. First sensitizer is excited to singlet state followed by intersystem crossing to triplet excited state. The direct absorption of light by $^3O_2$ to produce $^1O_2$ is a spin-forbidden process.

Type II

$$\text{Sens} + h\nu \rightarrow \text{Sens}^{1*}\ (\text{ISC}) \rightarrow \text{Sens}^{3*}$$

$$\text{Sens}^{3*} + {}^3O_2 \rightarrow {}^1\text{Sens} + {}^1O_2$$

$${}^1O_2 + \text{R} \rightarrow \text{Oxygenation}$$

Recently, however, another process has been observed (referred to, by some authors, as "Type IIb"), which results in oxygenation via radical process [76,78]. In Type IIb, triplet sensitizer interacts with dioxygen via electron transfer to yield superoxide; the later, or more likely its derivatives, initiate oxygenation [78,79]. Superoxide appears to be rather poor radical, which rarely initiates free radical autoxidative processes via H-abstraction or addition to double bond. Its conjugate acid HOO$^{\bullet}$, or another of its derivative HO$^{\bullet}$, are well-documented radical initiators [76]. Research in the case of Rose Bengal has suggested, however, that the source of the superoxide is in fact a reaction between the sensitizer and singlet oxygen [78,80].

Type IIb

$$\text{Sens}^{3} + {}^3O_2 \rightarrow [\text{Sens}^1 + {}^1O_2] \rightarrow \text{Sens}^{+\bullet} + O_2^{-\bullet}$$

$$\text{RH} + O_2^{-\bullet}\ (\text{or HOO}^{\bullet}) \rightarrow \text{Oxygenation}$$

Finally and most recently, a third "Type II" reaction (which will refer to as "Type IIc") has been observed with n-π^* sensitizers, in which the triplet sensitizer (generally an excited carbonyl) reacts with molecular oxygen generating a diradical peroxy species (e.g., $^{\bullet}$O-CR$_2$-OO$^{\bullet}$). The later may initiate radical processes itself or via its derivatives [76].

Type IIc

$$\text{Sens}^{3} + {}^3O_2 \rightarrow [\text{Sens}^1 + {}^1O_2] \rightarrow {}^{\bullet}\text{Sens-OO}^{\bullet}$$

$$\text{RH} + {}^{\bullet}\text{Sens-OO}^{\bullet} \rightarrow \text{Oxygenation}$$

As a rule $^1O_2$ and free-radical processes can be involved simultaneously and at different rate in photosensitized oxygenation. It is well known that, in general, high oxygen concentration favours the Type II photo-oxidation (*i.e.* energy transfer to triplet oxygen) and high substrate concentration favours radical pathway. Hence, several tests have been developed to discern between the two mechanisms:

- DABCO or DPBF (1,3-diphenylisobenzofurane) quenches $^1O_2$ reactions.

- On the other hand, free-radical inhibitors such as 2,6-di-t-butylphenol will inhibit radical mediated processes.

- Because of their low activation energies, the rates of singlet oxygenation are well known to be insensitive to reaction temperature; such is not the case with free-radical autoxidations.

- The reaction results should be compared with those obtained when $^1O_2$ is chemically generated from triphenyl phosphite ozonide.

1.7.5 Singlet oxygen detection

Listed below is a short survey of the most commonly cited methods for singlet oxygen detection.

- Scavengers: Indirect tests for singlet oxygen are based on the inhibiting effects of an additive on the rate of a photochemical reaction. Azide ion (N_3^-) is a useful water-soluble agent. The protective effect of azide is attributed to physical quenching:

  $$^1O_2 + N_3^- = {}^3O_2 + N_3^\bullet$$

  Other frequently employed water-soluble quenching agents include 1,4-diazabicyclo-[2.2.2]octane (DABCO), DPBF, ascorbic acid, and tryptophan.

- D_2O: D_2O can be used for indirect detection of $^1O_2$ presence because the lifetime of $^1O_2$ is more than 10-fold longer in D_2O than in H_2O. So, if a reaction in aqueous

solution is dependent on singlet oxygen, carrying it out in D_2O instead should greatly improve the reaction rate.

- Luminescence: As $^1O_2$ decays back to the ground state, some of the energy is emitted as light. The light from singlet oxygen appears in the infrared as 1268 nm band.

$O_2 (^1\Delta_g) \rightarrow O_2 (^3\Sigma_g^-) + h\nu$ (1268 nm)

- Electron paramagnetic resonance: A recent approach to singlet oxygen detection is based on electron paramagnetic resonance (EPR). EPR is a non-optical technique in which energy transfer between the intrinsic magnetism of unpaired electrons and an external magnetic field is measured with a sensitive microwave detection system.

1.8 References

[1] Brown, A.; Tcherniac, J.; *Ber. Dtsch. Chem. Ges.* **1907**, 40, 2709.
[2] de Diesbach, H.; von der Weid, E.; *Helv. Chim. Acta* **1927**, 10, 886.
[3] Linstead, R. P.; *J. Chem. Soc.* **1934**, 1016.
[4] Byrne, G. T.; Linstead, R. P.; Lowe, A. R.; *J. Chem. Soc.* **1934**, 1017.
[5] Dent, C. E.; Linstead, R. P.; *J. Chem. Soc.* **1934**, 1027.
[6] Dent, C. E.; Linstead, R. P.; *J. Chem. Soc.* **1934**, 1033.
[7] Linstead, R. P.; Lowe, A. R.; *J. Chem. Soc.* **1934**, 1022.
[8] Linstead, R. P.; Lowe, A. R.; *J. Chem. Soc.* **1934**, 1031.
[9] Neil B. McKeown; *The synthesis of symmetrical phthalocyanines* in The Porphyrin Handbook, Vol. 15, Academic Press, **2003**.
[10] Leznoff, C. C.; Lever, A. B. P.; *Phthalocyanines Properties and Applications*, Vol.1, **1989** VCH.

[11] Sharman, W. M.; van Lier, J. E.; *Synthesis of Phthalocyanine Precursors* in The Porphyrin Handbook, Vol. 15, Academic Press **2003**.

[12] Brodkin, V. F.; *J. Appl. Chem. USSR*, **1958**, 31, 803.

[13] Hurley, T. J.; Robinson, M. A.; Trotz, S. I.; *Inorg. Chem.* **1967**, 6, 389

[14] Oliver, S. W.; Smith, T. D.; *J. Chem. Soc. Perkin. Trans II*, **1987**, 1579.

[15] Gaspard, S.; Maillard, Ph.; *Tetrahedron*, **1987**, 43, 1083.

[16] Bauman, F.; Bienert, B.; Rösch, G.; Vollmann, H.; Wolf, W.; *Angew. Chem.* **1956**, 68, 133.

[17] Chambrier, I.; Cook, M. J.; *J. Chem. Res. (S)*, **1990**, 322.

[18] Molek, C. D.; Halfen, J. A.; Loe, J. C.; McGaff, E. W.; *Chem Commun.* **2001**, 2644.

[19] van der Pol, J. F.; Neeleman, E.; Nolte, R. J. M.; Zwikker, J. W.; Drenth, W.; *Macromol. Chem.* **1989**, 190, 2727.

[20] Berezin, B. D.; *Coordination Compounds of Porphyrins and Phthalocyanines*, **1981** John Wiley & Sons.

[21] Rosenthal, I.; Ben-Hur, E.; in Leznoff, C. C.; Lever, A. B. P.; *Phthalocyanines Properties and Applications* **1989** VCH, Vol. 1, 393-425.

[22] Rosenthal, I.; *Photochem. Photobiol.* **1991**, 53, 859-870.

[23] Henderson, B. W.; Dougherty, T. J.; *Photochem. Photobiol.* **1992**, 55, 145-157.

[24] Emmelius, M. K.; Pawlowski, G.; Vollman, H.; *Angew. Chem.* **1989**, 28, 1445-1470.

[25] Nicolson, M. M.; in Leznoff, C. C.; Lever, A. B. P.; *Phthalocyanines Properties and Applications*, New York, **1993** VCH, Vol. 3, 75-117.

[26] Brown, K. M.; Gleim, K. T.; Urban, P.; *Oil Gas* **1959**, 57, 73-78.

[27] Salazar, P.; In UOP Merox process. *Handbook of Petroleum Process* (Edited by R. A. Meyers), Part 9, McGraw-Hill, New York.

[28] Schneider, G.; Wöhrle, D.; Spiller, W.; Stark, J.; Schulz-Ekloff, G.; *Photochemistry and Photobiology*, **1994**, 60, pp. 333-342.

[29] Gerdes, R.; Bartels, O.; Schneider, G.; Wöhrle, D.; Schulz-Ekloff, G.; *International Journal of Photoenergy,* **1999**, Vol. 1, 41-47.

[30] Wöhrle, D.; Suvorova, O.; Gerdes, R.; Bartels, O.; Lapok, L.; Baziakina, N.; Makarov, S.; Slodek, A.; *Processes of Petrochemistry and Oil Refining* **2002**, 3(10), 30-46.

[31] Wöhrle, D.; Meissner, D.; Organic solar cells, in *Adv. Mater.* **1991**, 3, 129-138.

[32] Nazeeruddin, Md. K.; Humphry-Baker, M.; Grätzel, M.; Murrer, B. A.; *Chem. Commun.* **1998**, 719-720.

[33] Nazeeruddin, Md. K.; Humphry-Baker, M.; Grätzel, M.; Wöhrle, D.; Schnurpfeil, G.; Schneider, G.; Hirth, A.; Trombach, N.; *J. Porphyrins Phthalocyanines* **1999**, 3, 230-237.

[34] Piechocki, C.; Simon, J.; Skoulious, A.; Guillon, D.; Weber, P.; *J. Am. Chem. Soc.* **1982**, 104, 5245.

[35] Cammidge, A. N.; Cook, M. J.; Harrison, K. J.; McKeown, N. B.; *J. Chem. Soc., Perkin Trans.* **1991**, 1, 3053.

[36] Van der Pol, J. F.; Neeleman, E.; Zwikker, J. W.; Notte, R. J. M.; Drenth, W.; Aerts, J.; Visser, R.; Picken, S. J.; *Liq. Cryst.* **1989**, 6, 577.

[37] Batey, J.; Petty, M. C.; Roberts, G. G.; Wright, D. R.; *Electron. Lett.* **1984**, 20, 489.

[38] Zagal, J. H.; *J. Electroanal. Chem.* **1980**, 109, 389.

[39] Kilcuchi, T.; Sasaki, H.; Toshima, S.; *Chem. Lett.* **1980**, 5.

[40] Nicolson, M. M.; in Leznoff, C. C.; Lever, A. B. P.; *Phthalocyanine: Properties and Applications*, New York, VCH, **1996**, Vol. 4, 79-181.

[41] Ahuja, R. C.; Hauffe, K.; *Ber., Bunsenges. Phys. Chem.* **1980**, 84, 68.

[42] McKeown, N. B.; *Chem Industry* **1999**, 92.

[43] Law, K. Y.; in *Handbook of Organic Conductive Molecules and Polymers*, Nalwa, H. S. (Ed.),Wiley, Chichester, **1997**, Vol. 1, 487-551.

[44] Grund, A.; Kaltbeitzel, A.; Mathy, A.; Schwartz, R.; Bubeck, C.; Vernmehren, P.; Hanack, M.; *J. Phys. Chem.* **1992**, 96, 7450.

[45] Meller, A.; Ossko, A.; *Monatsh. Chem.* **1972**, 103, 150.

[46] Kietaibl, H.; *Monatsh. Chem.* **1974**, 105, 405.

[47] Claessens, Ch. G.; Gonyales-Rodriguey, D.; Torres, T.; *Chem. Rev.* **2002**, 102, 835-853.

[48] Geyer, M.; Plenzig, F.; Rauschnabel, J.; Hanack, M.; del Rey, B.; Sastre, A.; Torres, T.; *Synthesis* **1996**, 1139-1151.

[49] Kobayashi, N.; *J. Porphyrins Phthalocyanines* **1999**, 3, 453-467.

[50] Claessen, Ch. G.; Torres, T.; *Angev. Chem. Int. Ed.* **2002**, 41, 2561-2565.

[51] Claessens, Ch. G.; Torres, T.; *Chem. Eur. J.* **2000**, 6, 2168-2172.

[52] Kudrevich, S. V.; Gilbert, S.; van Lier, J. E.; *J. Org. Chem.* **1996**, 61, 5706-5707.

[53] Lee, S.; Suh, H.; *Bull. Korean Chem. Soc.* **1999**, Vol. 20, 9, 991-992.

[54] Zyskowski, Ch. D.; Kennedy, V. O.; *J. Porphyrins Phthalocyanines* **2000**, 4, 707-712.

[55] del Rey, B.; Torres, T.; *Tetrahedron Lett.* **1997**, 38, 5351-5354.

[56] Sastre, A.; Torres, T.; Hanack, M.; *Tetrahedron Lett.* **1995**, 36, 8501-8504.

[57] Kobayashi, N.; Kondo, R.; Nakajima, S.; Osa, T.; *J. Am. Chem. Soc.* **1990**, 112, 9640-9641.

[58] Weitmeyer, A.; Kliesch, H.; Wöhrle, D.; *J. Org. Chem.* **1995**, 60, 4900-4904.

[59] Ho Kang, S.; Kang, Y. S.; Zin, W. C.; Olbrechts, G.; Wostyn, K.; Clays, K.; Persoons, A.; Kim, K.; *Chem. Commun.* **1999**, 1661-1662.

[60] Martinez-Diaz, M. V.; del Rey, B.; Torres, T.; Agricole, B.; Mingotaud, C,; Cuvillier, N.; Rojo, G.; Agullo-Lopez, F.; *J. Mater. Chem.* **1999**, 9, 1521-1526.

[61] Sastre, A.; Torres, T.; Diay-Garcia, M. A.; Agullo-Lopez, F.; Dhenaut, C.; Brasselet, S.; Ledoux, I.; Zyss, J.; *J. Am. Chem. Soc.* **1996**,118, 2746-2747.

[62] del Rey, B.; Keller, U.; Torres, T.; Rojo, G.; Agullo-Lopez, F.; Nonell, S.; Marti, C.; Brasselet, S.; Ledoux, I.; Zyss, J.; *J. Am. Chem. Soc.* **1998**, 120, 12808-12817.

[63] Gouterman, M.; Sayer, Ph.; Shankland, E.; Smith, J. P.; *Inorg. Chem.* **1981**, 20, 87-92.

[64] Sayer, P.; Goutermen, M.; Connell, Ch.; *Acc. Chem. Res.* **1982**, 15, 73-79.

[65] Fujiki, M.; Tabei, H.; Isa, K.; *J. Am. Chem. Soc.* **1986**, 108, 1532-1536.

[66] Li, J.; Lakshminarayanapuram, R.; Subramanian, R.; Hanack, M.; *Chem. Commun.* **1997**, 679-680.

[67] Li, J.; Lakshminarayanapuram, R.; Subramanian, R.; Hanack, M.; *Eur. J. Org. Chem.* **1998**, 2759-2767

[68] Fox, J. P.; Goldberg, D. P.; *Inorg.Chem.* **2003**, 42, 8181-8191.

[69] Ichiro Okura; "Photosensitization of Porphyrins and Phthalocyanines", GIB, Tokyo **2000**.

[70] Thomas Oppenländer; "Photochemical Purification of water and air" 2003 Wiley-VCH.

[71] Jan Kopecky, "Organic Photochemistry: a visual approach", 1992 VCH.

[72] Barltrop, J. A.; Coyle, J. D.; *Excited States in Organic Chemistry* **1975**, Wiley: New York.

[73] Kearns, D. R.; Physical and chemical properties of singlet molecular oxygen. in *Chem. Rev.* **1971**, 71 (4), 395-427.

[74] Ameta, S. C.; Punjabi, P. B.; Chobisa, C. S.; Mangal, N.; Bhardwaj, R.; Singlet molecular oxygen. in *Asian J. Chem. Rev.* **1990**, 1 (2), 106-124.

[75] Dieter Woehrle, Michael W. Tausch, Wolf-Dieter Stohrer: Photochemie, 1998 Wiley-VCH.

[76] Frimer, A. A.; *The Spectrum* **2000**, Vol. 13, 9-16.

[77] Parmon, V.; Emeline, A.; V.; Serpone, N.; "Glossary of Terms in Photocatalysis and Radiocatalysis" in: *Intern. J. Photoenergy,* **2002**.

[78] Jefford, C. W.; Boschung, A. F.; *Helv. Chim. Acta* **1977**, 60, 2673-2685.

[79] Neckers, D. C.; *J. Photochem. Photobiol.* **1989**, 47, 1-29.

[80] Jefford, C. W.; Estrada, M. J.; Barchietto, G.; *Tetrahedron* **1987**, 43, 1737-1745.

2. Synthesis and characterization

2.1 Synthesis strategy

In order to induce water solubility, a number of functional groups have been added to the Pc framework, *e.g.* sodium salts of sulfonate, carboxylate, phosphonate as well as quaternary amine and polyethers [1]. Substitution with suitable groups can essentially be accomplished in two ways. The first method involves condensation of previously substituted precursors (phthalonitriles, 1,3-diiminoisoindolines and others) followed sometimes by further modifications. Thus, tetrasulfophthalocyanines are usually synthesized by cyclotetramerization of the sodium 4-sulfophthalate in melted urea in the presence of metal salt, ammonium chloride and ammonium molybdate [2,3]. Octacarboxyphthalocyanines are prepared by hydrolysis of octacyanophthalocyanines previously obtained from 1,2,4,5-tetracyanobenzene reacted with metal salt in solvents such as 1-propanol, 1-chloronaphthalene, picoline, sulfolane or DMF [4-7]. Phthalocyanines substituted with esters [8], sulfonamides [9] or phosphonate esters [10-12] can be successfully hydrolysed to give carboxylic acids, sulfonic acids and phosphonate acids, respectively. Quaternization of tertiary amines provides a valuable method of preparing water-soluble positively charged phthalocyanines [13]. The ester hydrolysis was used to prepare water-soluble phthalocyanine-centered dendrimers [14]. Octahydroxy- and tetrahydroxyphthalocyanies are synthesized by the cleavage of the ether bond and removal of alkoxy, methoxymethyloxy or benzyl protecting groups attached to the phthalocyanine core [15-17]. The second method involves the direct substitution onto a pre-existing phthalocyanine. An example of the latter is the sulfonation of the phthalocyanine what was thoroughly investigated during this work [18].

Chapter 2.2 deals with the synthesis, purification and characterization of four precursor compounds. Three of these precursors were synthesized according to procedures published elsewhere. 4-(Pyridyloxy)phthalonitrile (**3**) was synthesized with the intention of converting it to the metal-free phthalocyanines. Once the metal-free phthalocyanine was isolated, it could be converted to triazatetrabenzcorrole via phosphorus insertion

and ring reduction. 5-(Pyridyloxy)-1,3-diiminoisoindoline (**4**) was the precursor used in the synthesis of silicon (**14**, **15**) and germanium (**17**, **18**) phthalocyanines. 4-Iodophthalonitrile (**6**) was utilized for the synthesis of triiodosubphthalocyanine, which then via Sonogashira cross-coupling was converted to the water-soluble subphthalocyanines **35** and **36**. 4-[2-(2-pyridinyl)ethyl]phthalonitrile (**9**) obtained in a multistep reaction was proposed as a precursor for the synthesis of alkylated water-soluble subphthalocyanine. The choice of such precursors that results in dyes having 3-pyridyloxy, 2-(3-pyridynyl)ethynyl and 2-(2-pyridynyl)ethyl substituents was intentional. N-methylation or quaternization with 1,3-propanesultone of these functionalities give excellent water-soluble cationic and zwitterionic phthalocyanines and related compounds. Chapter 2.3 deals with the synthesis of nine water-soluble phthalocyanines. Both silicon and germanium sulfophthalocyanines – two precious photocatalysts - have been already reported in chemical literature, however, procedures described there lack many important details and proved to be irreproducible in our hands. Hence, the synthesis of silicon and germanium sulfophthalocyanines (**25**, **28**) was thoroughly reinvestigated. As a result new synthesis methods were proposed. Moreover, the synthesis of positively charged and zwitterionic silicon and germanium phthalocyanines (**14**, **15**, **17**, **18**) was investigated. Besides, sulfonated, cationic and zwitterionic metal-free phthalocyanines were obtained (**11**, **12**, **20**). Chapter 2.4 deals with the successful preparation of two water-soluble oxophosphorus(V) triazatetrabenzcorroles (**30**, **31**) that were synthesized via phosphorus insertion and ring contraction of the metal-free phthalocyanine (**10**). The synthesis of water-soluble subphthalocyanines is particularly challenging and difficult as many phthalonitriles successfully utilized during phthalocynines synthesis are useless for the subphthalocyanines. This is due to incompatibility of many functional groups and very reactive boron trichloride used during subphthalocyanines preparation. Chapter 2.5 summarizes efforts towards making these compounds water-soluble. Altogether, five new water-soluble subphthalocyanines were obtained. Chapter 2.6 deals with metal-free and zinc water-soluble porphyrins (**46**, **47**, **49**, **50**, **52**). Many water-soluble porphyrins have been described until now, some of them are also commercially available. These compounds offer interesting alternative to phthalocyanines, the photocatalytic properties of which have been investigated fairly well.

The intrinsic disadvantage of the synthesis of tetrasubstituted phthalocyanines and trisubstituted subphthalocyanines is the isomeric mixture formation. Many chemists working in the field of phthalocyanines chemistry have been dealing with the

particularly challenging task of single isomer synthesis. Although many attempts have been undertaken towards single isomer synthesis, this problem remains unsolved as yet.

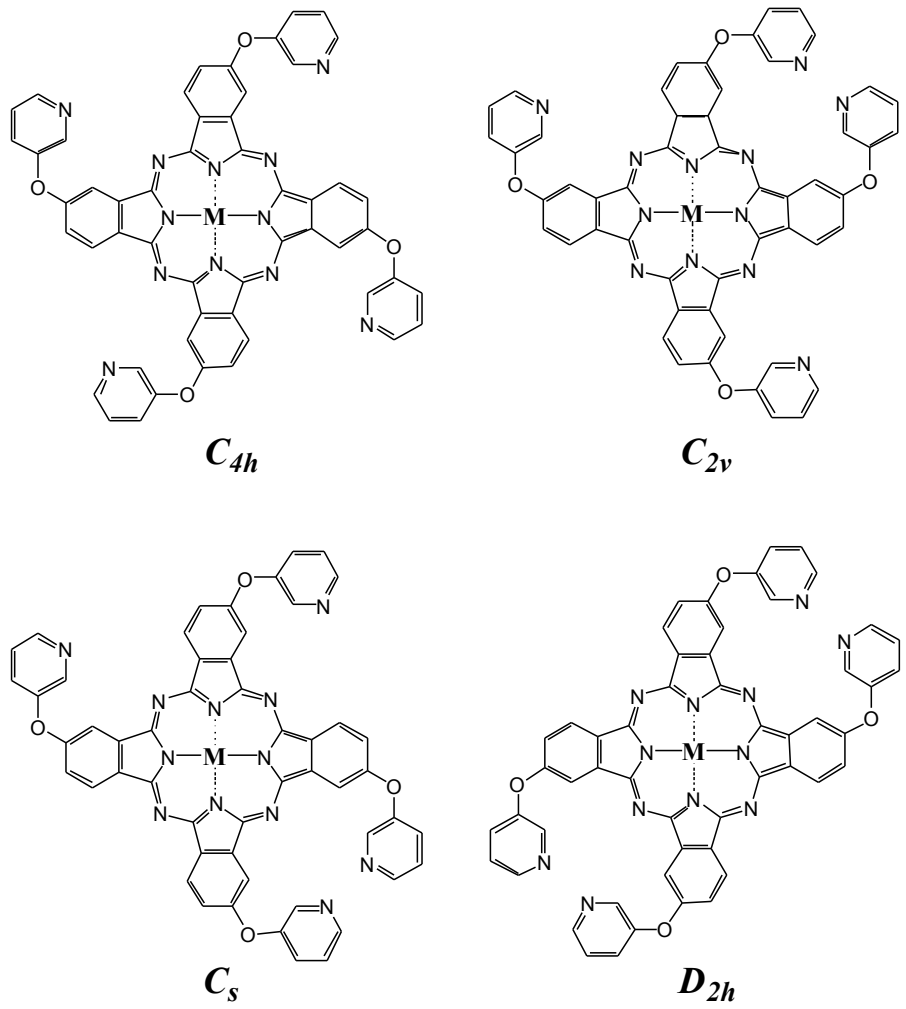

Figure 2.1. The four constitutional isomers possible for a tetrasubstituted phthalocyanine (M = metal).

The cyclotetramerization of monosubstituted precursors such as 4-(3-pyridyloxy)phthalonitrile or 5-(3-pyridyloxy)-1,3-diiminoisoindoline inevitably leads to a mixture of four constitutional isomers with C_{4h}, C_{2v}, C_s and D_{2h} symmetry (Fig. 2.1). Using specially designed HPLC columns the group of Hanack succeeded in separating individual phthalocyanine isomers, however, with varying degree of success for different derivatives [19]. During these investigations particularly tedious and difficult task of separating the reaction mixture for individual isomers has been omitted, as an isomeric mixture seems to be not less suitable for the photocatalytic application than a single isomer.

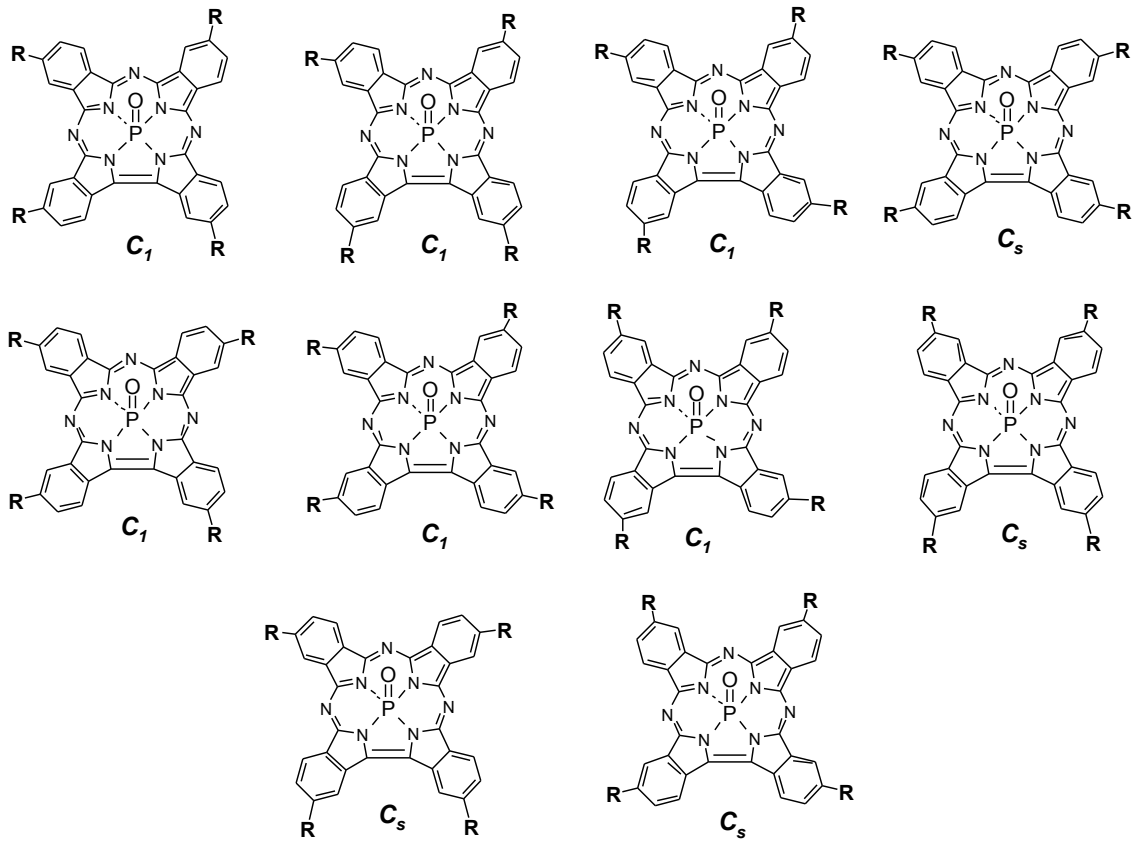

Figure 2.2. The ten regioisomers of triazatetrabenzcorroles possibly formed as a result of phosphorus insertion and ring contraction of tetrasubstituted meta-free phthalocyanines.

The utilization of tetrasubstituted metal-free phthalocyanines for the synthesis of triazatetrabenzcorroles gives consequently a mixture of ten different regioisomers that belong to the C_1 and C_s point group (Fig. 2.2). These isomers were not separated for individual components but used as such.

The utilization of monosubstituted phthalodinitrile precursors during subphthalocyanines synthesis results inevitably in a mixture of two regioisomers that belong to the C_1 and C_3 point group (Fig. 2.3). Moreover, each of these constitutional isomers is in turn a racemic mixture of enantiomers. These isomers have been successfully resolved for the first time by preparative HPLC by the group of Hanack *et al.* and later by the group of Torres [20].

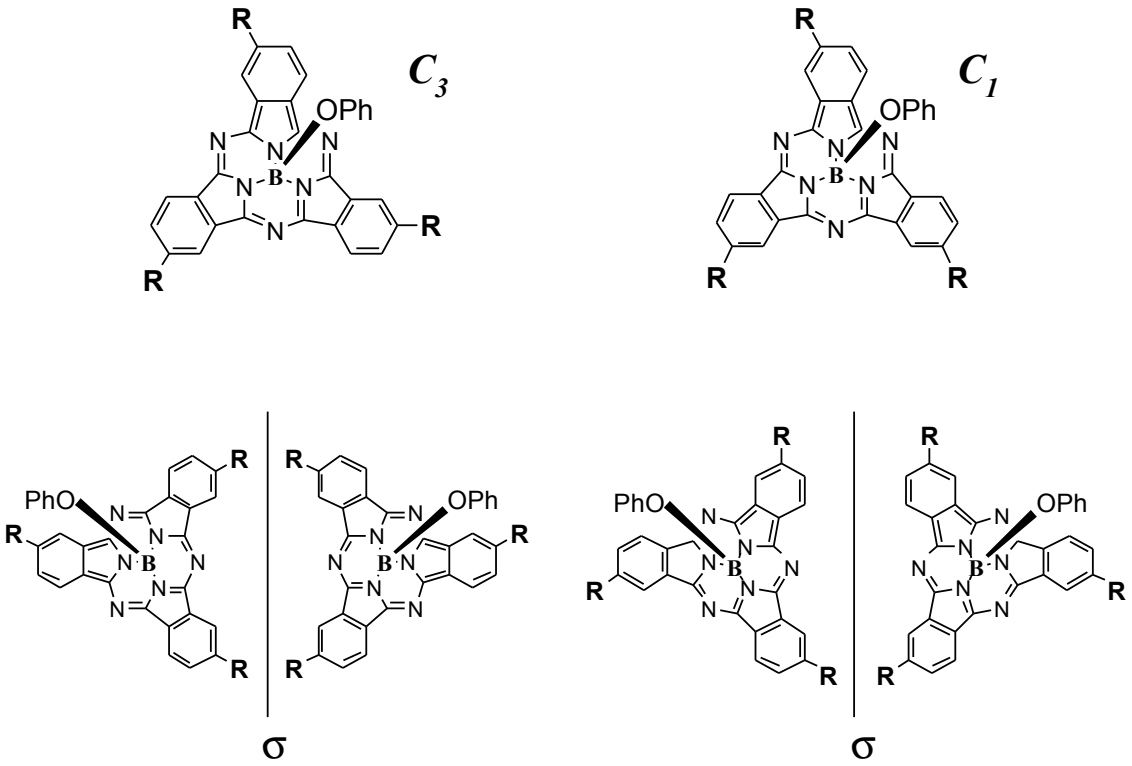

Figure 2.3. Regio- and enantiomers possible for the trisubstituted subphthalocyanine.

2.2 Synthesis of precursors

A multitude of differently substituted 1,2-disubstituted benzene derivatives can act as a useful precursors for phthalocyanines synthesis and these include phthalic acids, phthalic acid anhydrides, phthalonitriles, phthalimides, diiminoisoindolines and *o*-cyanobenzamides. By far the most versatile precursors are phthalonitriles and diiminoisoindolines. In this work derivatives of these two classes of compounds were chosen as starting materials during preparation of water-soluble phthalocyanines and subphthalocyanines. Following precursor compounds were prepared:

4-(Pyridyloxy)phthalonitrile (**3**). NO_2 is an excellent living group for nucleophilic aromatic substitution reactions. A plenty of nucleophiles can by introduced by this reaction, *e.g.* alcohols, thiols or amines.

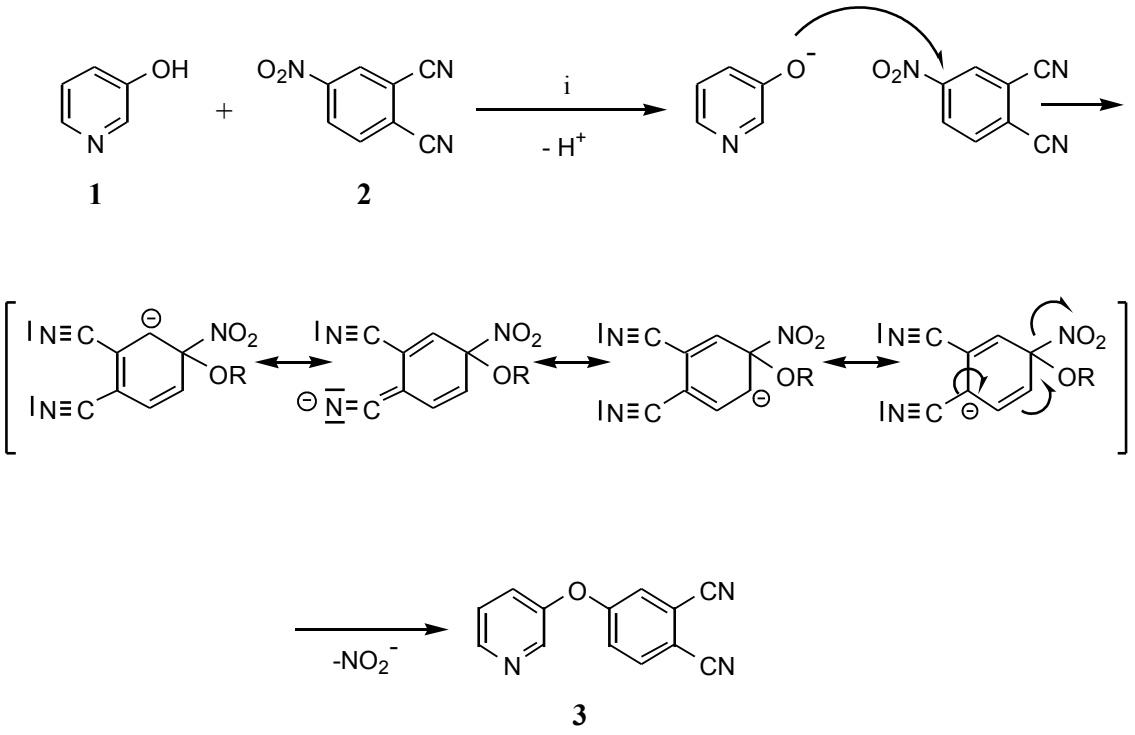

Figure 2.4. Synthesis of 4-pyridyloxyphthalonitrile (**3**) via nucleophilic aromatic substitution. Condition: (i) DMSO, K_2CO_3, N_2, RT, 5 days (80%).

Taking advantage of this reaction a very useful precursor for the synthesis of zwitterionic and positively charged photosensitizers was prepared according to the procedure described elsewhere [13,21]. Commercially available 4-nitrophthalonitrile was reacted with 3-hydroxypyridine in DMSO using potassium carbonate as a base [13,21]. The reaction mixture was stirred for five days at room temperature and the high purity product was finally isolated in a good 80 % yield. The IR spectrum confirmed the presence of CN group showing sharp, narrow band at 2228 cm^{-1} and the aromatic ether group characteristic vibrations appeared at 1280 and 1253 cm^{-1}. The EI-MS spectrum showed a molecular ion peak at *m/z* 221$[M]^+$ and two fragmentation ions peaks at *m/z* 127$[M\text{-}C_5H_4NO^-]^+$ and at *m/z* 78$[C_5H_4N]^+$.

5-(Pyridyloxy)-1,3-diiminoisoindoline (**4**). Diiminoisoindoline **4** was formed from the phthalonitrile **3** by reacting it with ammonia gas in the presence of sodium methoxide in methanol (Fig.2.4) according to [21]. The product could not be purified by column chromatography. Hence, after solvent removal and drying under vacuum, the highly hygroscopic product was used as such in the next step. The reaction mixture soon after initiation turned slightly greenish. This observation is consistent with the fact that

diiminoisoindolines display increased tendency towards cyclization and readily react to form phthalocyanines even at very mild conditions. The EI-MS spectrum showed intensive molecular ion peak at *m/z* 238 $[M]^+$ along with a peak at *m/z* 444 which may indicate the presence of diiminoisoindoline dimmer fragmentation ion, *i.e.* $[2M\text{-}NH]^+$. Diiminoisoindoline **4** proved to be excellent precursor for the synthesis of silicon and germanium water-soluble phthalocyanines.

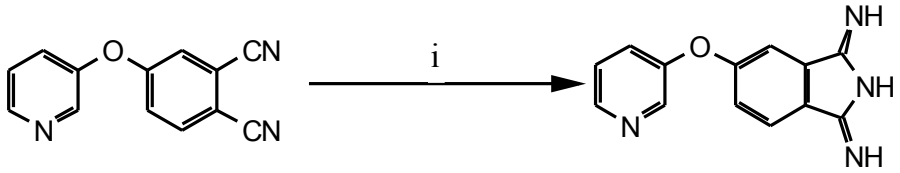

3 **4**

Figure 2.5. Synthesis of 5-(3-pyridyloxy)-1,3-diiminoisoindoline (**4**). Condition: (i) MeOH, MeONa, NH_3, 110°C, 4 h.

4-Iodophthalonitrile (**6**). Commercially available 4-aminophthalonitrile was utilized to prepare 4-iodophthalonitrile - an important precursor for the subphthalocyanines preparation. The amino group in 4-aminophthalonitrile can be readily used to append other functional groups to the phthalonitrile molecule. The diazotization of the 4-aminophthalonitrile was accomplished using traditional reaction conditions by treating the 4-aminophthalonitrile with sodium nitrite in aqueous acidic media [22]. The diazonium salt was used to add iodide to the molecule. This was achieved by reacting the diazonium salt with potassium iodide in water. Care must be taken to keep the reaction mixture at low temperature to avoid decomposition of the diazonium salt to 4-hydroxy substituted derivative. After column chromatography the product was isolated in a reasonable 56 % yield.

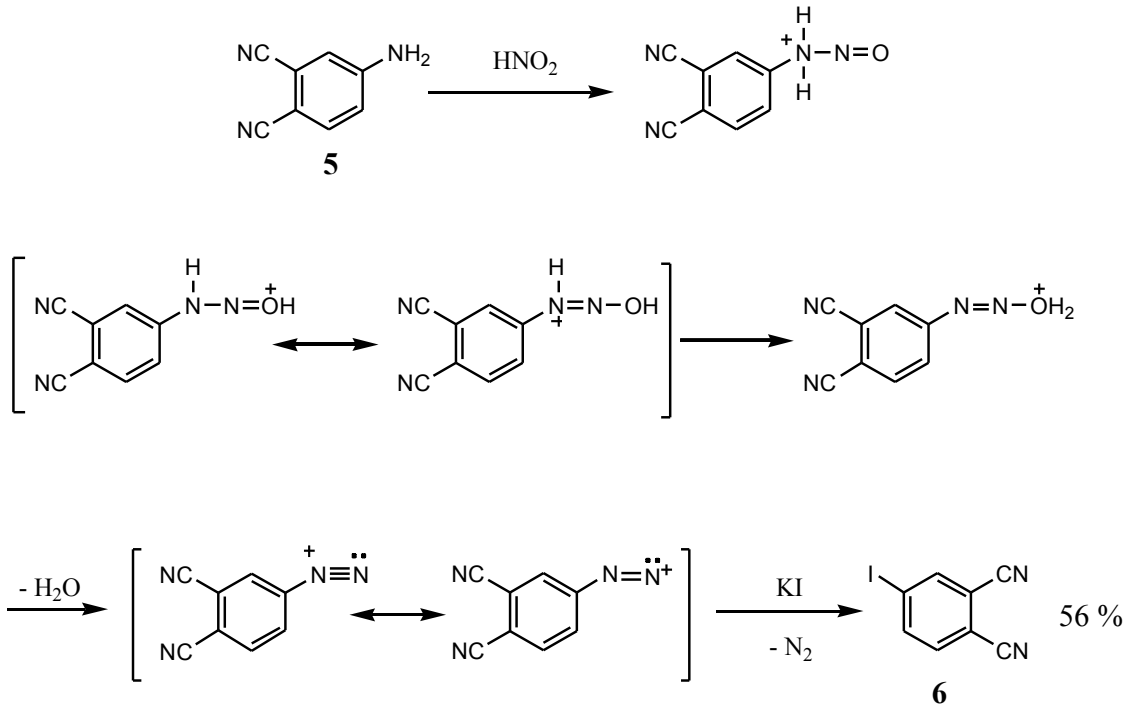

Figure 2.6. Synthesis of 4-iodophthalonitrile (**6**).

4-[2-(2-pyridinyl)ethyl]phthalonitrile (**9**). This phthalonitrile was proposed as a starting material for alkyl-substituted water-soluble subphthalocyanine **39**. Compound **9** was obtained in a two-step reaction; *i.e.* palladium-catalyzed coupling followed by hydrogenation of the triple bound (Fig. 2.7). The Sonogashira cross-coupling of commercially available terminal alkyne **7** with 4-iodophthalonitrile (**6**) involved palladium catalyst $PdCl_2(PPh_3)_2$ and CuI as a co-catalyst. Triethyamine as an organic base was added along with DMSO to enhance the solubility of reactants. Purification by column chromatography and subsequent crystallization furnished compound **8** in a 79 % yield. Mass spectrum unambiguously corroborates the identity of product; molecular ion peak found at *m/z* 229$[M]^+$. Furthermore, a very sharp band at 2218 cm^{-1} appeared in the IR spectrum clearly indicating presence of the carbon-carbon triple bond.

Catalytic hydrogenation of **8** with hydrogen over Pd on charcoal gave alkylated phthalonitrile **9** in good 71 % yield (Fig. 2.7). The identification of phthalonitrile **9** is based on ^{1}H-NMR data. Unlike the alkynylated phthalonitrile **8**, the new precursor displays two multiplets characteristic of alkyl protons. Moreover, the sharp signal at 2218 (C ≡ C) cm^{-1} observed in **8** disappeared and new bands could be observed at 2957, 2926 and 2863 cm^{-1}, respectively, indicating presence of alkyl chain.

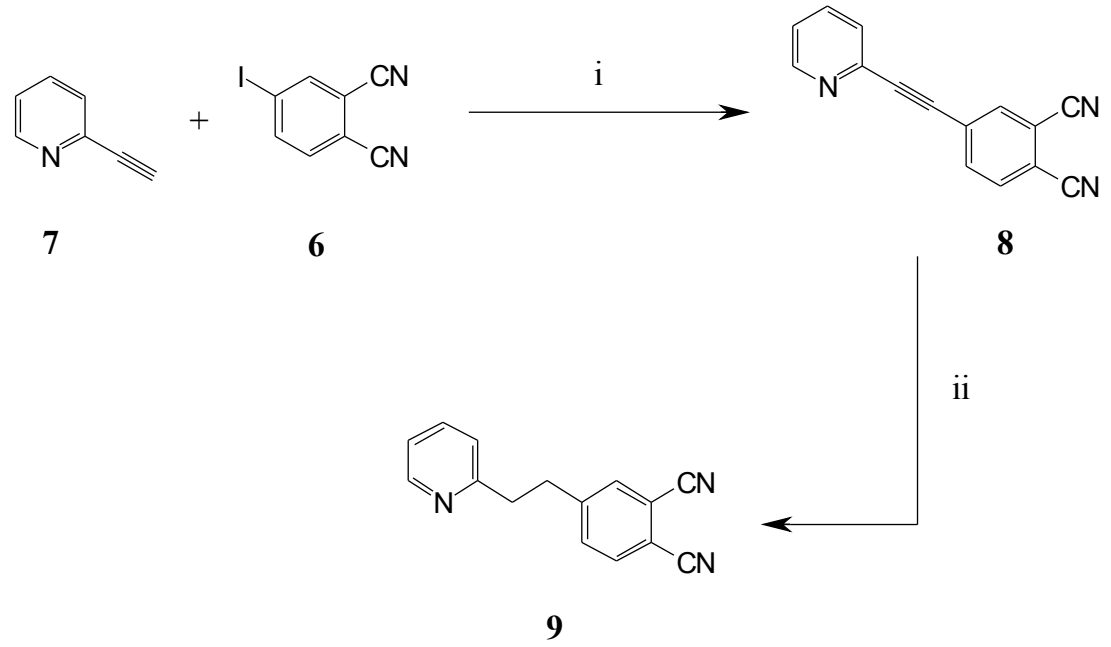

7 **6** **8** **9**

Figure 2.7. Synthesis of phthalonitrile **9** via palladium-catalyzed coupling followed by hydrogenation of the triple bound. Conditions: (i) $PdCl_2(PPh_3)_2$, NEt_3/DMSO, CuI, RT, 12 h, N_2 (79%), (ii) AcCN, RT, 2 h, Pd/C, H_2 (71%).

2.3 Synthesis of water-soluble phthalocyanines

2.3.1 Synthesis of positively charged and zwitterionic metal-free, silicon and germanium phthalocyanines

The positively charged **11** and zwitterionic **12** water-soluble phthalocyanines were prepared by a three-step procedure according to the procedure described by Wöhrle et al. [13]. The reaction of phthalonitrile **3**, the synthesis of which has been already described in chapter 2.2, with lithium in 1-pentanol at elevated temperature (140°C) afforded metal-free phthalocyanine **10** in a yield of 57 % [13]. The reaction is straightforward and starts immediately after the lithium is added to the pentanolate solution of phthalonitrile **3** (Fig. 2.8). The lithium was removed by acidic work-up and then the compound was purified by column chromatography. The compound **10** exhibits the typical UV-Vis spectrum of the metal-free phthalocyanine (recorded in DMF) that is

two strong absorptions in the visible region, one at 696 nm and the other one at 665 nm. The DCI-MS spectrum of phthalocyanine **10** shows peak at *m/z* 887 $[M+H^+]^+$. The analysis of compound **10** was also supported by IR spectrum. A high intensity stretching band was observed at ν = 1229 cm^{-1}. The band is characteristic of aromatic ether functionality Ar-O-Ar and was present in the IR spectra of all the compounds with 3-pyridyloxy substituent appended to the macrocycle as well as in the IR spectra of their water-soluble derivatives. The phthalocyanine **10** is characterized by good solubility in a very broad range of organic solvents, *i.e.* pyridine, methanol, CH_2Cl_2, DMF and many others.

The quaternization of 3-pyridyloxy groups in metal-free phthalocyanine **10** with methyl iodide or 1,3-propanesultone is a very straightforward reaction. The reaction of **10** with an excess of methyl iodide in DMF furnished an excellent water-soluble positively charged compound **11** in 98 % yield (Fig. 2.8). When the metal-free phthalocyanine was quaternized with an excess of 1,3-propanesultone the zwitterionic derivative **12** was obtained in 97 % yield (Fig. 2.8). In contrast to the positively charged phthalocyanine **11**, compound **12** was hardly soluble in water (see chapter 4.2 and Fig. 4.1). The UV-Vis spectra of **11** and **12** are presented in chapter 4.4 (Fig. 4.5).

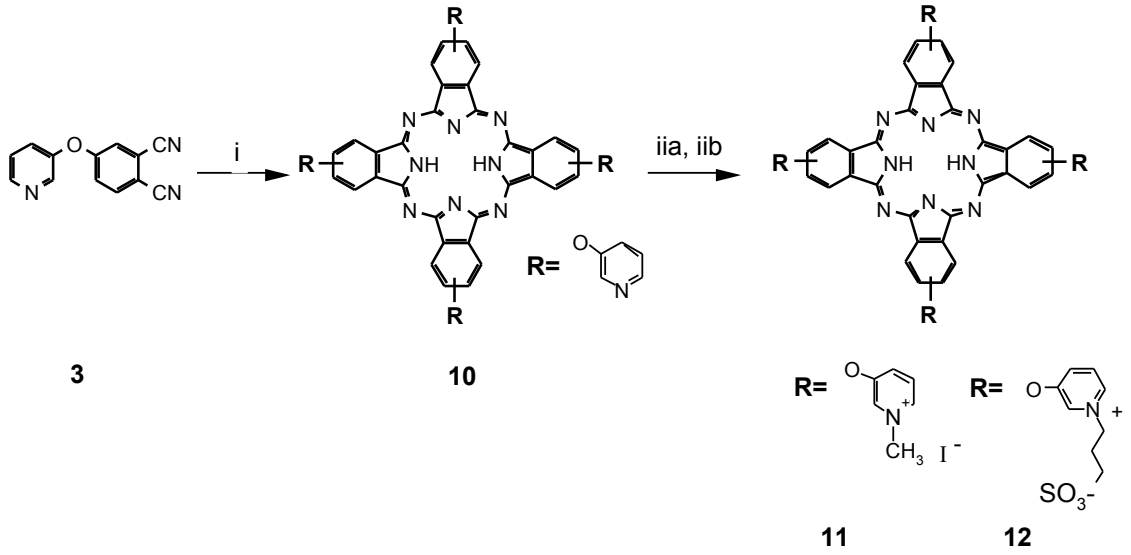

Figure 2.8. Synthesis of positively charged **11** and zwitterionic **12** metal-free phthalocyanine. Conditions: (i) Li, 1-pentanol, 140°C, 2 h, (ii) CH_3COOH, H_2O (57%), (iii) DMF, CH_3I, N_2, 50°C, 17 h (98%), (iv) DMF, 1,3-propanesultone, N_2, 50°C, 17 h (97%).

The reaction of metal-free phthalocyanine **10** with $SiCl_4$ in anhydrous pyridine, DMF or quinoline at elevated temperature (from 60°C to 180°C) did not yield silicon phthalocyanine **13**; instead the starting material was recovered. In 1997 Aoudia *et al.* reported a successful synthesis of a series of silicon-centered octabutoxyphthalocyanines *via* $HSiCl_3$ insertion into the metal-free phthalocyanine framework [22]. Thus, to a mixture of tributylamine, toluene and metal-free phthalocyanine **10** an excess of $HSiCl_3$ was added. The reaction mixture was stirred for 24 h. However, this method proved to be unreliable for the synthesis of Pc **13** as well. As judged by TLC only traces of the desired product could be detected in the reaction mixture. The method reported by Aoudia *et al.* was patterned after the unprecedented procedure developed by Kane and Lemke for the synthesis of (porphyrinato)silicon (IV) complexes [23]. In this latter route, the reaction requires conversion of the metal-free phthalocyanine into the dilithiophthalocyanine followed by the insertion of $HSiCl_3$ into the phthalocyanine core. Thus, dilithio salt was generated from metal-free phthalocyanine **10** and $LiN(SiMe_3)_2$ in THF at 60°C. After removal of solvent and $HN(SiMe_3)_2$ under vacuum, the anhydrous CH_2Cl_2 and $HSiCl_3$ was added at –78°C. The reaction mixture was stirred until reached room temperature. Surprisingly, only the starting material was recovered from the reaction mixture. Since, neither the insertion of $SiCl_4$ or $HSiCl_3$ into metal-free phthalocyanine **10** nor the insertion of $HSiCl_3$ into the alkali metal salt of phthalocyanine **10** gives good results, the “classical” method was tried out. By far the most widely applied rout to the silicon phthalocyanines is the cyclotetramerization of the precursor, often diiminoisoindoline, in the presence of tetrachlorosilane in dry quinoline [1].

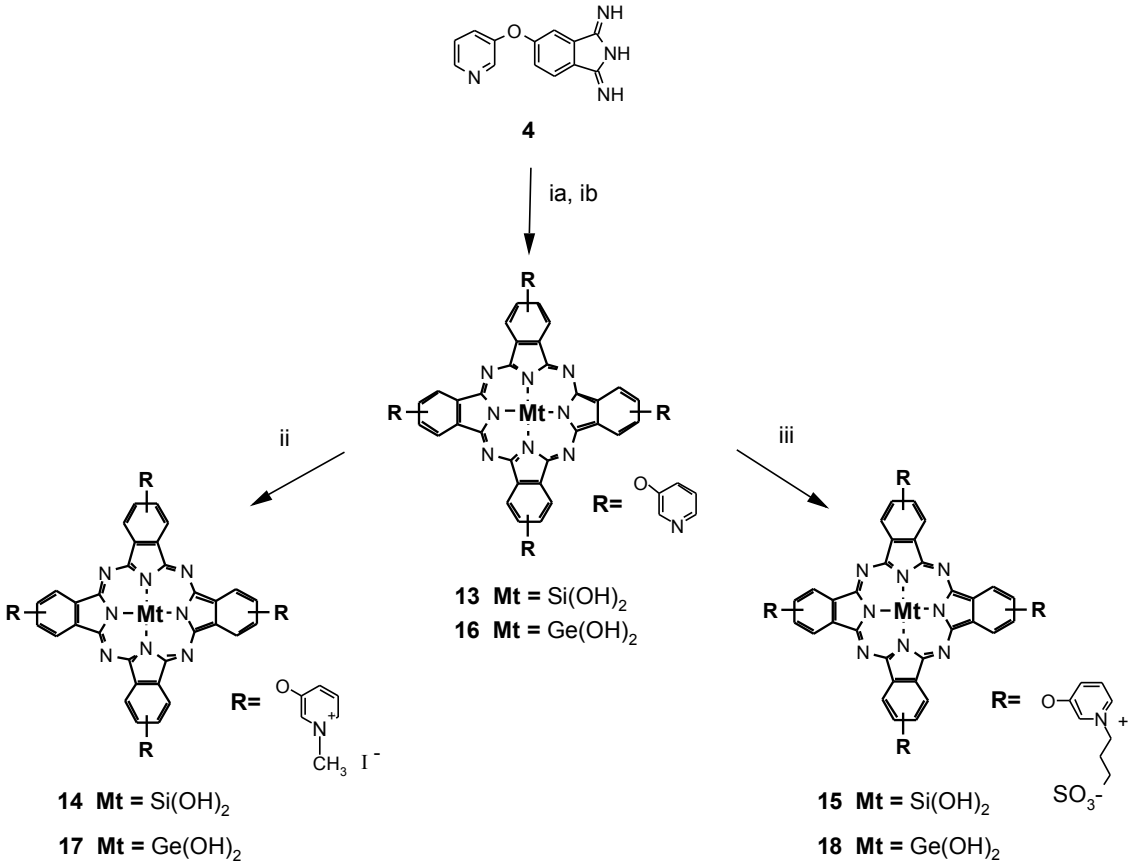

Figure 2.9. Synthesis of water-soluble silicon (**14**, **15**) and germanium (**17**, **18**) phthalocyanines. Conditions: (ia) $SiCl_4$, quinoline, 200°C, 1 h, then NH_4OH, H_2O (54% for **13**), (ib) $GeCl_4$, quinoline, 200°C, 2 h, then NH_4OH, H_2O (77% for **16**), (ii) CH_3I, DMF, 50°C, 17 h (83% for **14**, 88% for **17**), (iii) 1,3-propanesultone, DMF, 50°C, 17 h (64% for **15**, 81% for **18**).

Hence, the phthalonitrile **3** was reacted with $SiCl_4$ in anhydrous, freshly distilled quinoline at 200°C for 1 h (Fig. 2.9). The formation of silicon phthalocyanine **13** proceeds quickly and gives the product in 54 % yield. The chlorine atoms exchange was achieved by refluxing the reaction mixture with ammonia hydroxide overnight. The electrospray mass spectrum showed molecular ion peak at *m/z* 946 [M^-]. At the last step silicon phthalocyanine **13** was converted into the positively charged, water-soluble derivative **14**. The reaction requires stirring of phthalocyanine **13** with an excess of methyl iodide in DMF (Fig. 2.9). Water-soluble phthalocyanine was isolated in 83 % yield. In order to obtain zwitterionic derivative, phthalocyanine **13** was reacted with an excess of 1,3-propanesultone in DMF to give water-soluble compound **15** in 64 % yield.

Under the same reaction conditions as for the synthesis of water-soluble silicon phthalocyanines, the germanium water-soluble complexes were obtained in good yields. An endeavour to insert $GeCl_4$ into metal free phthalocyanine **10** according to the procedure reported by others has failed [24]. Hence, phthalonitrile **3** was reacted with $GeCl_4$ in anhydrous, freshly distilled quinoline at 200°C for 2 h (Fig.2.9). The chlorine atoms exchange has been achieved by refluxing the reaction mixture with ammonia hydroxide overnight. After the column chromatography the germanium phthalocyanine **16** was obtained in 77 % yield. In the ESI-MS spectrum of **16** a peak of ion resulted from loss of one molecule of water was found at *m/z* 974 $[M\text{-}H_2O]^+$. The calculated mass peak pattern is in good agreement with the observed results, taking into account the isotopic natural abundance of $^{70,\ 72,\ 73,\ 74,\ 76}Ge$. The quaternization of germanium phthalocyanine **16** with an excess of methyl iodide and 1,3-propanesultone gives two water-soluble germanium phthalocyanines, *i.e.* positively charged **17** and zwitterionic **18**, in reasonable yields (Fig. 2.9).

The intense bands at 1237-1278 cm^{-1} were seen in the IR spectra of silicon and germanium phthalocyanines **13**-**18** due to the presence of aromatic ether bonds (Ar-O-Ar). Besides, due to the presence of SO_3 group, zwitterionic phthalocyanines SiPcOPPS **15** and GePcOPPS **18** exhibit strong absorptions at 1208-1190 cm^{-1} (ν_{as}, SO_2) and 1089-1079 cm^{-1} (ν_{sym}, SO_2). The UV-Vis spectra of water-soluble phthalocyanines **14**, **15**, **17** and **18** are presented in chapter 4.4 (Fig. 4.7 and 4.8).

2.3.2 Synthesis of sulfonated metal-free, silicon and germanium phthalocyanines

The water-soluble metal-free tetrasulfophthalocyanines (**20**) has been obtained [36]. The reaction was simple achieved reacting magnesium acetate tetrahydrate with sodium 4-sulfophthalate (**19**), urea and ammonium chloride according to the well-known method reported by Weber and Busch [2]. The magnesium was easily removed from the phthalocyanine by acidic work-up. The metal-free phthalocyanine H_2PcTS **20** was obtained in 5 % yield (Fig. 2.10). The ESI-MS spectrum of **20** is described in subchapter 3.6 and the UV-Vis spectrum in subchapter 4.4 (Fig. 4.3).

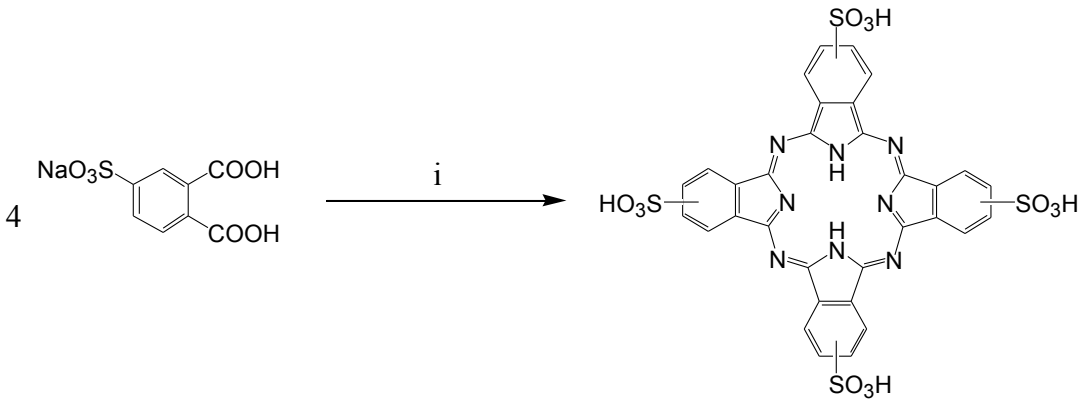

Figure 2.10. Synthesis of metal-free tetrasulfophthalocyanines H_2PcTS **20**. Conditions: (i) $Mg(CH_3COO)_2$, urea, NH_4Cl, 200°C, 16 h (5%).

An attempt to prepare silicon and germanium sulfophthalocyanine has been made during this work. Both compounds have been already reported in chemical literature, however, the procedures described therein lack many important details especially as to isolation and purification of the products [25]. Hence, the synthesis of silicon and germanium sulfophthalocyanines was thoroughly reinvestigated and new, detailed synthesis methods were proposed.

Innitialy the classical template cyclotetramerization of 4-sulfophthalic acid was tried out. Thus, silicon tetraacetate $Si(CH_3COO)_4$ was reacted with 4-sulfophthalic acid and ammonium chloride in melted urea at 200°C. The reaction did not give any traces of silicon tetrasulfophthalocyanine. Moreover, the reaction of metal-free tetrasulfophthalocyanine **20** and $Si(CH_3COO)_4$ did not allow to insert silicon into the phthalocyanine. Taking into account these two failures, it was decided to follow the method already reported in literature, *i.e.* sulfonation of the unsubstituted silicon phthalocyanine with oleum [25]. The first step was to prepare the unsubstituted silicon phthalocyanine.

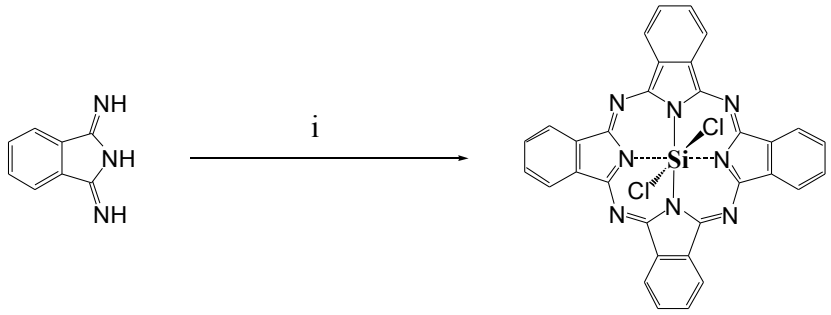

21 **22**

Figure 2.11. Synthesis of unsubstituted silicon phthalocyanine **22**. Conditions: (i) $SiCl_4$, quinoline, N_2, 200°C, 1 h.

The unsubstituted dichlorosilicon phthalocyanine **22** was prepared and characterized as early as in 1962 [26]. A modification of this method was applied during this work. A commercially available 1,3-diiminoisoidoline (**21**) was reacted with $SiCl_4$ in dry quinoline at 200°C for one hour (Fig. 2.11). Due to lack of solubility of **22**, none of the traditional methods used in laboratories could be applied to purify the product. Hence, the resulting phthalocyanine **22** was filtered off and washed with a variety of solvents to remove soluble impurities at least. Certainly, this method is insufficient as it leaves other insoluble impurities behind. It should be mentioned that during this work, the often cited method, *i.e.* dissolution in concentrated sulphuric acid, followed by precipitation in cold water, did not give better results with regard to purity of **22**.

Initially, the procedure described elsewhere, that is sulfonation of the parent phthalocyanine with oleum, was followed [25]. A sample of unsubstituted silicon phthalocyanine was treated with oleum (concentrated sulphuric acid containing 30 % of SO_3) at 75°C for 4 hours (Fig. 2.12). Surprisingly, no SiPcTS **25** was detected in the reaction mixture. Unexpectedly, during purification of the reaction mixture light green, water-soluble product was isolated. The UV-Vis spectrum of the unexpected product (in water) displayed a very sharp Soret band at 452 nm and a Q-band at 670 nm with intensity ca. half that of the Soret band (Fig. 2.13).

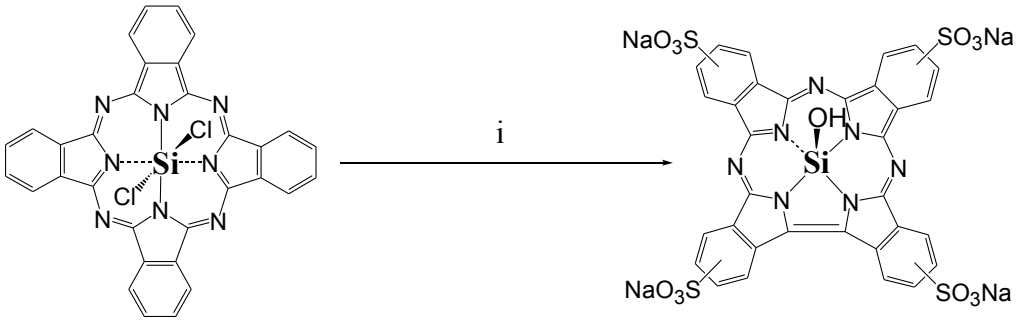

22 **23**

Figure 2.12. Treatment of $SiCl_2Pc$ **22** with oleum at 75°C gives Si(tbc)TS **23**. Conditions: (i) H_2SO_4 (30% SO_3), 75°C, 4 h, than NaOH, H_2O (10%).

The spectrum closely resembles that of the hydroxysilicon triazatetrabenzcorrole - the compound reported by Hanack *et al*. - and found to be the contracted phthalocyanine with one *meso*-nitrogen missing in the macrocycle framework [27]. Apparently, the dichlorosilicon phthalocyanine (**22**) was not only sulfonated but also underwent reduction to hydroxysilicon sulfotriazatetrabenzcorrole (**23**) during reaction. The mechanism of the ring contraction and formation of triazatetrabenzcorrole remains unknown and needs further investigations. The new compound **23** is stable both as a solid and in a solution.

The resulting reaction mixture was separated on RP-18 column with water as eluent. Besides obtaining ring-contracted compound **23**, a blue band was isolated as well. The blue fraction exhibits broad absorption band at 641 nm (Fig. 2.13). It closely resembles the UV-Vis spectrum of oligomeric silicon sulfophthalocyanine [28]. The concentrated sulphuric acid is a known dehydrating agent and obviously causes condensation of the silicon phthalocyanine into the oligomeric silicon sulfophthalocyanine with μ-oxo bridges.

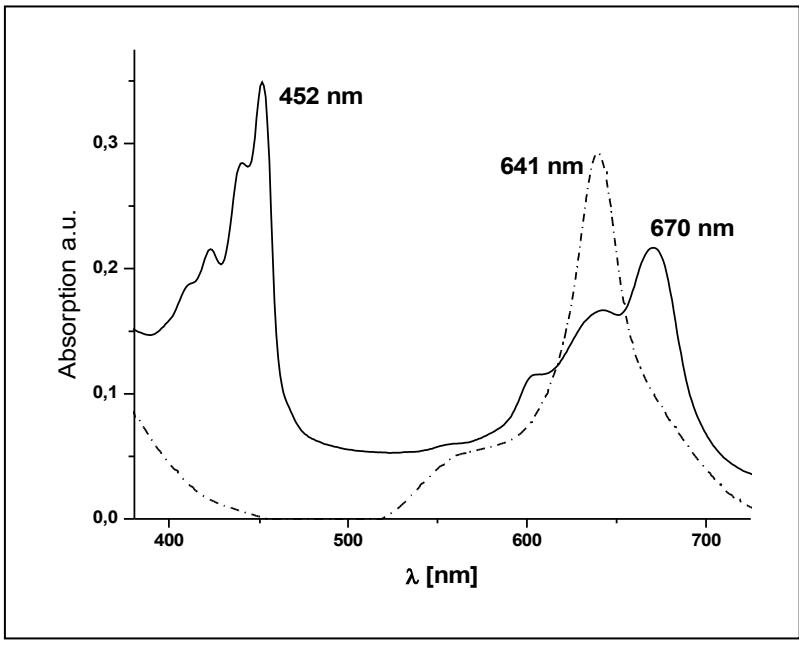

Figure 2.13. UV-Vis spectrum (in water) of green (regular trace) and blue (dashed trace) fraction isolated after sulfonation of the silicon phthalocyanine **22** with oleum.

Since sulfonation of the unsubstituted silicon phthalocyanine**22** with oleum did not yield the desired product, another approach was applied, *i.e.* chlorosulfonation followed by hydrolysis of the product. The reaction of silicon phthalocyanine **22** with chlorosulfonic acid conducted for 6 h, and then with thionyl chloride for 4 h yielded sulfochloride-substituted derivative **24** (Fig. 2.14). Chlorosulfonated silicon phthalocyanine **24** exhibits rather poor solubility in common organic solvents; hence, only simple washing with water, ethanol and acetone of the precipitated product was carried out. Chlorosulfonated silicon phthalocyanine **24** is disaggregated in DMF solution and exhibits Q-band at 674 nm along with Soret band at 356 nm. In the IR spectrum of chlorosulfonated silicon phthalocyanine **24** the very intense absorption band corresponding to the SO_2 vibrations appeared at 1172 cm^{-1} (S=O, ν_{as}). No satisfactory mass spectrum could be obtained for **24**.

The last part of the synthesis was hydrolysis of the chlorosulfonic groups in the **24**. Initially, the method reported by Gürek *et al*. [28] was followed. A sample of compound **24** was refluxed in a mixture of water and methanol (5:1). The UV-Vis spectrum of the reaction mixture showed intense band at 636 nm along with two other less intense bands at 658 nm and 671 nm. In the aforementioned publication, the authors claimed that the broad band at 630 nm could be attributed to the dimmers formation in solution. During

earlier investigations made in our laboratory, it was established that the dihydroxysilicon sulfophthalocyanine exists in an aqueous solution in a fully monomeric state [25]. The UV-Vis spectrum of this compound recorded in water solution exhibits intense, regular shape Q-band at 671 nm (see chapter 4.4).

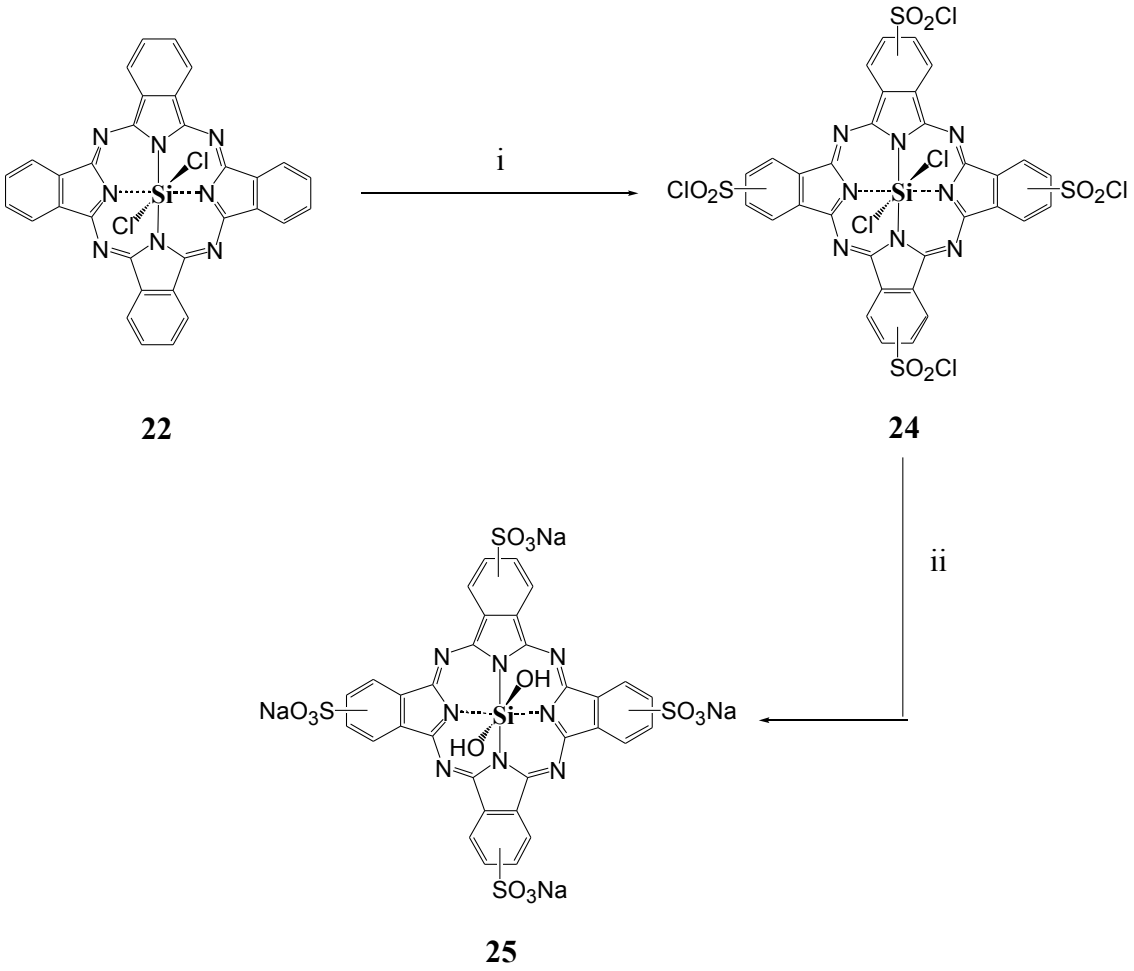

Figure 2.14. Synthesis of sulfonated silicon phthalocyanine **25**. Conditions: (i) $HClSO_3$, 130°C, 6 h, then $SOCl_2$, 85°C, 4 h (66%), (ii) H_2O, NaOH, pH < 10 (49%).

On the basis of these facts it can be rather concluded that these reaction conditions cause not only hydrolysis of the chlorosulfonic groups but also partial oligomerization of the silicon phthalocyanine. The broad band at 636 nm observed during the reaction closely resembles that observed for the oligomeric silicon sulfophthalocyanine with μ-oxo bridges [28]. In order to avoid the oligomerization side-reaction, it was decided to conduct the hydrolysis in water solution of NaOH (Fig. 214). During all reaction the pH was held below 10 to avoid fast decomposition of the SiPcTS **25**, which is known to be

unstable at higher pH [25]. UV-Vis spectrum of the reaction mixture diluted with water showed only one single narrow absorption band at 673 nm (ε = 82 000 $M^{-1}cm^{-1}$) (Fig. 4.3). The IR analysis showed the characteristic absorption bands corresponding to the SO_2 vibrations: 1194 (S=O, ν_{as}) cm^{-1} and 1035 (S=O, ν_{sym}) cm^{-1}.

The unsubstituted dihydroxygermanium phthalocyanine **26** was prepared and characterized for the first time in 1960 [29]. A modification of the published method was used during this work. As in the case of $SiCl_2Pc$ **22** a commercially available 1,3-diiminoisoindoline **21** was reacted with $GeCl_4$ in freshly distilled quinoline at 200°C for 2 hours (Fig. 2.15). The replacement of two chlorine atoms in **26** by hydroxy groups was achieved by adding ammonia solution to the reaction mixture. Due to lack of solubility of **26**, the compound was filtered off and used as such in the next step. The characterization of **26** was supported with ESI-MS. A peak at *m/z* 603 was identified and attributed to a positively charged ion $[M - OH^-]^+$.

The synthetic pathway to sulfonated germanium phthalocyanine **28** used in this study is shown in Figure 2.15. Dihydroxygermanium phthalocyanine (**26**) was converted into the corresponding sulfochloride-substituted derivative **27** by reacting it with chlorosulfonic acid and thionly chloride under inert atmosphere. The compound **27** was obtained in 87 % yield. In the IR spectrum of germanium phthalocyanine **27** the very intense absorption bands corresponding to the SO_2 vibrations are observed at 1173 cm^{-1} (S=O, ν_{as}) and 1028 cm^{-1} (S=O, ν_{sym}). Germanium phthalocyanine **27** like silicon phthalocyanine **24** shows very good solubility in DMF. The UV-Vis spectrum of **27** recorded in this solvent shows Q-band at 679 nm (ε = 109 000 $M^{-1}cm^{-1}$) and Soret band at 358 nm (ε = 40 000 $M^{-1}cm^{-1}$) and exhibits no aggregation in solution. No satisfactory mass spectrum could be obtained for **27**.

At the last step compound **27** was hydrolyzed to the water-soluble sulfonated phthalocynine **28**. By far the best results were obtained when the germanium chlorosulfonated phthalocyanine **27** was treated with a mixture of water and pyridine for 3 h at 80°C and then for 15 min with diluted ammonia solution (Fig. 2.15). In this way the dihydroxygermanium sulfophthalocyanine (**28**) in the form of ammonium salt was obtained in 41 % yield. The UV-Vis spectrum recorded in aqueous solution consists of regular shape Q-band at 680 nm (ε = 108 116 $M^{-1}cm^{-1}$) with no additional shoulders (see chapter 4.4 and Fig. 4.3 herein).

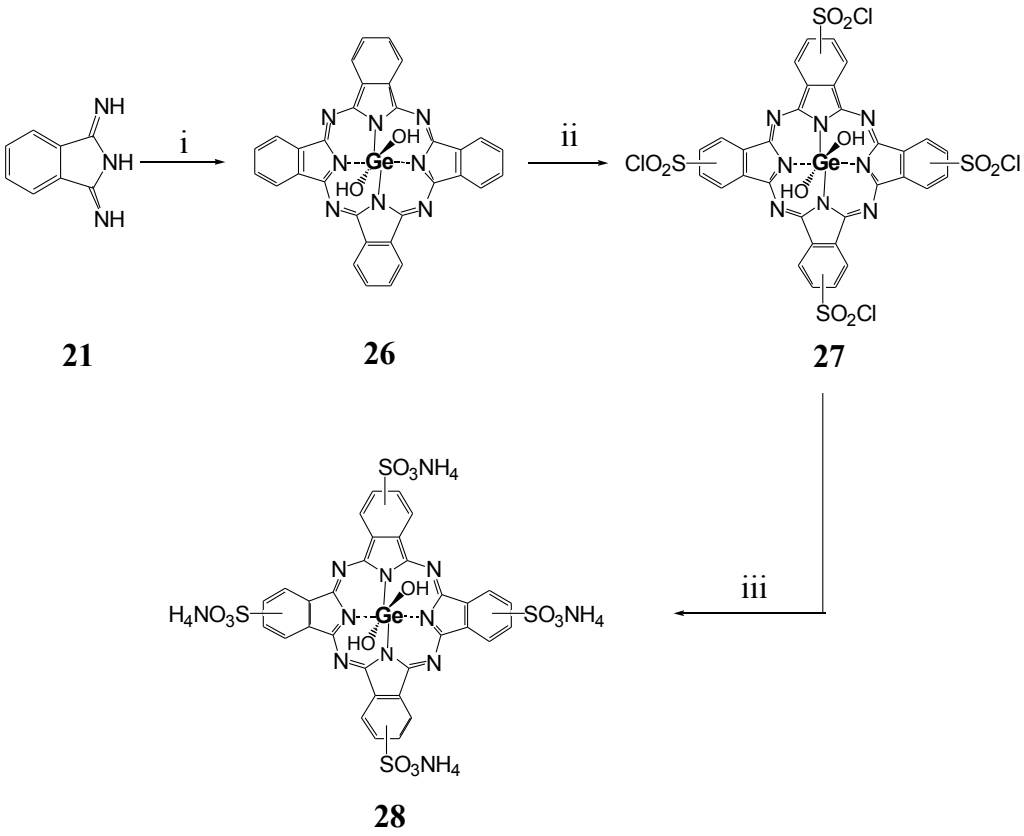

21 **26** **27** **28**

Figure 2.15. Synthesis of GePcTS **28**. Conditions: (i) $GeCl_4$, quinoline, 200°C, N_2, 2 h, then NH_4OH, quinoline, 100°C, 12 h (ii) $HClSO_3$, 130°C, 6h, then $SOCl_2$, 85°C, 4 h (87%), (iii) Py, H_2O, 80°C, 3 h, then NH_4OH, H_2O, 15 min. (41%).

Interesting was the comparison of the sulfonation of $Ge(OH)_2Pc$ (**26**) with the results obtained during sulfonation of $SiCl_2Pc$ (**22**). In 1986 Fujiki *et al.* reported a new compound obtained by reducing $GeCl_2Pc$ with $NaBH_4$. The compound was identified as a tetrapyrrole macrocycle, namely hydroxygermanium(IV) triazatetrabenzcorrole [30]. Taking into account that the sulfonation of $SiCl_2Pc$ **22** resulted in the ring-contracted hydroxysilicon triazatetrabenzcorrole **23**, it was foreseen that the sulfonation of $Ge(OH)_2Pc$ **26** would give in all likelihood sulfonated hydroxygermanium(IV) triazatetrabenzcorrole. Somewhat surprisingly, sulfonation of $Ge(OH)_2Pc$ **26** gives exclusively sulfonated dihydroxygermanium phthalocyanine. Moreover, even if the reaction is conducted at 100°C for 24 h no traces of ring-contracted product can be found in the reaction mixture. Apparently, the macrocycle $Ge(OH)_2Pc$ **26** is less susceptible to reduction when compared to $SiCl_2Pc$ **22**. On the basis of the performed experiments it can be stated that both chlorosulfonation followed by hydrolysis and

direct sulfonation with oleum of the unsubstituted dihydroxygermanium phthalocyanine (**26**) are suitable methods of obtainig water-soluble germanium sulfophthalocyanine **28**.

2.4 Synthesis of water-soluble oxophosphorus (V) triazatetrabenzcorroles

The reaction of PCl_3 with a metal-free phthalocyanine **10** in pyridine afforded the oxophosphorus(V) triazatetrabenzcorrole **29**. The product after two-time column chromatography on silica gel was obtained in a very good yield of 96 % (Fig. 2.17). The metal-free phthalocyanine seems to be immensely reactive with the pyridine/PCl_3 intermediate as the reaction initiates already at room temperature instantly after the PCl_3 is added.

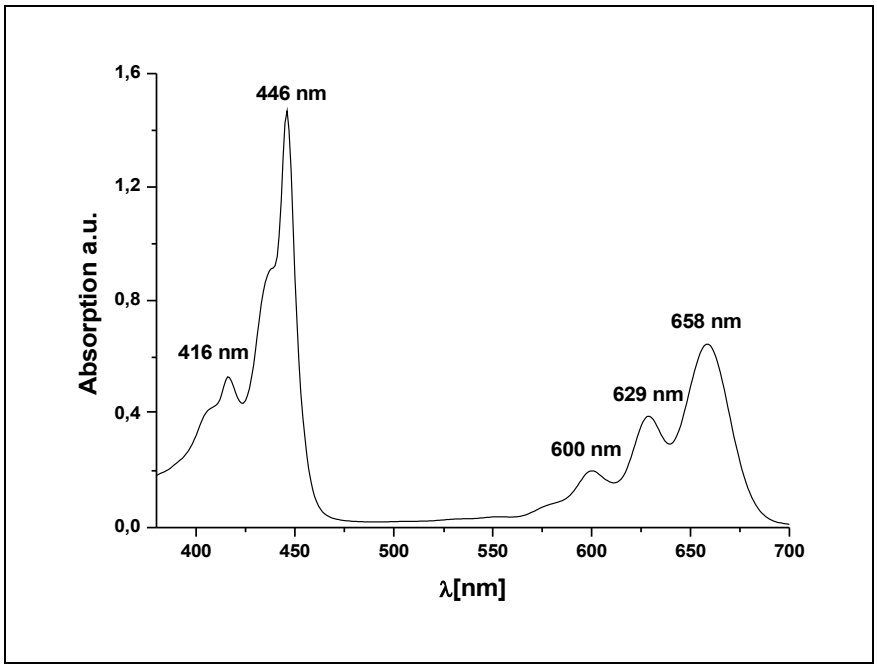

Figure 2.16. UV-Vis spectrum of oxophosphorus(V) triazatetrabenzcorrole **29** in DMF solution.

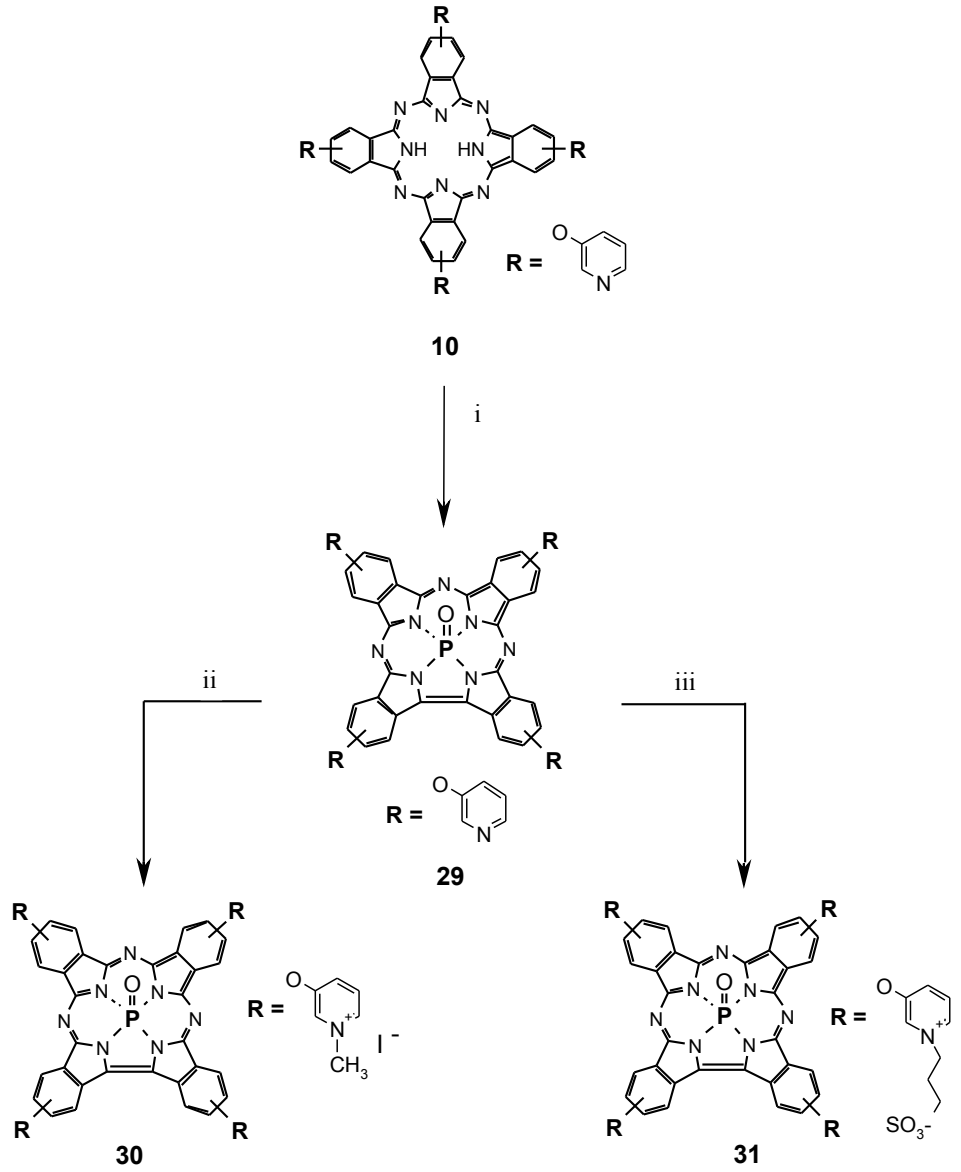

Figure 2.17. Synthesis of water-soluble oxophosphorus(V) triazatetrabenzcorroles **30** and **31**. Conditions: (i) Py, PCl_3, 120°C, N_2, 1.5 h (96%), (ii) DMF, CH_3I, 14 h, N_2, 50°C (93%), (iii) DMF, 1,3-propanesultone, 17 h, N_2, 50°C (78%).

The solution turns greenish, the previously observed split Q band at λ_{max} 668 nm and λ_{max} 698 nm disappears and new intense bands emerge in the visible region. Figure 2.16 shows the UV-Vis spectrum of oxophosphorus(V) triazatetrabenzcorrole recorded in DMF solution. Upon reduction of the metal-free phthalocyanine **10** to the triazatetrabenzcorrole **29** (abbrev. tbc) followed by a phosphorus insertion into tbc, the sharp Soret band displays red-shift and appears now at λ_{max} 446 nm. Moreover, the Soret

band is characterized by high intensity, nearly twice that of the Q band which in turn is blue-shifted compared to PcH_2 and emerges now at λ_{max} 658 nm along with two other, less intense bands at 629 nm and 600 nm. The DCI-MS spectrum evidently corroborates the structure. Only one peak at *m/z* 917 can be seen, which is in good agreement with the calculated mass value.

The reaction of **29** with an excess of methyl iodide and 1,3-propanesultone in DMF is a very straightforward reaction that gives two excellent water-soluble compounds **30** and **31** (Fig. 2.17). The reaction results in good yields: 93 % for the positively charged compound and 78 % for the zwitterionic derivative. Both water-soluble triazatetrabenzcorroles were successfully characterised with ESI-MS (chapter 3), IR (chapter 6) and UV-Vis (Fig. 4.4 in chapter 4.4) spectra.

2.5 Synthesis of water-soluble subphthalocyanines

To the best of our knowledge, merely one example of water-soluble SubPc has been reported till now. In 1996 van Lier *et al.* described the reaction of 4-(chlorosulfonyl)phthalonitrile with BBr_3 conducted in 1-chlorobenzene [31]. The reaction led to tris(chlorosulfonyl)SubPc. The latter was hydrolyzed in a mixture of water and pyridine to afford the pyridinium salt of tri(sulfo)SubPc in 60 % yield. Due to the hydrophilic substituents this SubPc exhibits water-solubility.

Synthesis of water-soluble subphthalocyanines remains particularly difficult task since many phthalonitriles successfully utilized during phthalocyanines synthesis are incompatible with very reactive boron trichloride, thus they are useless for the preparation of SubPcs. The present chapter summarizes efforts towards making these compounds water-soluble. Altogether, five new water-soluble subphthalocyanines have been obtained.

2.5.1 Synthesis of alkynyl-substituted water-soluble subphthalocyanines

Triiodosubphthalocyanine **32** was prepared from 4-iodophthalonitrile (**6**) following a standard procedure [32]. After reacting iodophthalonitrile **6** with BCl_3, phenol was added to exchange axial chloride in the resultant subphthalocyanine against a phenoxy group (Fig. 2.18). It improves solubility of the resulting subphthalocyanine **32** and its derivatives. On the other hand, it prevents subphthalocyanine form being hydrolyzed during workup procedure, chromatography and further reactions. Consequently, axial substitution may improve reaction yields. After the workup procedure, column chromatography gave **32** in 24 % yield. The compound **32**, and consequently its derivatives, consists of a mixture of two regioisomers that belong to the C_1 and C_3 point group. ^{1}H NMR spectrum of **32** shows signals corresponding to the protons of the axial phenoxy group. The aromatic protons close to the SubPc ring gave rise to very shielded doublet at 5.36 ppm (a consequence of the strong ring current produced by SubPc macrocycle). Moreover, a multiplet at 6.81-6.66 ppm corresponding to *metha* and *para* aromatic protons of the phenoxy group was observed. Besides, in the ^{1}H NMR spectrum three signals at 9.21(s) ppm, 8.56(d) ppm and 8.22(d) ppm corresponding to protons of the SubPc moiety were discernible.

Introduction of the 2-(3-pyridynyl)ethynyl group at the peripheral positions of the molecule allows its further quaternization with methyl iodide and thus makes it water-soluble. This was achieved by the methodology similar to that previously reported by Torres *et al.* [33]. The 2-(3-pyridynyl)ethynyl group was introduced at the peripheral positions, as outlined in Figure 2.18, by coupling SubPc **32** with an excess of 3-ethynylpyridine (**33**) in triethylamine (TEA) in the presence of $Pd(PPh_3)_2Cl_2$ and CuI as catalysts. As judged by TLC, the reaction gave a mixture of three compounds. These compounds were identified as mono- (**34c**), di- (**34b**) and tri-substituted (**34a**) subphthalocyanines (Fig. 2.18). The relative mobilities on thin-layer chromatography are **34c**>**34b**>**34a**. As expected, the more 2-(3-pyridynyl)ethynyl groups appended to the SubPc molecule the stronger is the interaction with the stationary phase and thus lower mobility.

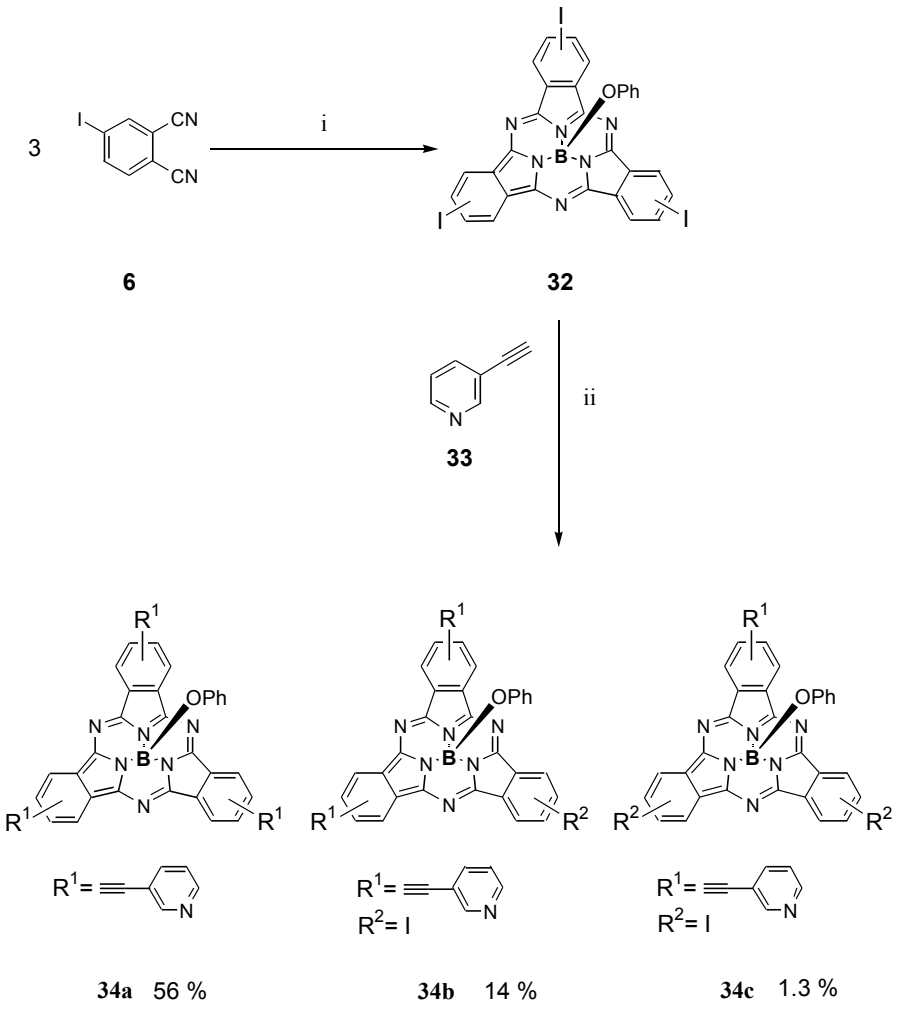

Figure 2.18. Synthesis of SubPc **32** and coupling it with 3-ethynylpyridine (**33**). Conditions: (i) BCl_3, p-xylene, 150°C, N_2, 1 h, then phenol, toluene, 120°C, 12 h (24%), (ii) $PdCl_2(PPh_3)_2$, CuI, TEA, RT, N_2, 20 h.

Treatment of **34a** with an excess of methyl iodide in DMF afforded new, positively charged, water-soluble SubPc **35** in 78 % yield. Quaternization of **34a** with an excess of 1,3-propanesultone gave the first ever reported zwitterionic subphthalocyanine **36** in 83 % yield (Fig. 2.19). The identities of both compounds were confirmed by ESI-MS (see chapter 3). Due to the presence of SO_3 group, in the IR spectrum of zwitterionic SubPc **36** strong absorptions at 1191 cm^{-1} (ν_{as}, SO_2) and 1043 cm^{-1} (ν_{sym}, SO_2) were discernible. The UV-Vis spectra of **35** and **36** are described in subchapter 4.4 (Fig. 4.10).

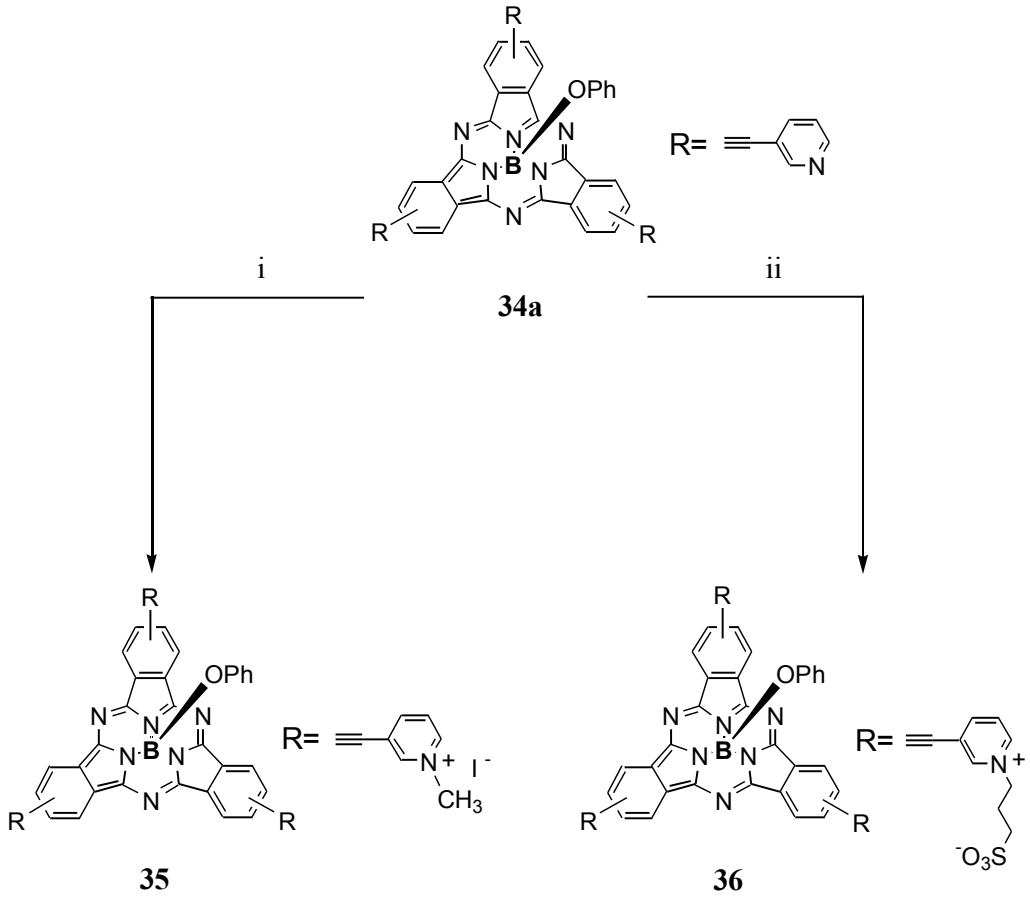

Figure 2.19. Synthesis of positively charged **35** and zwitterionic **36** subphthalocyanines. Conditions: (i) DMF, CH_3I, 50°C, N_2, 4 h (78%), (ii) DMF, 1,3-propanesultone, 50°C, N_2, 4 h (83%).

2.5.2 Synthesis of alkyl-substituted water-soluble subphthalocyanine

An attempt to prepare a new alkyl-substituted, water-soluble subphthalocyanine has been made. For this purpose a novel precursor compound has been designed and synthesized, *i.e.* 4-[2-(2-pyridinyl)ethyl]phthalonitrile (**9**) (see chapter 2.2). The new phthalonitrile **9** was reacted with BCl_3 in p-xylene according to standard procedure (Fig. 2.20). A wide temperature range, from 100°C to 160°C, was tested to find the optimum reaction conditions for the formation of SubPc **38**. The characteristic deep-purple colour of SubPc appears only at the very beginning of the reaction. Short after the reaction initiates the compound decomposes and can not be isolated.

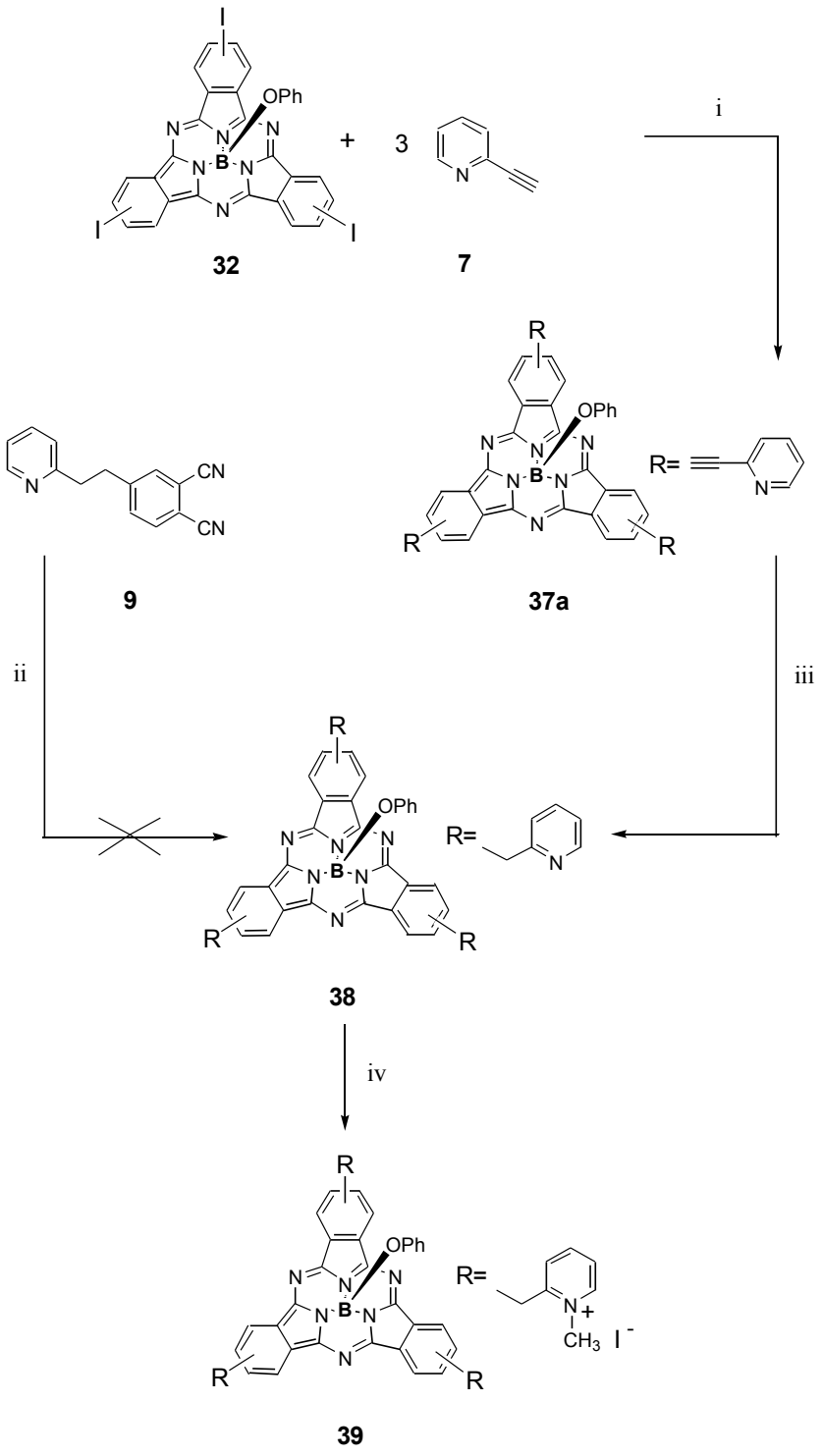

Figure 2.20. Synthesis of water-soluble SubPc **39** via Pd-catalyzed hydrogenation of the triple bond in alkynyl-substituted SubPc **37a**. Conditions: (i) $PdCl_2(PPh_3)_2$, CuI, TEA, RT, N_2, 20 h (42%), (ii) BCl_3, p-xylene, 100°C-160°C, 15 min, (iii) $AcCN/CH_2Cl_2$, Pd/C, H_2, 7 h (61%), (iv) DMF, CH_3I, RT, N_2, 4 h (87%).

There are very few examples of alkyl-substituted subphthalocyanines in chemical literature. Hanack *et al.* in his paper from 1996 described synthesis of hexamethyl-substituted SubPc and hexapentyl-substituted SubPc, both in very low yields (3 % and 5 %) [32]. Synthesis of subphthalocyanines with alkyl chains attached to the peripheral position is fairly difficult. This is due to the benzylic positions, which are known to be easily halogenable. Hence, alkyl-substituted phthalonitriles are incompatible with BCl_3. During our studies a new method was developed to circumvent this obstacle. This is the first time alkyl-substituted SubPc was obtained in such a good yield. This approach consists of two successive reactions, *i.e.* Sonogashira cross-coupling followed by Pd-catalyzed reduction of the triple bond with hydrogen.

An excess of the terminal alkyne, *i.e.* 2-ethynylpyridine (**7**), was coupled with triiodosubphthalocyanine (**32**) in triethylamine (TEA) at room temperature using $Pd(PPh_3)_2Cl_2$ and CuI as catalysts. After 20 h the reaction mixture consisted of three fractions as judged by TLC. The main product was identified as tri-substituted derivative **37a** and isolated in 42 % yield. The two other fractions were characterized as di-substituted **37b** and mono-substituted **37c** derivatives and isolated in 20 % and in 5 % yields respectively (Fig. 2.20). The analysis of UV-Vis spectra of **37a**, **37b** and **37c** in CH_2Cl_2 revealed pronounced tendency for both Q-band and Soret band to shift to shorter wavelength as a consequence of the increase of the π-conjugation system. Thus, the Q-band is centred at 570 nm for **37c**. It is red-shifted to 576 nm for compound **37b**. Whereas, for the SubPc **37a** the Q-band appears at 582 nm.

The unsaturated compound **37a** was dissolved in acetonitrile and CH_2Cl_2 was added to enhance the solubility of reactants. Treatment of **37a** with a stream of gaseous hydrogen in the presence of Pd/C catalyst gave compound **38** (Fig. 2.20). After the workup procedure, column chromatography on silica gel furnished a pink color SubPc **38** in 61 % yield. These findings open a new avenue toward synthesis of novel alkylated subphthalocyanines till now hardly available. In subphthalocyanine **38** the Q-band absorption occurs now at 564 nm and is blue-shifted comparing to SubPc **37a** indicating that the unsaturated carbon-carbon bond was reduced. In the IR spectrum of **38**, the strong absorption at 2213 cm^{-1} characteristic of triple carbon-carbon bond is not observed anymore. Instead new bands between 2857 and 2963 cm^{-1} appeared indicating alkyl functionality.

The reaction of SubPc **38** with an excess of methyl iodide in DMF at room temperature afforded a new, excellent water-soluble compound **39** in a yield of 87 % (Fig. 2.20). The identity of **39** was unambiguously corroborated by ESI-MS (see subchapter 3.4). A peak at *m/z* 282.8 $[M]^{3+}$ was found. The absorption maxima of **39** in water solution are described in chapter 4.

2.5.3 Synthesis of pyridyloxy-substituted water-soluble subphthalocyanine

The results obtained during synthesis of phthalocyanines using 3-pyridyloxyphthalonitrile (**3**) were very good. Hence, it was decided to employ phthalonitrile (**3**) for the preparation of new water-soluble SubPc. 3-Pyridyloxyphthalonitrile (**3**) was reacted with BCl_3 at 160°C for 15 minutes to afford SubPc **40** in 12 % yield (Fig. 2.21). Extension of the reaction time to more than 15 minutes as well as extention of the reaction temperature over 160°C lead to a dramatic decrease in the reaction yield. The resulting SubPc was reacted with phenol to exchange the axial chlorine for phenoxy group. This was necessary since column chromatography of axially chloro-substituted SubPc over silica gel yields considerably amount of axially hydroxy-substituted SubPc. The hydroxy-substituted SubPc sticks firmly to the silica gel, thus, separation and purification is impossible. Consequently, phenoxy group attached to the axial position enhances solubility of SubPc **40** as well as facilitates its purification. SubPc **40** proved to be fairly unstable compound. It has to be protected from intense light during column chromatography and it has to be stored solid. SubPc **40** was light-sensitive when dissolved in common organic solvents. When solution of **40** is exposed to a daily light, after 1-2 days it turns turquoise. The UV-Vis spectrum exhibits absorption typical for phthalocyanines. This may indicate spontaneous ring opening in SubPc **40** and conversion of the latter to Pc macrocycle.

Although 3-pyridyloxyphthalonitrile (**3**) gives excellent phthalocyanines, it seems to be rather poor precursor for SubPc synthesis. It is rather incompatible with very reactive BCl_3 and as a result it gives a plenty of by-products, which are difficult to remove from the target SubPc leading to low yields. In general, SubPcs with substituents attached to the peripheral positions via ether bonds appear to be unstable compounds. Moreover, reactions leading to SubPcs with ether groups are characterized by low yields. For

example S. Lee and H. Suh published synthesis of SubPc with 15-crown-5 subunits on the peripheral positions with merely 3.5 % yield [34].

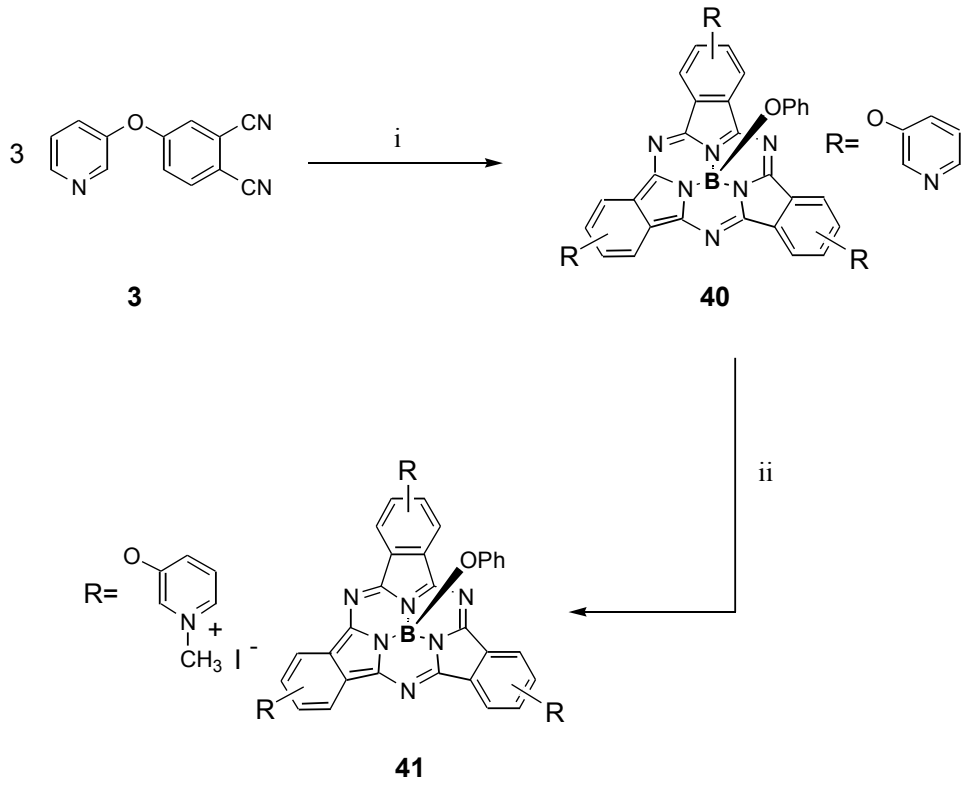

Figure 2.21. Synthesis of pyridyloxy-substituted water-soluble SubPc **41**. Conditions: (i) BCl_3, p-xylene, N_2, 160°C, 15 min, then phenol, DMF, N_2, 120°C, 2 h (12%), (ii) DMF, CH_3I, 50°C, N_2, 2 h (98%).

SubPc **40** was N-methylated with methyl iodide in DMF. The reaction gave new water-soluble SubPc **41** in 98 % yield. Both SubPc **40** and its water-soluble derivatives show in the IR spectra absorption at around 1272 cm^{-1} indicating ether group (Ar-O-Ar). The ESI-MS spectrum of **41** is described in subchapter 3.4.

2.5.4 Synthesis of axially substituted water-soluble subphthalocyanine

The subphthalocyanine molecule offers two possibilities of making it water-soluble; one possibility is the attachment of substituents having charged groups at the periphery of the molecule and the second possibility is to append the charged functionality at the axial position of the molecule [32,35]. An example of the latter strategy is the reaction of the commercially available chloro[subphthalocyaninato]boron(III) (**42**) with 3-hydroxypyridine (**1**) (Fig. 2.22).

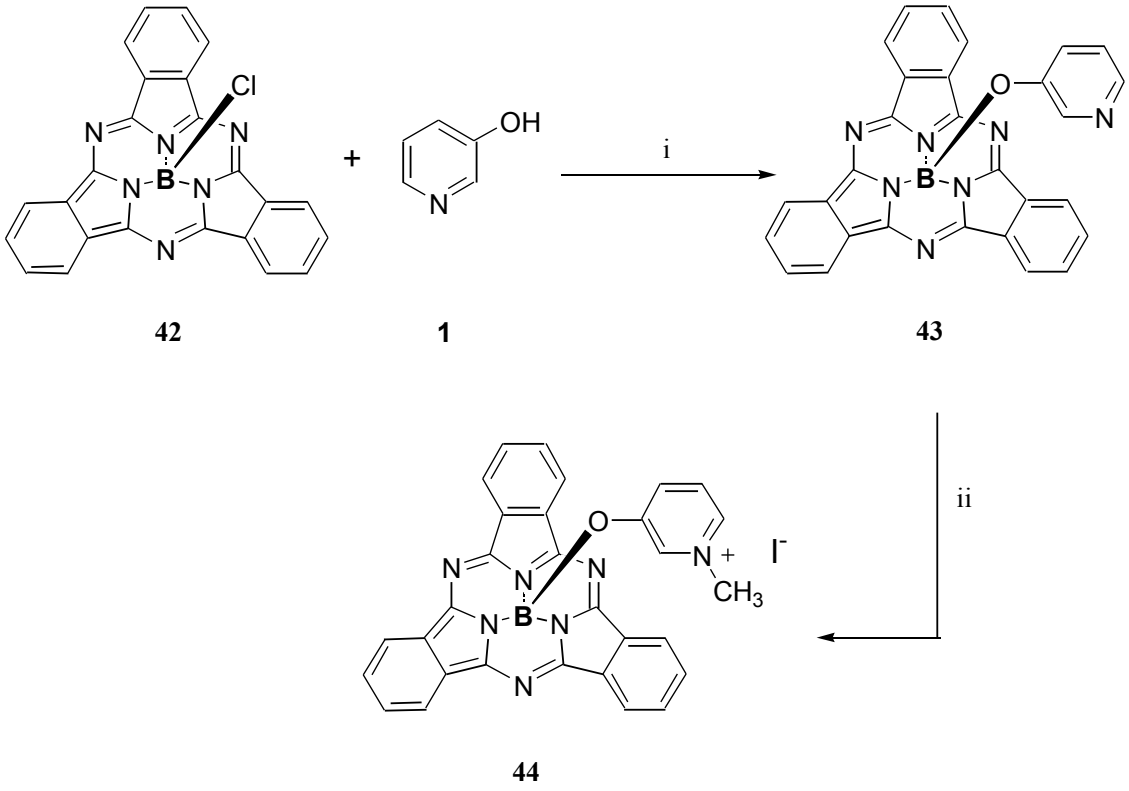

42 **1** **43**

44

Figure 2.22. Synthesis of axially substituted water-soluble subphthalocyanine **44**. Conditions: (i) toluene, 120°C, N_2, 12 h (63%), (ii) DMF, CH_3I, N_2, 2 h (93%).

Both compounds were reacted in toluene at 120°C to give new axially substituted subphthalocyanine **43** with 63 % yield. The assigned structure was confirmed by ESI-MS and ^{1}H-NMR. Two peaks were seen in the spectrum, *m/z* 490 $[M + H^+]^+$ and *m/z* 395 $[M - C_6H_4NO^-]^+$. The ^{1}H-NMR spectrum of **43**, apart from two multiplets attributed to the aromatic protons of the SubPc macrocycle, shows three signals with an integration ration of 1:2:1 for the protons corresponding to the axial 3-pyridyloxy group. The N-

methylation of **43** with an excess of methyl iodide was accomplished in DMF and after 2 h the final 3-(N-methyl)pyridyloxy[subphthalocyaninato]boron(III) iodide (**44**) was obtained with 93 % yield. The ESI-MS spectrum of **44** exibits two peaks, one at *m/z*: 504 $[M - I^-]^+$ and the other one at *m/z* 395 $[M - C_6H_7NOI^-]^+$ (see subchapter 3.4).

Somewhat surprisingly, even though the new subphthalocyanine **44** consists of bulky hydrophobic part and only one charged group attached to the axial position, it proved to be water-soluble. Of course subphthalocyanine **44** is much less water-soluble comparing to its peripheraly substituted derivatives described before. Nevertheless, water solution of **44** is intensely pink coloured. The UV-Vis spectrum of **44** recorded in DMF exhibits absorption at 656 nm (see chapter 4.3).

2.6 Synthesis of water-soluble porphyrins

Several tetraanionic, tetracationic and zwitterionic porphyrins were synthesized and characterized as photosensitizers during this study. Most of these porphyrins have been already described in chemical literature. Moreover, some of them are commercially available. Hence, only brief description of the reaction conditions and spectral characterization of these compounds is given in this chapter.

The commercially available metal-free *meso*-tetrakis(4-pyridyl)-porphyrin **45** was quaternized with methyl iodide and 1,3-propanesultone in DMF (Fig. 2.23). This way two water-soluble derivatives were obtained, *i.e.* tetracationic H_2PoOPM **46** and zwitterionic H_2PoOPPS **47**.

In order to obtain water-soluble zinc porphyrins in the first step free-base porphyrin **45** was metallated. It was accomplished by reacting **45** with zinc acetate in DMF (Fig. 2.23). The reaction was monitored by UV-Vis spectometry. The disappearance of four bands at 510, 543, 583 and 640 nm and appearance of two other bands instead at 557 nm and 597 nm upon metallation indicates that the reaction drawn to a close. DCI mass spectrometry corroborates that the porphyrin **45** was fully metallated. No peak from the metal-free porphyrin could be detected in the mass spectrum of the reaction product. Quaternization of zinc porphyrin **48** with methyl iodide and 1,3-propanesultone is a

straightforward reaction that leads to two excellent water-soluble porphyrins, *i.e.* positively charged **49** and zwitterionic porphyrin **50** (Fig. 2.23).

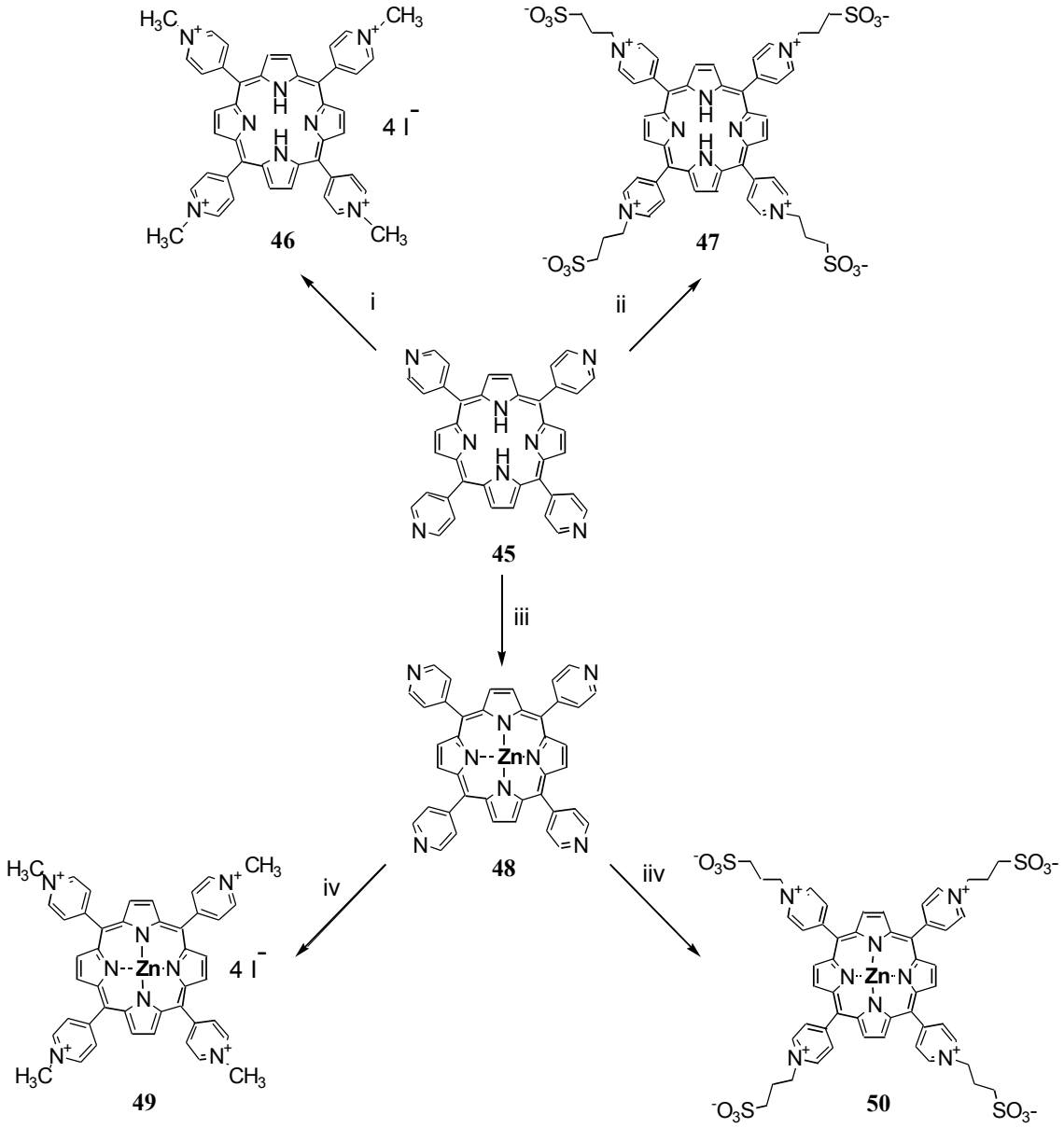

Figure 2.23. Synthesis of water-soluble porphyrins. Conditions: (i) DMF, CH_3I, 50°C, 18 h (96 %), (ii) DMF, 1,3-propanesultone, 80°C, 16 h (92 %), (iii) DMF, $Zn(CH_3COO)_2$, 100°C, 48 h (98 %), (iv) DMF, CH_3I, 50°C, 18 h (96 %), (iiv) DMF, 1,3-propanesultone, 80°C, 16 h (92 %).

Tetraanionic *meso*-tetrakis-(sulfonatophenyl)porphyrin-zinc(II) (**52**) (abbreviated as ZnPoTS) was obtained from the commercially available free-base porphyrin **51**. This

was done by reacting it with zinc acetate in DMF at 80°C (Fig. 2.24). After 24 h the zinc containing porphyrin **52** was isolated with 93 % yield.

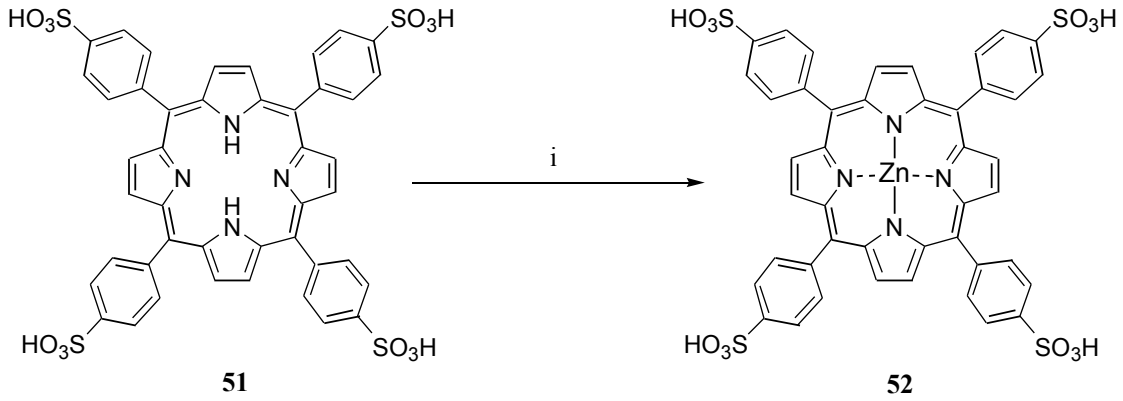

Figure 2.24. Synthesis of ZnPoTS **52** via insertion of zinc into the metal-free H_2PoTS **51**. Conditions: (i) $Zn(CH_3COO)_2$, DMF, 80°C, 24 h (94%).

Each porphyrin obtained during this study is characterized by a single Soret band located between 419 and 455 nm (see chapter 4, Fig. 4.9). The Soret band is always about 30 nm blue shifted upon metallation. Moreover, the less intense Q-band was discernible as four bands for metal-free porphyrins. Upon metallation due to the change of the symmetry the Q-band emerges as two bands located at ca. 569 nm and 615 nm. The Soret and Q-band molar absorptivities as well as maximum peak positions vary with porphyrin concentration in water solution. The spectral characterization of water-soluble porphyrins is also supported with ESI-MS. The results are summarized in chapter 3.

2.7 Conclusion

Investigations were carried out, aiming to prepare a set of differently charged, water-soluble compounds, potentially applicable as photocatalysts. The following macrocycles were investigated:

- metal-free, silicon and germanium phthalocyanines,
- oxophosphorus(V) and hydroxysilicon triazatetrabenzcorroles,
- subphthalocyanines,
- metal-free and zinc porphyrins.

Synthesis of all these compounds was undertaken purposely, *i.e.* to find possibly stable and efficient new photocatalyst useful in the photo-oxidation reactions (see chapter 5). Besides, of interest were multicomponent systems absorbing at different wavelengths of ultraviolet and visible irradiation. Moreover, the influence of central metal, charge and substituents on the photocatalytic properties of phthalocyanines and related compounds can be elucidate only after collecting substantial photocatalytic data on diverse compounds.

Cyclotetramerization of 4-(3-pyridyloxy)phthalonitrile (**3**) in 1-pentanol upon addition of lithium afforded metal-free phthalocyanine (**10**). The reaction of 5-(pyridyloxy)-1,3-diiminoisoindoline (**4**) with $SiCl_4$ in dry quinoline proved to be good method of obtaining silicon phthalocyanine **13** with 3-pyridyloxy substituents. Analogous reaction with the difference being use of $GeCl_4$ afforded germanium phthalocynine **16** substituted with 3-pyridyloxy groups. The reaction of metal-free **10**, silicon **13** and germanium **16** phthalocyanines with an excess of methyl iodide resulted in positively charged water-soluble dyes (**11**, **14**, **17**). The reaction of these phthalocyanines with 1,3-propanesultone in DMF furnished zwitterionic water-soluble compounds (**12**, **15**, **18**). Attempt to insert $SiCl_4$, $HSiCl_3$, $Si(CH_3COO)_4$ or $GeCl_4$ in to the metal-free phthalocyanine **10** has been made. Although the reaction was performed in various solvents at different conditions it did not give metallated phthalocyanines.

Metal-free sulfophthalocyanine (**20**) was obtained by the cyclotetramerization of 4-sulfophthalate in melted urea. Attempt to react $Si(CH_3COO)_4$ with 4-sulfophthalate in melted urea to give silicon sulfophthalocyanine has failed. Thus, the unsubstituted silicon phthalocyanine (**22**) was sulfonated with oleum according to published

procedure. The reaction, quite unexpectedly, resulted in ring-contracted product, namely hydroxysilicon sulfotriazatetrabenzcorrole (**23**). Examination of UV-Vis properties showed that Si(tbc)TS **23**, found as a main product, has dramatically red-shifted Soret band compared to the parent phthalocyanine. The Soret band found at 452 nm is of an intensity twice that of the Q-band. Moreover, the oligomeric silicon sulfophthalocyanine was found in the reaction mixture. The UV-Vis spectrum of the latter shows a broad band at 641 nm – typical of the oligomeric sulfonated phthalocyanine. There was no silicon sulfophthalocyanine in the reaction mixture. The chlorosulfonation of $SiCl_2Pc$ (**22**) followed by hydrolysis of the chlorosulfonated derivative **24** was found to be considerably better method compared to sulfonation of $SiCl_2Pc$ (**22**) with oleum. Water-soluble germanium sulfophthalocyanine (**28**) has been successfully obtained by chlorosulfonation and hydrolysis of the sulfochloride derivative **27**. Unlike $SiCl_2Pc$ (**22**), sulfonation of $Ge(OH)_2Pc$ (**26**) with oleum gives exlusively germanium sulfophthalocyanine (**28**). Apparently, $Ge(OH)_2Pc$ (**26**) is much less susceptible to reduction and ring contraction compared to $SiCl_2Pc$ (**22**). Both chlorosulfonation followed by hydrolysis and sulfonation with oleum of the unsubstituted parent phthalocyanine is suitable method to obtain water-soluble germanium sulfophthalocyanine (**28**). Both silicon and germanium sulfophthalocyanines exist in a monomeric state in water solution.

The reaction of metal-free phthalocyanine **10** with PCl_3 in pyridine resulted in ring-contracted compound, namely, oxophosphorus(V) triazatetrabenzcorrole **29**. This compound after reacting it with methyl iodide and 1,3-propanesultone gave two water-soluble dyes (**30**,**31**). Their water solutions are bright green and show two strong absorptions at ca. 446 nm and 658 nm.

The synthesis of five novel water-soluble SubPcs has been achieved. These are dyes bearing different substituents having always “pyridyl motif” that allows its N-substitution with methyl group or sulfopropyl chain.

4-Iodophthalonitrile (**6**) was cyclotrimerized to triiodosubphthalocyanine **32**. The latter was reacted with an excess of 3-ethynylpyridine (**33**) in the presence of palladium catalyst to yield 2-(3-pyridynyl)ethyl-substituted SubPc **34a**. N-methylation and quaternization of SubPc **34a** with 1,3-propanesultone afforded two water-soluble compounds: positively charged **35** and zwitterionic **36** SubPcs.

As attempt at converting 4-[2-(2-pyridinyl)ethyl]phthalonitrile (**9**) into alkyl-substituted subphthalocyanine **38** was unsuccessful, a new approach was developed. Thus, two successive reactions were employed: Sonogashira cross-coupling of an excess of the terminal alkyne **7** with triiodosubphthalocyanine **32** followed by Pd-catalyzed reduction of the triple bond with hydrogen. The novel 2-(2-pyridynyl)ethyl-substituted subphthalocyanine **38** was converted into the water-soluble derivative **39**. The results of these investigations indicate that Pd-catalyzed hydrogenation of alkynyl bond is compatible with the subphthalocyanine macrocycle, thus providing a convenient method for alkyl-substituted subphthalocyanines hardly available via cyclotrimerization of alkyl-substituted phthalonitriles. The quaternization of SubPc **38** with methyl iodide afforded excellent water-soluble SubPc **39**.

3-Pyridyloxyphthalonitrile (**3**) is an excellence precursor for the synthesis of water-soluble Pcs. For the first time it has been employed aiming to prepare 3-pyridyloxy substituted SubPc **41**. Thus, precursor **3** was reacted with BCl_3 to give SubPc **40**. The latter was N-methylated to the new water-sloluble SubPc **41**. Both SubPc **40** and its water-soluble derivative **41** proved to be light-sensitive. In general, SubPcs having ether groups appear to be unstable compounds. The solution of **41** exposed to a daily light turns blue indicating spontaneous ring opening and conversion to phthalocyanine macrocycle.

Chloro- and bromoSubPcs can be reacted with a variety of nucleophiles (carboxilic acids, phenyllithium, trialkylchlorosilanes, phenols or aliphatic alcohols) to afford axially substituted SubPcs. This reaction was utilized to obtain a new, interesting water-soluble SubPc. The reaction of commercially available chloroSubPc **42** with 3-hydroxypyridine (**1**) followed by N-methylation gave rise to SubPc **44** bearing positive charge at the axial substituent. The molecule comprises of bulky hydrophobic part and only one charge at the axial position, yet it gives intensely pink coloured water solutions.

Several tetraanionic, tetracationic and zwitterionic porphyrins (**46**, **47**, **49**-**52**) were synthetized aiming to reveal their photocatalytic properties (see chapter 5).

2.8 References

[1] Neil B. McKeown; *The synthesis of symmetrical phthalocyanines* in The Porphyrin Handbook, Vol. 15, Academic Press, **2003**.

[2] Weber, M. J. T.; Busch, D. H.; *Inorg. Chem.* **1965**, 4, 469.

[3] Sanchez, M.; Fache, E.; Bonnet, D.; Meunier, B.; *J. Porphyrins Phthalocyanines* **2001**, 5, 867-872.

[4] Wöhrle, D.; Hundorf, U.; *Macromol. Chem.* **1985**, 186, 2177.

[5] Dulog, L.; Gittinger, A.; *Mol. Cryst. Liq. Cryst.* **1992**, 213, 31.

[6] Sakamoto, K.; Ohno, E.; *Dyes Pigment.* **1997**, 35, 375.

[7] Solov`eva, L. I.; Lukyanets, E. A.; *J. Gen. Chem. USSR (Engl. Trans.)*, **1980**, 50, 907.

[8] Drechsler, U.; Pfaff, M.; Hanack, M.; *Eur. J. Org. Chem.* **1999**, 3441.

[9] Li, Z. P.; van Lier, J.; Leznoff, C. C.; *Can. J. Chem.* **1999**, 77, 138.

[10] Boyle, R. W.; van Lier, J. E.; *Synthesis*. **1995**, 1079.

[11] Boyle, R. W.; van Lier, J. E.; *Synlett.* **1993**, 5, 351-352.

[12] Sharman, W. M.; Kudrevich, S. V.; van Lier, J. E.; *Tetrahedron Lett.* **1996**,37, 5831.

[13] Wöhrle, D.; Iskander, N.; Graschew, G.; Sinn, H.; Friedrich, E.; Maier-Borst, W.; Stern, J.; Schlag, P. *Photochem. Photobiol.* **1990**, 51, 351-356.

[14] Kimura, M.; Nakada, K.; Yamaguchi, Y.; Hanabusa, K.; Shirai, H.; Kobayashi, N.; *Chem. Commun.* **1997**, 1215.

[15] Rosenthal, I.; Ben-Hur, E.; Greenbeg, S.; Concepcion-Lam, A.; Drew, D. M.; *Photochem. Photobiol.* **1987**, 46, 959.

[16] Leznoff, C. C.; Hu, M.; McArthur, C. R.; Qin, Y.; van Lier, J.; *Can. J. Chem.* **1994**, 72, 1990.

[17] Leznoff, C. C.; Vigh, S.; Svirskaya, P. I.; Greenberg, S.; Drew, D. M.; Ben-Hur, E.; Rosenthal, I.; *Photochem. Photobiol.* **1989**, 49, 279.

[18] Ali, H.; Langlois, R.; Wagner, J. R.; Brasseur, N.; Paquette, B.; van Lier, J. *Photochemistry and Photobiology* **1988**, Vol. 47, 5, 713-717.

[19] Hanack, M.; Geyer, M.; *J. Chem. Soc., Chem. Commun.* **1994**, 2253-2254.

[20] Claessens, C.G.; Torres, T.; *Tetrahedron Lett.* **2000**, 41, 6361-6365.

[21] Oliver, S. W.; Smith, T. D.; *Heterocycles,* **1984**, Vol 22, 9, 2047-2052.

[22] Leznoff, C. C.; Terekhov, D. S.; McArthur, C. R.; Vigh, S.; Li, J.; *Can J. Chem.* **1995**, 73,435.

[22] Aoudia, M.; Cheng, G.; Kennedy, V. O.; Kenney, M. E.; Rodgers, A. J.; *J. Am. Soc. Chem.* **1997**, 119, 6029-6039.

[23] Kane, K. M.; Lemke, F. R.; *Inorg. Chem.* **1995**, 34, 4085-4091.

[24] Rihter, B. D.; Kenney, M. E.; Ford, W. E.; Rodgers, A. J.; *J. Am. Chem. Soc.* **1990**, 112, 8064-8070.

[25] R. Gerdes, *Niedermoleculare und immobilisierte Phthalocyaninetetrasulfonsäuren als Photosensibilisatoren für die Photooxidation von Phenol und Chlorophenolen,* Doctoral Dissertation, Universität Bremen **2000**.

[26] Joyner, R. D.; Kenney, M. E.; *Inorg. Chem,* **1962**, Vol. 1, 236-237.

[27] Li, J.; Lakshminarayanapuram, R.; Subramanian, R.; Hanack, M.; *Chem. Commun.* **1997**, 679-680.

[28] Gürek, A. G.; Appel, G.; Mikalo, R. P.; Schmeißer, D.; *J. Porphyrins Phthalocyanines*, **2001**, 5, 751-757.

[29] Joyner, R. D.; Kenney, M. E.; *Inorg. Chem,* **1960**, 82, 5790-5791.

[30] Fujiki, M.; Tabei, H.; Isa, K.; *J. Am. Chem. Soc.* **1986**, 108, 1532-1536.

[31] Kudrevich, S. V.; Gilbert, S.; van Lier, J. E.; *J. Org. Chem.* **1996**, 61, 5706-5707.

[32] Geyer, M.; Plenzig, F.; Rauschnabel, J.; Hanack, M.; del Rey, B.; Sastre, A.; Torres, T.; *Synthesis* **1996**, 1139-1151.

[33] del Rey, B.; Torres, T.; *Tetrahedron Lett.* **1997**, 38, 5351-5354.

[34] Lee, S.; Suh, H.; *Bull. Korean Chem. Soc.* **1999**, Vol. 20, 9, 991-992.

[35] Claessens, Ch. G.; Gonyales-Rodriguey, D.; Torres, T.; *Chem. Rev.* **2002**, 102, 835-853.

[36] Schneider, G.; Wöhrle, D.; Spiller, W.; Stark, J.; Schulz-Ekloff, G.; *Photochem. Photobiol.*, **1994**, 60, pp. 333-342.

3. Electrospray Ionization Mass Spectrometry of Different Water Soluble Photosensitizers

3.1 Introduction

Electrospray Ionisation (ESI) and Matrix Assisted Laser Desorption Ionization (MALDI) are two, by far the most important now, ionisation methods for organic molecules. Moreover, both ESI-MS and MALDI-MS seem to be two most frequently utilized analytical tools for a variety of complex, high mass, non-volatile molecules and biomolecules. The method of producing charged droplets and a commonly accepted mechanism of ion formation from charged droplets in ESI is briefly described below.

The development of electrospray into a widely used practical method of sample ionisation was preceded by experiments carried out by Ryleigh. In 1882 Rayleigh had investigated the phenomenon that happens during the evaporation of solvent from a droplet that was electrically charged [1]. He found that as the solvent evaporates and droplet shrinks, the density of charges at the droplet surface increases to a certain critical value (referred to as a "Rayleigh limit"). At this point Coulomb repulsion overcomes surface tension and the droplet eventually explodes into a plenty of offspring droplets. The mechanism proposed by Dole further assumes that the offspring droplets resulting from Rayleigh instability continue to shrink as the solvent evaporates until the Rayleigh limit is reached again. The offspring droplets break up into a plurality of smaller droplets. A succession of Rayleigh instabilities ultimately lead to a single analyte molecule that retains some of the droplet`s charge. The charges are statistically distributed amongst the analyte`s available charge sites, leading to the possible formation of multiply charged ion. Around thirty years after Rayleigh`s pioneering work John Zeleny made the first systematic experiments (1914-1917) with that technique and confirmed Rayleigh`s theoretical predictions [2-4]. He passed a stream of conducting volatile solvent through a needle the tip of which was maintained at a high potential.

Zeleny observed that the intense electric field dispersed the emerging liquid into a fine spray of charged droplets.

In 1968 Malcolm Dole published his famous paper describing experiments in which the molecular weights of oligomers of polystyrene were measured using electrospray ionisation [5]. This was the first time that non-volatile molecules of such high molecular masses were measured. Moreover, Malcolm´s Dole´s paper had great impact on the development of ESI into a practical method of sample ionisation. In the 1980s, Fenn and Mann - inspired by the results obtained by Malcolm Dole - further developed the ESI mass spectrometry. They were able to measure mass spectra of some biological macromolecules, like cyclic peptide Cyclosporine A and Gramicidin S, as well as poly(ethylene glycol) oligomers. At the same time they explored the propensity for multiple charging and worked out the algorithm that transforms the multiple peaks into a single peak that would be obtained if the ions had a single charge. The work of John Fenn was awarded in 2002 by Nobel Prize for chemistry (the fourth time a Nobel Prize has been awarded to mass spectrometry pioneers) [6].

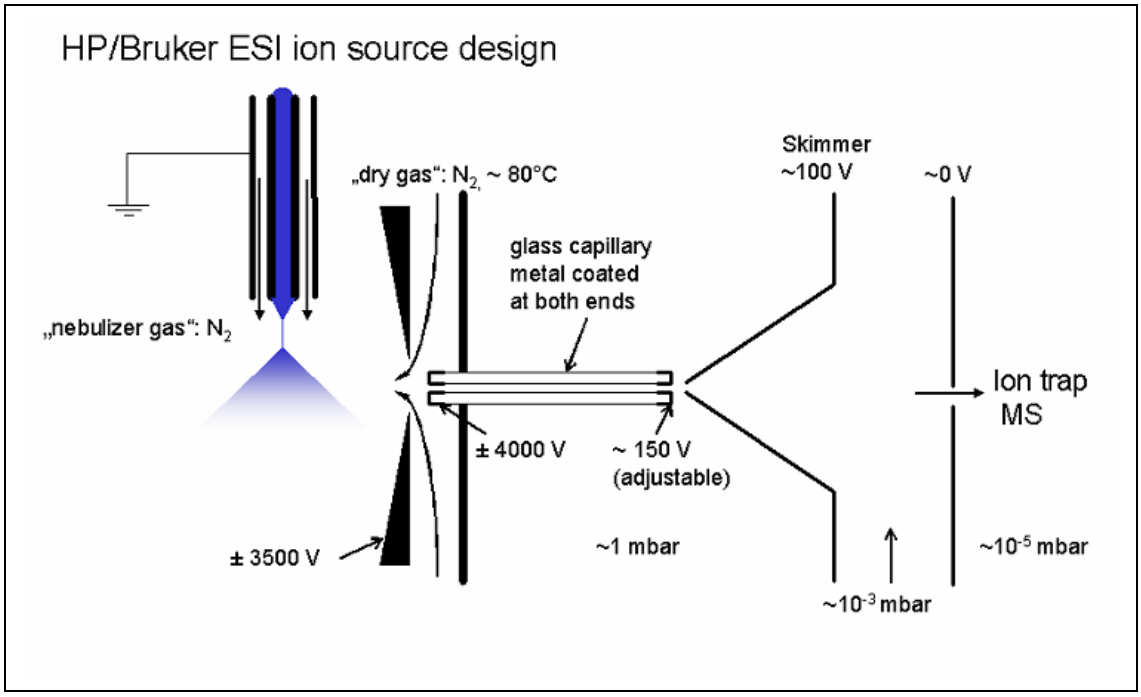

Figure 3.1. The basic components of an ESI source (by courtesy of Dr. Thomas Dülcks).

In Figure 3.1 schematic representation of electrospray ion source is depicted. The analyte solution is introduced to the source through the syringe pump or as the eluent flow from liquid chromatography. The analyte solution is passed through the electrospray needle. The exit tip of electrospray needle is maintained at a high potential difference with respect to the opposing electrode (typically in the range from 3 to 6 kV) [7]. The charged droplets are repelled from the needle towards the source sampling cone on the counter electrode. The droplets traverse the space between the needle tip and the nozzle in the stream of dry nitrogen, counter-current to the flux of charged droplets, to facilitate the evaporation of solvent. Thus, as the solvent evaporates, the droplet shrinks bringing the surface charges closer together until the resulting Coulomb repulsion overcomes surface tension leading to explosion of the droplet into a offspring droplets according to the mechanism that was described above. In sum, a stream of conducting polar solvent is dispersed into plurality of highly charged droplets by an intense electric field. This process of shrinking followed by explosions repeats until naked charged analyte molecules appear. The naked charged molecule enters the vacuum system through the glass capillary and then through the skimmer into the analyser [7].

3.2 Aim of this study and literature survey on the ESI-MS of water soluble phthalocyanines

Surprisingly, relatively little data on the ESI-MS of water-soluble phthalocyanines have been reported by authors working on these compounds. Most frequently the authors cite in the experimental part merely the parent ion and, hardly ever give information on fragmentation of the molecule. The mass spectral methods, in particular ESI-MS and MALDI-MS, seem to be underestimated in phthalocyanines structure elucidation, although in many cases mass spectrometry can be superior to NMR since aggregation and poor solubility limit the usefulness of this method. Significantly more work has been dedicated to porphyrins [8,9].

For example, to the best of our knowledge no detailed spectra of the zwitterionic phthalocyanines have been reported until now. More data are available on sulfonated phthalocyanines, as they have attracted attention as photodynamic agents in chemotherapy of cancer. Some results on decontamination of red blood cell

concentrates for transfusion using phthalocyanines have been published as well. Moreover, water-soluble phthalocyanines have been intensively investigated as a photocatalysts in water media for intoxication of environmental contaminations - to mention all but few of the applications of these water-soluble dyes. Thus, M. Bressan et al. published the ESI mass spectrum of ruthenium (II) sulfophthalocyanine, made via template condensation, for which the catalytic properties were investigated [10]. They observed the parent ion and a number of peaks attributed to sodium attachment. Then, two water soluble metal sulfophthalocyanines, namely nickel (II) and cobalt (II), and their oxidation products were characterized by ESI mass spectrometry [11]. Zinc and alumina sulfophthalocyanines have attracted attention as potential PDT agents. Hence, an effort towards structure elucidation using ESI and other mass spectrometry techniques has been made [12,13]. The alkylammonium salts of various metallo sulfophthalocyanines were studied using ESI-MS as well [14]. Recently, Dixon and co-workers have reported detailed description of the positive and negative ESI mass spectra of copper, cobalt, zinc and metal-free sulfophthalocyanines [15]. Some of these compounds were made using the template synthesis, *i.e.* cyclotetramerization of the sulfophthalic acid, and others were made via sulfonation of the unsubstituted phthalocyanine. Interestingly, depending on the synthesis method the compounds showed somewhat different mass spectra. It has been reported that the sulfonation can give phthalocyanines with more than one sulfonate. In this work the ESI mass spectra were compared with spectra obtained by matrix-assisted laser desorption/ionization (MALDI).

In the present studies we were interested in exploring the usefulness of the electrospray mass spectrometry in investigation of the water-soluble dyes. A very broad range of differently charged compounds has been scrutinized: porphyrins, phthalocyanines, subphthalocyanines and triazatetrabenzcorroles. The focus was not only on obtaining molecular ion peaks but also on exploring the fragmentation patterns of these compounds. We were particularly interested in good ESI mass spectra of the sulfonated phthalocyanines, which have been an ongoing issue in our laboratory for a long time. The question of the extent of sulfonation of the unsubstituted silicon and germanium phthalocyanines, an important photocatalysts [16], remains open and ESI mass spectrometry could be helpful in solving this problem.

3.3 Experimental – instrumentation and sample preparation

ESI mass spectra were recorded using the Bruker Esquire-LC which is a HPLC/MS system that consists of an Agilent HP 1100 liquid chromatography system and an ion trap mass detector. Both components can be used separately. The instrument is characterized by a mass range of 50-2200 amu (in standard mode) and up to 6000 amu (maximum value). Following resolution is attainable: in standard mode 0.6 amu FWHM, and minimum peak width 0.2 amu FWHM. Acquisitions were carried out in both positive and negative ion modes.

Samples were prepared by taking less than one mg of compound and dissolving it in approximately 0.4 ml of water. This solution was further diluted prior to analysis with an appropriate solvent or mixture of solvents. For positively charged compounds the following solvents proved to be useful: H_2O, MeOH, or mixture of both (1:1) as well as ACN/DMF (10:1). For zwitterions DMSO/MeOH, MeOH/DMF (100:1), DMF, H_2O/ACN (1:10) as well as H_2O/MeOH (1:20) were applied. In some cases addition of 0.1% of formic acid was necessary. The bulk of tetrasulfonated dyes could be analyzed exclusively upon dilution with buffer solution, *i.e.* 50 mM water solution of ammonium formate. All the samples were introduced in to the electrospray source at a flow rate of 2 μL/min.

3.4 ESI mass spectra of positively charged compounds

A significant loss of the N-methyl group was seen for H_2PcOPM **11**, SubPcOPM **41** and ZnPoOPM **49**. On the other hand, in the case of SubPcOPM **35**, SubPcOPM **39** and SiPcOPM **14** the positive ion mode ESI spectrum revealed the presence of quasi-molecular ions only, *i.e. m/z* 278.4 $[M\text{-}3I^-]^{3+}$, *m/z* 282.8 $[M\text{-}3I^-]^{3+}$ and *m/z* 251 $[M\text{-}4I^-]^{4+}$ respectively (Fig. 3.2).

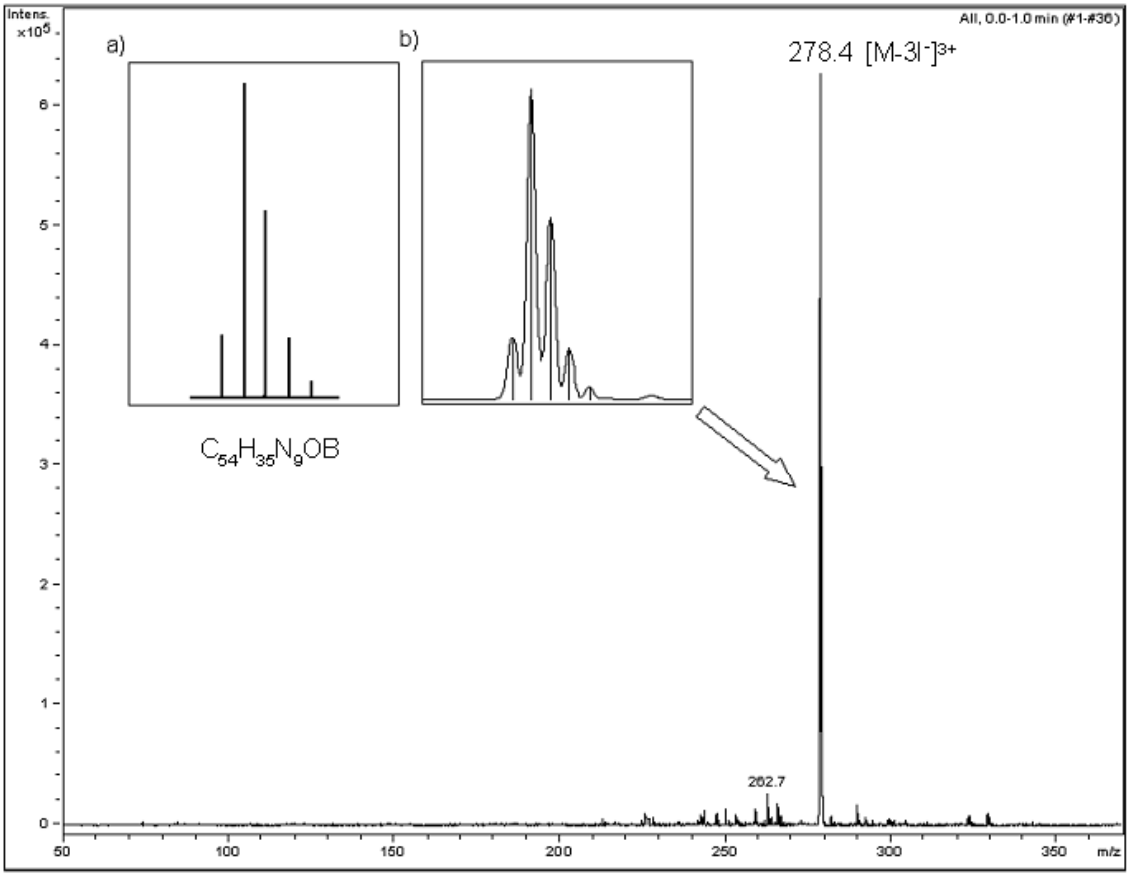

Figure 3.2. Positive ion mode ESI mass spectrum of SubPcOPM **35**. The inset shows the calculated (a) and observed (b) isotopic pattern of SubPcOPM **35**.

The positive ion mode ESI spectrum of SubPcOPM **41** showed the quasi-molecular ion at *m/z* 270.4 $[M\text{-}3I^-]^{3+}$ and an abundance of singly and doubly charged ions. Among them, a peak at *m/z* 1066 indicated an ion resulting from loss of one iodide counter-ion, *i.e.* $[M\text{-}I^-]^+$. Peaks at *m/z* 924 and *m/z* 990 were attributed to loss of one methyl group as

well as two iodide anions, *i.e.* $[M\text{-}CH_3^+\text{-}2I^-]^+$, and axial phenyl group loss along with loss of one iodide anion, *i.e.* $[M\text{-}I^-\text{-}C_6H_5^+\text{+}H^+]^+$. Among the doubly charged ions the most abundant one was that of two iodide counter-ions loss, *i.e. m/z* 469 $[M\text{-}2I^-]^{2+}$. Of interest were peaks at *m/z* 360.7 and *m/z* 431.1 indicating axial phenyl group loss: $[M\text{-}3I^-\text{-}C_6H_5^+\text{-}CH_3^+\text{+}H^+]^{2+}$ and $[M\text{-}C_6H_5^+\text{-}2I^-\text{+}H^+]^{2+}$.

Interestingly, only in the case of SubPcOPM **41** the negative ion mode ESI spectrum could be recorded. The most prominent peak in the spectrum was that of the iodide attachment, *i.e. m/z* 1320 $[M+I^-]^-$ (Fig. 3.3).

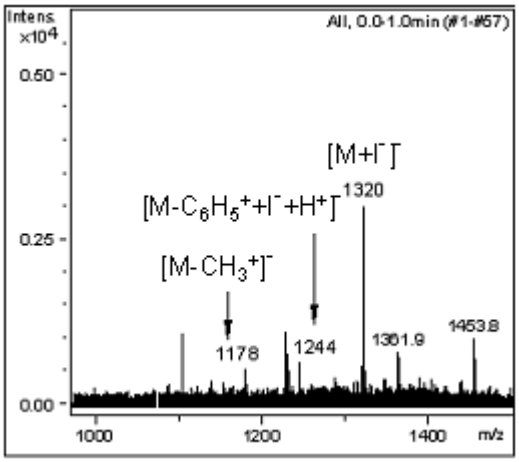

Figure 3.3. Negative ion mode ESI mass spectrum of SubPcOPM **41**.

The ESI mass spectrum of GePcOPM **17** revealed a moderately intense peak ascribed to the quasi-molecular ion, *i.e. m/z* 263 $[M\text{-}4I^-]^{4+}$. The most intense peak at *m/z* 236.6 fitted to an ion of the following composition: $[M\text{-}4I^-\text{-}Ge(OH)_2\text{+}2H^+]^{4+}$. Apparently under the ionization conditions germanium was pushed out from the macrocycle and exchanged for two protons.

Similarly, demetallation was observed in the case of positively charged zinc porphyrin ZnPoOPM **49**: *m/z* 169.3 $[M\text{-}4I^-\text{-}Zn^{2+}\text{+}2H^+]^{4+}$ (Fig. 3.4). Moreover, the high intensity peak at *m/z* 185 matched the quasi-molecular ion, $[M\text{-}4I^-]^{4+}$. Loss of one and two N-methyl groups was seen as well: *m/z* 241.4 $[M\text{-}4I^-\text{-}CH_3^+]^{3+}$ and *m/z* 355 $[M\text{-}4I^-\text{-}2CH_3^+]^{2+}$.

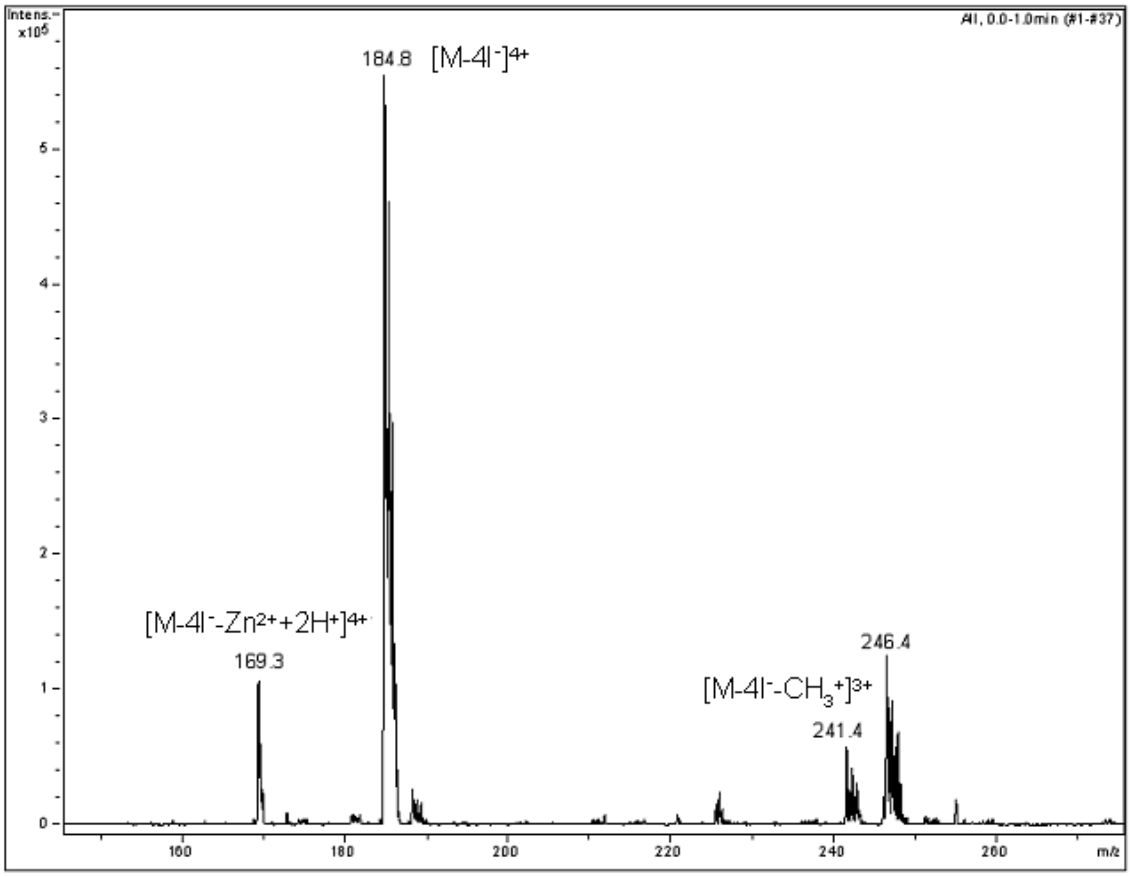

Figure 3.4. ESI mass spectrum of ZnPoOPM **49**.

Surprisingly, for PO(tbc)OPM **30** the addition of one molecule of water was observed (Fig. 3.5). A series of three peaks were appropriate for doubly, triply and quadruple charged species: *m/z* 623.9 $[M\text{-}2I^{-}+H_2O]^{2+}$, *m/z* 373.6 $[M\text{-}3I^{-}+H_2O]^{3+}$, *m/z* 248.6 $[M\text{-}4I^{-}+H_2O]^{4+}$. No peak corresponding to the loss of N-methyl group was discernible.

The most prominent peak in the spectrum of the positively charged metal-free phthalocyanine H_2PcOPM **11** was attributed to the quasi-molecular ion, *i.e. m/z* 236.6 $[M\text{-}4I^{-}]^{4+}$, two others matched loss of one and two N-methyl groups: *m/z* 310.5 $[M\text{-}4I^{-}\text{-}CH_3^{+}]^{3+}$ and *m/z* 458.4 $[M\text{-}4I^{-}\text{-}2CH_3^{+}]^{2+}$.

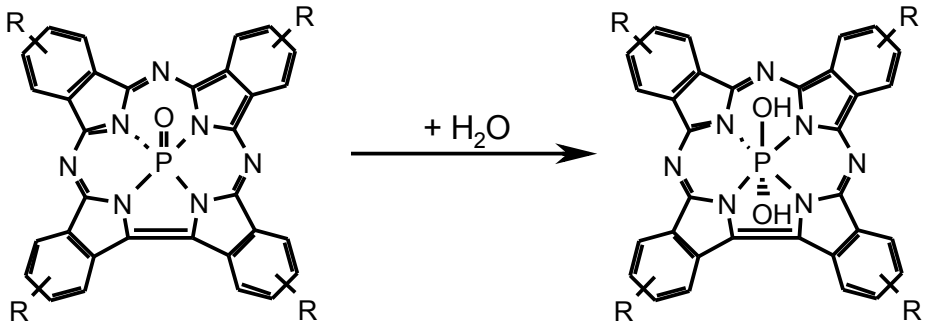

m/z 244.25 $[M\text{-}4I^-]^{4+}$ *m/z* 248.6 $[M\text{-}4I^-+H_2O]^{4+}$

Figure 3.5. Proposed structure of a new species after water molecule addition to the coordination sphere of phosphorus(V) in the PO(tbc)OPM **30**[17].

The table 3.1 summarizes identified positive and negative ions for the positively charged macrocyclic compounds.

Table 3.1. List of the identified positive and negative ions for positively charged water-soluble compounds.

Compound	m/z	Assignment
H_2PcOPM (11)	236.6	$[M\text{-}4I^-]^{4+}$
	310.5	$[M\text{-}4I^-\text{-}CH_3^+]^{3+}$
	458.4	$[M\text{-}4I^-\text{-}2CH_3^+]^{2+}$
SiPcOPM (14)	251.3	$[M\text{-}4I^-]^{4+}$
GePcOPM (17)	263	$[M\text{-}4I^-]^{4+}$
	236.6	$[M\text{-}4I^-\text{-}Ge(OH)_2+2H^+]^{4+}$
PO(tbc)OPM (30)	248.6	$[M\text{-}4I^-+H_2O]^{4+}$
	373.6	$[M\text{-}3I^-+ H_2O]^{3+}$
	623.9	$[M\text{-}2I^-+ H_2O]^{2+}$
SubPcOPM (35)	278.4	$[M\text{-}3I^-]^{3+}$

SubPcOPM (**39**)	282.8	$[M-3I^-]^{3+}$
SubPcOPM (**41**)	270.4	$[M-3I^-]^{3+}$
	282	$[M-OPh-2I^-+H^+]^{3+}$
	1066	$[M-I^-]^+$
	924	$[M-CH_3^+-2I^-]^+$
	990	$[M-C_6H_5^+-I^-+H^+]^+$
	469	$[M-2I^-]^{2+}$
	360.7	$[M-3I^--C_6H_5^+-CH_3^++H^+]^{2+}$
	431.1	$[M-C_6H_5^+-2I^-+H^+]^{2+}$
	398.2	$[M-3I^--CH_3^+]^{2+}$
	1320	$[M+I^-]^-$
	1178	$[M-CH_3^+]^-$
	1228	$[M-PhO^-+I^-+H^+]^-$
	1244	$[M-C_6H_5^++I^-+H^+]^-$
SubPc (**44**)	504	$[M-I^-]^+$
	395	$[M-C_6H_7ONI^-]^+$
ZnPoOPM (**49**)	185	$[M-4I^-]^{4+}$
	169.3	$[M-4I^--Zn^{2+}+2H^+]^{4+}$
	241.4	$[M-4I^--CH_3^+]^{3+}$
	355	$[M-4I^--2CH_3^+]^{2+}$

3.5 ESI mass spectra of zwitterionic compounds

A set of zwitterionic compounds was also investigated by ESI mass spectrometry. In general, the positive ion mode gave better results than the negative one. A series of peaks at intervals of 122 Da indicating loss of the sulfopropyl unit could be observed. Additionally, loss of the H_2SO_3 (82 Da) moiety was detected in some cases.

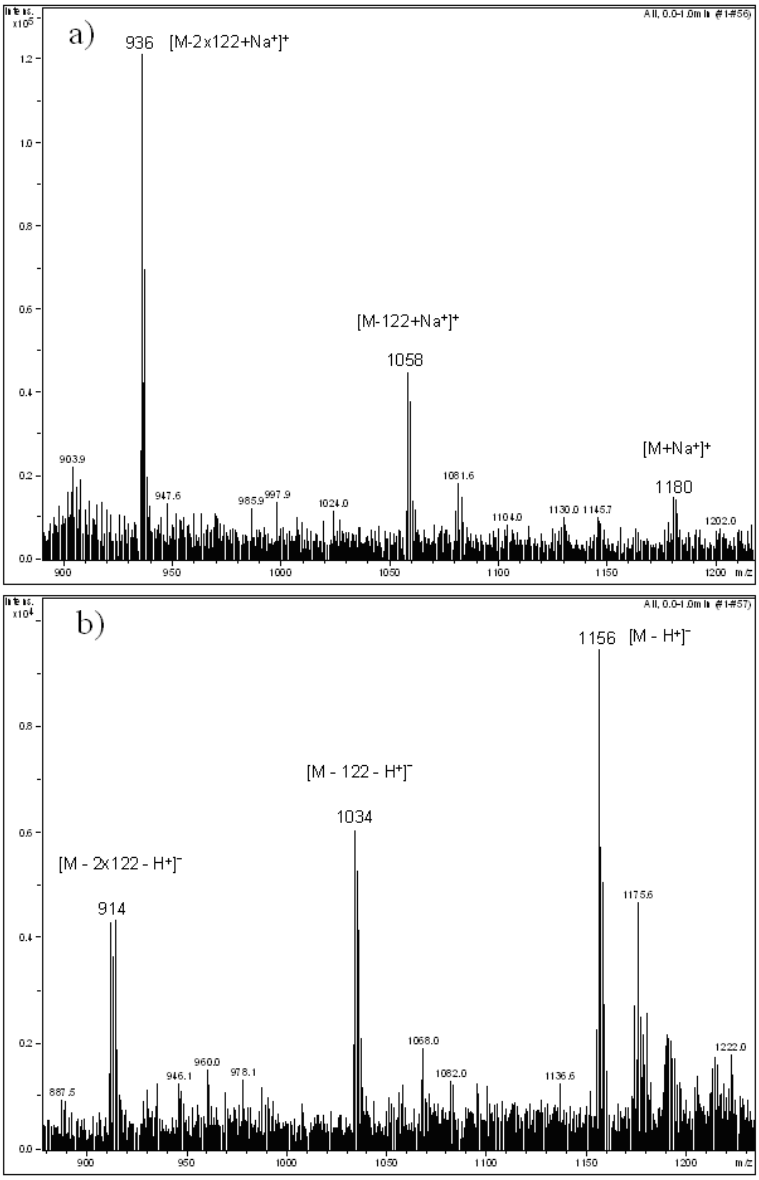

Figure 3.6. Positive a) and negative b) ion mode ESI mass spectra of SubPcOPPS **36**.

Only in the case of SubPcOPPS **36** an interpretable negative ion mode spectrum was obtained (Fig. 3.6). A sharp signal appeared at *m/z* 1156 $[M\text{-}H^+]^-$ together with two other

peaks corresponding to loss of one and two sulfopropyl units, respectively: at *m/z* 1034 $[M\text{-}122\text{-}H^+]^-$ and *m/z* 912 $[M\text{-}2x122\text{-}H^+]^-$. On the other hand, the positive ion mode ESI spectrum revealed the presence of ions resulting from sodium attachment. Thus, the low intensity peak at *m/z* 1180 could be attributed to an ion of the following composition: $[M+Na^+]^+$. Two other intense peaks were attributed to ions resulting from loss of the sulfopropyl unit; *i.e. m/z* 1058 $[M–122+Na^+]^+$ and *m/z* 936 $[M\text{-}2x122+Na^+]^+$.

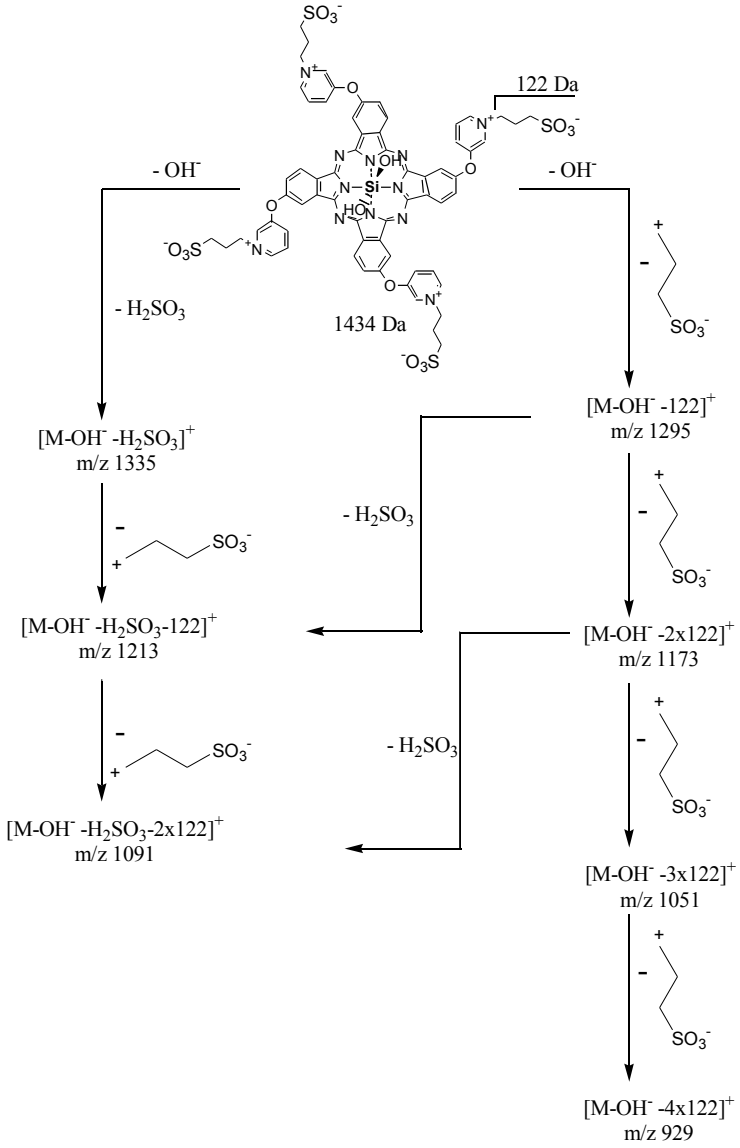

Figure 3.7. Fragmentation pattern observed in the positive ion mode ESI mass spectrum of SiPcOPPS **15**. Two series of peaks were discernible and attributed to loss of sulfopropyl unit or H_2SO_3 moiety.

The positive ion mode ESI-MS spectrum of SiPcOPPS **15** was fairly complex and comprised two sets of peaks corresponding to singly charged ions (Fig. 3.7). The loss of

the sulfopropyl unit or H_2SO_3 moiety was always accompanied by loss of one axial OH^- group, *i.e.* positive ion formation was due to the cleavage of OH^- from the neutral molecule. In other words positive ion formation was due to cleavage of OH^- from neutral molecule. Hence, peaks centred at *m/z* 1295, *m/z* 1173, *m/z* 1051 and *m/z* 929 matched loss of one, two, three and four sulfopropyl chains, respectively. A low intensity peak at *m/z* 1335 fitted to loss of the H_2SO_3 moiety. Furthermore, two peaks of moderate intensity were discerned and attributed to loss of one and two sulfopropyl units: *m/z* 1213 $[M\text{-}OH^-\text{-}H_2SO_3\text{-}122]^+$ and *m/z* 1091 $[M\text{-}OH^-\text{-}H_2SO_3\text{-}2x122]^+$. No demetallation under electrospray ionization conditions was observed for SiPcOPPS **15**.

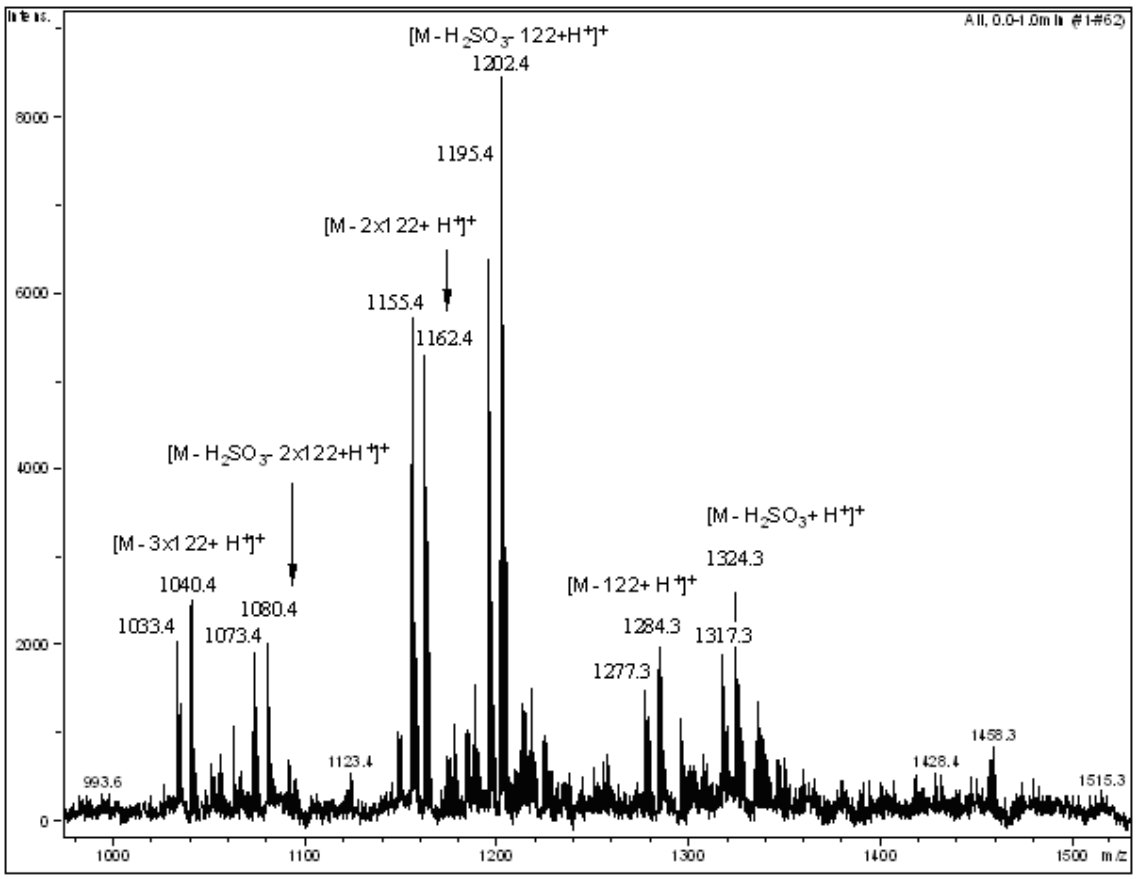

Figure 3.8. Positive ion mode ESI mass spectrum of PO(tbc)OPPS **31**. Every peak in the spectrum is accompanied by a peak, which is always centered at a 7 Da lower value.

In general, the positive ion mode spectrum of spectrum of PO(tbc)OPPS **31** revealed two series of peaks, one of which matched to successive loss of one, two and three sulfopropyl chains followed by proton attachment: *m/z* 1284 $[M–122+H^+]^+$, *m/z* 1162

$[M\text{-}2x122+H^+]^+$, *m/z* 1040 $[M\text{-}3x122+H^+]^+$, while the other set of peaks could be attributed to loss of a H_2SO_3 unit, a sulfopropyl chain and a proton attachment: *m/z* 1324 $[M\text{-}H_2SO_3+H^+]^+$, *m/z* 1202 $[M\text{-}H_2SO_3\text{–}122+H^+]^+$, *m/z* 1080 $[M\text{-}H_2SO_3\text{-}2x122+H^+]^+$. Interestingly, every described peak has its counterpart in the spectrum, which is always centred at a 7 Da lower value (*e.g. m/z* 1162 Da and *m/z* 1162 – 7 = 1155 Da). However, the origin and composition of ions attributed to these peaks remain unclear (Fig. 3.8).

The positive ion mode spectrum of ZnPoOPPS **50** did not reveal the presence of a quasi-molecular ion. There was no peak indicating loss of H_2SO_3 moiety as well. The positive ion mode ESI showed two series of peaks corresponding to singly charged ions. The most intensive peak was ascribed to loss of two sulfopropyl chains and sodium attachment, *i.e. m/z* 947 $[M\text{-}2x122+Na]^+$. Two less intensive peaks matched loss of one and three sulfopropyl moieties accompanied by sodium attachment: *m/z* 1069 $[M\text{–}122+Na]^+$ and *m/z* 825 $[M\text{-}3x122+Na]^+$. Analogously, two low intensity peaks were discernible and easily attributed to proton attachment: *m/z* 925 $[M\text{-}2x122+H^+]^+$ and *m/z* 803 $[M\text{-}3x122+H^+]^+$. No demetallation under electrospray ionization conditions was observed for ZnPoOPPS **50**.

The positive ion mode spectrum of metal-free porphyrin H_2PoOPPS **47**, as in the case of zinc porphyrin ZnPoOPPS **50**, did not reveal either a quasi-molecular ion or loss of H_2SO_3 moiety. Doubly and triply charged peaks resulting from proton or sodium attachment were found: *m/z* 576 $[M+2Na^+]^{2+}$, *m/z* 554 $[M+2H^+]^{2+}$ and *m/z* 370 $[M+3H^+]^{3+}$. Moreover, there were peaks corresponding to loss of one up to four sulfopropyl units.

Neither positive nor negative ESI showed reasonable spectra for H_2PcOPPS **12** and GePcOPPS **18**. In Table 3.2 identified peaks of positive and negative ions for the zwitterionic water-soluble macrocyclic complexes are listed.

Table 3.2. Identified positive and negative ions for zwitterionic water-soluble compounds.

Compound	m/z	Assignment
SiPcOPPS (15)	1295	$[M\text{-}OH^{-}\text{-}122]^{+}$
	1173	$[M\text{-}OH^{-}\text{-}2x122]^{+}$
	1051	$[M\text{-}OH^{-}\text{-}3x122]^{+}$
	929	$[M\text{-}OH^{-}\text{-}4x122]^{+}$
	1335	$[M\text{-}OH^{-}\text{-}H_2SO_3]^{+}$
	1213	$[M\text{-}OH^{-}\text{-}H_2SO_3\text{-}122]^{+}$
	1091	$[M\text{-}OH^{-}\text{-}H_2SO_3\text{-}2x122]^{+}$
PO(tbc)OPPS (31)	1284	$[M\text{-}122+H^{+}]^{+}$
	1162	$[M\text{-}2x122+H^{+}]^{+}$
	1040	$[M\text{-}3x122+H^{+}]^{+}$
	1324	$[M\text{-}H_2SO_3+H^{+}]^{+}$
	1202	$[M\text{-}H_2SO_3\text{-}122+H^{+}]^{+}$
	1080	$[M\text{-}H_2SO_3\text{-}2x122+H^{+}]^{+}$
SubPcOPPS (36)	1180	$[M+Na^{+}]^{+}$
	1058	$[M\text{-}122+Na^{+}]^{+}$
	936	$[M\text{-}2x122+Na^{+}]^{+}$
	1156	$[M\text{-}H^{+}]^{-}$
	1034	$[M\text{-}122\text{-}H^{+}]^{-}$
	912	$[M\text{-}2x122\text{-}H^{+}]^{-}$
H_2PoOPPS (47)	576	$[M+2Na^{+}]^{2+}$
	554	$[M+2H^{+}]^{2+}$
	370	$[M+3H^{+}]^{3+}$
	741	$[M\text{-}3x122+H^{+}]^{+}$
	619	$[M\text{-}4x122+H^{+}]^{+}$
	493	$[M\text{-}122+2xH^{+}]^{2+}$
	432	$[M\text{-}2x122+2xH^{+}]^{2+}$
	247	$[M\text{-}3x122+3H^{+}]^{3+}$

	1007	$[M-122+Na^+]^+$
	885	$[M-2x122+Na^+]^+$
ZnPoOPPS (50)	1069	$[M-122+Na^+]^+$
	947	$[M-2x122+Na^+]^+$
	925	$[M-2x122+H^+]^+$
	825	$[M-3x122+Na^+]^+$
	803	$[M-3x122+H^+]^+$

3.6 ESI mass spectra of negatively charged compounds

Contrary to the expectation that molecule with negatively charged functionalities should rather give better negative ion ESI mass spectra, excellent positive ion ESI spectra were recorded for sulfonated phthalocyanines. Moreover, the bulk of the investigated compounds gave exclusively positive ion ESI mass spectra with the only exception being H_2PcTS **20** and SiPcTS **25**, for which negative ions were detected. One should mention that although many attempts were undertaken in our laboratory for a very long time, we had not been able to obtain any satisfactory results with sulfonated compounds. Finally, it was found that the presence of ammonium formate $HCOONH_4$ (volatile buffer) in the spraying solution is essential for obtaining good ESI spectra. However, one has to point out that the role of ammonium formate in the ionization process remains obscure. Independently of what is the role of this organic salt, it works and it furnishes us with an excellent tool, until now not available in our laboratory, for the analysis of sulfonated phthalocyanines.

A sample of SiPcTS **25** obtained by chlorosulfonation of the silicon phthalocyanine **22** was studied both in the positive and the negative ion mode. The positive ion mode ESI-MS showed a series of peaks, one of which, at *m/z* 895, corresponds to the protonated monomeric form $[M+H^+]^+$. The negative ion mode ESI-MS revealed the quasi-molecular ion peak at *m/z* 893 $[M-H^+]^-$ and two other peaks of high intensity. The peaks at *m/z* 813 and *m/z* 733 were attributed to loss of one SO_3, *i.e.* $[M-SO_3-H^+]^-$, as well as

two SO_3, *i.e.* $[M\text{-}2SO_3\text{-}H^+]^-$, moieties. The positive ion mode ESI-MS showed peaks which could be attributed to loss of one axial OH^- group: *m/z* 877 $[M\text{-}OH^-]^+$, *m/z* 797 $[M\text{-}OH^-\text{-}SO_3]^+$ and *m/z* 717 $[M\text{-}OH^-\text{-}2SO_3]^+$. The most intensive peaks in the positive ion mode originated from di- and trisulfonated silicon phthalocyanine: *m/z* 735 $[M\text{-}2SO_3\text{+}H^+]^+$ and *m/z* 815 $[M\text{-}SO_3\text{+}H^+]^+$. No evidence for demetallation of SiPcTS **25** was found (Fig. 3.9).

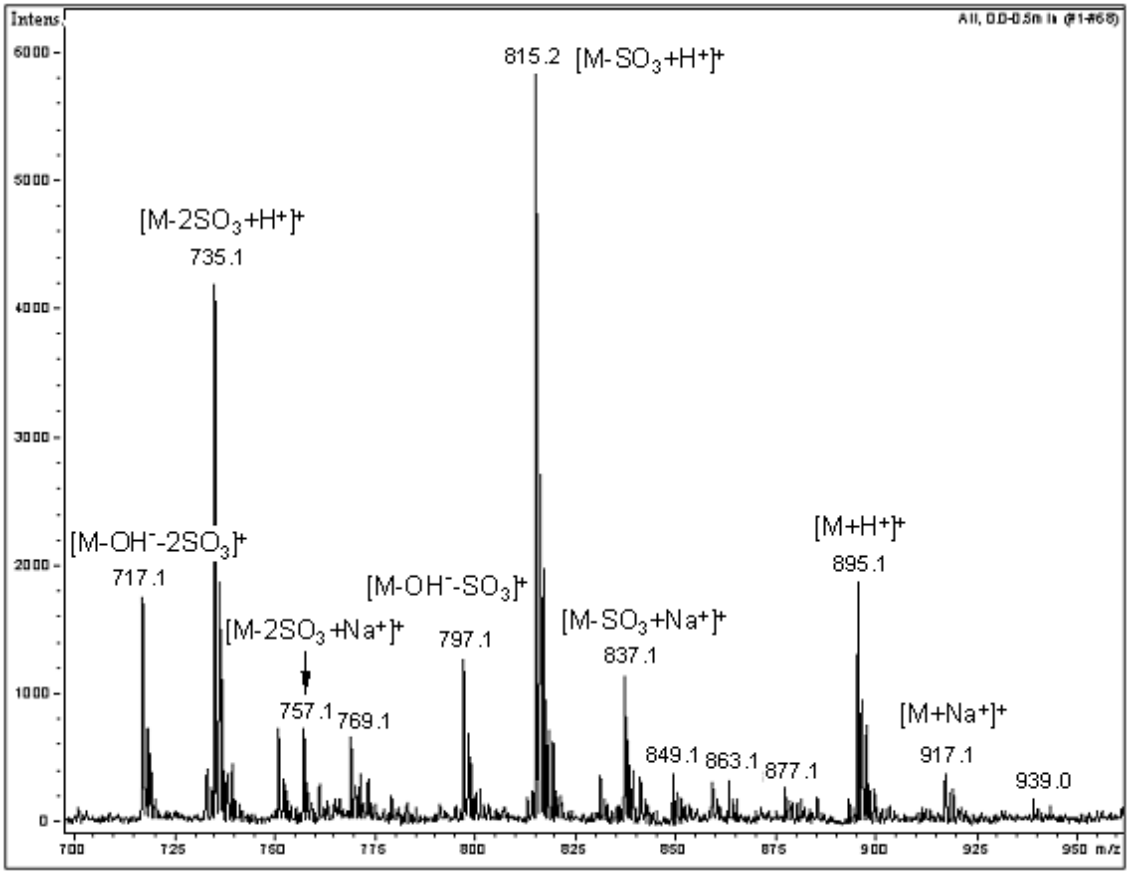

Figure 3.9. Positive ion ESI mass spectrum of SiPcTS **25** in 50 mM aqueous ammonium formate solution (M refers to $SiPc(SO_3H)_4$).

For GePcTS **28**, obtained by chlorosulfonation of GePc **26**, only a positive ion ESI spectrum could be obtained. No quasi-molecular ion peak was discernible for GePcTS **28**. The peak at *m/z* 923 for the singly charged moiety appeared, clearly indicating loss of one OH^- group: $[M\text{-}OH^-]^+$. Intensive peaks at *m/z* 843 and *m/z* 763 reflect loss of one and two SO_3 moieties: $[M\text{-}OH^-\text{-}SO_3]^+$, $[M\text{-}OH^-\text{-}2SO_3]^+$. Two significant sodium adduct peaks were also observed; *i.e. m/z* 865 $[M\text{-}OH^-\text{-}H^+\text{-}SO_3\text{+}Na^+]^+$ and *m/z* 785 $[M\text{-}OH^-\text{-}H^+\text{-}2SO_3\text{+}Na^+]^+$.

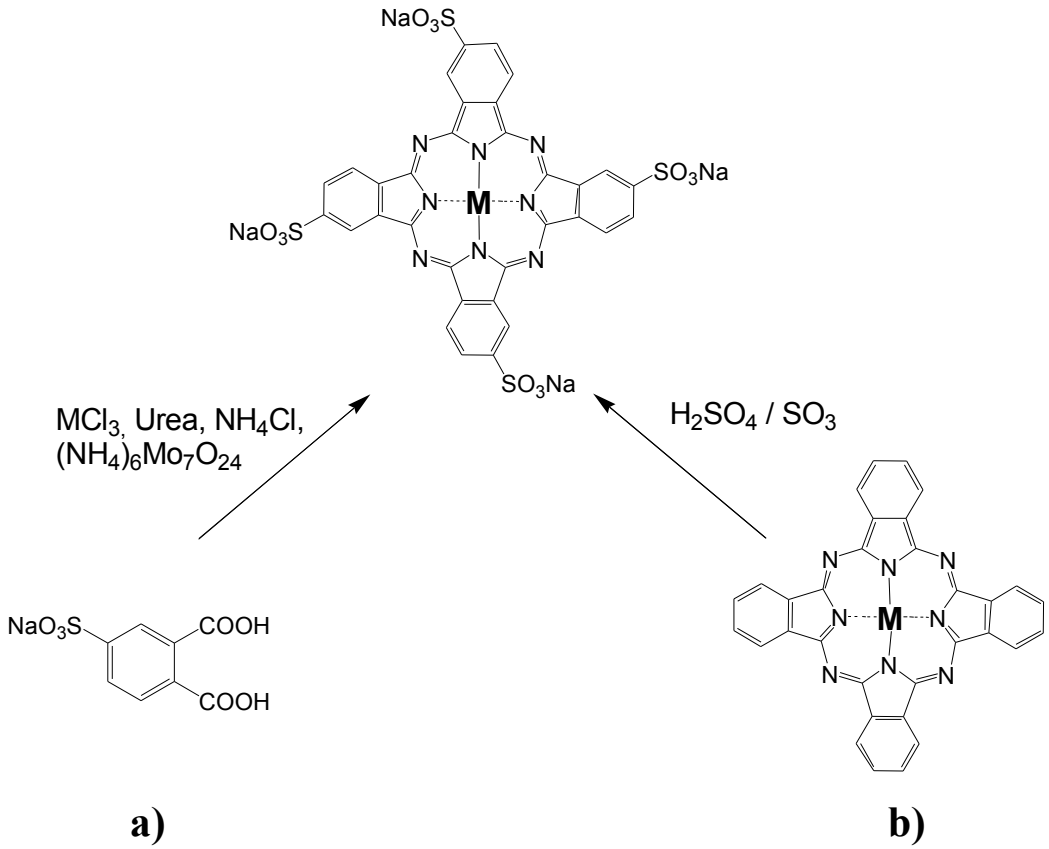

Figure 3.10. Synthesis of sulfophthalocyanines via template cyclotetramerization of 4-sulfophthalic acid is expected to give exclusively the tetrasulfonated product, a). The direct sulfonation of an unsubstituted phthalocyanine may result in a mixture of differently substituted phthalocyanines, b).

Both SiPcTS **25** and GePcTS **28** were produced by chlorosulfonation of the corresponding phthalocyanines. However, it remains questionable whether chlorosulfonation gives purely tetrasulfonated compounds or rather results in a mixture of products with various extent of sulfonation. Hence, a set of phthalocyanines obtained via template cyclotetramerization of 4-sulfophthalic acid was investigated: ZnPcTS **53**, GaPcTS **55**, AlPcTS **54** and H_2PcTS **20**. This method is expected to give exclusively phthalocyanines with four sulfonates (Fig. 3.10). A comparison of the spectra of compounds obtained via sulfonation and template cyclotetramerization is expected to give an interesting piece of information, namely to answer the question whether the peaks attributed to loss of SO_3 units in SiPcTS **25** and GePcTS **28** really originate from fragmentation process or rather indicate that the sample is a mixture of differently substituted species.

Thus, ZnPcTS **53** gave only one peak in the positive ion mode at *m/z* 897 for the singly charged, protonated ion $[M+H^+]^+$. There was no peak indicating loss of sulfonate.

The positive ion ESI spectrum of AlPcTS **54** was successfully recorded. The spectrum showed loss of OH^- group and a set of peaks attributed to mono-, di-, tri- and tetrasodium adducts. As before no peaks attributed to mono-, di- and trisulfonated form of AlPc were found (Fig. 3.11).

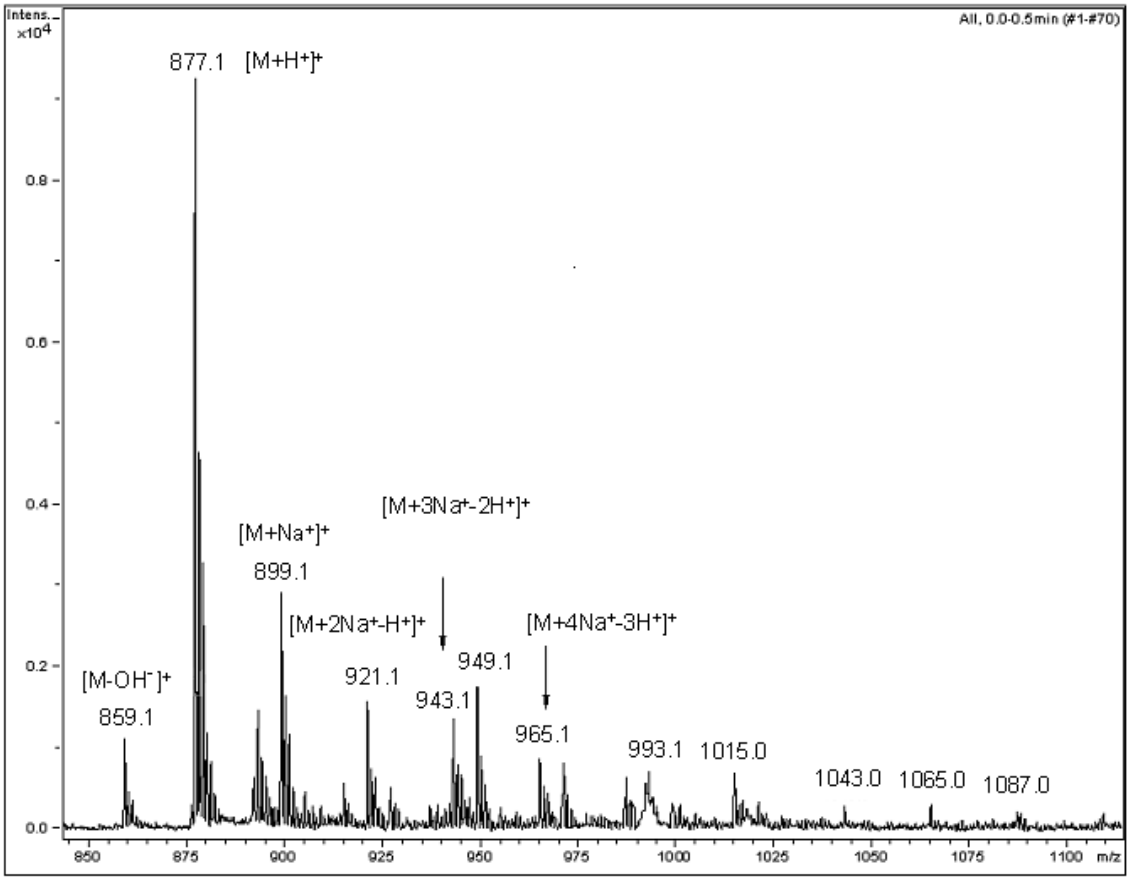

Figure 3.11. Positive ion ESI mass spectrum of AlPcTS **54** in 50 mM aqueous ammonium formate solution (M refers to $AlPc(SO_3H)_4$)..

The positive ion ESI spectrum of GaPcTS **55** was nearly identical with that observed for AlPcTS **54**. The positive ion mode ESI spectrum of GaPcTS **55** showed the presence of a mono-protonated tetrasodium adduct at *m/z* 1007 $[M-3H^++4Na^+]^+$. However, the most intensive peak could be attributed to an ion derived from loss of one axial OH^- group, *i.e. m/z* 901 $[M-OH^-]^+$. A series of peaks at intervals of 22Da indicated mono-, di- and trisodium adducts of a molecule derived from axial OH^- group loss: *m/z* 923 $[M-H^++Na^+-OH^-]^+$, *m/z* 945 $[M-2H^++2Na^+-OH^-]^+$ and *m/z* 967 $[M-3H^++3Na^+-OH^-]^+$. The

peak at *m/z* 989 matched the singly charged tetrasodium adduct, $[M-4H^{+}+4Na^{+}-OH^{-}]^{+}$. No evidence for loss of SO_3 was found.

Contrary to the cases mentioned above, the mass spectrum of H_2PcTS **20**,obtained via template cyclotetramerization of 4-sulfophthalic acid, showed loss of SO_3 moiety. The positive ion ESI spectrum revealed peak at *m/z* 755 that could be clearly attributed to the trisulfonated moiety; *i.e.* $[M+H^{+}-SO_3]^{+}$. Similarly, the negative ion ESI-MS confirmed the presence of trisulfonated ion: *m/z* 753 $[M-H^{+}-SO_3]^{-}$. These results clearly indicate that under the ionization conditions cleavage of the S-benzene bond might occur leading to the corresponding tri-sulfophthalocyanine.

Taking into account the results obtained for H_2PcTS **20**, an unambiguous answer for the question of the extent of sulfonation of phthalocyanines is not possible. Disulfonated or trisulfonated species present in the product would give the same mass spectrum as loss of a sulfonate in the mass spectrum of purely tetrasulfonated SiPcTS **25** or GePcTS **28**. However, no evidence for penta-sulfonated phthalocyanines, or phthalocyanines of higher degree of sulfonation, was found. These results are in contrast with those reported by D. W. Dixon *et al*. [15]. They found mass spectral evidence for penta-sulfonated species when these species were made by sulfonation of the metal-free phthalocyanine. It seems to be rather reasonable to consider sulfonated silicon and germanium phthalocyanines obtained during this work as a mixture of compounds with four, three and two sulfonates. There was no peak indicating monosulfonated phthalocyanine.

In Table 3.3 all identified peaks for sulfonated phthalocyanines are listed. In case of **25**, **28**, **53**, **54** and **55** M refers to the metal containing tetrasulfonated phthalocyanine molecule $Pc(SO_3H)_4$. In case of metal-free phthalocyanine **20** M refers to $H_2Pc(SO_3H)_4$.

Table 3.3. ESI-MS of buffer solution (50 mM water solution of ammonium formate) of sulfonated dyes.

Compound	*m/z*	Assignment
H_2PcTS (20)	835	$[M+H^+]^+$
	857	$[M+Na^+]^+$
	755	$[M-SO_3+H^+]^+$
	833	$[M-H^+]^-$
	753	$[M-SO_3-H^+]^-$
Si(tbc)TS (23)	908	$[M+2Na^+-H^+]^+$
	886	$[M+Na^+]^+$
	806	$[M-SO_3+Na^+]^+$
	862	$[M-H^+]^-$
	782	$[M-SO_3-H^+]^-$
SiPcTS (25)	939	$[M+2Na^+-H^+]^+$
	917	$[M+Na^+]^+$
	895	$[M+H^+]^+$
	877	$[M-OH^-]^+$
	837	$[M-SO_3+Na^+]^+$
	815	$[M-SO_3+H^+]^+$
	797	$[M-OH^--SO_3]^+$
	757	$[M-2SO_3+Na^+]^+$
	735	$[M-2SO_3+H^+]^+$
	717	$[M-OH^--2SO_3]^+$
	893	$[M-H^+]^-$
	813	$[M-SO_3-H^+]^-$
	733	$[M-2SO_3-H^+]^-$
GePcTS (28)	923	$[M-OH^-]^+$
	843	$[M-OH^--SO_3]^+$
	763	$[M-OH^--2SO_3]^+$
	865	$[M-OH^--SO_3+Na^+-H^+]^+$
	785	$[M-OH^--2SO_3+Na^+-H^+]^+$

ZnPcTS (53)	897	$[M+H^+]^+$
AlPcTS (54)	877	$[M+H^+]^+$
	859	$[M-OH^-]^+$
	899	$[M+Na^+]^+$
	921	$[M+2Na^+-H^+]^+$
	943	$[M+3Na^+-2H^+]^+$
	965	$[M+4Na^+-3H^+]^+$
GaPcTS (55)	901	$[M-OH^-]^+$
	989	$[M-OH^-+4Na^+-4H^+]^+$
	1007	$[M+4Na^+-3H^+]^+$
	923	$[M-OH^-+Na^+-H^+]^+$
	945	$[M-OH^-+2Na^+-2H^+]^+$
	923	$[M-OH^-+Na^+-H^+]^+$
	967	$[M-OH^-+3Na^+-3H^+]^+$
	985	$[M+3Na^+-2H^+]^+$
	1029	$[M+5Na^+-H^+]^+$

3.7 Conclusion

NMR is a useful technique for many soluble phthalocyanine derivatives. However, in many cases obtaining of good NMR spectra may be hindered, if possible, by the very strong tendency of phthalocyanine derivatives to aggregate in solution, resulting in brodening and strong dependence of peak positions on concentration. Therefore, mass spectrometry, in particular ESI and MALDI, are becoming indispensable tools in the analysis of these compounds. In this work the usefulness of ESI mass spectrometry in the characterisation of water-soluble phthalocyanines and related compounds was investigated. ESI-MS proved to be an excellent analytical technique for most of the investigated charged water-soluble photosensitizers as it does not suffer from aggregation phenomenon and strong intermolecular interactions characteristic for zwitterions. Furthermore, ESI-MS, as a very soft ionization technique, usually provides direct information regarding the compound investigated, *i.e.* the quasi-molecular ion peak.

A careful examination of the ESI-MS spectra revealed several processes, *i.e.*:

- N-demethylation, characteristic for positively charged compounds.
- Loss of the sulfopropyl moiety, characteristic for zwitterions.
- Loss of axial substituents, *i.e.* $C_6H_5O^-$ or $C_6H_5^+$ found for SubPc`s, as well as loss of the $OH^-$ group observed for AlPcTS, SiPc`s and GePc`s.
- Elimination of H_2SO_3 (*m/z* 82), characteristic for zwitterions.
- Loss of SO_3 (*m/z* 80) observed for sulfonated compounds.
- Demetallation, however, observed only for GePcOPM **17** and ZnPoOPM **49**.
- Water addition, observed for PO(tbc)OPM **30**.

ESI-MS helped to shed light on structural characteristic of the sulfophthalocyanines obtained via chlorosulfonation of the unsubstituted parent compound; they seem to be composed of a mixture of di-, tri- and tetrasulfophthalocyanines – no evidence of mono- and pentasulfophthalocyanines has been found. For the first time in our laboratory the ESI-MS has been successfully implemented for characterization of sulfophthalocyanines.

3.8 References

[1] Rayleigh, Lord; *Phil. Mag.* **1882**, 14, 184.

[2] Zeleny, J,; *Phys. Rev.* **1914**, 3, 69.

[3] Zeleny, J; *Proc. Comb. Phil. Soc.* **1915**, 18, 17.

[4] Zeleny, J.; *Phys. Rev.* **1917**, 10, 1.

[5] Dole, M.; Mack, L. L.; Hines, R. L.; Mobley, R. C.; Ferguson, R. C.; Alice, M. B.; *J. Chem. Phys.* **1968**, 49, 2240-2249.

[6] Fenn, J. B.; *Electrospray wings for molecular elephants*, Nobel Lecture, December 8, **2002**.

[7] de Hoffmann, E.; Charette, J.; Stroobant, V.; "Spektrometria mass", Wydawnictwo Naukowo-Techniczne, Warszawa **1998**.

[8] Batinic-Haberle, I.; Stevens, R. D.; Fridovich, I.; *J. Porphyrins Phthalocyanines*, **2000**, 4, 217-227.

[9] Kachadourian, R.; Srinivasan, N.; Haney, C. A.; Stevens, R. D.; *J. Porphyrins Phthalocyanines*, **2001**, 5, 507-511.

[10] Bressan, M.; Celli, N.; d`Alessandro, N.; Liberatore, L.; Mprvillo, A.; Tonucci, L.; *J .Organometal. Chem.* **2000**, 594, 416-420.

[11] d`Alessandro, N.; Tonucci, L.; Dragani, L.; Morvillo, A.; Bressan, M.; *J. Porphyrins Phthalocyanines,* **2003**, 7, 484-492.

[12] Beeby, A.; FitzGerald, S.; Stanley, C. F.; *Photochem. Photobiol.* **2003**, 74, 566.

[13] Kudrevich, S. V.; Brasseur, N.; La Mmadelaine, C.; Gilbert, S, van Lier J. E.; *J. Med. Chem.* **1997**, 40, 3897.

[14] Sanchez, M.; Fache, E.; Bonnet, D.; Meunier, B.; *J. Porphyrins Phthalocyanines* **2001**, 5, 867.

[15] Dixon, D. W.; Gill, A. F.; Sook, B. R.; Characterization of Sulfonated Phthalocyanines by Mass Spectrometry and Capillary Electrophoresis, *J Porphyrins Phthalocyanines*, in press.

[16] Gerdes, R.; Bartels, O.; Schneider, G.; Wöhrle, D.; Schulz-Ekloff, G.; *Polym. Adv. Technol.* **2001**, 12, 152-160.

[17] Fox, J. P.; Goldberg, D. P.; *Inorg. Chem*. **2003**, 42, 8181-8191.

4. Optical Properties of New Water Soluble Photosensitizers In Solution

4.1 Introduction

In the reported results, conditions under which the measurements were made are explicitly stated. In chapters 4.2 and 4.3 results concerning solubility, absorption in aqueous system, extinction coefficients and emission maxima are tabulated. Chapter 4.4 collects data that illustrate the effects of substituents, pH, electrolytes and addition of disaggregating agents. The aggregation behaviour is studied qualitatively by comparison of the UV-Vis spectra at different pH values and in the presence and absence of surfactants.

4.2 Solubility

All the positively charged compounds, with the exception of axially substituted, positively charged SubPc **44**, exhibit good solubility in water (see Table 4.1). SubPc **44** is only sparingly soluble in water as it has only one charge at the bulky hydrophobic group. SubPc **44** to some extent is soluble in CH_2Cl_2 and acetone. All alkylated products are excellent soluble in organic solvents like DMF and DMSO. Both solvents significantly reduce aggregation of the positively charged compounds. N-methylation has no influence on the position of Q-band. Table 4.1 collects all data concerning solubility of the positively charged dyes.

Table 4.1. Solubility of positively charged photosensitizers (+++ very good solubility, ++ moderate solubility, + only sparingly soluble, - not soluble).

Compound	Solubility					
	H_2O	**DMF**	**DMSO**	**MeOH**	**Acetone**	**CH_2Cl_2**
H_2PcOPM **11**	+++	+++	+++	++	-	-
SiPcOPM **14**	+++	+++	+++	++	-	-
GePcOPM **17**	+++	+++	+++	++	-	-
PO(tbc)OPM **30**	+++	+++	+++	+++	-	-
SubPc **35**	+++	+++	+++	++	-	-
SubPc **39**	+++	+++	+++	++	-	-
SubPc **41**	+++	+++	+++	++	-	-
SubPc **44**	+	+++	+++	++	++	++
H_2PoOPM **46**	+++	+++	+++	++	-	-
ZnPoOPM **49**	+++	+++	+++	++	-	-

Zwitterionic compounds exhibit lower solubility in water in comparison to the positively charged derivatives (see Table 4.2). It was observed that the solubility is greatly increased at higher pH value or in water solution of inorganic salts (*e.g.* 6 M KCl solution), in other words in solution of higher ionic strength [1]. This feature can be probably explained on the basis of strong intermolecular interaction, caused by attractive forces between negative and positive functionality. Such interaction would lead to "intermolecular net" formation. In some cases the attractive forces seem to be particularly strong what entirely prevents water solubility (*e.g.* H_2PcOPPS **12**). Figure 4.1 shows hypothetical structure of the intermolecular net formed by zwitterionic metal-free phthalocyanine **12**. This undesirable interactions lead not only to lower solubility but also to decrease of the photocatalytic activity, as molecules from the intermolecular net efficiently quench other excited molecules present nearby. An essential prerequisite

during photocatalytic measurements is monomerization of the photosensitizer in solution [2].

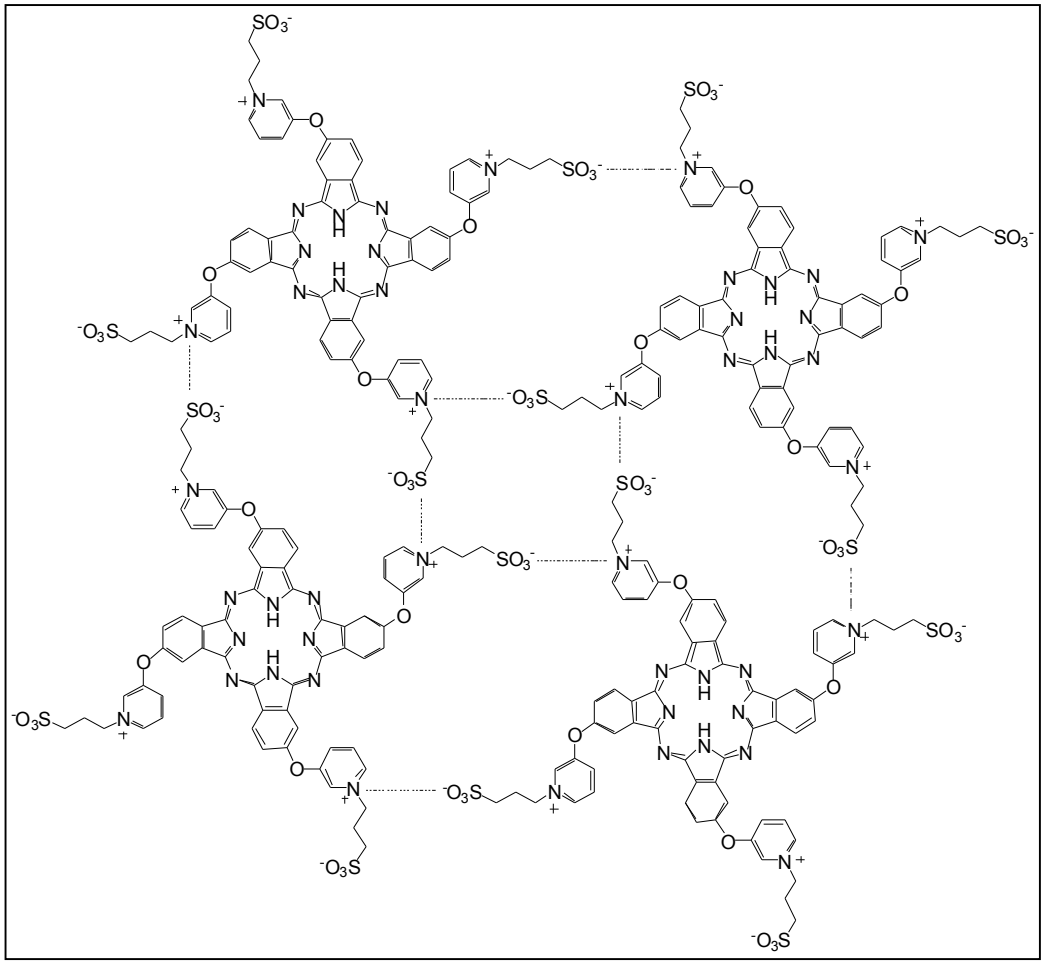

Figure 4.1. Hypothetical structure of the intermolecular net formed by the zwitterionic metal-free phthalocyanine **12**.

Table 4.2 collects all the data concerning solubility of zwitterionic dyes.

Negatively charged compounds H_2PcTS **20**, Si(tbc)TS **23**, SiPcTS **25** and GePcTS **28** show excellent solubility in water (see Table 4.3). Unlike H_2PcTS **20** and Si(tbc)TS **23**, both SiPcTS **25** and GePcTS **28** are only slightly soluble in DMF.

Table 4.2. Solubility of zwitterionic photosensitizers (+++ very good solubility, ++ moderate solubility, + only sparingly soluble, - not soluble).

Compound	Solubility					
	H_2O	**DMF**	**DMSO**	**MeOH**	**Acetone**	**CH_2Cl_2**
H_2PcOPPS **12**	-	-	+	-	-	-
SiPcOPPS **15**	+++	-	++	++	-	-
GePcOPPS **18**	++	-	+	-	-	-
PO(tbc)OPPS **31**	+++	+	++	+	-	-
SubPc **36**	++	+	++	-	-	-
H_2PoOPPS **47**	+++	-	+	+	-	-
ZnPoOPPS **50**	+++	+	+++	++	-	-

Table 4.3. Solubility of negatively charged photosensitizers (+++ very good solubility, ++ moderate solubility, + only sparingly soluble, - not soluble).

Compound	Solubility					
	H_2O	**DMF**	**DMSO**	**MeOH**	**Acetone**	**CH_2Cl_2**
H_2PcTS **20**	+++	++	+	+	-	-
Si(tbs)TS **23**	+++	++	+	+	-	-
SiPcTS **25**	+++	+	+	-	-	-
GePcTS **28**	+++	+	+	-	-	-

4.3 Bands position and absorption coefficients

Each group of the dye shows the characteristic Q and Soret band absorption. The position of the absorption band and the value of the absorption coefficient strongly

depend on solvent, pH value and presence of additives like SDS, CTAC or electrolytes. The position of Q and Soret bands as well as their absorption coefficients were measured and collected in Table 4.4. Spectra are given in chapter 4.4.

Table 4.4. UV-Vis data of the water-soluble dyes: bands positions, extinction coefficients and fluorescence (recorded in DMF, unless indicated otherwise).

COMPOUND	**SOLVENT**	**ABSORPTION [nm] (ε x 10^5 M^{-1} cm^{-1})**	**FLUORESCENCE [nm]**
H_2PcOPM **11**	H_2O, pH 13, SDS 0.1M. H_2O, pH 7, SDS 0.1M.	673(0.75), 608. 694(1.5), 659(1.3).	681
H_2PcOPPS **12**	H_2O, pH 13, SDS 0.1M. H_2O, pH 7, SDS 0.1M.	693(0.51), 671(0.78). 695(1.00), 661(0.91).	
SiPcOPM **14**	H_2O, pH 13, SDS 0.1M. H_2O, pH 7, SDS 0.1M.	675(1.22), 641(0.58). 675(1.24), 642(0.61).	678
SiPcOPPS **15**	H_2O, pH 13, SDS 0.1M.	678(1.45), 609(0.31).	
GePcOPM **17**	H_2O, pH 13, SDS 0.1M. H_2O, pH 7, SDS 0.1M.	678(0.89),645(0.38),613(0.3). 678(0.33), 643(0.52).	681
GePcOPPS **18**	H_2O, pH 13, SDS 0.1M.	678(0.89), 644(0.61).	
H_2PcTS **20**	H_2O, pH 13, CTAC 0.1M. H_2O, pH 7, CTAC 0.1M.	679(0.55), 611. 696(0.62), 663(0.63).	677(in H_2O)
Si(tbc)TS **23**	H_2O, pH 13. H_2O, pH 7.	671(0.23), 454(0.48), 441, 425, 412. 670(0.2), 643, 452(0.33), 441, 423.	677
SiPcTS **25**	H_2O, pH 7.	673(0.82), 604.	677
GePcTS **28**	H_2O, pH 7.	680(1.08), 609(0.23), 354(0.51).	680
PO(tbc)OPM **30**	H_2O, pH 13, SDS 0.1M. H_2O, pH 7, SDS 0.1M.	659(0.96), 620(0.43), 595(0.3), 445(2.9), 437(1.08), 416(0.63). 658(0.84), 634, 601, 443(1.96),	

		413.	
PO(tbc)OPPS **31**	H_2O, pH 13, SDS 0.1M.	659(0.84), 621(0.41), 596(0.27), 445(1.55), 416(0.57).	
	H_2O, pH 7, SDS 0.1M.	658(0.69), 636, 602, 443(1.6), 414.	
SubPc **35**	H_2O.	585(0.75), 285(0.74), 216(0.81).	
SubPc **36**	H_2O, 0.6 M KCl.	579(0.2), 547(0.21), 286(0.46), 205(0.6).	
SubPc **39**	H_2O.	567(0.31), 309(0.17).	582(in H_2O)
SubPc **41**	H_2O.	562(0.21).	
SubPc **44**	DMF.	565(0.64).	576
H_2PoOPM **46**	H_2O, pH 13, SDS 0.1M.	421, 441, 580.	
	H_2O, pH 7.	419, 515, 550, 581, 637.	
H_2PoOPPS **47**	H_2O, pH 13, SDS 0.1M.	426, 514, 578.	
	H_2O, pH 7.	420, 516, 553, 581, 638.	
ZnPoOPM **49**	H_2O, pH 13, SDS 0.1M.	452, 569, 609.	
	H_2O, pH 7, SDS 0.1M.	446, 567, 609.	
ZnPoOPPS **50**	H_2O, pH 13, SDS 0.1M.	451, 569, 615.	
	H_2O, pH 7, SDS 0.1M.	455, 569, 615.	

4.4 Aggregation - effect of additives, pH value, electrolytes and solvent

The phenomenon of aggregation is generally viewed as an association of molecules in solution. In the case of phthalocyanines, aggregation is usually depicted as a coplanar interaction of rings progressing from monomer to dimmer and higher order structures.

The driving force for aggregation process is a non-covalent attractive interaction of the π electron system of the phthalocyanine rings [1].

Water-soluble phthalocyanines have been widely investigated due to their photocatalytic ability to generate singlet oxygen [1,2,3]. The singlet oxygen generation requires that the photosensitizer be in the monomeric state in an aqueous medium. A very effective approach to circumvent aggregation phenomenon is to employ surfactants, which form micelles in which photosensitizer molecule may be disaggregated. The structures of two detergents that were used during these investigations are depicted in Figure 4.2.

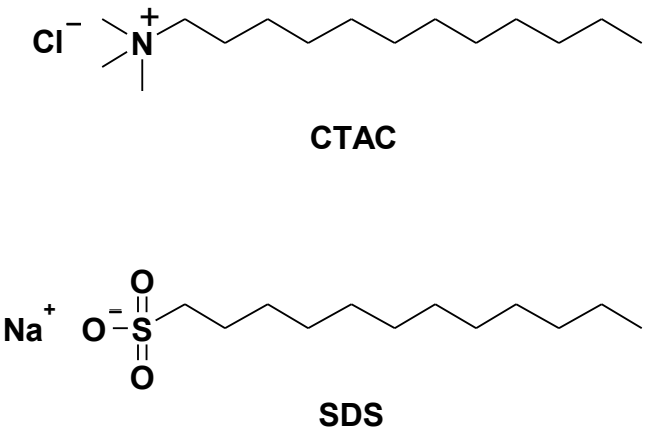

Figure 4.2. Structures of two surfactants: CTAC and SDS.

All water-soluble compounds prepared during this work have charged groups at their periphery, such as a sulfonate or quaternary aromatic amine (pyridyl). The nature of the charge determines choice of detergent as the ionic photosensitizers disaggregate better in micelles formed from surfactants with opposite charge [3]. For example, sulfonated phthalocyanine is bound to the cationic head group of the CTAC at the micelle interface, while its long hydrophobic chain interacts with the phthalocyanine ring and screens it from forming aggregates [1].

Increasing the ionic strength by addition of simple inorganic salts such as KCl or NaCl to the aqueous solution of zwitterionic dye results in a substantial improvement of solubility and, to some extent, decrease in the aggregation. The added salt has the effect of reducing attractive forces between oppositely charged groups, *i.e.* sulfonate and quaternary amine. This way, the intermolecular net is destroyed. In some cases (*e.g.* H_2PcOPPS **12**) the intermolecular attractive forces are so strong that the only way to get the compound soluble at neutral pH is addition of inorganic salt.

Aggregation results primarily from attractive interactions between two or more molecules. Thus, solvents that will have the most pronounced effects on reducing aggregation will be those that compete with the aggregation interactions. It was observed in many instances that solvents with a higher dielectric constant like DMF, DMSO or pyridine are able to screen the π-π interaction between dyes molecules [1]. Addition of water miscible organic solvents (DMF, pyridine, alcohols) to aqueous solutions of phthalocyanines and other investigated compounds has often the effect of reducing aggregates formations.

Negatively charged sulfonated phthalocyanines

Compounds SiPcTS **25** and GePcTS **28** show excellent solubility in water with strong absorption at 673 nm (ε_{H2O} = 82 000 $M^{-1}cm^{-1}$) for **25** and 680 nm (ε_{H2O} = 108 000 $M^{-1}cm^{-1}$) for **28**, respectively. An important feature of SiPcTS **25** and GePcTS **28** is lack of aggregation in a very wide range of concentrations [2]. Addition of oppositely charged detergent, CTAC, has no influence on the appearance of the UV-Vis spectra of **25** and **28**. The lack of aggregation is one of the factors that make SiPcTS **25** and GePcTS **28** so good as photocatalysts for photo-oxidation in water medium. Tetrasulfonated phthalocyanines have been well-studied. This system is complicated by having relatively small hydrophilic ionic peripheral groups appended to hydrophobic phthalocyanine ring. Beside attractive π-π interactions, there are coulomb repulsive forces from the negative charge of the sulfonate groups. Interestingly, in water the tetrasulfonated phthalocyanines have some of the highest dimmerization constants ever measured [1]. It is, for instance, well known that ZnPcTS, AlPcTS, CuPcTS or FePcTS readily aggregate in water solution.

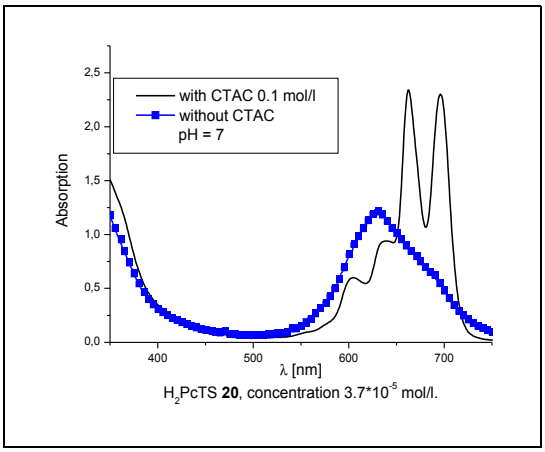

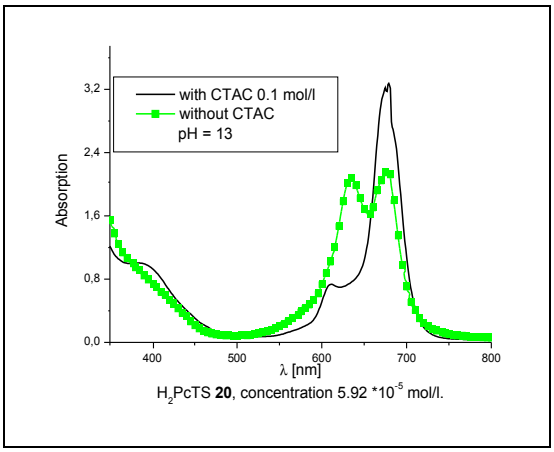

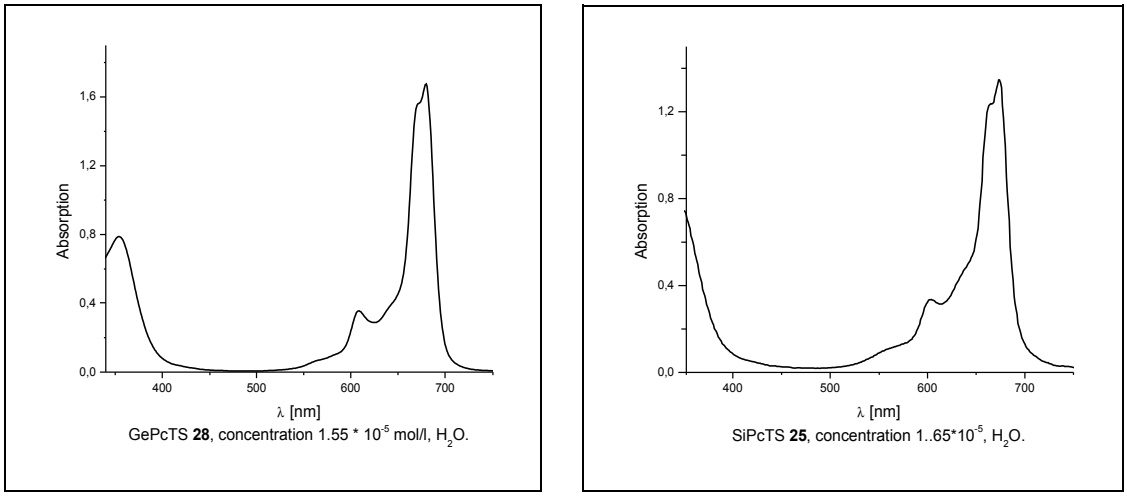

Figure 4.3. UV-Vis spectra of GePcTS **28** and SiPcTS **25** recorded at pH 7 in water solution. UV-Vis spectra of H_2PcTS **20** were recorded at pH 7 and pH 13, in the presence and absence of CTAC surfactant.

Taking into account the literature data for sulfonated phthalocyanines, the following conclusion can be drawn: the kind of metal being incorporated into Pc macrocycle and the axial hydroxyl groups are really decisive for the lack of aggregation in the case of SiPcTS **25** and GePcTS **28**. The metal-free H_2PcTS **20**, contrary to SiPcTS **25** and GePcTS **28**, is highly aggregated in water solution at pH 7. The extent of aggregation is reduced by addition of the cationic surfactant CTAC. At pH 13 in the absence of surfactant the Q band diminishes in intensity and a new broad band at 634 nm emerges. At pH 7 in the absence of CTAC the metal-free H_2PcTS **20** occurs in a highly aggregated state.

Positively charged and zwitterionic oxophosphorus(V) triazatetrabenzcorroles

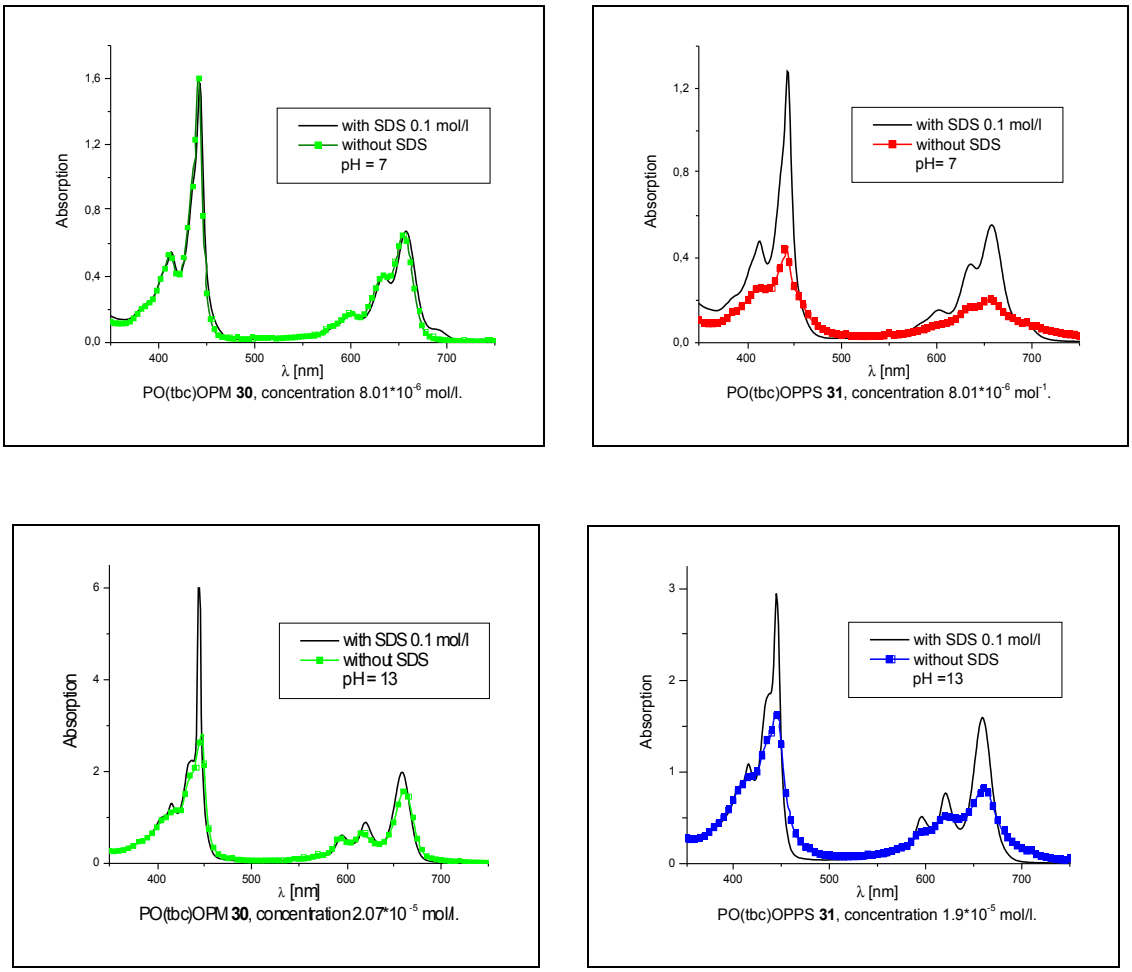

Figure 4.4. UV-Vis spectra of PO(tbc)OPM **30** and PO(tbc)OPPS **31** recorded at pH 7 and pH 13 in water solution, in the presence and absence of SDS surfactant.

More recently, triazatetrabenzcorroles have attracted attention due to their unique spectral properties. Their solutions are light green, giving UV-Vis spectra with a strong absorption at *ca.* 446 nm (Soret band with intensity twice that of the Q-band) and at *ca.* 658 nm (Q-band) (Fig. 4.4). PO(tbc)OPM **30** seems to be disaggregated at neutral pH as the appearance of the UV-Vis spectra recorded in the absence of SDS resembles that recorded upon addition of SDS. In that case low aggregation might be a cooperative effect of electrostatic repulsion and axial ligand that makes the coplanar association more difficult to occur. Zwitterionic PO(tbc)OPPS **31** displays to some extent intermolecular interactions as the absorption coefficient of the main band drops from ε = 160 000 $M^{-1}cm^{-1}$ in the presence of SDS to ε = 57 000$M^{-1}cm^{-1}$ in the absence of SDS, respectively.

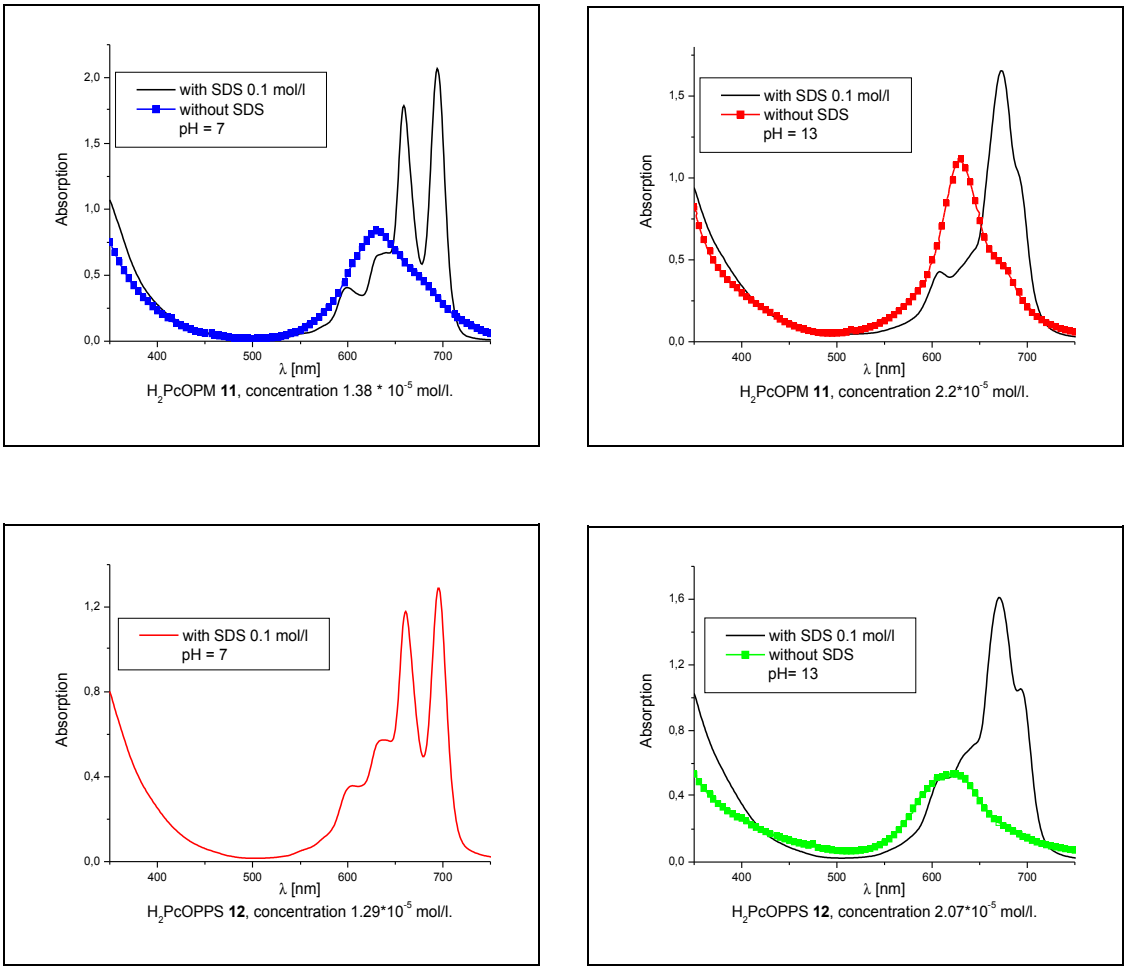

Figure 4.5. UV-Vis spectra of H_2PcOPM **11** and H_2PcOPPS **12** recorded in aqueous solution at pH 7 and pH 13, in the presence and absence of SDS detergent.

The metal-free phthalocyanines **11** and **12** have C_{2h} symmetry and show, typical in that case, a doublet at 695 nm and 661 nm together with a weaker band at 605 nm. The two bands in the region 661-695 nm are the split Q-band (Fig. 4.5). The partially resolved broad absorption band at shorter wavelength, *i.e.* at around 639 nm, has been attributed to dimmer or higher aggregates. In the absence of surfactant SDS at pH 7 and at pH 13 the UV-Vis spectrum of positively charged phthalocyanine **11** is entirely affected by aggregation process. At the higher pH, the very weakly acidic cavity protons of this free-base phthalocyanine are abstracted causing the symmetry increase from C_{2h} to C_{4h} resulting in the Q-band split disappearance. Thus, the Q-band is now observed as a single band 673 nm. The zwitterionic H_2PcOPPS **12** exhibits immensely strong

intermolecular interaction, hence, it could be solubilized at neutral pH only upon addition of detergent.

Negatively charged sulfonated hydroxysilicon triazatetrabenzcorrole

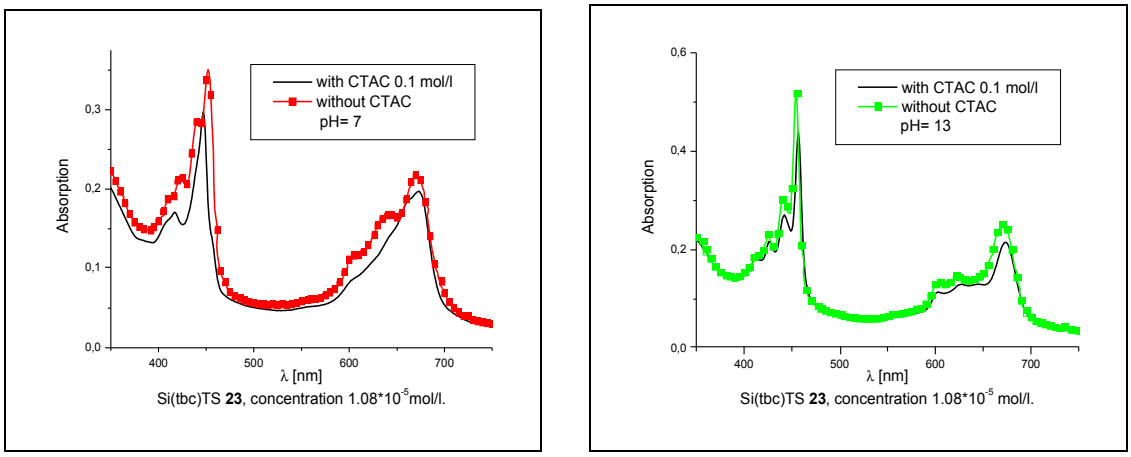

Figure 4.6. UV-Vis spectra of Si(tbc)TS **23** recorded at pH 7 and pH 13 in the presence and absence of CTAC detergent.

The addition of cationic detergent CTAC to the water solution of Si(tbc)TS **23** has rather insignificant influence on the appearance of the UV-Vis spectrum (Fig. 4.6). Presumable, the axial ligand may have some influence on lower aggregation in that case. An aggregate structure of this monoaxially substituted molecule would involve a cofacial association with the axial ligands oriented outward, this way higher aggregates could be probably avoided.

Positively charged and zwitterionic silicon phthalocyanines

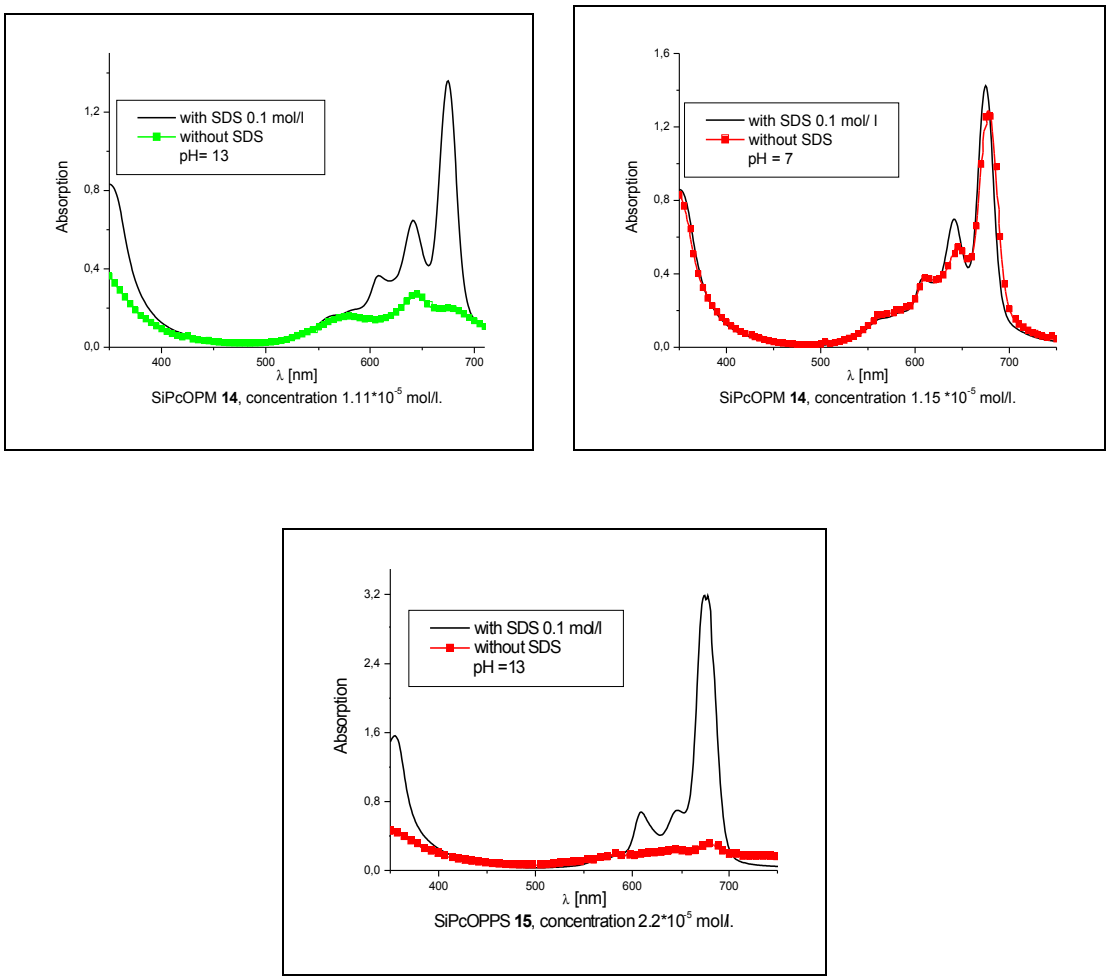

Figure 4.7. UV-Vis spectra of SiPcOPM **14** and SiPcOPPS **15** recorded at pH 7 and pH 13, in the presence and absence of SDS detergent.

Positively charged SiPcOPM **14** could be only partially disaggregated by the anionic SDS independently of the pH value (Fig. 4.7). The Q-band at 675 nm is always accompanied by a strong band at around 641 nm, which is attributed to aggregated form of phthalocyanine. Zwitterionic SiPcOPPS **15** is strongly disaggregated at higher pH value by the anionic SDS, but the SDS becomes ineffective at neutral pH as the intermolecular interactions are strong enough to prevent solubility.

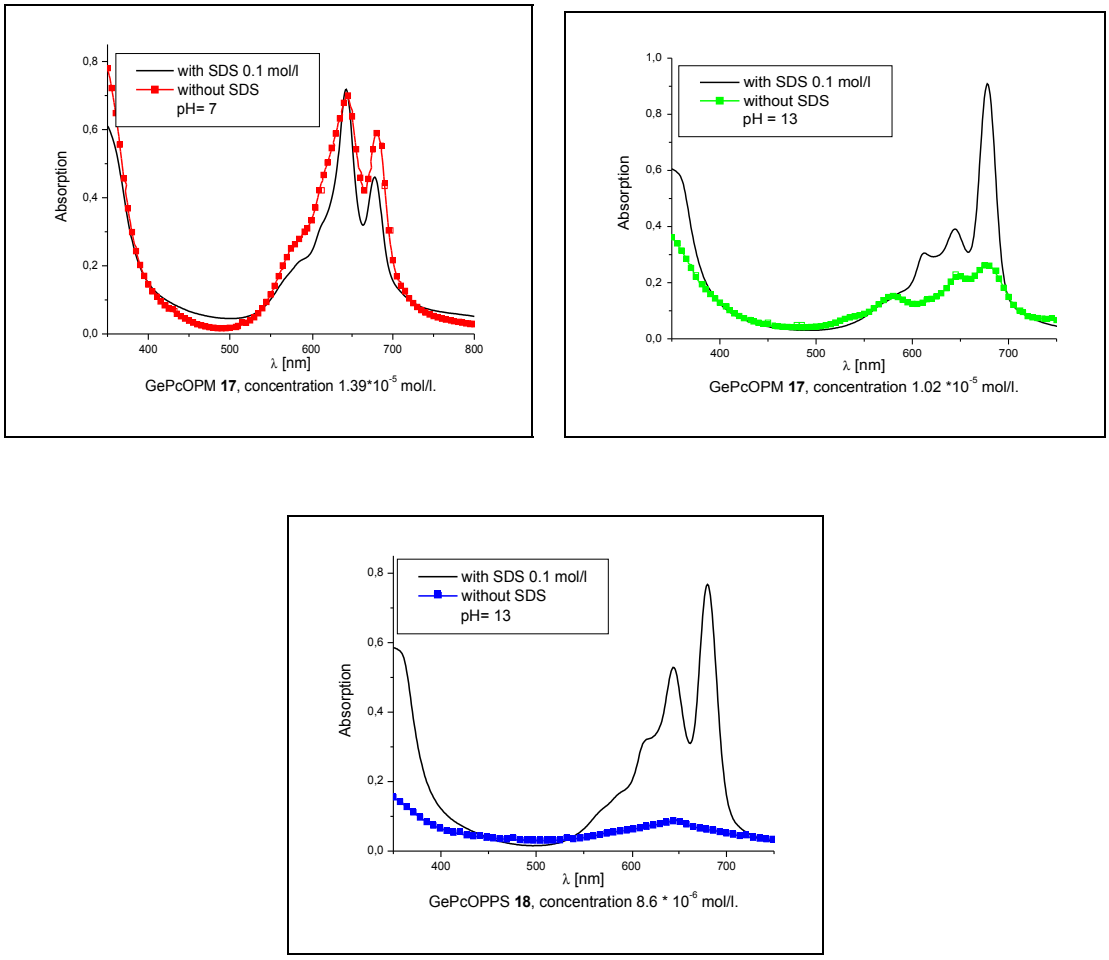

Figure 4.8. UV-Vis spectra of GePcOPM **17** and GePcOPPS **18** recorded at pH 7 and pH 13, in the presence and absence of SDS detergent.

Figure 4.8 shows that both GePcOPM **17** and GePcOPPS **18** exhibit very strong aggregation in solution. Positively charged GePcOPM **17** could be partially disaggregated by the action of anionic SDS at pH 13. At pH 7 in the presence or absence of detergent the UV-Vis spectrum is dominated by intense absorption at around 645 nm arising from strong aggregation.

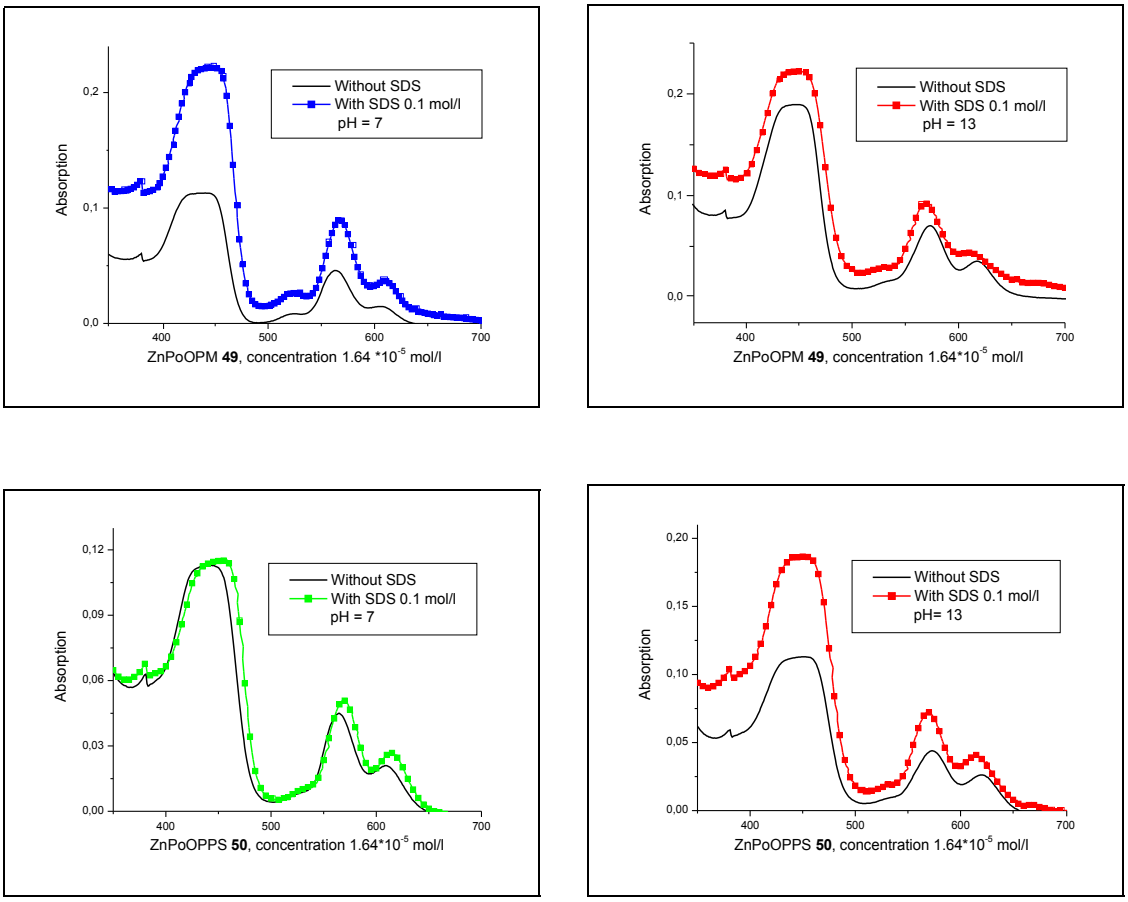

Figure 4.9. UV-Vis spectra of ZnPoOPM **49** and ZnPoOPPS **50** recorded at pH 7 and pH 13, in the presence and absence of SDS detergent.

The UV-Vis spectra of water-soluble zinc porphyrins are dominated by broad Soret band centred at around 445 nm (Fig. 4.9). An addition of oppositely charged detergent to the aqueous solution of water-soluble porphyrins ZnPoOPM **49** and ZnPoOPPS **50** results in increase of the intensity of the absorption bands indicating tendency toward aggregation in water solution. In comparison with zinc porphyrins, the metal-free porphyrins H_2PoOPM **46** and H_2PoOPPS **47** exhibit blue shift of the Soret band to around 420 nm in water solution at pH 7. Due to symmetry of the metal-free porphyrins the Q-band exists as a four bands at around 515 nm, 550 nm, 581 nm and 637 nm.

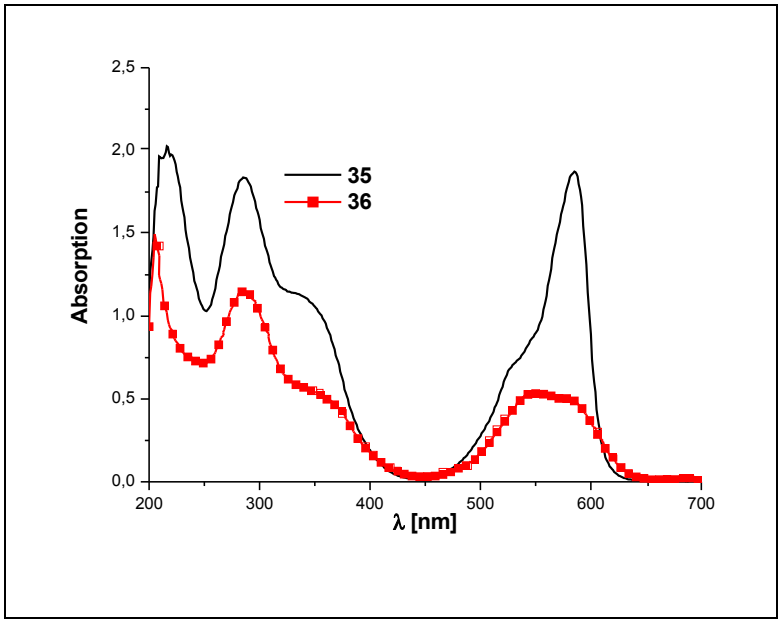

Figure 4.10. UV-Vis spectra of positively charged subphthalocyanine **35** in water solution and zwitterionic subphthalocyanine **36** in 0.6 M water solution of KCl. Concentration 2.49 x 10^{-5} M.

Subphthalocyanines present nonplanar cone-shaped structure with axial substituents attached to boron and placed in the opposite direction of the open bowl [5,6]. This structural feature is decisive for the lack of aggregation (Fig. 4.10). The positively charged SubPcs remain disaggregated in water solution pH 7 in a very wide range of concentrations. The addition of anionic detergent SDS to the water solution of positively charged SubPcs has insignificant influence on the appearance of the UV-Vis spectrum. The only exception proved to be zwitterionic SubPc **36**, which exhibit strong intermolecular interaction, observed for all compounds of this type. Hence, SubPc **36** could be solubilized only upon addition of electrolyte (0.6 M KCl) to the aqueous solution.

4.5 Conclusion

Summarising all discussed results it can be concluded that aggregation tendency decreases in the following order:

H_2PcOPM, H_2PcOPPS, H_2PcTS, GePcOPM, GePcOPPS, SiPcOPM, SiPcOPPS >> PO(tbc)OPPS > PO(tbc)OPM, Si(tbc)TS, ZnPoOPM, ZnPoOPPS, H_2PoOPM, H_2PoOPPS >> SubPcs(positively charged), GePcTS, SiPcTS.

The results that were discussed in this chapter explicitly show that aggregation is a very complex phenomenon. On the one hand, it depends on the structure of the molecule, especially on the bulkiness of the substituents, and, on the other hand, it is complicated by coulombic, hydrophobic and strong π-electron interaction. The positively charged compounds investigated during this work have "electron rich" peripheral substituents that could presumably increase the π-π interaction between molecules and additionally enhance aggregation in water solution. Moreover, there is a noticeable response of the state of aggregation to the varying physical environment, *i.e.* solvent, presence of electrolytes, pH and addition of surfactants [1].

4.6 References

[1] Snow, A. W. in *The Porphyrin Handbook* (K.M. Kadish, K.M. Smith, R. Guilard, Editors), Vol. 17 Phthalocyanines: Properties and Materials, pp. 129-176; Elsevier Science **2003**.

[2] R. Gerdes, *Niedermoleculare und immobilisierte Phthalocyaninetetrasulfonsäuren als Photosensibilisatoren für die Photooxidation von Phenol und Chlorophenolen,* Doctoral Dissertation, Universität Bremen, **2000**.

[3] Schneider, G.; Wöhrle, D.; Spiller, W.; Stark, J.; Schulz-Ekloff, G.; *Photochem. Photobiol.*, **1994**, 60, pp. 333-342.

[4] Gerdes, R.; Bartels, O.; Schneider, G.; Wöhrle, D.; Schulz-Ekloff, G.; *Interna. J. Photoenergy,* **1999**, Vol. 1, 41-47.

[5] Claessens, Ch. G.; Gonzales-Rodriguez, D.; Torres, T.; *Chem. Rev.* **2002**, 102, 835-853.

[6] Geyer, M.; Plenzig, F.; Rauschnabel, J.; Hanack, M.; del Rey, B.; Torres, T.; *Synthesis*, **1996**, 1139-1151.

5. Photocatalytic properties

5.1 Introduction

The purpose of the present chapter is to present results concerning photocatalytic activities of different photosensitizers obtained during these investigations. In particular, special attention has been given to the following points:

- Tetrapyrrolic compounds such as phthalocyanines, triazatetrabenzcorroles, subphthalocyanines and porphyrins have been proposed as photocatalysts in photo-oxidation reaction. A common feature of all employed photosensitizers is their water solubility. This has been achieved by adding suitable functional groups to the Pc framework, *e.g.* sulfonate and quaternary aromatic amine (see chapter 2). The efficiency of sensitised photo-oxidation, the influence of substrate structure on the photo-oxidation efficiency as well as on the sensitizer photostability were studied.
- The singlet oxygen generation requires that the photosensitizer be in the monomeric state in an aqueous medium. Otherwise in aggregates dissipation of the energy of the excited state readily takes place (so-called self-quenching) (see chapter 1.6). A very effective approach to circumvent aggregation phenomenon is to employ surfactants that form micelles in which photosensitizer molecules may be disaggregated (see chapter 4.4). Hence, all photocatalytic measurements were performed in water solution in the absence and presence of surfactants that let the charged photosensitizer molecules be in their monomeric state. This way, by comparison of two such measurements, an important piece of chemical information can be obtained, *i.e.* the extent and influence of aggregation process on the photocatalytic activity can be followed.
- One solution to the long-standing problem of sensitizer recovery and reuse is the use of polymer-bound singlet oxygen sensitizers. Because all investigated compounds have charged groups at their periphery, such as sulfonate (negatively charged) or quaternary aromatic amine (positively charged and zwitterions), immobilization on ion exchanger is possible. Therefore, the reactivity of

sensitizers dissolved in solution has been compared with the reactivity of polymer-immobilized dyes.

- During the photo-oxidation of 2-mercaptoethanol and phenol the photosensitizers may oxidatively decompose. The degradation of photosensitizers investigated during this work was followed by measuring the UV-Vis absorption intensity at the beginning and after termination of the photo-oxidation. Of special interest are photosensitizers, which exhibit increased stability towards intense light and oxygen.
- The action spectra obtained for phthalocyanines, porphyrins and triazatetrabenzcorroles show that each photosensitizer is photocatalytically active solely in the area of absorption (Q-band and Soret band). In principle, there is no activity in the region between absorption maxima. So far, chemists in their work have involved single photosensitizer, this means that only small fraction of the solar spectrum is exploited. The fraction of light collected by the sensitizer must be increased to improve efficiency of the catalytic system. In order to overcome this obstacle it is proposed to utilize panchromatically absorbing system, consisted of several dyes, absorbing at different wavelengths.

Below some comments to the preceding points will be given, this let the reader better understand subject of the present chapter.

The term of **photocatalysis** was introduced in the 1930s [1]. In general, the term refers to the catalytic reaction that takes place under the action of light. However, it has to be pointed out that there is variety of possible processes having often different mechanisms that fall under the umbrella of “photocatalysis”. In general, at the beginning of the photocatalytic process a photosensitizer molecule or semiconductor absorbs light energy. Light absorption causes an electron transition (or energy transfer) from the ground state to an excited state of the photosensitizer, or from the valence band to the conduction band of the semiconductor. In the next step electron transfer (or energy transfer) takes place between the excited state and a molecule of substrate leading to chemical process(es) resulting in a final reaction product. At the conclusion of the photocatalytic cycle the photosensitizer or semiconductor comes back to its ground state. Now the photosensitizer/semiconductor is fully regenerated and ready to be excited again by the action of light. Consequently, the photochemical reaction is

repeated again. In other words the photosensitizer/semiconductor acts as a **photocatalyst**.

The investigations that have been made during this work and the following chapter refer to photocatalysis by photosensitizer molecules only and the reaction under consideration is the photo-oxidation. It has to be pointed out that phthalocyanines can be active during photocatalytic oxidation process either via **energy transfer** (**Type II**) or via **electron transfer** (**Type III**). However, many reports show that the rout via $^1O_2$ (Type II) is predominant in photo-oxidation of many biological substrates and pollutants present in the environment.

The Type II is characterized by initial interaction between the excited photosensitizer and a molecule of oxygen in its ground state. In the first step a molecule of photosensitizer absorbs light. This causes excitation of a photosensitizer to singlet excited state ($Sens^{1*}$) followed by intersystem crossing (ISC) to triplet excited state ($Sens^{3*}$). The lowest electronic state of oxygen is a triplet ground state ($^3O_2$, $^3\Sigma_g^-$) with two unpaired electrons distributed in the highest occupied orbitals. The energy is now transferred from the triplet excited state of photosensitizer to the triplet ground state of oxygen resulting in singlet oxygen ($^1O_2$, $^1\Delta_g$). The direct absorption of light by $^3O_2$ to produce $^1O_2$ is a spin-forbidden process. Singlet oxygen ($^1O_2$) is a highly reactive species that easily reacts with a molecule of substrate (R) resulting in a new oxygenised product.

Type II

$$Sens + h\nu \rightarrow Sens^{1*} (ISC) \rightarrow Sens^{3*}$$

$$Sens^{3*} + {}^3O_2 \rightarrow {}^1Sens + {}^1O_2$$

$$^1O_2 + R \rightarrow Oxygenation$$

Furthermore, another plausible pathway, that is photoinduced electron transfer, should be taken into account. In that case the sensitizer triplet ($Sens^{3*}$), formed via intersystem crossing of the exited singlet state sensitizer ($Sens^{1*}$), interacts directly with a molecule of oxygen in its ground state ($^3O_2$) resulting in the superoxide radical anion ($O_2^{\bullet-}$) as the reactive species. Moreover, the sensitizer triplet ($Sens^{3*}$) may interact directly with a molecule of substrate leading to a chain of further reactions.

Type III

$$Sens^{3*} + R \rightarrow Sens^{-\bullet} + R^{+\bullet}$$

$$Sens^{-\bullet} + {}^3O_2 \rightarrow Sens + O_2^{-\bullet}$$

$$Sens^{3*} + {}^3O_2 \rightarrow Sens^{+\bullet} + O_2^{-\bullet}$$

$$Sens^{+\bullet} + R \rightarrow Sens + R^{+\bullet}$$

$$R^{+\bullet} + O_2^{-\bullet} \rightarrow \text{Oxygenation}$$

Photocatalysis appears to be alluring for creating new energy resources based on solar energy. Intensive investigation have been made on all over the world aimed at the construction of an artificial system able to convert solar energy into electricity or able to cleave water affording useful fuels. However, it has to be pointed out that the artificial system that would be as efficient as the nature occurring photosynthesis as yet has not been obtained. A well-known example of photocatalytic process is water cleavage by UV light on TiO_2 photoanode and platinum counter electrode. Later this process was modified by coating semiconductor material with dyes (usually metal complex) absorbing at longer wavelengths where the colourless TiO_2 remains inactive due to the band gap [2-4]. Moreover, new type solar cells are based on photocatalytic process. These solar cells, called Graetzel`s cells, utilize nanometer-sized titanium dioxide ($TiO_2$) film covered with dye, (typically $Ru(dcbpy)_2(SCN)_2$, where dcbpy is 4,4`-dicarboxyl-4,4´-bipyridine) [5-8]. An efficiency of about 10% was reported for Graetzel`s cell which makes it comparable to the efficiency of amorphous silicon photovoltaic cells.

Another example of photocatalytic process is photooxygenation. **Photooxygenation** is an example of photosensitized process; during this light induced process incorporation of molecular oxygen into a molecular entity takes place. This process is of great industrial importance. The synthesis of some fine chemicals is achieved via photo-oxidation reaction. The photo-oxidations of α-terpine to (±)-ascaradiol and cyclopentadiene to (Z)-4,5-epoxy-2-penten-1-on in the presence of chlorophyll as photosensitizer have been investigated [9,10]. The synthesis of 5-hydroxy-5H-furan-2-one from furfural in the presence of oxygen and methylene blue or Rose Bengal as photosensitizers has been reported as well [11,12]. Finally, the photo-oxidation of (S)-(-)citronellol to rose oxide with oxygen and Rose Bengal as photosensitizer is applied in

industry [13-15]. The importance of chemical reactions driven by the action of light (photooxygenation in particular) stems from the excellent chemo-, regio- and stereoselectivity in many cases unattainable via more “classical” synthetic approach. Only a cursory glance at the handbooks dealing with photochemistry shows that the ene- as well as [4+2]-cycloaddition reaction are the most important chemical reactions of organic compounds with singlet oxygen obtained during photosensitization. These photochemical reactions allow obtaining of allylic hydroperoxides and endoperoxides, both very important intermediates in the synthesis of allylic alcohols, epoxy alcohols, 1,4-diols, vicinal diols and saturated polyols to mention all but few important products. Among all photocatalytic processes that have been reported in chemical literature, photooxygenation seems to be one of the most important also because of its potential application in wastewater cleaning [16]. A well-known example of the latter is the photocatalytic destruction of halogenated hydrocarbons and other environmentally toxic compounds by TiO_2 as photoexcitable semiconductor. In this process TiO_2 is exposed to solar radiation. The disadvantage of TiO_2 as photocatalyst is the band gap (3.2 eV, $\leq$ 387 nm). It means that titanium dioxide works only in the UV region where only approximately 3 % of solar radiation is effective. In order to improve efficiency of this process it was decided to employ photosensitizers absorbing in the visible region of radiation as the region between λ = 390 - 780 nm embraces around 49 % of the solar radiation. Investigations dedicated to the application of water-soluble photosensitizers in the purification of water have been an ongoing issue in our laboratory for a long time. For instance, results concerning application of water-soluble photosensitizers in the photo-oxidation of sulfide [17,18], 2-mercaptoethanol [19], phenol and its halogenated derivatives [20-22] have been reported by our group in many chemical journals. It is also worth mentioning that some of the sulfonated phthalocyanines investigated in our laboratory entered first successful trials on a semi-industrial scale. Sulfonated phthalocyanines proved to be promising candidate for photocatalysts useful in the photochemical wastewater treatment. Moreover, due to high activity and stability of the polymer bound Si(IV) sulfophthalocyanine a patent application was made by the PROSYS company in Bremen. The idea of such wastewater treatment is based on the usage of three inexhaustible natural resources: oxygen (present in the air), photons (from sunlight), water (as environmentally friendly solvent).

A good photosensitizer necessitates not only favourable photophysical parameters, but also it has to be stable enough to ensure longevity of the photcatalytic system. It is of

special importance for any of such system to be used on a practical scale. It has to be cheap, efficient and stable. Therefore, during this study, besides photocatalytic activity, the susceptibility towards photobleaching was evaluated for each compound. **Photobleaching**, known also as a photodegradation, is a process whereby the dye molecule degrades in the presence of light. Phthalocyanines and other photosensitizers are known to cause their own degradation. After irradiation with intense light the singlet oxygen is produced that will destroy the phthalocyanine molecule by a mechanism proposed by Schnurpfeil *et al.* (Fig. 5.1) [23]. The mechanism suggests singlet oxygen [4+2] cycloaddition to the phthalocyanine pyrrole units. As final reaction product phthalimide was found. The mechanism closely resembles that known for the reaction of 1,3-diphenylisobenzofuran (DPBF) and singlet oxygen.

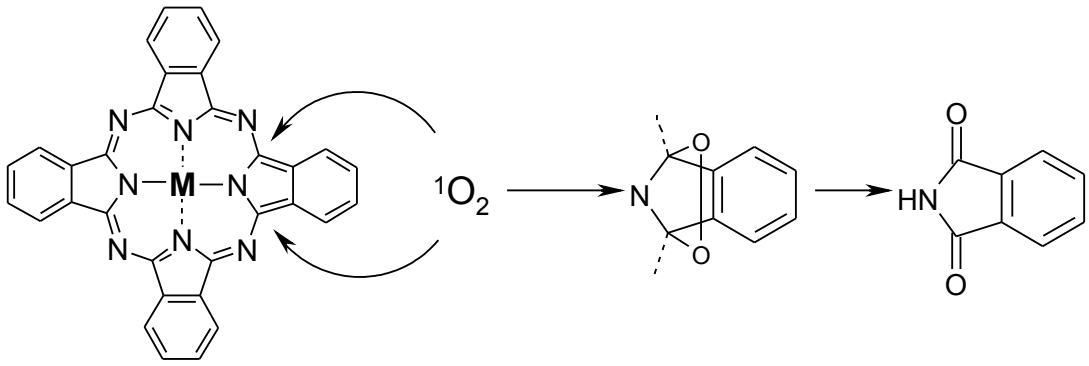

Figure 5.1. Proposed mechanism of photodegradation of phthalocyanines by the action of singlet oxygen.

One should point out that in addition to singlet oxygen mediated photobleaching another process can be involved in the photodegradation of sensitizer molecules. It was found that photodegradation of sensitizer is pH dependent. Moreover, photo-oxidations carried out at the same reaction conditions but for different substrates (trichlorophenol, pentachlorophenol and *p*-chlorophenol were compared) differ as to the extent of sensitizer photobleaching [24]. In other words, experiments have shown that the nature of the substrate, namely electron-acceptor properties, plays a vital role in the photobleaching. This finding indicates that electron transfer from the excited sensitizer to substrate may be considered as a first step in the sensitizer photobleaching process. It was observed that addition of the reductants inhibited the photobleaching; most probably the oxidized sensitizer is reduced back to its initial form [24]. Thus, Ozoemana

et al. [24] proposed the following sequence of reaction to describe the photodegradation of sensitizer via electron transfer pathway:

$$MPc^{*} + substrate \rightarrow MPc^{\bullet+} + substrate^{\bullet-}$$

$$MPc^{\bullet+} \rightarrow photodegradation\ products$$

$$MPc^{\bullet+} + red \rightarrow MPc + red_{ox}$$

where MPc^{*} is the excited metallophthalocyanine and red is the reductant.

5.2 Photo-oxidation of 2-mercaptoethanol

In order to measure photocatalytic activity of phthalocyanines and other photosensitizers obtained during these studies, 2-mercaptoethanol was employed as a substrate to be oxidized (see subchapter 6.3.2). The stochiometry of the photo-oxidation of 2-mercaptoethanol is known, hence, it appears to be good test reaction [18,19,25]. Detailed studies were dedicated to the explanation of the mechanism of thiols catalytic oxidation [26]. Such process is of great technical importance in the petroleum industry where it is necessary to separate the sulfur-containing pollutants from the petroleum. It is accomplished by washing the gasoline fractions of petroleum with aqueous alkaline solution in the extractor. In this way extracted product is obtained along with waste solution containing mercaptanes. In the second step Co (II) phthalocyanine sulfonic acid is added as catalyst and air is passed through the solution. Mercaptanes are oxidized to disulfides and easily separated. In the mercaptanes sweetening process (MEROX) the charcoal-supported Co (II) phthalocyanine is used as solid catalyst [27-29]. This process is catalytic oxidation, hence, requires no light. It embraces catalyzed and uncatalyzed step. Different mechanisms have been proposed in the literature regarding the CoPc catalyzed oxidation of thiols to disulfide [26]. The reaction begins with nucleophilic coordination of thiolate to Co(II) followed by addition of O_2 and formation of a paramagnetic superoxo complex. The formal state of oxidation of sulphur rises from –2 to –1. The detailed investigation revealed the reaction rate follows an enzyme-like two-substrate Michaelis-Menten kinetics with respect to both thiol and oxygen [30-36]. Hence, ternary complex formation is postulated to explain the observed kinetic

behavior. Furthermore, the formation of hydrogen peroxide with its concomitant catalytic decomposition was experimentally proved [32].

$$R\text{-}SH \rightarrow R\text{-}S^- + H^+$$
$$MPc + R\text{-}S^- \rightarrow (R\text{-}S^-)MPc$$
$$(R\text{-}S^-)MPc + O_2 \rightarrow (R\text{-}S^-)MPc(O_2)$$
$$(R\text{-}S^-)MPc(O_2) \rightarrow R\text{-}S^\bullet + MPc + O_2^{-\bullet}$$
$$R\text{-}S^- + O_2^{-\bullet} \rightarrow R\text{-}S^\bullet + O_2^{2-}$$
$$MPc + O_2^{2-} + 2\ H^+ \rightarrow MPc + H_2O + \tfrac{1}{2}\ O_2$$
$$2\ R\text{-}S^\bullet \rightarrow R\text{-}S\text{-}S\text{-}R$$

The overall reaction for the thiol oxidation is given in the following equation (the numbers in brackets are the oxidation state of sulphur):

$$4\ R\text{-}S^-\ (\text{-II}) + O_2 + 2\ H_2O \rightarrow 2\ R\text{-}S\text{-}S\text{-}R\ (\text{-I}) + 4\ OH^-$$

The oxidation of thiols to disulfides is an important biological and industrial process. Thus, numerous attempts have been made towards determining the plausible mechanism of catalytic thiol oxidation using different thio compounds like 2-mercaptoethanol, cysteine, alkyl mercaptan and thioglycolic acid.

In the case of catalytic process paramagnetic Pc complexes (cobalt (II), vanadyl (IV)) with unfilled d orbitals are successfully employed as catalysts. They are able to coordinate reversibly and activate oxygen. On the other hand, it has been shown that Pc complexes with diamagnetic central metal having closed shell electron configuration (Zn(II), Al(III)OH, Si(IV)$(OH)_2$) as well as metal-free phthalocyanines are effective photosensitizers and thus they are useful photocatalysts [19,18,22]. It has been found that irradiation of such phthalocyanines in their absorption region, that is, Q-band and Soret band, gives rise to singlet oxygen production and consequently efficient photo-oxidation. Hence, not only catalytic oxidation but also photocatalytic thiols oxidation was investigated by many chemists. Depending on the kind of substituents on the phthalocyanine, the photo-oxidation results in mainly sulfonic acid (S(+IV)) and sulfate (S(+VI)) formation.

$$2\ R\text{-}S^- + 3\ O_2 + (h\nu) \rightarrow 2\ R\text{-}SO_3^-\ (\text{also } R\text{-}SO_4^{2-})$$

It is rather difficult to determine the exact reaction mechanism, as several intermediates of RS^- like RSO_n^- and of RSSR like $RS(O)_nSR$ or $RS(O)_nS(O)_mR$ are possible. In 1994 Gerhard Schneider et al. proposed a few partial reaction that could be involved in the mechanism of thiol photo-oxidation catalyzed by zinc phthalocyanine [19].

$$ZnPc + h\nu \rightarrow {}^{S}ZnPc^{*} \text{ (ISC)} \rightarrow {}^{T}ZnPc^{*}$$

$${}^{T}ZnPc^{*} + O_2 \rightarrow ZnPc + {}^{1}O_2$$

$$R\text{-}S^- + {}^{1}O_2 \rightarrow R\text{-}S^{\bullet} + O_2^{-\bullet}$$

$$R\text{-}S^- + O_2^{-\bullet} + H^+ \rightarrow R\text{-}S^{\bullet} + HO_2^-$$

$$2\ R\text{-}S^{\bullet} \rightarrow R\text{-}S\text{-}S\text{-}R$$

$$R\text{-}S^-,\ R\text{-}S^{\bullet},\ R\text{-}S\text{-}S\text{-}R + {}^{1}O_2,\ O_2^{-\bullet} \rightarrow R\text{-}SO_n^-,\ R\text{-}S(O)_nS\text{-}R,\ R\text{-}S(O)_nS(O)_m\text{-}R$$

Thus, irradiation of the phthalocyanine leads to singlet oxygen ($^1O_2$) formation according to Type II reaction. It is supposed that singlet oxygen reacts with the thiolate anion leading to cyclic thiolate-peroxo species, and then to thiol radical, and superoxide anion radical. The very reactive superoxide anion radical reacts with thiolate resulting in the formation of peroxide (HO_2^-). The latter can participate in the oxidation of thiolate anion as well. Coupling of two R-S$^\bullet$ radicals leads up to the formation of disulfide. Finally, reaction of $^1O_2$ and $O_2^{-\bullet}$ with different thiol derivatives results in sulfur containing products of higher oxidation state, like RSO_n^-, $RS(O)_nSR$ and $RS(O)_nS(O)_mR$.

5.3 Photo-oxidation of phenol

Phenol and its chlorinated derivatives (trichlorophenol TCP, pentachlorophenol PCP) are notorious environmental pollutant. Chlorophenols are commonly used as pesticides, insecticides, in wood preservation, pulp and paper manufacturing [38]. These compounds have a bad reputation for toxicity, persistence in the environment and ability to accumulate in aquatic organisms [39]. For this reason one can find them listed in both the U.S. Environmental Protection Agency list and the European Community red list of priority pollutants. Therefore, studies towards the degradation of these compounds have received much attention. Biological treatment of chlorophenols proved to be unsuitable method as it leads to the formation of products that are even more toxic than chlorophenol itself (polychlorinated dibenzo-*p*-dioxins and dibenzofurans) [40]. Two highly effective methods have been proposed by Meunier and Collins [41-43]. In both

methods hydrogen peroxide is used as the oxidant leading to partial mineralization of chlorphenols. CO_2, CO, chlorinated and nonchlorinated carboxylic acids and several oxidatively coupled compounds were identified as the final products [41-43].

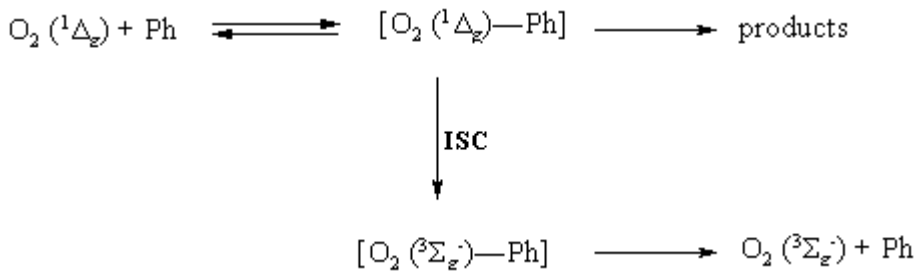

Figure 5.2. Phenol and singlet oxygen form an exciplex that later disintegrates.

The photocatalytic activity of the photosensitizers obtained during this study was tested on 2-mercaptoethanol. However, in some cases additional experiments were carried out employing phenol as a substrate to be oxidized (see subchapter 3.3.3). Phenol appears to be notable candidate for test compound, as the stochiometry and mechanism of its photo-oxidation is known. The mechanism of the photo-oxidation of phenol with low-molecular-weight photosensitizers was studied in detail [20,44,45]. The reactions in D_2O and in the presence of sodium azide unambiguously showed that singlet oxygen is involved in the photo-oxidation process of phenol [44]. It is also known that phenol and its derivatives form an exciplex with singlet oxygen [$^1O_2$—Ph], which disintegrates according to two different pathways (Fig. 5.2). After intersystem crossing the exciplex disintegrates back to the educt molecules, i.e. $O_2(^3\Sigma_g^-)$ and Ph, it is so-called physical quenching. On the other hand, the chemical quenching leads via [2+4]-cycloaddition to a hydroperoxycyclohexadienone (Fig. 5.3). The formation of hydroperoxycyclo-hexadienone via photoinduced electron transfer as an alternative to cycloaddition was postulated as well [20]. The hydroperoxycyclohexadienone easily decomposes resulting in *p*-benzoquinone. During the photo-oxidation the initially colourless solution turns deep brown. The UV-Vis spectrum of the brown coloured solution exhibits an intense absorption at 245 nm corresponding to *p*-benzoquinone. Then the solution turns yellow indicating that the oxidation proceeds further and ultimately it becomes nearly colourless again.

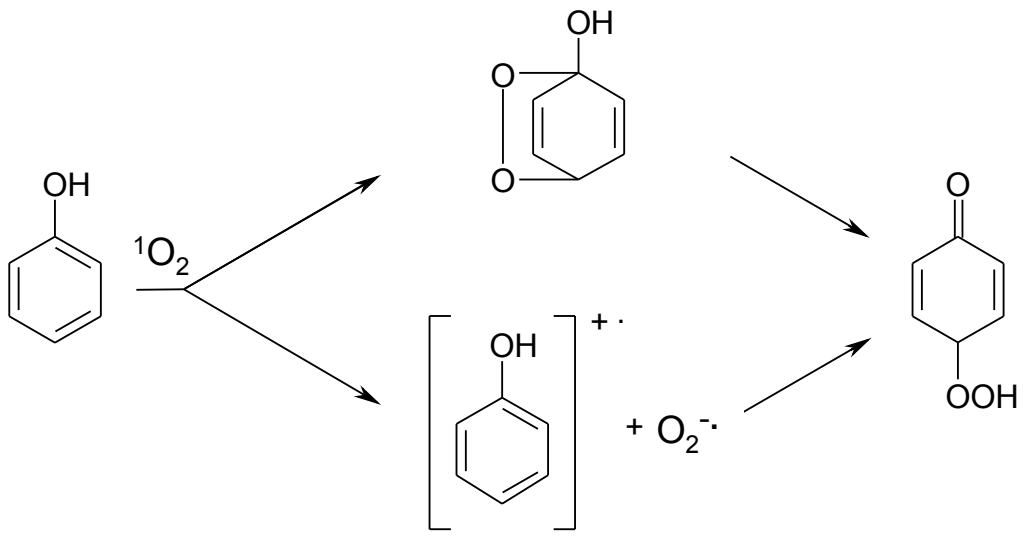

Figure 5.3. The reaction of phenol with singlet oxygen gives hydroperoxycyclohexadienone that easily decomposes to *p*-benzoquinone.

It has been shown that the photo-oxidation of phenol proceeds more efficiently at higher pH [22]. Hence, the reaction proceeds in aqueous solution at pH 13 or, in some cases, at pH 10 under consumption of ~ 3.5 mol of oxygen per 1 mol of phenol. *p*-Benzoquinone formed by the reaction of 1 mol of phenol and 1 mol of singlet oxygen was found as intermediate (Fig. 5.4). Further consumption of 1 mol of singlet oxygen and 1.5 mol of triplet oxygen results in simple carboxylic acids (maleic or fumaric acid) and carbonate formation. The singlet oxygen participation in the reaction is essential as no reaction occurs without irradiation.

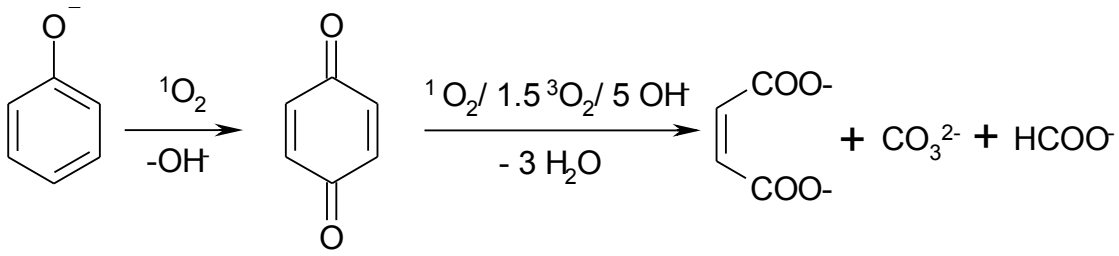

Figure 5.4. Photo-oxidation of phenolate anion leads to simple carboxylic acids and carbonate formation.

A total mineralization of phenol to CO_2 and water would require 7 mol of oxygen. The photo-oxidation of phenol is characterized by several consecutive steps and therefore by complex kinetics.

$$C_6H_6O + 7\,O_2 \longrightarrow 6\,CO_2 + 3\,H_2O$$

Therefore, a total mineralization of 0.36 mmol of phenol (the amount of phenol that was used during the photo-oxidation experiment) requires 30.8 ml of oxygen.

5.4 Photocatalytic activity of positively and zwitterionically charged oxophosphorus(V) triazatetrabenzcorroles

2-mercaptoethanol photo-oxidation

For the first time the photocatalytic activities of oxophosphorus(V) triazatetrabenzcorroles has been studied. Two excellent water-soluble compounds were tested, *i.e.* positively charged PO(tbc)OPM **30** and zwitterionic PO(tbc)OPPS **31**. Data are collected in Table 5.1 and presented in Figure 5.5.

Table 5.1. Photocatalytic oxidation of 2-mercaptoethanol by PO(tbc)OPM **30** and PO(tbc)OPPS **31**.

Compound	Conditions	O_2 consumed after 3 h [ml]	Photodegradation of dye in %	Molar ratio O_2/substrate	TON [min^{-1}]/ RR_i [ml $O_2 \cdot min^{-1}$]
PO(tbc)OPM	pH 13, SDS	19.1	38	1.1	134 / 0.82
PO(tbc)OPM	pH 13	17	73	0.99	85 / 0.52
PO(tbc)OPM on IRA-120	pH 13	13.8	100	0.8	6.5 / 0.16
PO(tbc)OPPS	pH 13, SDS	17.1	34	1	103.4 / 0.63
PO(tbc)OPPS	pH 13	11.1	21	0.64	31 / 0.19
PO(tbc)OPPS on IRA-402	pH 13	50	100	2.9	29 / 0.71

The oxophosphorus(V) triazatetrabenzcorroles exhibit tendency to form aggregates in water solution (see chapter 4.4). Hence, the activities of PO(tbc)OPM **30** and PO(tbc)OPPS **31** in non-micellar solution are lower comparing to the activities measured in a solution containing oppositely charged detergent SDS due to monomerization. The photocatalytic activities were investigated at pH 13 as both **30** and

31 proved to be very stable at high pH value. The positively charged photosensitizer **30** exhibits better stability in micellar solution (photodegradation of dye was estimated at 38 % after 3 h reaction time), therefore, higher oxygen consumption (19.1 ml) during the photo-oxidation of 2-mercaptoethanol. When the photo-oxidation is performed in a non-micellar solution the turnover number drops from 134 [min^{-1}] for SDS containing solution to 85 [min^{-1}]. At the same time 73 % of the photosensitizer decomposes after 3 h reaction time. Analogous situation is evident for zwitterionic **31**, which is characterized by higher activity and stability in the presence of detergent. Positively charged **30** loaded on cation exchanger Amberlite IRA-120 showed very poor photocatalytic activity and low oxygen consumption.

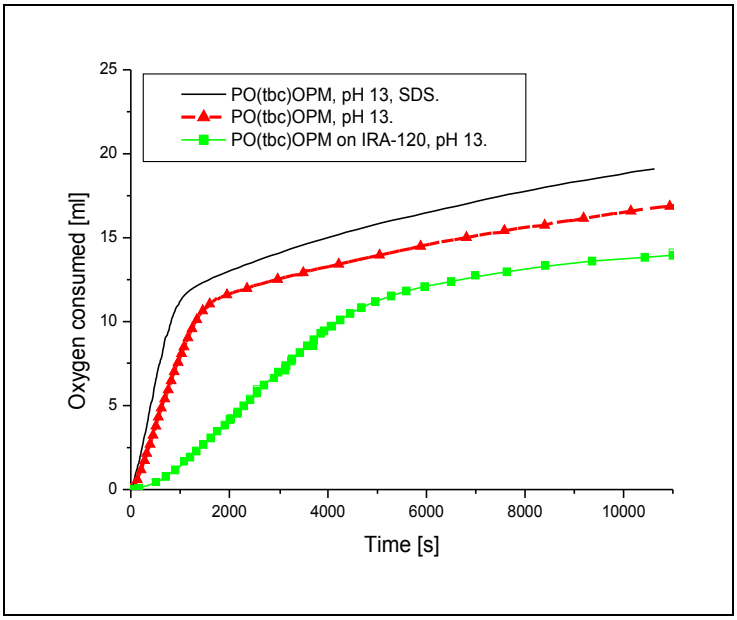

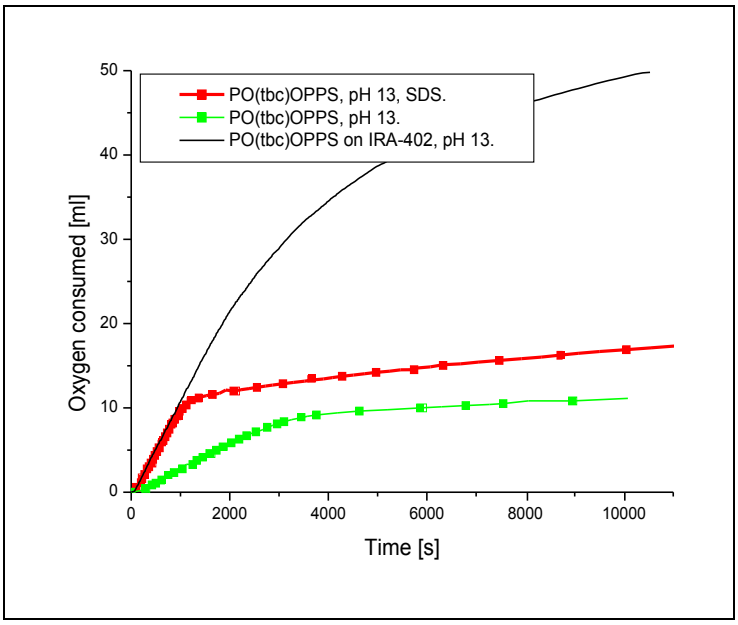

Figure 5.5. Photo-oxidation of 2-mercaptoethanol in aqueous solution at pH 13 with PO(tbc)OPM **30** and PO(tbc)OPPS **31** as photocatalysts.

The poor activity and low oxygen consumption is caused by fast photobleaching. The total degradation was observed after 3h of irradiation. On the other side, zwitterionic PO(tbc)OPPS **31** loaded on anion exchanger Amberlite IRA-402 exhibited enormously high oxygen uptake (50 ml) although it is totally photobleached during photo-oxidation. Interestingly, when the reaction was repeated at the same experimental conditions but without 2-mercaptoethanol consumption of 10.52 ml oxygen was found along with total photobleaching of the dye. After the reaction is over the solution becomes non-transparent and turns milky in hue. It follows that the polymer itself must be photo-oxidized during the course of reaction.

In Figure 5.6 the photoaction spectrum of PO(tbc)OPM **30** in the presence of SDS at pH 13 based on normalized TON is compared with the absorption spectrum. The highest activity is found in the Q-band as well as in the Soret band. No activity can be seen in the region between these two bands.

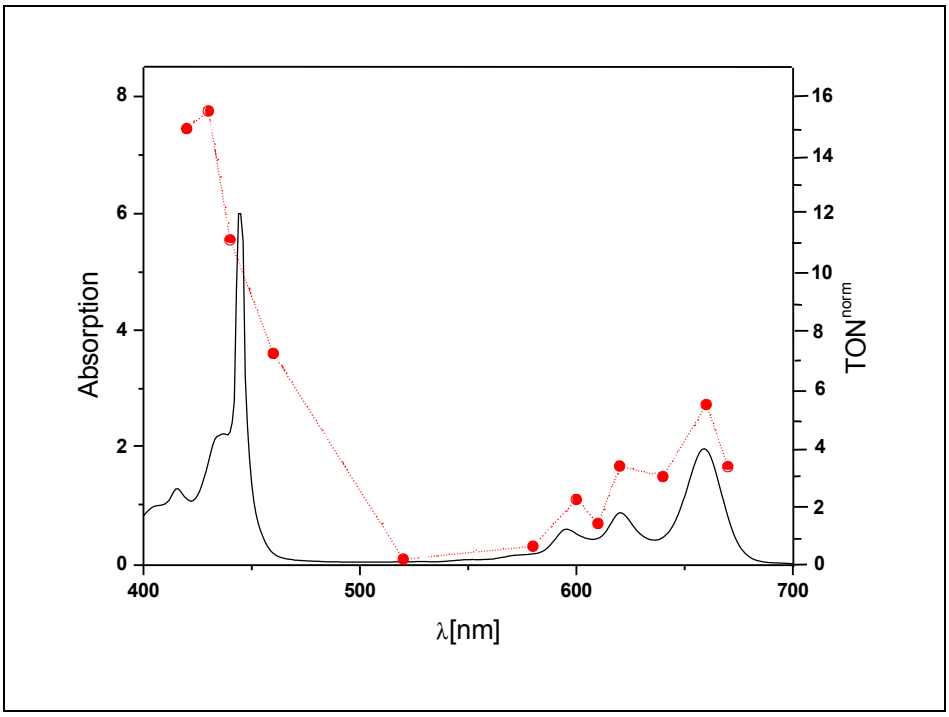

Figure 5.6. Photoaction spectrum (--●--) of PO(tbc)OPM **30** obtained during photo-oxidation of 2-mercaptoethanol in aqueous solution in the presence of SDS at pH 13. The solid line represents the absorption spectrum of PO(tbc)OPM **30** in aqueous solution in the presence of SDS at pH 13.

Many studies have shown that the singlet oxygen-mediated photo-oxidation (Type II) is a predominant pathway in the case of phthalocyanines (see chapter 5.1) [18,24,46]. However, there has been no report on the photo-oxidation using triazatetrabenzcorroles as photosensitizers. In order to have a better insight into the processes involved in the photo-oxidation catalysed by triazatetrabenzcorroles some additional measurements have been done. The participation of singlet oxygen in the reaction can be determined easily by doing two additional measurements: one in D_2O and the other one in the presence of sodium azide. Singlet oxygen is known to has a longer lifetime in deuterated solvents. On the other hand, NaN_3 is a physical quencher that deactivates $^1O_2$. Therefore, the initial reaction rate increases in D_2O and decreases after addition of sodium azide. The initial reaction rate RR_i measured during photo-oxidation of 2-mercaptoethanol at pH 13, in the presence of SDS, using PO(tbc)OPM **30** as photosensitizer amounted to 0.82 [ml $O_2 \cdot min^{-1}$]. It rose to 0.97 [ml $O_2 \cdot min^{-1}$] in D_2O and dropped to 0.21 [ml $O_2 \cdot min^{-1}$] in a solution containing the singlet oxygen quencher (NaN_3). Thus, it is obvious that singlet oxygen participates in this reaction. These data

show that addition of NaN_3 resulted in 74% inhibition of the photo-oxidation. The concentration of NaN_3 in the experiment was $2.5 \cdot 10^{-3}$ mol l^{-1}. Further increase of NaN_3 concentration did not change the initial reaction rate, thereby indicating full quenching of singlet oxygen. The above results show that the photo-oxidation of 2-mercaptoethanol under our experimental conditions the Type II is predominant. Test was made indicating the formation of hydrogen peroxide (H_2O_2) as a side product of the reaction. This finding suggests that simultaneously to the singlet oxygen pathway (Type II), electron transfer (Type III) occurs resulting in the superoxide radical anion ($O_2^{\bullet-}$) as the reactive species.

Phenol photo-oxidation

Additionally, the photo-oxidation of phenol by PO(tbc)OPM **30** and PO(tbc)OPPS **31** was studied to compare results with those obtained during photo-oxidation of 2-mercaptoethanol. The results are summarized in Table 5.2. In the case of PO(tbc)OPM **30**, the differences in the activities, expressed as initial reaction rates RR_i, are more pronounced comparing with the photo-oxidation of 2-mercaptoethanol. The initial reaction rate RR_i for PO(tbc)OPM **30** reaches value 1.16 [mlO_2/min] in the presence of surfactant and drops to the value 0.28 [mlO_2/min] in non-micellar solution. However, the final oxygen consumption is comparable. As a general tendency in all investigated cases it can be seen that the photocatalysts are more stable during photo-oxidation of phenol than during photo-oxidation of 2-mercaptoethanol. Hence, the photodegradation of PO(tbc)OPM **30** during photo-oxidation of phenol was around 16 % and increased to 34 % during photo-oxidation of 2-mercaptoethanol. The zwitterionic PO(tbc)OPPS **31** in the micellar solution exhibits lower activity comparing to PO(tbc)OPM **30**, *i.e.* RR_i 0.55 [ml/min]. However, the oxygen uptake is rather comparable in both cases. Merely 7 % of PO(tbc)OPPS **31** vanished after 3 h reaction time. When the PO(tbc)OPPS **31** is loaded on ion exchanger Amberlite IRA-402 36 ml of oxygen is consumed, which is more than required for total mineralization of 0.36 mmol of phenol. As it was suggested before the polymer itself can be partially photo-oxidized. Interestingly, the stability of polymer-immobilized PO(tbc)OPPS **31** was noticeably better (loss of 44% of dye was observed) during photo-oxidation of phenol, while in the case of photo-oxidation of 2-mercaptoethanol the photosensitizer was totally bleached.

Table 5.2. Photocatalytic oxidation of phenol in aqueous solution at pH 13 by water-soluble PO(tbc)OPM **30** and PO(tbc)OPPS **31**.

Compound	Conditions	O_2 consumed after 3 h [ml]	Photodegradation of dye in %	Molar ratio O_2/phenol	TON [min^{-1}]/ RR_i [ml $O_2 \cdot min^{-1}$]
PO(tbc)OPM	pH 13, SDS	25.1	16	2.9	190 / 1.16
PO(tbc)OPM	pH 13	25.6	-	2.9	47 / 0.28
PO(tbc)OPPS	pH 13, SDS	24.3	8	2.8	90 / 0.55
PO(tbc)OPPS	pH 13	23.4	6	2.7	27 / 0.17
PO(tbc)OPPS on IRA-402	pH 13	36	44	4.1	20 / 0.48

Additionally, measurements were carried out to estimate the efficiency of Type II and Type III processes in the photo-oxidation of phenol. Thus, the addition of singlet oxygen quencher, sodium azide NaN_3, to the solution containing PO(tbc)OPM **30** and SDS at pH 13, resulted in 61% inhibition of the photooxidation of phenol. Thereby, this finding indicates that the relative contribution of electron transfer (Type III) for the case when phenol is employed as a substrate is higher comparing to photo-oxidation of 2-mercaptoethanol. Again hydrogen peroxide was detected in the reaction mixture as a side product. The results obtained provide evidence for participation of the superoxide radical anion ($O_2^{\bullet -}$) in the reaction.

5.5 Photocatalytic activity of sulfonated Si(IV), Ge(IV) and metal-free phthalocyanines

2-mercaptoethanol photo-oxidation

The photocatalytic activities of three different sulfophthalocyanines (Si(IV), Ge(IV) and metal-free) were investigated. The silicon **25** and germanium **28** sulfophthalocyanines are examples of dyes, which are fully disaggregated in aqueous solution (see chapter 4.4 and Figure 4.3), which is a fundamental prerequisite for good photosensitizer. Thus, presence of detergent is not required in that case. The results obtained during photo-oxidation of 2-mercaptoethanol with SiPcTS as sensitizer are collected in Table 5.3 and depicted in Figure 5.7.

Table 5.3. Photo-oxidation of 2-mercaptoethanol by silicon sulfophthalocyanine **25**.

Compound	Conditions	O_2 consumed after 3 h [ml]	Photodegradation of dye in %	Molar ratio O_2/substrate	TON [min^{-1}]/ RR_i [ml $O_2 \cdot min^{-1}$]
SiPcTS	pH 10,	11.9	10	0.7	97 / 0.59
SiPcTS on IRA-402	pH 10	18.4	64	1	25 / 0.61
SiPcTS on IRA-958	pH 10	19.5	45	1.13	14 / 0.34

The SiPcTS **25** decomposes within a few seconds in micellar solution at pH 13. Thus, the photo-oxidation was carried out at pH 10 (Table 5.3). After a good RR_i, the reaction slows down and finally after 3 h reaction time the oxygen uptake of 11.9 ml was found, which indicates that 2-mercaptoethanol is not fully oxidized. Around 25.7 ml of oxygen is required to convert the amount of thiol used in experiment to sulfonic acid. It can not be attributed to loss of sensitizer since SiPcTS **25** is relatively stable photosensitizer, hence it is still present in the solution after 3 h. Interestingly, when after 3 hours another portion of substrate was injected to the reaction mixture the results where comparable as to the RR_i and final oxygen uptake. The reaction was repeated four times by injecting additional portion of 2-mercaptoethanol. Each time kinetic curves were comparable indicating that the activity of SiPcTS **25** remains largely unaffected. In addition to homogeneous reaction, the polymer bound SiPcTS **25** was utilized for the photo-oxidation. Two different anion exchangers were used in the experiments. The amount of consumed oxygen in case of heterogeneous photocatalysis was higher compared to the experiment with photosensitizer dissolved in a solution. Unfortunately, relatively high loss of dye was observed at the conclusion of the reaction: 64% in case of SiPcTS immobilized on IRA-402 and 45% in case of SiPcTS loaded on IRA-958. High photodegradation makes the reuse of polymer immobilized SiPcTS impossible.

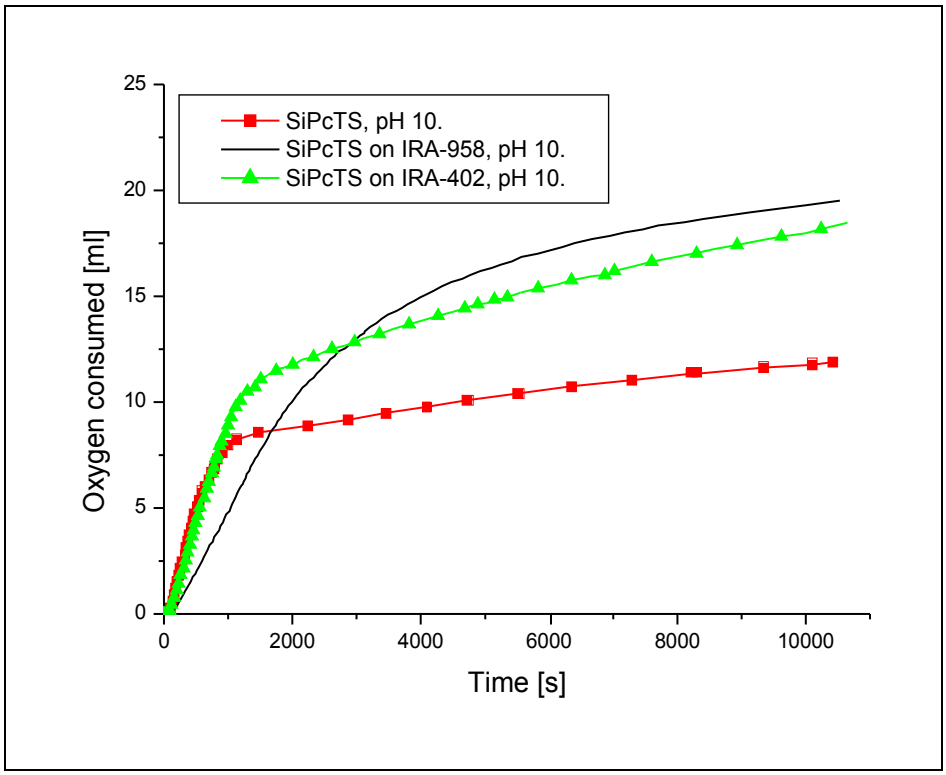

Figure 5.7. Photo-oxidation of 2-mercaptoethanol in aqueous solution at pH 10 with SiPcTS **25** as photosensitizer.

In 2001 Gerdes et al. described results concerning photocatalytic activity of SiPcTS in the photo-oxidation of phenol, cyclopentadiene and (S)-(-)-citronellol [22,44]. High activity along with extraordinary stability of the SiPcTS immobilized on anion exchanger IRA-400 enabling repeated use of such photosensitizer was claimed. The results obtained during this work, with 2-mercaptoethanol as substrate, contrast sharply with those reported by Gerdes et al. The polymer bound SiPcTS demonstrated especially low photostability during photo-oxidation of thiol.

Like in case of SiPcTS **25**, the GePcTS **28** vanishes within a few seconds in micellar solution at pH 13. Hence, measurements were carried out in aqueous solution at pH 10. The results obtained during photo-oxidation of 2-mercaptoethanol with GePcTS as sensitizer are collected in Table 5.4 and depicted in Figure 5.8. The GePcTS **28** is somewhat more active in a solution compared to SiPcTS **25**. The RR_i measured for GePcTS in the homogeneous reaction amounts to 0.95 [$mlO_2 \cdot min^{-1}$]. In addition, the experiments were carried with GePcTS **28** ionically bound to two different anion exchangers. Higher oxygen uptake was observed compared to homogeneous reaction, but on the other side very low photostability was observed.

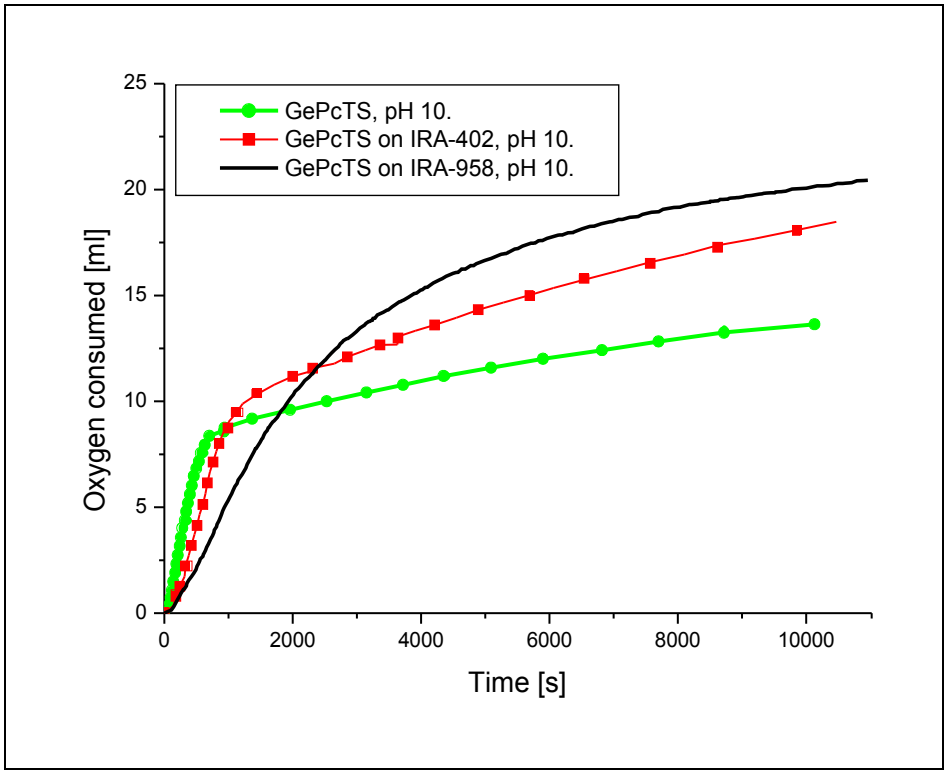

Figure 5.8. Photo-oxidation of 2-mercaptoethanol in aqueous solution at pH 10 with GePcTS **28** as photosensitizer.

When the GePcTS **28** immobilized on IRA-402 was employed as photocatalyst as much as 90% loss of dye was found. On the other hand, for GePcTS **28** loaded on IRA-958 better photostability is achieved, namely 49% of dye is bleached. The results obtained for SiPcTS **25** and GePcTS **28** are comparable as to photocatalytic activity, stability and oxygen consumption.

Table 5.4. Photo-oxidation of 2-mercaptoethanol germanium sulfophthalocyanine **28**.

Compound	**Conditions**	**O_2 consumed after 3 h [ml]**	**Photodegradation of dye in %**	**Molar ratio O_2/substrate**	**TON [min^{-1}]/ RR_i [ml $O_2 \cdot min^{-1}$]**
GePcTS	pH 10	13.6	13	0.8	154.5 / 0.95
GePcTS on IRA-402	pH 10	18.5	90	1.1	27.2 / 0.67
GePcTS on IRA-958	pH 10	20.5	49	1.2	14.8 / 0.36

Data concerning photo-oxidation of 2-mercaptoethanol by H_2PcTS **20** are collected in Table 5.5 and depicted in Figure 5.9. The H_2PcTS **20** exhibits good stability at higher

pH, thus all measurements were carried out at pH 13. Unlike SiPcTS **25** and GePcTS **28**, the metal-free sulfophthalocyanie **20** remains strongly aggregated in water solution in the absence of CTAC (see chapter 4.4 and Fig. 4.3). Hence, in the absence of detergent H_2PcTS **20** exhibits low activity, both RR_i and oxygen uptake is negligible. Upon addition of CTAC the activity is somewhat improved, however, the initial reaction rate still remains rather low. The oxygen consumption is also low as the photosensitizer decomposes gradually during the course of reaction, resulting in 78% loss of dye after 3 h of irradiation. H_2PcTS **20** immobilized on Amberlite IRA-402 and IRA-958 proved to be extremely unstable. Because of pronounced tendency to aggregate in aqueous solution along with poor photostability, metal-free sulfophthalocyanine **20** is a very bad candidate for photosensitizer.

Table 5.5. Photo-oxidation of 2-mercaptoethanol by metal-free sulfophthalocyanine **20**.

Compound	Conditions	O_2 consumed after 3 h [ml]	Photodegradation of dye in %	Molar ratio O_2/substrate	TON [min^{-1}]/ RR_i [ml $O_2 \cdot min^{-1}$]
H_2PcTS	pH 13, CTAC	12.2	78	0.7	41.1 / 0.25
H_2PcTS	pH 13	7.6	35	0.44	18.4 / 0.11
H_2PcTS on IRA-402	pH 13	23.4	100	1.37	21.5 / 0.53
H_2PcTS on IRA-958	pH 13	9.1	92	0.53	11 / 0.27

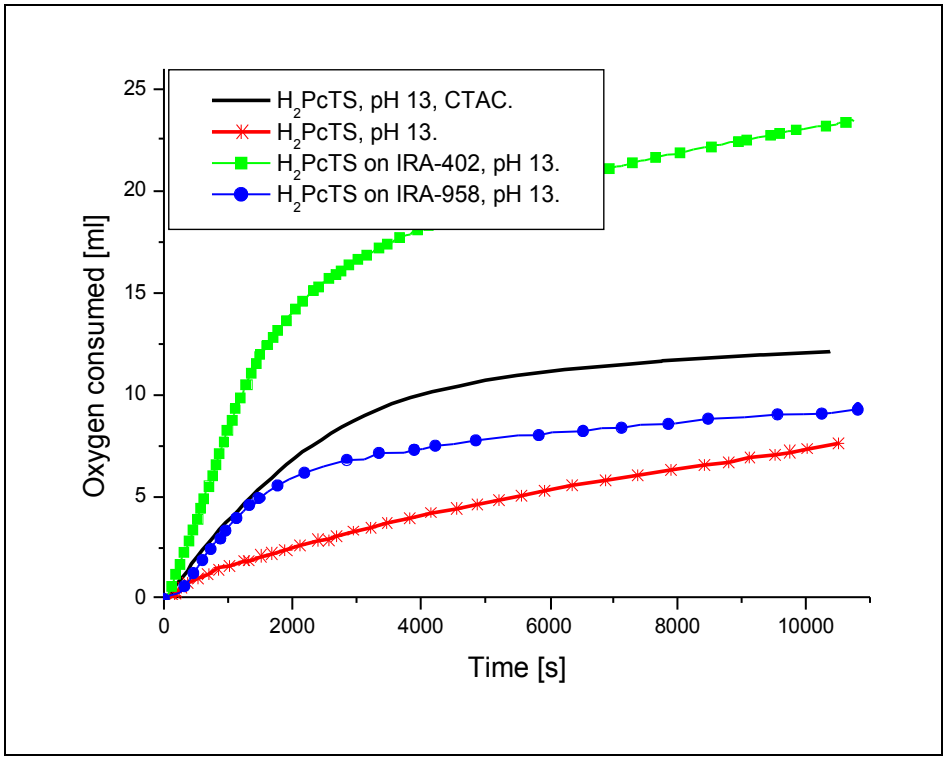

Figure 5.9. Photo-oxidation of 2-mercaptoethanol in aqueous solution at pH 13 with H_2PcTS **20** as photosensitizer.

5.6 Photocatalytic activity of sulfonated hydroxysilicon(IV) triazatetrabenzcorrole

2-mercaptoethanol photo-oxidation

For the first time the photocatalytic activity of hydroxysilicon(IV) triazatetrabenzcorrole was studied. Date are collected in Table 5.6. Addition of the cationic detergent to the aqueous solution of **23** had insignificant influence on the initial reaction rate and final oxygen consumption, indicating that the photosensitizer exists mainly in a non-aggregated form (see chapter 4.4 and Fig. 4.6). The photodegradation of **23** in the presence of CTAC was around 65 % and 59 % in a non-micellar solution. It was observed that the activity of Si(tbc)TS **23** depends on pH value. At pH 10 the initial reaction rate was decreased to RR_i 0.33 [$mlO_2 \cdot min^{-1}$], and only 6.24 ml of oxygen was consumed. On the other hand, at pH 13 increase of the RR_i to 0.83 [$mlO_2 \cdot min^{-1}$] and oxygen consumption to 18.2 ml was seen. The photodegradation of **23** was unaffected by pH value. Loss of around 63 % of photosensitizer was observed after 3 h of irradiation at pH 10. The photosensitizer Si(tbc)TS **23** was loaded on basic anion exchanger IRA-402.

Table 5.6. Photo-oxidation of 2-mercaptoethanol by Si(tbc)TS **23**.

Compound	Conditions	O_2 consumed after 3 h [ml]	Photodegradation of dye in %	Molar ratio O_2/substrate	TON [min^{-1}]/ RR_i [ml $O_2 \cdot min^{-1}$]
Si(tbc)TS	pH 13, CTAC	18.2	65	1.06	136 / 0.83
Si(tbc)TS	pH 13	17	59	0.99	119.5 / 0.73
Si(tbc)TS on IRA-402	pH 13	50	-[a]	2.9	37 / 0.9

[a] could not be measured accurately

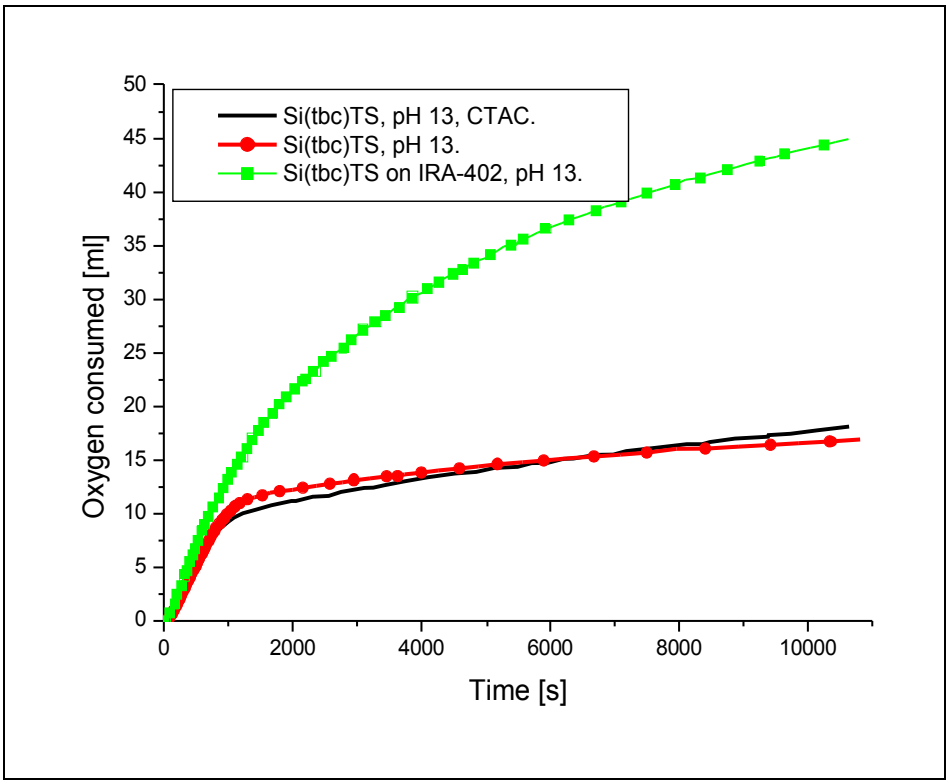

Figure 5.10. Photo-oxidation of 2-mercaptoethanol in aqueous solution at pH 13 using Si(tbc)TS **23** as photosensitizer.

Unexpectedly high oxygen consumption was observed (around 50 ml). The oxygen consumption was higher than it is expected from the stochiometry of 2-mercaptoethanol photo-oxidation (around 25.7 ml of O_2 corresponds to the formation of 2-hydroxyethanesulfonic acid). This result may indicate that the singlet oxygen and the superoxide radical anion ($O_2^{\bullet-}$) formed during reaction is involved in the photo-oxidation of polymer. After reaction the solution becomes non-transparent and turns milky in hue indicating polymer degradation.

Phenol photo-oxidation

Additionally, the activity of Si(tbc)TS **23** in the photo-oxidation of phenol was studied (Table 5.7). Photo-oxidation of phenol with Si(tbc)TS **23** was measured in micellar and non-micellar solution. The final oxygen consumption in both cases was similar but higher initial reaction rate was measured in non-micellar solution, *i.e.* 0.55 [mlO_2 /min].

Table 5.7. Photo-oxidation of phenol by Si(tbc)TS **23**.

Compound	Conditions	O_2 consumed after 3 h [ml]	Photodegradation of dye in %	Molar ratio O_2/phenol	TON [min^{-1}]/ RR_i [ml $O_2 \cdot min^{-1}$]
Si(tbc)TS	pH 13, CTAC	27.2	42	3.08	60.5 / 0.37
Si(tbc)TS	pH 13	25.6	30	2.9	90 / 0.55
Si(tbc)TS on IRA-402	pH 13	32	15	3.64	21 / 0.52
Si(tbc)TS on IRA-958	pH 13	48.4	10	5.5	18.4 / 0.45

Somewhat higher photodegradation was observed in a micellar solution (around 42%) as in previous experiments with 2-mercaptoethanol. When the photocatalytic reaction is performed with Si(tbc)TS **23** immobilized on IRA-402 a 32 ml of oxygen uptake was measured. This value may roughly correspond to the complete mineralization of phenol; the calculated value is around 30.7 ml of oxygen for the quantity of phenol used during experiment. Surprisingly, around 48 ml of oxygen is consumed when the dye is loaded on IRA-958. The photodegradation on both polymers is comparable, *i.e.* 15 % for IRA-402 and 10 % in case of IRA-958. These results clearly show that the choice of ion exchanger is crucial to the photocatalytic process. However, the question as to how the polymer affects the photocatalytic activity remains opens. The advantage of Si(tbc)TS **23** as photocatalyst is that the tendency towards aggregation in an aqueous solution is very low, hence, the presence of detergent is not required during reaction.

5.7 Photocatalytic activity of positively and zwitterionically charged silicon phthalocyanines

2-mercaptoethanol photo-oxidation

Two water-soluble silicon phthalocyanines were investigated, *i.e.* positively charged SiPcOPM **14** and zwitterionic SiPcOPPS **15** (Tab. 5.8). Both phthalocyanines are examples of compounds exhibiting pronounced tendency towards aggregates formation in aqueous solution (see chapter 4.4 and Fig. 4.7), resulting in negligible activity. Even at pH 13 upon addition of surfactant SDS to the water solution of SiPcOPM **14** and SiPcOPPS **15** the activities (RR_i, final oxygen consumption) are not increased (Fig. 5.11). Obviously, in micellar solution both photosensitizers are still highly aggregated

and dissipation of energy of the excited state readily occurs. The SiPcOPM **14** showed only 13% photodegradation after 3 h of irradiation. However, this could be rather attributed to low singlet oxygen production than good stability per se. Both dyes were loaded on ion exchangers. The results with polymer-loaded SiPcOPM **14** and SiPcOPPS **15** were unsatisfactory as to the RR_i and oxygen consumption. For example SiPcOPPS immobilized on IRA-402 was totally photobleached during the course of reaction.

Table 5.8. Photocatalytic oxidation of 2-mercaptoethanol in aqueous solution at pH 13 by water-soluble silicon phthalocyanines **14** and **15**.

Compound	Conditions	O_2 consumed after 3 h [ml]	Photodegradation of dye in %	Molar ratio O_2/substrate	TON [min^{-1}]/ RR_i [ml $O_2 \cdot min^{-1}$]
SiPcOPM	pH 13, SDS	7.3	13	0.4	15 / 0.09
SiPcOPM	pH 13	5.5	34	0.3	9 / 0.05
SiPcOPM on IRA-120	pH 13	8.1	7	0.5	3 / 0.07
SiPcOPPS	pH 13, SDS	4	54	0.2	5.8 / 0.04
SiPcOPPS	pH 13	6.9	38	0.4	13.2 / 0.08
SiPcOPPS on IRA-402	pH 13	8.3	100	0.5	2.9 / 0.07

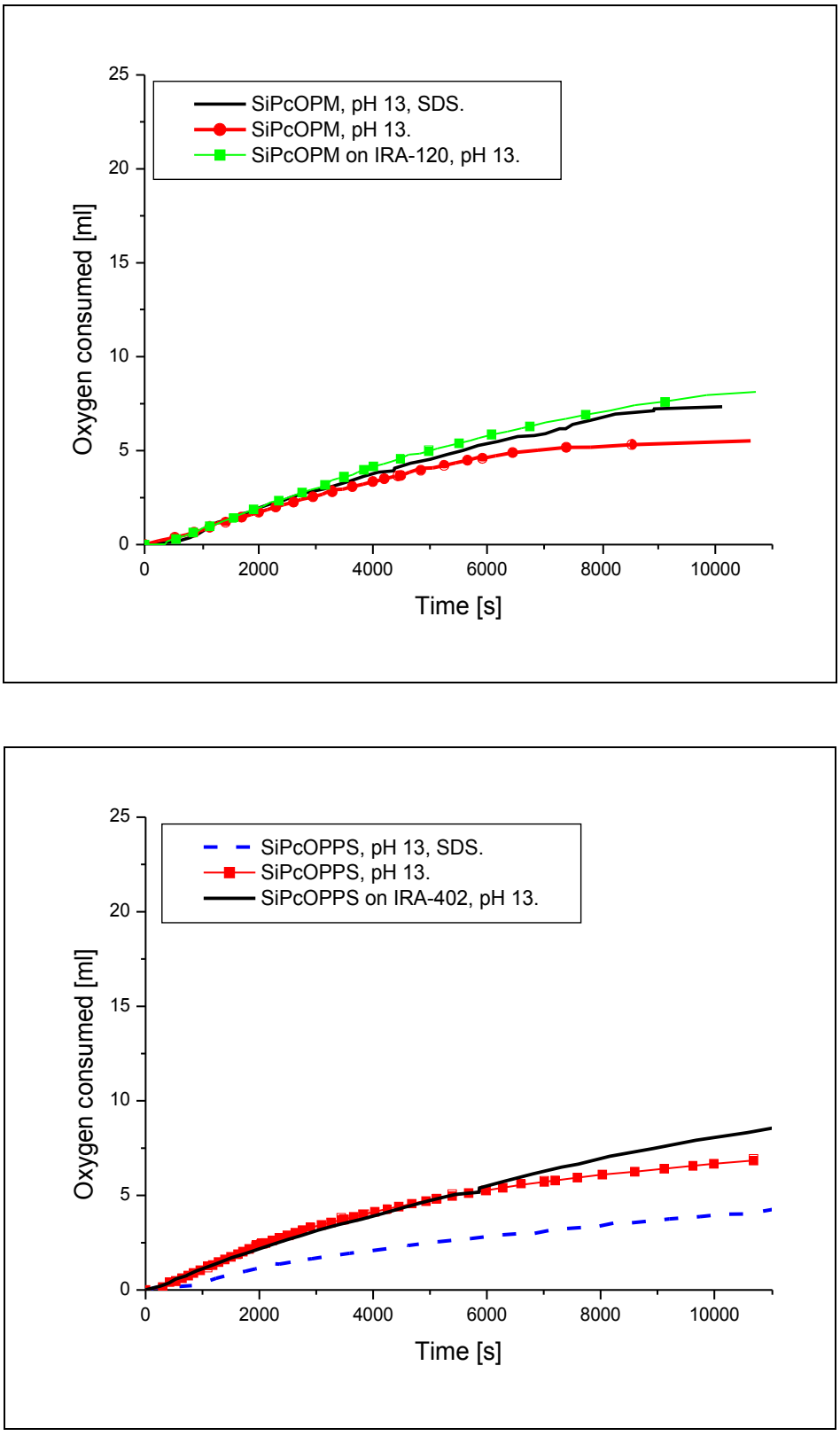

Figure 5.11. Photo-oxidation of 2-mercaptoethanol in aqueous solution at pH 13 with SiPcOPM **14** and SiPcOPPS **15** as photocatalysts.

5.8 Photocatalytic activity of positively and zwitterionically charged germanium phthalocyanines

2-mercaptoethanol photo-oxidation

The photocatalytic activities of GePcOPM **17** and GePcOPPS **18** are vastly superior to the activities of their silicon-containing counterparts. Data are collected in Table 5.9 and depicted in Figure 5.12. The homogeneous reaction could be conducted at pH 13 since both germanium phthalocyanines proved to be stable at high pH. Both GePcOPM **17** and GePcOPPS **18** turned out to be efficient photosensitizers for the photo-oxidation of 2-mercaptoethanol. However, the presence of anionic detergent (SDS) was essential for good photocatalytic activity. The activities of GePcOPM **17** and GePcOPPS **18** in the presence of SDS are comparable. Photo-oxidation of 2-mercaptoethanol results in TON of 106 [min^{-1}] for GePcOPM **17** and 97 [min^{-1}] for GePcOPPS **18**, respectively. Subsequent addition of another portion of substrate to the reaction mixture containing GePcOPM **17** resulted in a similar kinetic curve, indicating that after 3 h the activity of photosensitizer remains in principle the same. In the absence of anionic surfactant considerable decrease of the activity of **17** and **18** was seen. Moreover, in the absence of detergent 100% photodegradation was measured.

Table 5.9. Photo-oxidation of 2-mercaptoethanol by GePcOPM **17** and GePcOPPS **18**.

Compound	Conditions	O_2 consumed after 3 h [ml]	Photodegradation of dye in %	Molar ratio O_2/substrate	TON [min^{-1}]/ RR_i [ml $O_2 \cdot min^{-1}$]
GePcOPM	pH 13, SDS	18.4	24	1.07	106 / 0.65
GePcOPM	pH13	-[a]	100		-[a]
GePcOPM on IRA-120	pH 13	6.9	45	0.4	2.8 / 0.07
GePcOPPS	pH 13, SDS	17.4	14	1	97.6 / 0.6
GePcOPPS	pH 13	3	100	0.17	-[b]
GePcOPPS on IRA-120	pH 13	7.2	-[c]	0.42	2.7 / 0.07

[a] due to rapid photodegradation could not be measured, [b] due to low activity could not be measured accurately, [c] could not be measured accurately

The phthalocyanines **17** and **18** are strongly aggregated in water solution (see chapter 4.4 and Fig. 4.8). Thus, the addition of detergent is necessary for the photocatalysis. The

UV-Vis spectra of germanium phthalocyanines in aqueous solution at pH 13, even in the presence of SDS detergent, exhibit intense absorption at around 645 nm, which is characteristic of aggregated form. Both photosensitizers were loaded on cation exchanger IRA-120. However, poor activity, low oxygen consumption along with high photobleaching make such heterogeneous system useless as photocatalyst.

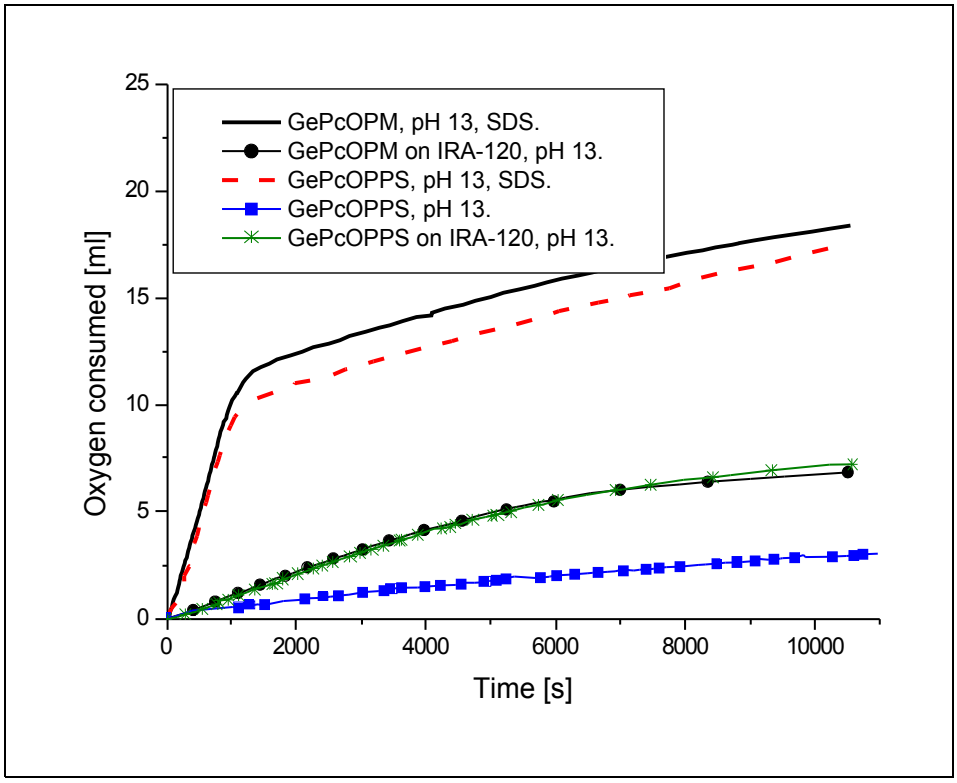

Figure 5.12. Photo-oxidation of 2-mercaptoethanol in aqueous solution at pH 13 with GePcOPM **17** and GePcOPPS **18** as photocatalysts.

5.9 Photocatalytic activity of positively and zwitterionically charged metal-free phthalocyanines

2-mercaptoethanol photo-oxidation

Data obtained during photo-oxidation of 2-mercaptoethanol employing metal-free phthalocyanines as photosensitizers are collected in Table 5.10 and showed in Figure 5.13. Addition of surfactant SDS to the water solution of metal-free phthalocyanines H_2PcOPM **11** and H_2PcOPPS **12** results in a strong increase of the photocatalytic activity. Obviously, without detergent the phthalocyanines were highly aggregated (see chapter 4.4 and Fig. 4.5) and dissipation of energy of the excited state occurs. Both metal-free phthalocyanines remain virtually inactive as photocatalysts in the absence of appropriate detergent.

Table 5.10. Photo-oxidation of 2-mercaptoethanol by H_2PcOPM **11** and H_2PcOPPS **12**.

Compound	Conditions	O_2 consumed after 3 h [ml]	Photodegradation of dye in %	Molar ratio O_2/substrate	TON [min^{-1}]/ RR_i [ml $O_2 \cdot min^{-1}$]
H_2PcOPM	pH 13, SDS	14.6	70	0.85	147 / 0.9
H_2PcOPM	pH13	2.3	80	0.13	3 / 0.02
H_2PcOPM on IRA-120	pH 13	-[a]	-[a]		-[a]
H_2PcOPPS	pH 13, SDS	14.1	64	0.8	109 / 0.67
H_2PcOPPS	pH 13	2.9	6	0.17	3.6 / 0.02

[a] no activity

For example the initial reaction rate (RR_i) for H_2PcOPM **11** in the monomeric state is 0.9 [ml/min] and decreases to 0.02 [ml/min] in the absence of detergent. From the Figure 5.13 it follows that after a very rapid initial phase of the photo-oxidation of 2-mercaptoethanol slow subsequent step is observed. After approximately 12 ml of oxygen is consumed the reaction slows down. Both H_2PcOPM **11** and H_2PcOPPS **12** dissolved in micellar aqueous solution show relatively high TON but low total oxygen uptake. Moreover, both H_2PcOPM **11** and H_2PcOPPS **12** show very high photodegradation, *i.e.* 70 % for H_2PcOPM **11** and 64 % for H_2PcOPPS **12** in micellar solution after 3 h of irradiation, respectively. Positively charged phthalocyanine **11** immobilized on cation exchanger Amberlite IRA-120 exhibits no photocatalytic activity.

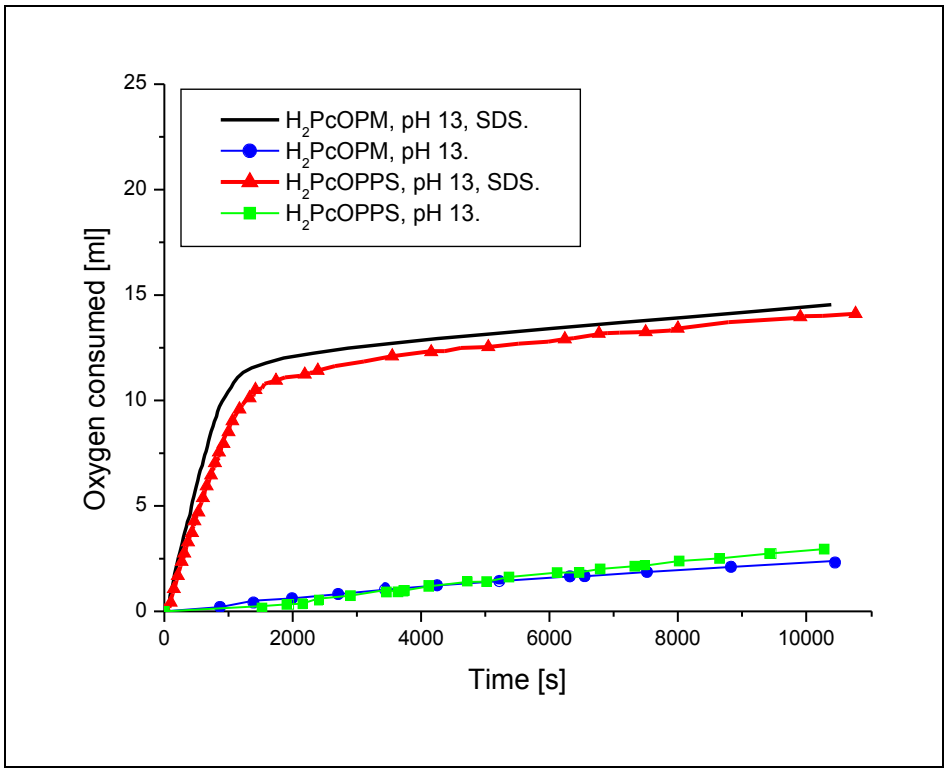

Figure 5.13. Photo-oxidation of 2-mercaptoethanol in aqueous solution at pH 13 with H_2PcOPM **11** and H_2PcOPPS **12** as photocatalysts.

High photodegradation, low oxygen consumption along with high aggregation tendency make the metal-free phthalocyanines H_2PcOPM **11** and H_2PcOPPS **12** very bad candidates for the photocatalysts in the photo-oxidation reaction.

5.10 Photocatalytic activity of differently charged zinc porphyrins

2-mercaptoethanol photo-oxidation

Photocatalytic data concerning activity of zinc porphyrins are collected in Table 5.11. All porphyrins synthesized during this work proved to be very stable at pH 13. Addition of detergent results in monomerization of porphyrins (see chapter 4.4 Fig. 4.9) and consequently in increased photocatalytic activity. Regarding final oxygen consumption, photocatalytic activity along with stability, ZnPoOPM **49** and ZnPoOPPS **50** exhibited

the most interesting results of all investigated compounds. On the other hand, negatively charged ZnPoTS **52** showed poor activity and stability towards photobleaching.

Table 5.11. Photo-oxidation of 2-mercaptoethanol by ZnPoOPM **49**, ZnPoOPPS **50** and ZnPoTS **52**.

Compound	Conditions	O_2 consumed after 3 h [ml]	Photodegradation of dye in %	molar ratio O_2/substr.	TON [min^{-1}]/ RR_i [ml $O_2 \cdot min^{-1}$]
ZnPoOPM	pH 13, SDS	22.1	0	1.3	145 / 0.89
ZnPoOPM	pH 13	17.8	80	1.04	50 / 0.3
ZnPoOPM on IRA-120	pH 13	15.2	16	0.9	8 / 0.19
ZnPoOPPS	pH 13, SDS	23.1	2.6	1.34	338 / 2.07
ZnPoOPPS	pH 13	19.2	75	1.1	97 / 0.59
ZnPoOPPS on IRA-402	pH 13	31.1	-[a]	1.8	18.5 / 0.45
ZnPoTS	pH 13, CTAC	11.6	93	0.67	95 / 0.58
ZnPoTS	pH 13	4.4	79	0.26	8 / 0.05
ZnPoTS on IRA-402	pH 13	14.4	100	0.84	25 / 0.61

[a] could not be measured accurately

Positively charged ZnPoOPM **49** in micellar solution is characterized by an excellent stability. No disappearance of dye after 3 h of irradiation was observed. Another portion of 2-mercaptoethanol was injected to the reaction vessel after 3 h, the apparatus was flushed with oxygen and the reaction was run again. Both initial reaction rate, TON and consumption of oxygen after 3 h reaction time was the same as for the first measurement. It follows that ZnPoOPM **49** is extremely stable during photo-oxidation of thiol. The amount of oxygen consumed under irradiation at pH 13 and in the presence of detergent SDS after 3 h (22.1 ml) roughly corresponds to the formation of 2-hydroxyethanesulfonic acid.

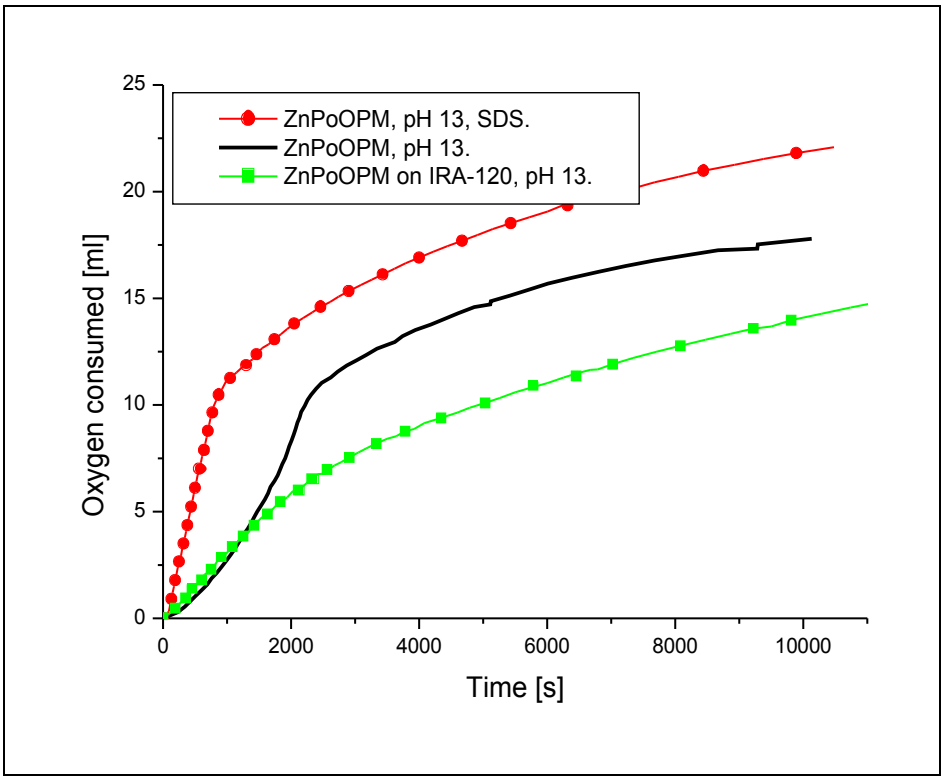

Figure 5.14. Photo-oxidation of 2-mercaptoethanol in aqueous solution at pH 13, sensitised by ZnPoOPM **49**.

The photocatalytic activity of ZnPoOPM **49** decreases considerably in the absence of SDS. In a micellar solution the initial reaction rate was 0.89 [mlO_2/min] whereas in a non-micellar solution the initial reaction rate dropped to 0.3 [mlO_2/min], very high degradation occurred (80 %) as well as lower oxygen uptake (17.8 ml) was observed comparing to measurement in micellar solution. The immobilization of **49** on Amberlite IRA-120 did not improve the photocatalytic activity of positively charged zinc porphyrin. Merely 15.2 ml of oxygen was consumed after 3 h of irradiation and 16 % loss of dye occurred. The participation of singlet oxygen in the photo-oxidation catalysed by positively charged zinc porphyrin **49** was easily determined by additional measurement in D_2O. A sharp increase in activity was seen in deuterated solvent due to longer lifetime of $^1O_2$ in D_2O. Thus, a surge of TON from 145 [min^{-1}] in water solution to 235 [min^{-1}] in D_2O was observed. On the other hand, the addition of singlet oxygen quencher (NaN_3, $2.5 \cdot 10^{-3}$ mol/l) to a micellar solution of ZnPoOPM **49** resulted in a discernible decline of TON to 21 [min^{-1}]. These results show that presence of sodium azide results in 85% inhibition of the photo-oxidation of 2-mercaptoethanol. Thus, the

main process involved in this reaction is the singlet-oxygen mediated (Type II) photo-oxidation and to a much lesser extent electron transfer pathway (Type III).

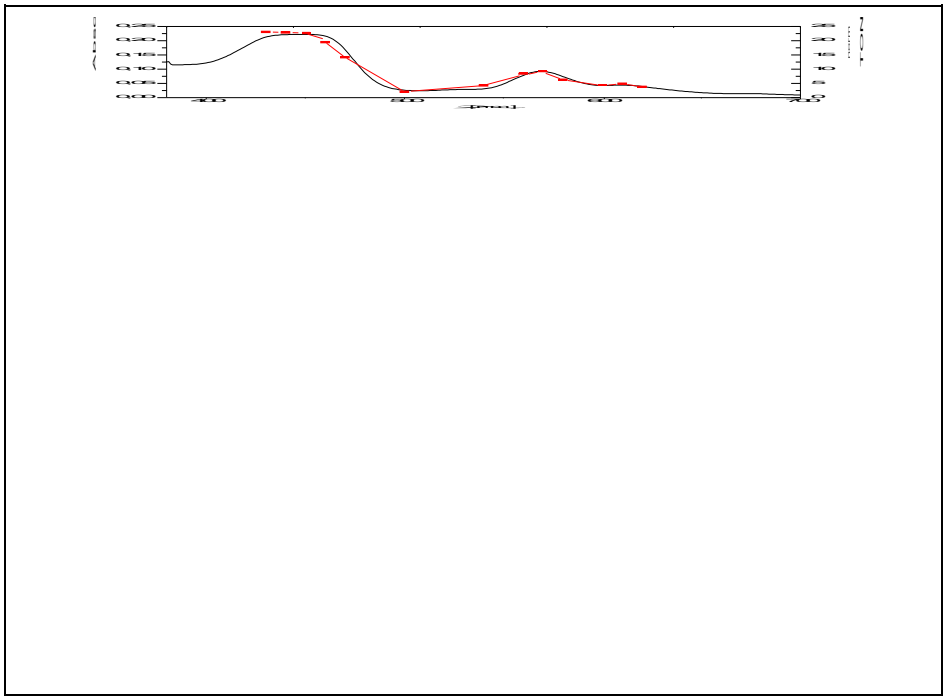

Figure 5.15. Photoaction spectrum (--■--) of ZnPoOPM **49** obtained during photo-oxidation of 2-mercaptoethanol in aqueous solution in the presence of SDS at pH 13. The solid line represents the absorption spectrum of ZnPoOPM **49** in aqueous solution in the presence of SDS at pH 13.

In Figure 5.15 the photoaction spectrum of ZnPoOPM **49** in the presence of SDS at pH 13 based on normalized TON is compared with the absorption spectrum. The highest activity is found in the region of Soret band as well as in the Q-band. No activity can be seen in the region between these two bands.

The zwitterionic ZnPoOPPS **50** exhibits the highest activity ever measured during this investigation. A very high TON was found in the presence of surfactant SDS, *i.e.* 338 [min^{-1}]. However, the turnover number drops to around 97 [min^{-1}] when the measurement is made in a non-micellar solution. After 3 h 23 ml of oxygen was consumed, the amount which corresponds to the 2-hydroxyethanesulfonic acid formation. Somewhat lower oxygen consumption (*i.e.* 19.2 ml) occurs in a non-micellar solution. As in the case of ZnPoOPM **49**, participation of detergent is crucial for the stability of photocatalyst. Hence, when the photosensitizer **50** is fully monomerized in a micellar solution only 2.6 % loss of dye is observed. On the other hand, considerably

degradation of photocatalyst is measured in a non-micellar solution, *i.e.* 75 %. The heterogeneous photocatalytic reaction with ZnPoOPPS **50** immobilized on Amberlite IRA-402 gives high oxygen consumption, around 31 ml, but at the same time most of the porphyrin is bleached. It will be shown that also in the case of phenol photo-oxidation the homogeneous photocatalysis is superior to the heterogeneous reaction with regard to RR_i and stability.

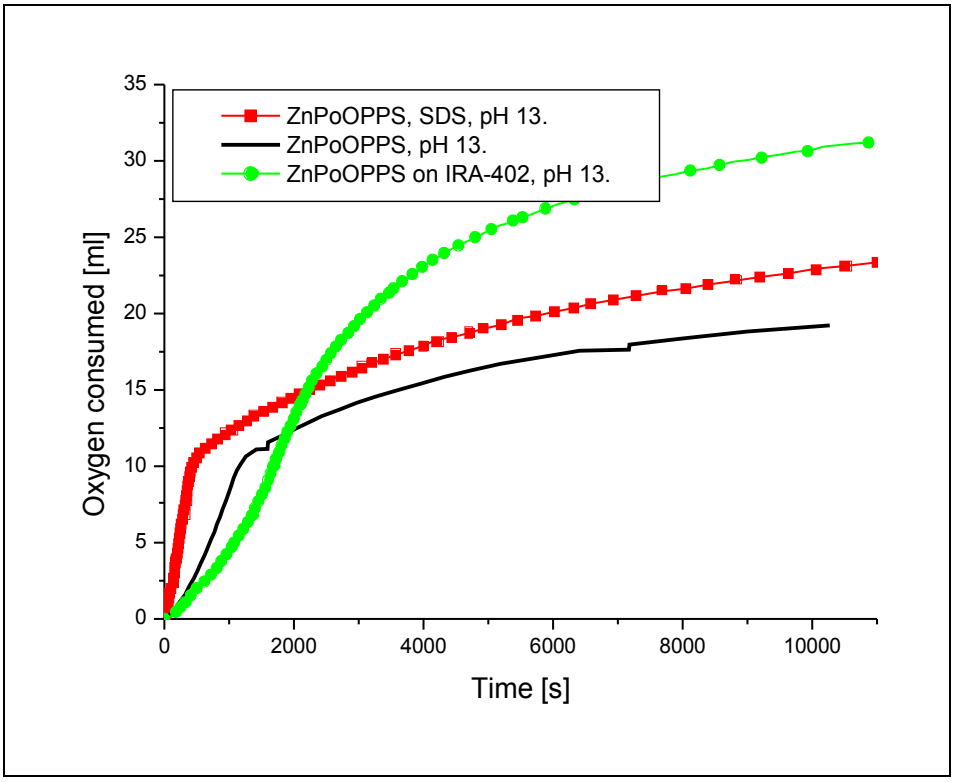

Figure 5.16. Photo-oxidation of 2-mercaptoethanol in aqueous solution at pH 13, sensitised by ZnPoOPPS **50**.

The negatively charged zinc porphyrin **52** proved to be very poor photocatalyst. This behaviour can be accounted for by its enhanced photodegradation during the course of reaction. 93% photodegradation after 3 h of illumination was observed when the reation was ran in the presence of detergent CTAC. Equally bad stability, that is 79%, was found for the reaction in a non-micellar solution. ZnPoTS **52** could be bound to anion exchanger Amberlite IRA-402. However, after relatively good initial step the reaction slows down due the extensive photodegradation (100%).

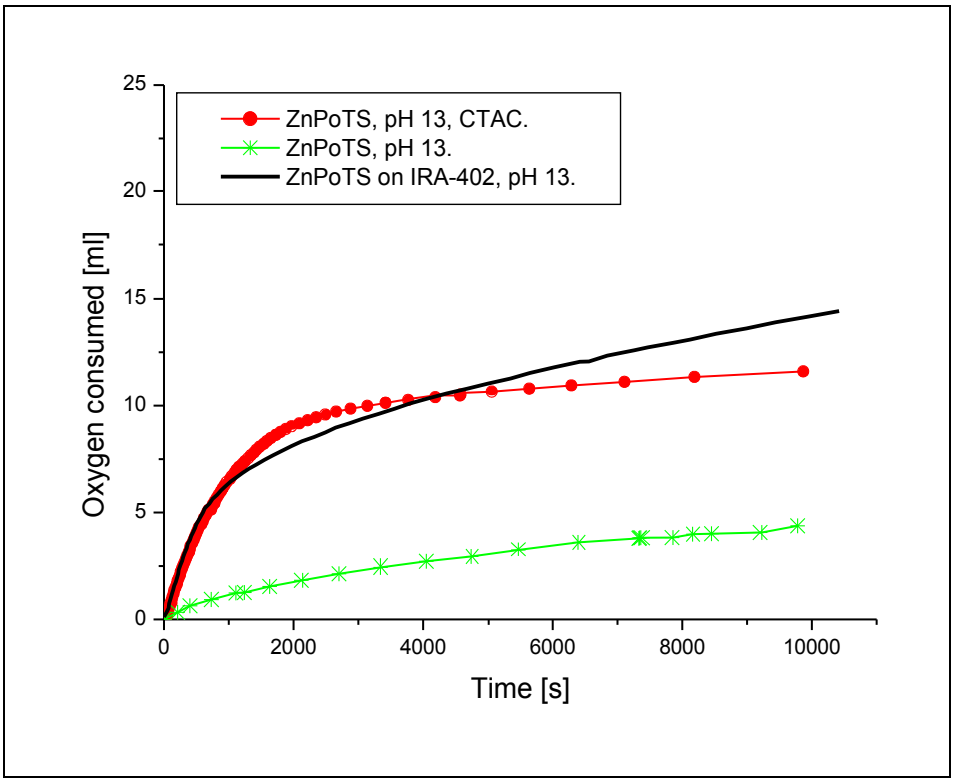

Figure 1.17. Photo-oxidation of 2-mercaptoethanol in aqueous solution at pH 13, sensitised by ZnPoTS **52**.

Phenol photo-oxidation

Additionally, the photo-oxidation of phenol with ZnPoOPM **49** and ZnPoOPPS **50** as photosensitizers was studied (Tab. 5.12). The results obtained indicate extraordinary activity of both compounds in a micellar solution. The initial reaction rate measured for ZnPoOPM **49** amounted to 0.96 [mlO_2/min], for zwitterionic compound was even higher, that is 1.2 [mlO_2/min]. The zwitterionic porphyrin **50** is characterized by a very good stability, *i.e.* only 8% of dye disappears at the conclusion of the reaction. When ZnPoOPPS **50** was loaded on anion exchanger Amberlite IRA-402 the activity expressed as RR_i was low, however the oxygen uptake was better comparing to homogeneous reaction (30 ml O_2). Unfortunately, significant degradation (72%) makes such heterogeneous photocatalyst unsuitable for repeated use.

Table 5.12. Photo-oxidation of phenol by ZnPoOPM **49** and ZnPoOPPS **50**.

Compound	Conditions	O_2 consumed after 3 h [ml]	Photodegradation of dye in %	Molar ratio O_2/phenol	TON [min^{-1}]/ RR_i [ml $O_2 \cdot min^{-1}$]
ZnPoOPM	pH 13, SDS	26.4	14	3	158 / 0.96
ZnPoOPM	pH 13	27.4	14	3.1	51 / 0.31
ZnPoOPPS	pH 13, SDS	26.5	8	3	197 / 1.2
ZnPoOPPS	pH 13	25.1	55	2.9	84 / 0.51
ZnPoOPPS on IRA-402	pH 13	30.1	72	3.4	14.4 / 0.35

In general, both positively charged and zwitterionic zinc porphyrins are very efficient photosensitizers for activation of oxygen in the photo-oxidation of 2-mercaptoethanol and phenol. Addition of positively charged detergent SDS greatly enhances the initial reaction rate and oxygen consumption (see chapter 4.4 and Fig. 4.9). Moreover, in micellar solution compounds **49** and **50** exhibit excellent stability (photodegradation between 0% and 2.6%). On the other hand, significant degradation (75%-80%) was observed in a no-micellar solution resulting in a lower activity (RR_i) and oxygen uptake. The heterogeneous reaction catalyzed by ZnPoOPPS **50** loaded on Amberlite IRA-402 is characterized by high oxygen consumption but lower activity compare to the homogeneous reaction. The UV-Vis reflectance spectrum indicates considerable degradation of zinc porphyrin **50**.

5.11 Photocatalytic activity of positively and zwitterionically charged metal-free porphyrins

2-mercaptoethanol photo-oxidation

The photocatalytic properties of two metal-free porphyrins were investigated (Tab. 5.13). The photo-oxidation of 2-mercaptoethanol catalysed by H_2PoOPM **46** and H_2PoOPPS **47** resulted in a good TON (131 [min^{-1}] and 150 [min^{-1}]), indicating high photocatalytic activity of both sensitizers, as well as high oxygen uptake (*ca.* 20 ml), indicating that the substrate is almost completely oxidized. However, presence of detergent is required to ensure monomerization of porphyrins (see chapter 4.4). In the absence of detergent high degradation (80-83%) and lower oxygen consumption

(around 14 ml) occurs. The comparison of photocatalytic data obtained during photo-oxidation of 2-mercaptoethanol and phenol reveals that there is strong influence of the substrate structure on the photo-oxidation efficiency, as well as on the sensitizer photodegradation.

Table 5.13. Photo-oxidation of 2-mercaptoethanol by H_2PoOPM **46** and H_2PoOPPS **47**.

Compound	Conditions	O_2 consumed after 3 h [ml]	Photodegradation of dye in %	Molar ratio O_2/substrate	TON [min^{-1}]/ RR_i [ml $O_2 \cdot min^{-1}$]
H_2PoOPM	pH 13, SDS	19.8	52	1.15	131 / 0.8
H_2PoOPM	pH 13	13.9	80	0.8	121 / 0.74
H_2PoOPPS	pH 13, SDS	20.1	67	1.2	150 / 0.92
H_2PoOPPS	pH 13	14.1	83	0.8	130 / 0.79

Phenol photo-oxidation

Data obtained during photo-oxidation of phenol employing metal-free porphyrins as photosensitizers are collected in Table 5.14 and depicted in Figure 5.18.

Both H_2PoOPM **46** and H_2PoOPPS **47** show good activity (RR_i 0.45-0.6 [mlO_2 min^{-1}]). Moreover, very high stability was observed for both compounds when the reaction is conducted in the presence of appropriate detergent. Only 7% of positively charged H_2PoOPM **46** vanished from the solution after 3 h reaction time. The zwitterionic porphyrin H_2PoOPPS **47** exhibits extraordinary stability, *i.e.* no loss of dye was observed during photocatalytic reaction. After conclusion of the reaction another portion of phenol was injected to the reaction vessel, the equipment was flushed with oxygen and the reaction conducted again. The kinetic curve obtained in the second reaction was identical with the first one (TON, RR_i and oxygen uptake) indicating excellent stability and efficiency of the photocatalyst.

Table 5.14. Photo-oxidation of phenol by H_2PoOPM **46** and H_2PoOPPS **47**.

Compound	Conditions	O_2 consumed after 3 h [ml]	Photodegradation of dye in %	Molar ratio O_2/phenol	TON [min^{-1}]/ RR_i [ml $O_2 \cdot min^{-1}$]
H_2PoOPM	pH 13, SDS	25.6	7	2.9	74 / 0.45
H_2PoOPM	pH 13	19.9	68	2.25	47 / 0.29
H_2PoOPPS	pH 13, SDS	25.8	0	2.9	98 / 0.6
H_2PoOPPS	pH 13	23.6	65	2.7	64 / 0.4

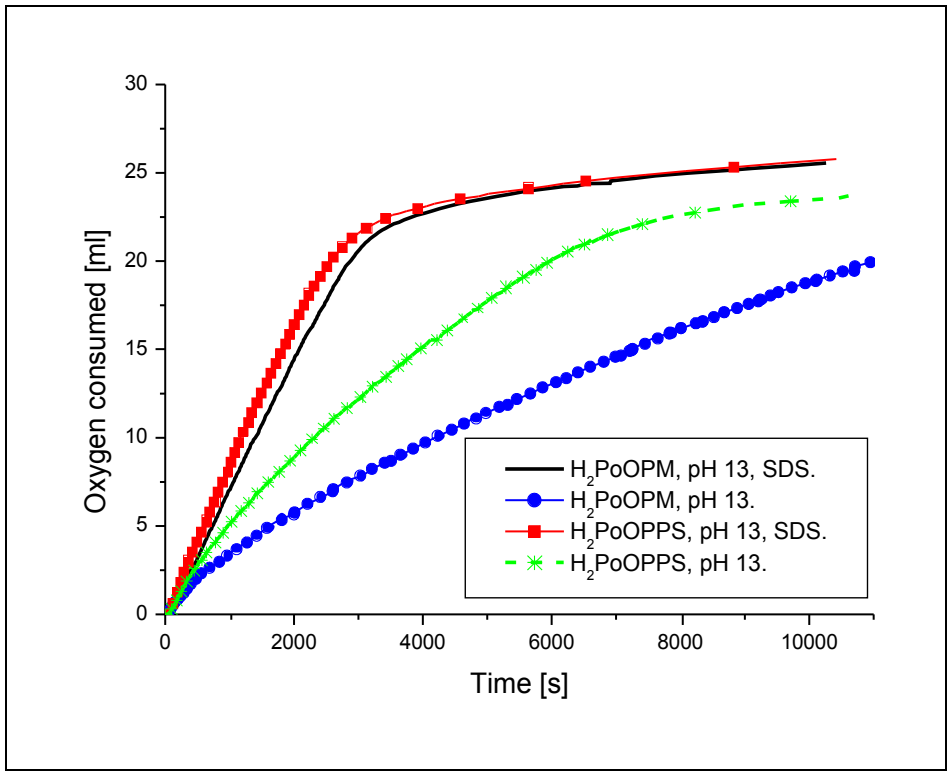

Figure 5.18. Photo-oxidation of phenol in aqueous solution at pH 13 with H_2PoOPM **46** and H_2PoOPPS **47** as photocatalysts.

As in case of thiol photo-oxidation the reaction in a micellar solution is superior to the photo-oxidation in a non-micellar solution, since both activities and stabilities are significantly enhanced. In the absence of detergent considerably loss of photosensitizer occurred (65-68%) as well as initial reaction rate and oxygen consumption was lesser.

5.12 Photocatalytic activity of panchromatically absorbing photosensitizers

The action spectra obtained for phthalocyanines, porphyrins and triazatetrabenzcorroles show that each photosensitizer is photocatalytically active solely in the area of absorption (Q-band and Soret band). In principle, there is no activity in the region between absorption maxima. The idea of panchromatically absorbing systems rests on the assumption that phthalocyanines, porphyrins, triazatetrabenzcorroles and other dye molecules coupled together would be capable of collecting a considerable fraction of the solar spectrum, much more than each of these compounds would be able being used

separately. In the photocatalytic experiments the incident beam of light consists of photons of different energies. Using one photosensitizer only small fraction of the spectrum of light is effectively utilized to drive the photochemical process. In this chapter it will be shown that combination of a few photosensitizers greatly improve the reaction efficiency leading to rapid photo-oxidation of 2-mercaptoethanol.

In the first experiment two zwitterionic compounds were investigated, *i.e.* triazatetrabenzcorrole **31** and germanium phthalocyanine **18**. The reaction was carried out at pH 13 in the presence of detergent SDS (Tab. 5.15) as zwitterions exhibit increased tendency towards aggregates formation. The UV-Vis spectrum of the mixture of GePcOPPS **18** and PO(tbc)OPPS **31** exhibits absorption in the regions of 678-596 nm and 416-445 nm (see chapter 4.4 and Fig. 4.4 as well as Fig. 4.8). Combination of both zwitterionic sensitizers gives rise to pronounced increase of the initial reaction rate to 0.9 [ml O_2 min^{-1}], while for the single compound it amounts to around 0.6 [ml O_2 min^{-1}] (Fig. 5.19). The oxygen consumption found for single dye is around 13 ml. The photo-oxidation of thiol with a combination of phthalocyanine **18** and triazatetrabenzcorrole **31** yielded 16.4 ml oxygen uptake after 1 h. Thus, it has been shown that two-component catalytic system is more effective than single photosensitizer. Under homogeneous condition at a concentration of 5 μmol/l no mutual quenching of the excited states between two compounds was observed thereby the photocatalytic activity was maintained.

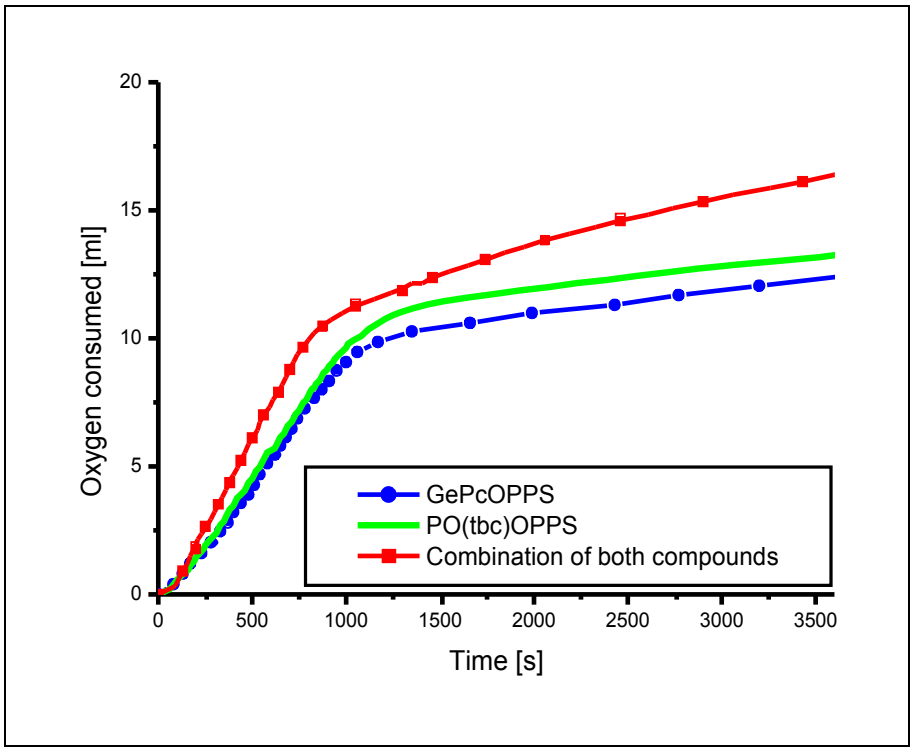

Figure 5.19. Photo-oxidation of 2-mercaptoethanol at pH 13 in the presence of SDS 0.1 mol/l with: PO(tbc)OPPS **31** (——), GePcOPPS **18** (–♦–) and combination of both photosensitizers (–■–). Concentration of dye: 5 (μmol/l).

Table 5.15. Photo-oxidation of 2-mercaptoethanol by PO(tbc)OPPS **31**, GePcOPPS **18** and combination of both compounds.

Compound	**Conditions**	**Oxygen consumed after 1 h in [ml]**	**Molar ratio O_2/substrate**	**RR_i [ml O_2·min^{-1}]**
PO(tbc)OPPS	pH 13, SDS	13.3	0.77	0.63
GePcOPPS	pH 13, SDS	12.4	0.73	0.6
Combination of compounds	pH 13, SDS	16.39	0.95	0.9

In the following experiment two negatively charged photosensitizers with sulfonate groups were investigated. One of them is the hydroxysilicon triazatetrabenzcorole **23** and the other one is the well-known photosensitizer zinc sulfophthalocyanine **53**. Figure 5.20 represents results obtained for combination of two sulfonated sensitizers. The UV-Vis spectrum shows that mixture of both compounds enables collecting of light between 680-600 nm and 454-412 nm (see chapter 4.3 and 4.4). The reaction was conducted in an alkaline aqueous solution with oppositely charged detergent CTAC. As in the preceding experiment the utilization of combination of Si(tbc)TS **23** and ZnPcTS **53**

resulted in enhancement of reaction rate for the oxidation of 2-mercaptoethanol. The initial reaction rate observed for single sensitizer was between 0.83-0.87 [ml O_2 min^{-1}]. In case of combined dyes RR_i increased to 1.3 [ml O_2 min^{-1}]. Moreover, in a relatively short reaction time 2-mercaptoethanol is completely oxidized to 2-hydroxyethanesulfonic acid. These results clearly demonstrate remarkable improvement of the catalytic activity of the panchromatically absorbing system consisted of two dyes active at different wavelengths. However, by far the best result was obtained for three-component panchromatically absorbing system.

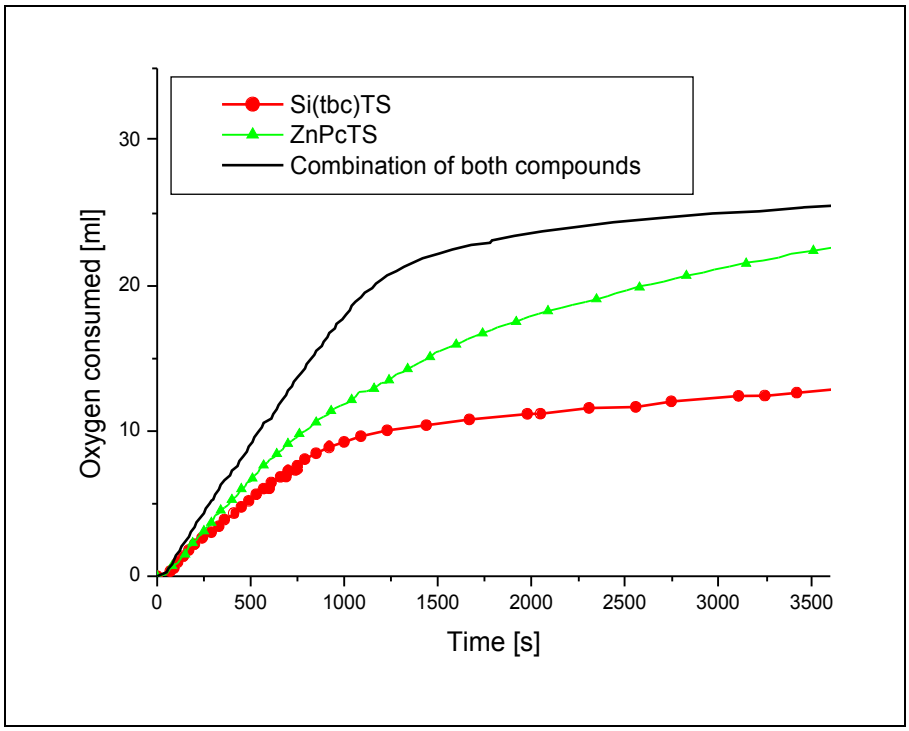

Figure 5.20. Photo-oxidation of 2-mercaptoethanol at pH 13 in the presence of CTAC 0.1 mol/l with: Si(tbc)TS **23** (—♦—), ZnPcTS **53** (–▲–) and combination of both photosensitizers (——). Concentration of dye: 5 (μmol/l).

Table 5.16. Photo-oxidation of 2-mercaptoethanol by Si(tbc)TS **23**, ZnPcTS **53** and combination of both compounds.

Compound	Conditions	Oxygen consumed after 1 h in [ml]	Molar ratio O_2/substrate	RR_i [ml $O_2 \cdot min^{-1}$]
Si(tbc)TS	pH 13, CTAC	12.7	0.7	0.83
ZnPcTS	pH 13, CTAC	22.4	1.3	0.87
Combination of compounds	pH 13, CTAC	24.6	1.4	1.3

In the last experiment three compounds absorbing at different wavelengths were combined together, each of them at the concentration of 5 μmol/l (Tab. 517). The reaction was conducted at pH 13 upon addition of detergent to avoid aggregation. The UV-Vis spectrum of the solution containing combined photosensitizers exhibits absorption in the regions of 416-452 nm and 569–768 nm (see also chapters 4.3 and 4.4).

Table 5.17. Photo-oxidation of 2-mercaptoethanol by PO(tbc)OPM **30**, GePcOPM **17**, ZnPoOPM **49** and combination of **30**, **17** and **49**.

Compound	Conditions	Oxygen consumed after 1 h in [ml]	Molar ratio O_2/substrate	RR_i [ml $O_2 \cdot min^{-1}$]
PO(tbc)OPM	pH 13, SDS	14.6	0.85	0.82
GePcOPM	pH 13, SDS	13.9	0.8	0.65
ZnPoOPM	pH 13, SDS	16.4	0.96	0.89
Combination of compounds	pH 13, SDS	20.5	1.2	3

Combination of three positively charged photosensitizers, *i.e.* triazatetrabenzcorrole **30**, germanium phthalocyanine **17** and zinc porphyrin **49**, gave an excellent improvement of the initial reaction rate (increase of RR_i to 3 [ml $O_2 \cdot min^{-1}$] was found) and oxygen uptake. After 1 h of irradiation 20.5 ml of oxygen was consumed, which is significantly better result compare to the reaction sensitized by single compound. For example, the use of single photosensitizer ZnPoOPM **49** resulted in 16.4 ml oxygen consumption after 1 h reaction time. It was demonstrated that homogeneous three-component system is capable of collecting considerable fraction of light resulting in around 3-fold enhancement of the reaction rate for the oxidation of 2-mercaptoethanol in water.

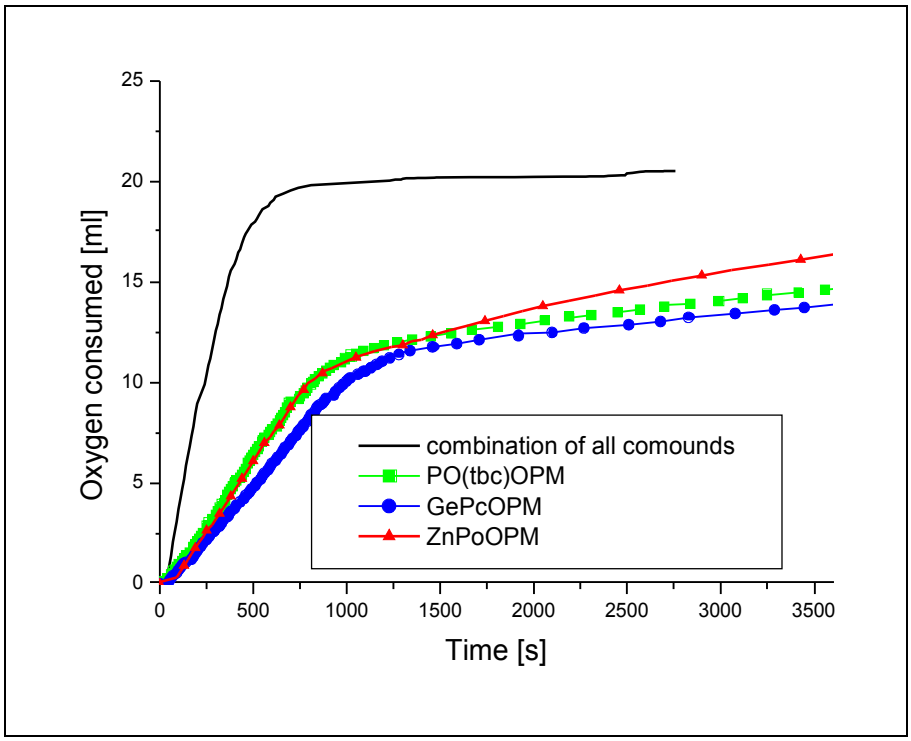

Figure 5.21. Photo-oxidation of 2-mercaptoethanol at pH 13 in the presence of SDS 0.1 mol/l with: PO(tbc)OPM **30** (—■—), GePcOPM **17** (–♦–), ZnPoOPM **49** (–▲–) and a combination of all three dyes (—). Concentration of dye: 5 (μmol/l).

5.13 Conclusion

The purpose of the present chapter was to present results concerning photocatalytic activities of different water-soluble photosensitizers obtained during these investigations. The following trend in activity expressed as TON during homogeneous photo-oxidation of 2-mercaptoethanol in the presence of appropriate detergent was found:

ACTIVITY IN THE PRESENCE OF DETERGENT

ZnPoOPPS >> GePcTS, H_2PoOPPS, H_2PcOPM, ZnPoOPM > Si(tbc)TS, PO(tbc)OPM, H_2PoOPM > H_2PcOPPS, GePcOPM, PO(tbc)OPPS, GePcOPPS, SiPcTS, ZnPoTS >> H_2PcTS, SiPcOPM, SiPcOPPS.

In the absence of detergent the trend in activity expressed as TON during homogeneous photo-oxidation of 2-mercaptoethanol is different:

ACTIVITY IN A NON-MICELLAR SOLUTION

H_2PoOPPS, H_2PoOPM > Si(tbc)TS > ZnPoOPPS, PO(tbc)OPM, ZnPoOPM > PO(tbc)OPPS > H_2PcTS, SiPcOPPS > SiPcOPM, ZnPoTS, H_2PcOPPS, H_2PcOPM.

For instance, the replacement of ZnPoOPPS **50** by metal-free porphyrins H_2PoOPPS **47** and H_2PoOPM **46** is observed. Decreasing order of activities is closely related to aggregation tendencies (see chapters 4.4 and 4.5) as well as to photostabilities of investigated photosensitizers.

The following trend in photostability during homogeneous photo-oxidation of 2-mercaptoethanol in the presence of appropriate detergent was found:

PHOTOSTABILITY

ZnPoOPM, ZnPoOPPS >> GePcTS, SiPcTS, GePcOPPS > PO(tbc)OPM, PO(tbc)OPPS, GePcOPM > H_2PcTS, H_2PcOPM, H_2PcOPPS, Si(tbc)TS, ZnPoTS, H_2PoOPM, H_2PoOPPS >> SubPc`s.

By far the most stable are ZnPoOPM **49** and ZnPoOPPS **50**. A very insignificant, if any, photodegradation was measured for these two compounds, *i.e.* between 0 and 2 %. Good stability was found for two sulfophthalocyanines, *i.e.* SiPcTS **25** and GePcTS **28**,

and zwitterionic phthalocyanine GePcOPPS **18**. Moderately stable are triazatetrabenzcorroles PO(tbc)OPM **30** and PO(tbc)OPPS **31**. All water-soluble subphthalocyanines obtained during this work exhibit no photocatalytic activity due to rapid degradation. They are unstable in aqueous solution at high pH, which is required to ionise the substrate (2-mercaptoethanol and phenol). Moreover, immediately after the light source is switched on, the initially pink solution turns colourless, indicating total photobleaching. A lack of photostability makes subphthalocyanines useless as photosensitizers.

It has been demonstrated that the substrate strongly affects both stability and activity of photosensitizers. Therefore, photo-oxidation of 2-mercaptoethanol was, in some cases, compared with photo-oxidation of phenol. For example, metal-free porphyrin H_2PoOPPS **47** was employed as photocatalyst in the photo-oxidation of thiol resulting in 67% degradation of dye. The same photosensitizer was utilized in the photo-oxidation of phenol. Somewhat surprisingly, no degradation was observed in this case.

Action spectra obtained during these studies confirmed that the photosensitizers are active only at the wavelengths of absorption of the monomers. Moreover, absorption of light both at Q-band and at Soret band gives rise to photocatalytic activity of the photosensitizer. There is no activity in the region between absorption maxima. This finding drew our attention towards panchromatically absorbing systems that would be capable of collecting considerably fraction of light resulting in enhancement of the photocatalytic activity. It has been demonstrated that coupling of a few dyes absorbing at different wavelengths leads to increase of the efficiency of the photo-oxidation of 2-mercaptoethanol. By far the best results were obtained for the three-component system consisted of positively charged zinc porphyrin, triazatetrabenzcorrole and germanium phthalocyanine.

The water-soluble photosensitizers could be easily bound to the ion exchangers. Only a cursory glance at the data in tables shows that the choice of ion exchanger is crucial for the course of reaction. The initial reaction rate, final oxygen consumption and even photostability of dyes strongly depend on the choice of ion exchanger.

Most of the investigated compounds immobilized on ion exchanger exhibit lower photostability comparing to the homogeneous reaction. For instance 13 % of GePcTS **28** disappears from the non-micellar solution after 3 hours of irradiation, while as much as 90 % photodegradation occurs when analogous reaction is performed with GePcTS **28** bound to the Amberlite IRA-402. Equally telling is the case of PO(tbc)OPM **30**: 38 % of the dye degrades from the micellar reaction solution after 3 h of irradiation, while

the use of PO(tbc)OPM ionically bound to the ion exchanger IRA-120 causes total photobleaching. Moreover, the type of ion exchanger may strongly influence photostability of dyes. For example GePcTS **28** was bound to two different resins with quaternary ammonium functionalities: IRA-402, which is a styrene/DVB resin, and IRA-958, which is an acrylic-based resin. Significantly better photostability was found for the phthalocyanine **28** bound to the IRA-958 (45 % photodegradation). GePcTS **28** immobilized on IRA-402 is fairly unstable, around 90 % loss of phthalocyanine was observed.

In addition, the use of photosensitizer bound to ion exchanger in every case resulted in a drop of turnover number (TON) comparing to the homogeneous reaction. This is because the photosensitizer is present in the polymer and thus oxygen and substrate have to diffuse inside the ion exchanger. Furthermore, drop of TON was always accompanying by high oxygen uptake. It was observed that the use of anion exchangers like Amberlite IRA-402 and IRA-958 results in higher oxygen uptake compared to the homogeneous reaction. In some cases unexpectedly high oxygen consumption occurred. It was shown that the polymer itself could be photo-oxidized as well. Moreover, both 2-mercaptoethanol and phenol exist in a solution in anionic form and thus increase in the local concentration of the thiolate and phenolate on the anion exchanger is possible. The utilization of cation exchanger IRA-120 results in low oxygen consumption. This may be due to electrostatic repulsion between negatively charged thiolate and phenolate ions and negatively charged polymer.

The reactions in D_2O and in the presence of NaN_3 unambiguously show that singlet oxygen ($^1O_2$) is involved in the photo-oxidation of 2-mercaptoethanol. Thus, the energy transfer (Type II) from the excited sensitizer to triplet oxygen ($^3O_2$) is the predominant process in the photocatalytic reaction under consideration. Simultaneously to energy transfer, however to lesser extent, the photoinduced electron transfer (Type III) is possible. Hydrogen peroxide (H_2O_2) was detected in the reaction mixture indicating that the superoxide radical anion ($O_2^{\bullet-}$) as the reactive species was present in the reaction solution.

The experimental results presented in this chapter suffice to show that the photocatalysis (with phthalocyanines and related tetrapyrrolic macrocycles) continues to be a very sensitive function of sensitizer structure (central metal, peripheral substituents), reaction condition (presence of detergent, pH) and even choice of substrate to be photooxidized. Thereby, our ability to predict the course of the photocatalytic process in a rational manner is severely limited.

5.14 References

[1] Parmon, V.; Emeline, A.; V.; Serpone, N.; "Glossary of Terms in Photocatalysis and Radiocatalysis" in: *Intern. J. Photoenergy,* **2002**.

[2] Fujishima, A. (Ed.), *TiO_2 Photocatalysis – Fundamentals and Applications*, BKC Publishers, Tokyo, 1999.

[3] Kalyanasundaram, K.;Grätzel, M. (Eds.), *Photosensitization and Photocatalysis Using Inorganic and Organometallic Compounds*, Kluver Academic Publishers, Dordrecht, 1993.

[4] Kaneko, M.; Okura, I. (Eds.), *Photocatalysis – Science and Technology*, Springer-Verlag, Berlin, 2002.

[5] O`Regan, B.; Grätzel, M.; *Nature*, **1991**, 353, 737.

[6] Hagfeld, A.; Grätzel, M.; *Acc. Chem. Res.* **2000**, 33, 269.

[7] Grätzel, M.; *Nature* **2001**, 414, 338.

[8] Nazeeruddin, Md. K.; Humphry-Baker, R.; Grätzel, M.; Murrer, A.; *Chem. Commun.* **1998**, 721.

[9] Schenk, G. O.; *Angew. Chem.* **1952**, 64, 12.

[10] Schenk, G. O.; Ziegler, K.; *Naturwissenschaften*, **1944**, 32, 157.

[11] Esser, P.; Pohlmann, B.; Scharf, H. D.; *Angew. Chem.* **1994**, 106, 2093.

[12] Funken, K. H.; *Nachr. Chem. Tech. Lab.* **1992**, 40, 793.

[13] Ohloff, G.; Lienhard, B., *Helv. Chim. Acta*, **1965**, 48, 182.

[14] Snowden, R. L.; Linder, S. M.; Muller, B. L.; Schulte-Elte, K. H.; *Helv. Chim. Acta*, **1987**, 70, 1879.

[15] Hoepfner, W.; Weyerstrahl, P.; *Liebigs Ann. Chem.* **1986**, 99.

[16] Thomas Oppenländer; "Photochemical Purification of water and air" 2003 Wiley-VCH.

[17] Spiller, W.; Wöhrle, D.; Schulz-Ekloff, G.; Ford, W. T.; Schneider, G.; Stark, J.; *Photochem. Photobiol.* **1996**, A 95, 161-173.

[18] Gerdes, R.; Bartels, O.; Schneider, G.; Wöhrle, D.; Schultz-Ekloff, G.; *Intern. J. Photoenergy*, **1999**, 1, 41-47.

[19] Schneider, G.; Wöhrle, D.; Spiller, W.; Stark, J.; Schultz-Ekloff, G.; *Photochem. Photobiol.,* **1994**, 60, pp. 333-342.

[20] Gerdes, R.; Wöhrle, D.; Spiller, Schneider, W., Schnurpfeil, G.; Schulz-Ekloff, G.; *Photochem. Photobiol.* **1997**, 111, 65-74.

[21] Gerdes, R.; Wöhrle, D.; Schneider, G.; Vetters, R.; Schulz-Ekloff, G.; *J. Inf. Recording* **1998**, 24, 223-227.

[22] Gerdes, R.; Bartels, O.; Schneider, G.; Wöhrle, D.; Schulz-Ekloff, G.; *Polym. Adv. Technol.* **2001**, 12, 152-160.

[23] Schnurpfeil, G.; Sobbi, A.; Spiller, W.; Kliesh, H.; Wöhrle, D.; *J. Porphyrins Phthalocyanines*, **1997**, 1, 159.

[24] Ozoemana, K.; Kuznetsova, N.; Nyokong, T.; *J. Mol. Catal.* **2001**, A 176, 29-40.

[25] Wöhrle, D.; Schlettwein, D.; Schnurpfeil, G.; Schneider, G.; Karmann, E.; Yoshida, T.; Kaneko, M.; *Polymers for Advanced Technologies*, Vol. 6, 118-130.

[26] Kimura, M.; Shirai, H.; in *The Porphyrin Handbook*, Vol. 19 Applications of Phthalocyanines, pp. 151-1776; Elsevier Science **2003**.

[27] Meyers, R. A.; *Handbook of Petroleum Refining Processes*, McGrow-Hill, New York 1986.

[28] Wöhrle, D.; Suvorova, O.; Gerdes, R.; Bartels, O.; Lapok, L.; Baziakina, N.; Makarov, S.; Slodek, A.; *Processes of petrochemistry and oil refining*, **2002**, 10, 3.

[29] Sharipov, A. Kh.; Kovtunenko, S. V.; *Petroleum Chemistry* **1997**, 37, 558.

[30] Dolanski, J.; Wagnerova, D. M.; Veprek-Siska, J.; *Collection Czechoslov. Chem. Commun.* **1976**, 41, 2326.

[31] Schutten, J. H.; Piet, P.; German, A. L.; *Macromol. Chem.* **1979**, 180, 2341.

[32] Schutten, J. H.; Beelen, T. P. M.; *J. Mol. Catal.* **1981**, 10, 85.

[33] Brouwer, W. M.; Piet, P.; German, A. L.; *Polym. Commun.* **1983**, 24, 216.

[34] Brouwer, W. M.; Piet, P.; German, A. L.; *J. Mol. Catal.* **1984**, 22, 297.

[35] Brouwer, W. M.; Piet, P.; German, A. L.; *Macromol. Chem.* **1984**, 184, 363.

[36] Brouwer, W. M.; Piet, P.; German, A. L.; *Polym. Bull.* **1982**, 8, 245.

[37] Brouwer, W. M.; Traa, P. A. M.; de Weerd, T. J. W.; Piet, P.; German, A. L.; *Angev. Makromol. Chem.* **1984**, 128, 133.

[38] Crosby, D. G.; Beynon, K. I.; Greve, P. A.; Korte, F.; Still, G. G.; Vonk, J. W.; *Pure Appl. Chem.* **1981**, 53, 1051.

[39] Angeletti, G.; Bjorsethi, A.; Organic Micropollutants in Aquatic Environment, Kluwer Academic Publishers, Dordrecht, **1991**.

[40] Oeberg, L. G.; Rappe, C.; *Chemosphere*, **1992**, 25, 46.

[41] Sorokin, A.; Seris, J. L.; Meunier, B.; *Science* **1995**, 268, 1163.

[42] Sorokin, A.; Dezard, S. S.; Poullain, D.; Noel, J. P.; Meunier, B.; *J. Am. Chem. Soc.* **1996**, 118, 7410.

[43] Gruptta, S. S.; Stadler, M.; Noser, C. A.; Anindya, G.; Bradley, S.; Dieter, L.; Horwitz, C. P.; Schramm, K. W.; Collins, T. J.; *Science* **2002**, 296, 205.

[44] R. Gerdes, *Niedermoleculare und immobilisierte Phthalocyanintetrasulfonsäueren als Photosensibilisatoren für die Photooxidation von Phenol und Chlorphenolen*. Ph.D. Thesis, Universität Bremen **2000**.

[45] Gerdes, R.; Wöhrle, D.; Spiller, W.; Stark, J.; Schulz-Ekloff, G.; *Photochem. Photobiol.* **1998**, 111, 65.

[46] Spiller, W.; Kliesch, H.; Wöhrle, D.; Hackbarth, S.; Röder, B.; Schnurpfeil, G.; *J. Porphyrins Phthalocyanines*, **1998**, 2, 145-158.

6. Experimental

6.1 Materials and methods

All solvents were dried and distilled prior to use. Pyridine was distilled from calcium hydride under nitrogen. Triethylamine used during Sonogashira cross-coupling was freshly distilled and deoxygenated by bubbling a stream of nitrogen through the solvent for 15 min. The absence of oxygen in these reactions is essential in order to avoid the formation of homocoupling compounds from the terminal alkyne. Most of the reactions were carried out under nitrogen atmosphere. The reaction mixtures during subphthalocyanines synthesis and purification procedures were protected against light. 3-Hydroxypyridine (**1**), 4-nitrophthalonitrile (**2**), 4-aminophthalonitrile (**5**), 4-sulfophthalic acid and 1,3-diiminoisoindoline (**21**) were obtained from commercial sources. Sulfonated phthalocyanines, *i.e.* ZnPcTS (**53**), AlPcTS (**54**) and GaPcTS (**55**), were obtained via template synthesis according to the procedures described elsewhere [1].

UV-Vis absorption spectra were recorded with a Perkin Elmer Lambda 2/Lambda 9, VARIAN DMS 200. Emission spectra were measured on a Perkin Elmer LS 50 spectrometer. ESI mass spectra were recorded using the Bruker Esquire LC which is a HPLC/MS system that consists of a Agilenta/HP 1100 liquid chromatography system and ion trap mass detector. EI and DCI mass spectra were recorded on Finnigan MAT 8200 which is double-focusing instrument with reverse Nier-Johnson geometry. In EI method the sample was introduced directly into ion source and bombarded with a beam of highly energetic electrons (70 eV). In DCI method the sample is ionized by reaction with a reagent gas, usually ammonia. FT-IR spectra were obtained using KBr pellet on a Perkin Elmer BIORAD SPC-3200 FTS7. ^{1}H NMR spectra were measured on a Bruker DPX-200 Avance. The spectra were measured in deuterated solvents at room temperature with chemical shifts related to tetramethylsilane. In the reporting of ESI data for sulfonated phthalocyanines M refers to $Pc(SO_3H)_4$.

6.2 Synthetic procedures

6.2.1 4-(3-Pyridyloxy)phthalonitrile (**3**).

This synthesis is a modified version of the method described elsewhere [2]. 4-Nitrophthalonitrile (**2**) (8.7 g, 50 mmol) and an excess of 3-hydroxypyridine (**1**) (7.13 g, 75 mmol) were dissolved in 100 ml of dry DMSO under inert gas. Dry potassium carbonate (13.8 g, 100 mmol) was added. After 48 h stirring at room temperature next portion of potassium carbonate was added (10 g, 72 mmol). After 72 h the mixture was added to 500 ml of water. Precipitate was washed thoroughly with water. The isolated and dried product was dissolved in hot ethanol and active charcoal was added. After filtration ethanol solution was poured into water. Precipitate was filtered, washed with water and dried. Chromatography on silica gel with CH_2Cl_2 afforded solid product that was dissolved in acetone and slowly poured to water. This way white crystals of high purity were obtained. Yield 8.73 g (80%). M = 221.22 g/mol, $C_{13}H_7N_3O$.

IR (KBr): ν = 3107, 3070, 3039, 2228 (CN), 1596, 1574, 1566, 1487, 1424, 1314, 1280 (Ar-O-Ar), 1253 (Ar-O-Ar), 1216, 1084, 1025, 956, 892, 854, 820, 706, 615, 527 cm^{-1}.

^{1}H-NMR (200 MHz, DMSO-D_6): δ = 8.52 (m, 1H), 8.40 (s, 1H), 8.12 (d, 1H), 7.9 (dd, 1H), 7.71 (m, 1H), 7.54 (m, 1H), 7.49 (dd, 1H).

EI-MS (200°C, 70 eV): *m/z* 221$[M]^+$, 127$[M^+-C_5H_4NO]$, 78$[C_5H_4N]^+$.

6.2.2 5-(3-Pyridyloxy)-1,3-diiminoisoindoline (**4**)

This method is a modified version of the synthesis describe elsewhere [3]. 4-(3-pyridyloxy)phthalonitrile (**3**) (1 g, 4.52 mmol) was added to a mixture of dry methanol (100 ml) and sodium methoxide (50 mg, 0.93 mmol). Anhydrous ammonia gas was bubbled through the stirred suspension for 45 min. The mixture was then refluxed and maintained at 110°C for 3.5 h with continuous bubbling of ammonia gas. The reaction mixture became slightly greenish. After cooling the methanol was removed at reduced pressure. Any attempt to purify by column chromatography and isolate the product failed. Hence, the hygroscopic product was dried under vacuum at 80°C and used directly without any purification. M = 238.25 g/mol, $C_{13}H_{10}N_4O$.

EI-MS (205°C, 70 eV): *m/z* 238$[M]^+$, 222$[M-NH_2^-]^+$, 78$[C_5H_4N]^+$.

6.2.3 4-Iodophthalonitrile (6)

In order to obtain compound **6** the procedure described elsewhere was followed [4]. 4-Aminophthalonitrile (**5**) (3.1 g, 21.7 mmol) was added to a mixture of crushed ice and 60 ml of concentrated hydrochloric acid. $NaNO_2$ (2.35 g, 34.1 mmol) was dissolved in 20 ml of water and added dropwise to the mixture. The temperature was maintained below 5 °C all the time (!). The mixture was stirred for 1.5 h and filtered. The solution was added dropwise to 50 ml of cold water solution of KI (5.44 g, 32.8 mmol). The brown reaction mixture was cooled in an ice bath and stirred for 0.5 h. The product was extracted from the water solution with toluene. The extracts were washed thoroughly with water, 5 % $NaHCO_3$, water and aqueous solution of $Na_2S_2O_3$ and again with water. The crude product was purified by column chromatography on silica gel with toluene. 3.09 g (56 %) of white solid was obtained. M = 254.03 g/mol, $C_8H_3N_2I$.

IR (KBr): ν = 3091, 3060, 3016, 2231 (CN),1946, 1811, 1573, 1556, 1543, 1470, 1389, 1374, 1277, 1265, 1205, 1179, 1073, 907, 842, 836, 581, 527, 476 cm^{-1}.

EI-MS (200°C, 70 eV): *m/z* 254$[M]^+$.

6.2.4 4-[2-(2-Pyridynyl)ethynyl]phthalonitrile (8)

The mixture of 0.3 g (1.18 mmol) of 4-iodophthalonitrile (**6**), $Pd(PPh_3)_2Cl_2$ (17 mg, 0.0242 mmol) and CuI (59 mg, 0.031 mmol) was dissolved in a mixture of freshly distilled and deoxygenated triethylamine (5 ml) and DMSO (4 ml). Then 0.24 ml (2.356 mmol) of deoxygenated 2-ethynylpyridine (**7**) was added via syringe and the solution was stirred for 12 h under argon. The solvent was evaporated and the crude product was purified by column chromatography with silica gel. Initially a mixture Et_2O/PE (1:1) was used to remove unreacted compound and then Et_2O/CH_2Cl_2 (1:1) to collect the desired product. The product was further purified by second column chromatography with CH_2Cl_2 as eluent to remove most of the yellow impurities. Final purification involved the crystallization from CH_2Cl_2/PE and gave 213 mg (79 %) of the product as white crystals. M = 229.24 g/mol, $C_{15}H_7N_3$.

IR (KBr): ν = 3104, 3061, 3040, 3027, 2238 (CN), 2229 (CN), 2218 (C ≡ C), 1598, 1584, 1562, 1546, 1489, 1463, 1431, 1395, 1323, 1286, 1274, 1154, 1107, 1093, 1046, 992, 916, 840, 779, 738, 629, 527, 471 cm^{-1}.

EI-MS (200°C, 70 eV): *m/z* 229$[M]^+$.

6.2.5 4-[2-(2-Pyridynyl)ethyl]phthalonitrile (**9**)

To 1.2 g (5.23 mmol) of 4-[2-(2-pyridynyl)ethynyl]phthalonitrile (**8**) dissolved in 150 ml of acetonitrile was added 0.8 g of palladium on charcoal (10%). A stream of dry hydrogen was bubbled through the stirred suspension for 2 h. The solvent was evaporated and the residue was purified by column chromatography on silica gel using initially acetone/PE (1:1) to remove impurities and then acetone/PE (1:0.5) to collect the product in 71 % yield as white solid. M = 233.27 g/mol, $C_{15}H_{11}N_3$.

IR (KBr): ν = 3102, 3053, 2957, 2926, 2863, 2234 (CN), 1599, 1577, 1562, 1492, 1477, 1453, 1426, 1273, 1234, 1193, 1101, 1029, 937, 856, 830, 800, 723, 708, 642, 627, 615, 588, 531, 500, 468 cm^{-1}.

^{1}H-NMR (200 MHz, D_6-acetone): δ = 3.01-3.09 (m, 2H), 3.14-3.23 (m, 2H), 7.27 (q, 1H), 7.64 (dt, 1H), 7.80 (dd, 1H), 7.97 (t, 1H), 7.98 (s, 1H), 8.41 (dd, 1H), 8.45 (d, 1H).

EI-MS (200°C, 70 eV): *m/z* 233$[M]^+$, 92$[C_6H_6N]^+$.

R_f (silica gel, acetone/PE 1:1): 0.38.

6.2.6 2,9,16,23-Tetrakis-(3-pyridyloxy)phthalocyanine (**10**)

4-(3-Pyridyloxy)phthalonitrile (**3**) (3 g, 13.74 mmol) was dissolved in 80 ml of pentan-1-ol [12]. Lithium solid (0.8 g) was added in small portion to the reaction mixture. The solution turned dark-blue. The reaction mixture was stirred at 140°C for 2 h under argon. The mixture was acidified with glacial acetic acid (60 ml) then diluted with water and left overnight. The pentanol layer was separated and washed thoroughly with water. The solvent was evaporated and the crude product chromatographed on silica gel with a mixture pyridine/PE 1:1 with gradual increase in pyridine concentration in the eluent to pyridine/PE 10:2. Yield: 57 % (1.74 g). M = 886.89 g/mol, $C_{52}H_{30}O_4N_{12}$.

IR (KBr): ν = 3030, 1612, 1572, 1501, 1471, 1422, 1396, 1337, 1319, 1229(C-O-C), 1188, 1113, 1091, 1011, 926, 816, 746, 705 cm^{-1}.

UV-Vis (DMF) λ nm (ε x 10^5): 696(1.36), 666(1.53).

DCI-MS (positive, NH_3): *m/z* 887$[M+H^+]^+$.

6.2.7 2,9,16,23-Tetrakis-[3-(N-methyl)pyridyloxy]phthalocyanine tetraiodide (**11**)

A quantity of 100 mg (0.113 mmol) of metal-free 2,9,16,23-tetrakis-(3-pyridyloxy)phthalocyanine (**10**) was dissolved in DMF (10 ml) [12]. An excess of methyl iodide (5 ml, 80 mmol) was added and the solution was stirred for 17 h under nitrogen at 50°C. The methyl iodide was evaporated and the reaction product was precipitated with CH_2Cl_2 (200 ml), filtered off and washed with CH_2Cl_2, EtOH and acetone. The compound was dissolved in water and after filtration isolated by freeze-drying. Yield: 98 % (162 mg). M = 1454.65 g/mol, $C_{56}H_{42}N_{12}O_4I_4$.

IR (KBr): ν = 3024, 1613, 1581, 1500, 1469, 1420, 1395, 1308, 1275(C-O-C), 1198, 1158, 1116, 1092, 1012, 960, 915, 827, 811, 742, 713, 661 cm^{-1}.

UV-Vis (H_2O, pH 13, SDS 0.1 mol/l) λ nm (ε x 10^5): 673(0.75), 608.

UV-Vis (H_2O, pH 7, SDS 0.1 mol/l) λ nm (ε x 10^5): 694(1.5), 659(1.3).

ESI-MS (positive ion mode) *m/z*: 236.6$[M\text{-}4I^-]^{4+}$, 310.5$[M\text{-}4I^-\text{-}CH_3^+]^{3+}$, 458.4$[M\text{-}4I^-\text{-}2CH_3^+]^{2+}$.

Fluorescence (DMF) λ: 681.

6.2.8 2,9,16,23-Tetrakis-[3-(3-propanesulfonic acid)pyridiniumoxy]-phthalocyanine (**12**)

A quantity of 100 mg (0.113 mmol) of metal-free 2,9,16,23-tetrakis-(3-pyridyloxy)phthalocyanine (**10**) and 1,3-propanesultone (1 g, 8.19 mmol) were dissolved in DMF (10 ml) and kept at 50°C for 17 h under nitrogen with stirring. The product was precipitated with CH_2Cl_2 (250 ml), filtered off and washed with plenty of CH_2Cl_2 and acetone to remove excess of 1,3-propanesultone. The compound was dried at 80°C to give 60 mg (97 %) of solid product. M = 1375.47 g/mol, $C_{64}H_{54}O_{16}N_{12}S_4$.

IR (KBr): ν = 3052, 2941, 1615, 1583, 1502, 1474, 1322, 1276(C-O-C), 1201(S=O, ν_{as}), 1093, 1040(S=O, ν_{sym}), 941, 815, 745, 682, 612, 526 cm^{-1}.

UV-Vis (H_2O, pH 13, SDS 0.1 mol/l) λ nm (ε x 10^5): 693(0.51), 671(0.78).

UV-Vis (H_2O, pH 7, SDS 0.1 mol/l) λ nm (ε x 10^5): 695(1.00), 661(0.91).

6.2.9 Dihydroxysilicon 2,9,16,23-tetrakis-(3-pyridyloxy)phthalocyanine (13)

Dry 5-(3-pyridyloxy)-1,3-diiminoisoindoline (**4**) obtained from 1 g of 4-(3-pyridyloxy)phthalonitrile (**3**) was placed in a 100 ml two-necked round-bottomed flask, equipped with magnetic stirrer and a reflux condenser.10 ml of freshly distilled quinoline was added to the flask and $SiCl_4$ (0.5 ml, 4.35 mmol) was transferred with the aid of syringe at room temperature under inert gas atmosphere. The reaction was stirred at 180°C for 15 min and than at 200°C for 45 min. The formation of a green precipitate took place. After being cooled 20 ml of water solution of ammonia hydroxide (25%) was added to the reaction mixture and stirring was continued overnight. After the water phase was evaporated the residue was diluted with DMF. The mixture was poured into 400 ml of water and the precipitate thus obtained was collected by filtration, washed thoroughly with DMF/water 1:2, with water only and then with acetone. The crude product was chromatographed on silica gel using CH_2Cl_2 to remove first yellow and greenish impurities. The desired compound was then eluted as a blue band using CH_2Cl_2/MeOH 2:1. After solvent evaporation second chromatography was applied using $CHCl_3$ and then $CHCl_3$/MeOH 9:1 to get rid of impurities. Finally product was eluted with $CHCl_3$/MeOH 6:4. Removal of the solvent resulted in 0.578 g of deep-blue solid. Yield (with respect to the phthalonitrile used): 54 %. M = 946.97 g/mol, $C_{52}H_{30}N_{12}O_6Si$.

IR (KBr): ν = 3058, 1614, 1574, 1519, 1472, 1412, 1331, 1238(C-O-C), 1125, 1079, 1060, 1021, 956, 820(Si-OH), 758, 734, 706, 538 cm^{-1}.

UV-Vis (DMF) λ nm (ε x 10^5): 676(0.56), 608(0.13).

ESI-MS (negative ion mode) *m/z*: 946[M^-].

6.2.10 Dihydroxysilicon 2,9,16,23-tetrakis-[3-(N-methyl)pyridyloxy]-phthalocyanine tetraiodide (14)

A quantity of 150 mg (0.158 mmol) of dihydroxysilicon 2,9,16,23-tetrakis-(3-pyridyloxy)phthalocyanine (**13**) was dissolved in DMF (10 ml). An excess of methyl iodide (2 ml, 32 mmol) was added and the solution was stirred for 19 h under nitrogen at 50°C. The methyl iodide was evaporated and the reaction product was precipitated with CH_2Cl_2, filtered off and washed with CH_2Cl_2, EtOH and acetone. The compound was dissolved in water and after filtration isolated by freeze-drying. Yield: 200 mg (83 %). M = 1514.73 g/mol, $C_{56}H_{42}N_{12}O_6SiI_4$.

IR (KBr): ν = 3026, 2941, 1614, 1582, 1501, 1471, 1409, 1330, 1275(C-O-C), 1124, 1083, 1061, 966, 826(Si-OH), 756, 663, 541 cm^{-1}.

UV-Vis (H_2O, pH 13, SDS 0.1 mol/l) λ nm (ε x 10^5): 675(1.22), 641(0.58).

UV-Vis (H_2O, pH 7, SDS 0.1 mol/l) λ nm (ε x 10^5): 675(1.24), 642(0.61).

ESI-MS (positive ion mode) *m/z*: 251.3$[M\text{-}4I^-]^{4+}$.

Fluorescence (DMF) λ: 678 nm.

6.2.11 Dihydroxysilicon 2,9,16,23-tetrakis-[3-(3-propanesulfonic acid)-pyridiniumoxy]phthalocyanine (**15**)

60 mg (0.063 mmol) of dihydroxysilicon 2,9,16,23-tetrakis-(3-pyridyloxy)phthalocyanine (**13**) and 1,3-propanesultone (0.5 g, 4.09 mmol) were dissolved in DMF (10 ml) and kept at 50°C for 19 h under nitrogen with stirring. The product was precipitated with CH_2Cl_2, filtered off and washed with plenty of CH_2Cl_2 and acetone to remove excess of 1,3-propanesultone. The product was dried at 80°C to give 58 mg (64 %). M = 1435.55 g/mol, $C_{64}H_{54}N_{12}O_{18}SiS_4$.

IR (KBr): ν = 3047, 1615, 1582, 1501, 1473, 1414, 1331, 1276(C-O-C), 1190(S=O, ν_{as}), 1126, 1079(S=O, ν_{sym}), 1041, 957, 818(Si-OH), 757, 735, 677, 604, 525 cm^{-1}.

UV-Vis (H_2O, pH 13, SDS 0.1 mol/l) λ nm (ε x 10^5): 678(1.45), 609(0.31).

ESI-MS (positive ion mode) *m/z*: 1295$[M\text{-}OH^-\text{-}122]^+$, 1173$[M\text{-}OH^-\text{-}2x122]^+$, 1051$[M\text{-}OH^-\text{-}3x122]^+$, 929$[M\text{-}OH^-\text{-}4x122]^+$, 1335$[M\text{-}OH^-\text{-}H_2SO_3]^+$, 1213$[M\text{-}OH^-\text{-}H_2SO_3\text{-}122]^+$, 1091$[M\text{-}OH^-\text{-}H_2SO_3\text{-}122]^+$.

6.2.12 Dihydroxygermanium 2,9,16,23-tetrakis-(3-pyridyloxy)phthalo-cyanine (**16**)

Dry 5-(3-pyridyloxy)-1,3-diiminoisoindoline (**4**) obtained from 1.5 g of 4-(3-pyridyloxy)phthalonitrile (**3**) (6.78 mmol) was placed in a 100 ml two-necked round-bottomed flask, equipped with magnetic stirrer and a reflux condenser. 10 ml of freshly distilled quinoline was added to the flask and 0.5 ml of $GeCl_4$ (4.29 mmol) was transferred with the aid of syringe at room temperature under inert gas atmosphere. The reaction was stirred at 200°C for 2 h. The formation of a green precipitate took place. After being cooled 20 ml of water solution of ammonia hydroxide (25%) and 20 ml of pyridine was added to the reaction mixture and stirring was continued overnight. The reaction mixture was poured into 500 ml of water and the green precipitate thus obtained was collected by filtration, washed thoroughly with DMF/water 1:2, with water only and then with acetone. The crude product was dissolved in a mixture of CH_2Cl_2/MeOH and chromatographed on silica gel using initially CH_2Cl_2/MeOH (9:1) to remove first impurities. The desired compound was then eluted as a blue-green band

using CH_2Cl_2/MeOH 6:4. Removal of the solvent resulted in 1.29 g of deep-blue solid. Yield (with respect to the phthalonitrile used): 77 %. M = 991.50 g/mol, $C_{52}H_{30}N_{12}O_6Ge$.
IR (KBr): ν = 3058, 1614, 1574, 1500, 1472, 1424, 1405, 1347, 1320, 1237(C-O-C), 1123, 1086, 1055, 1022, 954, 810, 749, 734, 707, 644 cm^{-1}.
UV-Vis (DMF) λ nm (ε x 10^5): 680(1.93), 612(0.42), 365(0.84).
ESI-MS (positive ion mode) *m/z*: 974$[M-H_2O]^+$.

6.2.13 Dihydroxygermanium 2,9,16,23-tetrakis-[3-(N-methyl)pyridyloxy]-phthalocyanine tetraiodide (17)

A quantity of 100 mg (0.1 mmol) of dihydroxygermanium 2,9,16,23-tetrakis-(3-pyridyloxy)phthalocyanine (**16**) was dissolved in DMF (10 ml). An excess of methyl iodide (5 ml, 80 mmol) was added and the solution was stirred for 16 h under nitrogen at 50°C. The methyl iodide was evaporated and the reaction product was precipitated with CH_2Cl_2 (400 ml), filtered off and washed with CH_2Cl_2, EtOH and acetone. The compound was dissolved in water and after filtration isolated by freeze-drying. Yield: 138 mg (88 %). M = 1559.25 g/mol, $C_{56}H_{42}N_{12}O_6GeI_4$.
IR (KBr): ν = 3024, 2941, 1613, 1582, 1500, 1469, 1405, 1346, 1275(C-O-C), 1217, 1122, 1089, 1056, 966, 887, 742, 663 cm^{-1}.
UV-Vis (H_2O, pH 13, SDS 0.1 mol/l) λ nm (ε x 10^5): 678(0.89), 645(0.38), 613(0.3).
UV-Vis (H_2O, pH 7, SDS 0.1 mol/l) λ nm (ε x 10^5): 678(0.33), 643(0.52).
ESI-MS (positive ion mode) *m/z*: 263$[M-4I^-]^{4+}$, 236.6$[M-4I^--Ge(OH)_2+2H^+]^{4+}$.
Fluorescence (DMF) λ: 681 nm.

6.2.14 Dihydroxygermanium 2,9,16,23-tetrakis-[3-(3-propanesulfonic acid)-pyridiniumoxy]phthalocyanine (18)

50 mg (0.05 mmol) of dihydroxygermanium 2,9,16,23-tetrakis-(3-pyridyloxy)phthalocyanine (**16**) and 1,3-propanesultone (0.5 g, 4.09 mmol) were dissolved in DMF (10 ml) and kept at 50°C for 16 h under nitrogen with stirring. The product was precipitated with CH_2Cl_2, filtered off and washed with plenty of CH_2Cl_2 and acetone to remove excess of 1,3-propanesultone. The compound was dissolved in hot water and placed in dialysis tube than immersed into the distilled water. The dialysis was carried out for a few hours with frequently changed water. The product was isolated by freeze-drying. Yield: 60 mg (81 %). M = 1480.08 g/mol, $C_{64}H_{54}N_{12}O_{18}GeS_4$.
IR (KBr): ν = 3052, 1614, 1582, 1501, 1470, 1406, 1347, 1330, 1278(C-O-C), 1208(S=O, ν_{as}), 1089(S=O, ν_{sym}), 1040, 954, 886, 820, 743, 683, 610, 523 cm^{-1}.

UV-Vis (H_2O, pH 13, SDS 0.1 mol/l) λ nm (ε x 10^5): 678(0.89), 644(0.61).

6.2.15 Sodium 4-sulfophthalate (19)

100 ml of commercially available 50% aqueous solution (262,4 mmol) of 4-sulfophthalic acid was neutralized with NaOH (10.5 g, 262.4 mmol). The solution was stirred for 0.5 h and water was removed by freeze-drying. White, highly hygroscopic solid was obtained (70.3 g). M = 236.11 g/mol, $C_8H_5O_7Na$.

6.2.16 2,9,16,23-Tetrasulfophthalocyanie (20)

H_2PcTS **20** was prepared by template synthesis starting from magnesium acetate tetrahydrate (5.76 g, 26.85 mmol), sodium 4-sulfophthalate (**19**) (16 g, 60 mmol), urea (21.5 g, 358 mmol) and ammonium chloride (1.6 g, 30 mmol) [13]. All compounds were ground in mortar and placed in 1000 ml flask equipped with magnetic stirring and reflux. The mixture was stirred and heated at 140°C for 0.5 h. Then the mixture was heated to 200°C and kept at this temperature for 16 h under argon. After cooling to room temperature hydrochloric acid (140 ml, 1M solution) was added and the suspension was stirred for 0.5 h. Then 400 ml of acetone was added slowly. After cooling in refrigerator the suspension was centrifuged and the precipitate was collected. The deep-blue solid was redissolved in small portion of water, reprecipitated with acetone and centrifuged. The procedure was repeated. The blue solid was collected and dried. Yield: 0.62g(5%). M = 834.81 g/mol, $C_{32}H_{18}O_{12}N_8S_4$.

IR (KBr): ν = 3081, 1720, 1637, 1505, 1410, 1319, 1189(S=O, ν_{as}), 1136, 1109, 1029(S=O, ν_{sym}), 901, 838, 744, 690, 647, 622, 585 cm^{-1}.

UV-Vis (H_2O, pH 13, CTAC 0.1 mol/l) λ nm (ε x 10^5): 679(0.55), 611.

UV-Vis (H_2O, pH 7, CTAC 0.1 mol/l) λ nm (ε x 10^5): 696(0.62), 663(0.63).

ESI-MS (positive ion mode) *m/z*: 835$[M+H^+]^+$, 857$[M+Na^+]^+$, 755$[M-SO_3+H^+]^+$.

ESI-MS (negative ion mode) *m/z*: 833$[M-H^+]^-$, 753$[M-SO_3-H^+]^-$.

Fluorescence (H_2O) λ: 677nm.

6.2.17 Dichlorosilicon phthalocyanine (22)

The synthesis of dichlorosilicon phthalocyanine was based on the modified method described elsewhere [5]. A mixture of 1,3-diiminoisoindoline (**21**) (6 g, 41.33 mmol), $SiCl_4$ (6.7 ml, 58.36 mmol) and freshly distilled quinoline (40 ml) was brought quickly to reflux. The resulting solution was maintained at 200°C for 1 h. Upon cooling the

mixture was diluted with a mixture of 200 ml of CH_2Cl_2 and 100 ml of DMF. The mixture was then centrifuged and the product washed with a mixture of CH_2Cl_2/DMF (1:1), CH_2Cl_2, and acetone and dried to yield 8.71 g of purple solid. M = 611.52 g/mol, $C_{32}H_{16}N_8Cl_2Si$.

IR (KBr): ν = 1651, 1610, 1531, 1473, 1429, 1400, 1336, 1290, 1163, 1121, 1080, 961, 913, 760, 733, 465(Si-Cl), 429 cm^{-1}.

6.2.18 Hydroxysilicon 4,11,18,25-tetrasulphotriazatetrabenzcorrole tetrasodium salt (**23**)

A dry sample of $SiCl_2Pc$ **22** (1g, 1.635 mmol) was placed in 100 ml round-bottomed flask and 20 ml of oleum (sulphuric acid containing 30 % of SO_3) was added. The mixture was heated to 75°C over a period of 4 h with stirring under argon. After cooling to room temperature, the mixture was poured slowly into crushed ice and the resulting solution was filtered, than diluted to 600 ml. The mixture was neutralized with solid sodium hydroxide and brought to slightly alkaline pH (ca. pH 7-8) and left overnight. The resulting sodium sulphate crystals were discarded and an ethanol was added dropwise to the solution to precipitate next portion of fine sodium sulphate crystals. The crystals were washed with a small volume of water and discarded. The ethanol was evaporated and the solution volume was reduced to 100 ml. Next portion of sodium sulphate was removed by very gently precipitation with an ethanol. The precipitation with an ethanol was repeated till no more sodium sulphate could be removed by this method. However, the sample still contains traces of sulphate, which were removed by short dialysis. Water volume was reduced to about 10 ml and the solution was placed into the dialysis tube and immersed into the distilled water. The dialysis was conducted only till no more sulphate anions could be detected in washing solution (reaction with $BaCl_2$). **Caution**: in order to avoid loss of compound the dialysis should not be carried out longer than it is necessary to remove the sulphate anions! While the dialysis is finished water is removed by freeze-drying. The product consisted of two fractions, one of them was green and the other one blue, which were separated on RP-18 column with water as eluent. The sample was dissolved in 5 ml of water and subjected to a long column. Only the head of the first band was pure enough to be collected. The rest of the fractions were collected together and the water volume was reduced to 5 ml on a rotary evaporator. The solution was subjected to the same column filled with the RP-18 and separation was repeated. The R_f value difference between green and blue fraction is insignificant. Hence, the separation had to be repeated many times (in this experiment

more than 20 separations were carried out). The water was removed by freeze-drying, affording 154 mg (ca. 10 %) of green solid. M = 951.80 g/mol, $C_{32}H_{13}N_7O_{13}S_4Na_4Si$.
IR (KBr): ν = 1636, 1385, 1194(S=O, ν_{as}), 1127, 1079, 1035(S=O, ν_{sym}), 974, 606 cm^{-1}.
UV-Vis (H_2O, pH 13) λ nm (ε x 10^5): 671 (0.23), 454(0.48), 441, 425, 412.
UV-Vis (H_2O, pH 7) λ nm (ε x 10^5): 670(0.2), 643, 452(0.33), 441, 423.
ESI-MS (positive ion mode) *m/z*: 908$[M+2Na^+-H^+]^+$, 886$[M+Na^+]^+$, 806$[M-SO_3+Na^+]^+$.
ESI-MS (negative ion mode) *m/z*: 862$[M-H^+]^-$, 782$[M-SO_3-H^+]^-$.
Fluorescence (DMF) λ: 677 nm.

6.2.19 Dichlorosilicon 2,9,16,23-tetrachlorosulphophthalocyanie (24)

$SiCl_2Pc$ **22** (3 g) and chlorosulfonic acid (30 ml) was kept at 130°C under nitrogen for 6 h. The solution was cooled to 85°C and 12 ml of thionyl chloride was gradually dropped into the mixture. The reaction was held at 85°C for 4 h, and the reaction mixture poured into crushed ice with vigorous stirring. The product was filtered and washed with water ethanol and acetone, respectively, and dried under vacuum to give 2.38 g (66 % yield relating to 1,3-diiminoisoindoline). M = 1005.56 g/mol, $C_{32}H_{12}N_8Cl_6O_8SiS_4$.
IR (KBr): ν = 1717, 1634, 1522, 1400, 1371, 1335, 1172(S=O, ν_{as}), 1085, 963, 466(Si-Cl) cm^{-1}.
UV-Vis (DMF) λ nm (ε x 10^5): 674(0.77), 604(0.15), 356(0.3).

6.2.20 Dihydroxysilicon 2,9,16,23-tetrasulphophthalocyanie tetrasodium salt (25)

The suspension of $Si(OH)_2Pc(SO_2Cl)_4$ (**24**) (0.3 g, 0.298 mmol) in 50 ml of water was placed in 250 ml flask and refluxed at 80°C with 5 ml of 0.1N NaOH solution. After 24 hours pH value was 2.4. After this time next portion of 0.1N NaOH solution (4 ml) was added to raise pH to value 9. The hydrolysis was continued at 80°C for 24 hours. pH value dropped to 6.4 again and another portion of 0.1N sodium hydroxide solution was added (1 ml). After 20 hours the pH value was recorded to be ca. 8.4. The hydrolysis is completed when the pH value does not decrease any more. **Caution:** to avoid decomposition pH value should not be higher than 10! Water volume was reduced to about 10 ml and the solution was placed in dialysis tube and immersed into the distilled

water. The dialysis was conducted only till no more chloride anions could be detected in washing solution (reaction with $AgNO_3$). **Caution**: the dialysis should not be conducted longer than it is necessary to remove chloride anions since the dialysis membrane is permeable for the sulfonated phthalocyanines as well! While the dialysis is finished water is removed by freeze-drying to give solid (143 mg, 49 %). M = 982.82 g/mol, $C_{32}H_{14}N_8Na_4O_{14}SiS_4$.

IR (KBr): ν = 1639, 1602, 1580, 1520, 1397, 1335, 1194(S=O, ν_{as}), 1124, 1078, 1035(S=O, ν_{sym}), 990, 920, 813, 750, 730, 690, 671, 633, 581, 523 cm^{-1}.

UV-Vis (H_2O) λ nm (ε x 10^5): 673(0.82), 604.

ESI-MS (positive ion mode) *m/z*: 939$[M+2Na^+-H^+]^+$, 917$[M+Na^+]^+$, 895$[M+H^+]^+$, 877$[M-OH^-]^+$, 837$[M-SO_3+Na^+]^+$, 815$[M-SO_3+H^+]^+$, 797$[M-OH^--SO_3]^+$, 757$[M-2SO_3+Na^+]^+$, 735$[M-2SO_3+H^+]^+$, 717$[M-OH^--2SO_3]^+$.

ESI-MS (negative ion mode) *m/z*: 893$[M-H^+]^-$, 813$[M-SO_3-H^+]^-$, 733$[M-2SO_3-H^+]^-$.

Fluorescence (DMF) λ: 677 nm.

6.2.21 Dihydroxygermanium phthalocyanine (26)

The synthesis of dihydroxygermanium phthalocyanine (**26**) was based on the modified method described elsewhere [6]. A mixture of dry 1,3-diiminoisoindoline (**21**) (6 g, 41.33 mmol), $GeCl_4$ (3.15 ml, 27.03 mmol) and freshly distilled quinoline (30 ml) was brought quickly to reflux. The resulting solution was maintained at 200°C for 2 h. Upon cooling the mixture was hydrolysed with a 30 ml of ammonia solution (25 %). The reaction mixture was stirred overnight at 100°C. Then the mixture of 60 ml of concentrated hydrochloric acid and water (1:1) was added to the reaction mixture. The mixture was diluted with 600 ml of water and the resulted precipitate was collected by decantation and than filtration. The resulting solid was washed thoroughly with water and than acetone to remove brown impurities. The dry product was treated with concentrated sulfuric acid (450 ml) and the resulting mixture was diluted with enough water to precipitate all the phthalocyanine (ca. 6 l). The precipitate was centrifuged and the product washed thoroughly with water to yield 6.39 g of blue solid. M = 619.16 g/mol, $C_{32}H_{18}N_8GeO_2$.

IR (KBr): ν = 3062, 1610, 1512, 1471, 1426, 1335, 1290, 1167, 1123, 1081, 905, 757, 728, 644, 575, 512 cm^{-1}.

ESI-MS (positive ion mode) *m/z*: 603$[M-OH^-]^+$.

6.2.22 Dihydroxygermanium 2,9,16,23-tetrachlorosulfophthalocyanie (**27**)

$Ge(OH)_2Pc$ (**26**) (2.5 g) and chlorosulfonic acid (21 ml) was kept at 130°C under nitrogen for 6 h. The solution was cooled to 85°C and 9.2 ml of thionyl chloride was gradually dropped into the mixture. The reaction was held at 85°C for 4 h, and the reaction mixture poured into crushed ice with vigorous stirring. The product was filtered and washed with water and ethanol, respectively. The solid was then washed with acetone prior to drying under vacuum to give 3.54 g (87 %) of solid product. M = 1013.20 g/mol, $C_{32}H_{14}N_8Cl_4O_{10}GeS_4$.

IR (KBr): ν = 3086, 1633, 1508, 1398, 1373, 1338, 1250, 1227, 1173(S=O, ν_{as}), 1083, 1054, 1028(S=O, ν_{sym}), 915, 760, 741, 637, 582, 545 cm^{-1}.

UV-Vis (DMF) λ nm (ε x 10^5): 679(1.09), 358(0.4).

6.2.23 Dihydroxygermanium 2,9,16,23-tetrasulfophthalocyanie tetrammonium salt (**28**)

The suspension of $Ge(OH)_2Pc(SO_2Cl)_4$ (**27**) (0.5 g, 0.493 mmol) in 50 ml of a mixture consisting of equal volumes of water and pyridine was placed in 250 ml flask and refluxed at 80°C for 3 h. After filtration the pyridine was removed under reduced pressure and the water was removed by freeze-drying. The solid sample was dissolved in 50 ml of water and 10 ml of ammonia solution (25 %) was added. The solution was stirred for 15 min at room temperature and water was removed under reduced pressure. The product was dissolved in small quantity of water than placed in dialysis tube and immersed into the distilled water. The dialysis was conducted only till no more chloride anions could be detected in washing solution (reaction with $AgNO_3$). **Caution**: in order to avoid loss of product the dialysis should not be conducted longer than it is necessary to remove chloride anions, as the dialysis membrane is permeable for the sulfonated phthalocyanines as well! While the dialysis is finished water is removed by freeze-drying to give 33 mg (41 %) of solid product. M = 1007.54 g/mol, $C_{32}H_{30}N_{12}O_{14}GeS_4$.

IR (KBr): ν = 3187, 1720, 1636, 1607, 1509, 1397, 1333, 1196(S=O, ν_{as}), 1124, 1084, 1034(S=O, ν_{sym}), 915, 770, 742, 632, 583, 517 cm^{-1}.

UV-Vis (H_2O, pH 7) λ nm (ε x 10^5): 680(1.08), 609(0.23), 354(0.51).

ESI-MS (positive ion mode) *m/z*: 923$[M\text{-}OH^-]^+$, 843$[M\text{-}OH^-\text{-}SO_3]^+$, 763$[M\text{-}OH^-\text{-}2SO_3]^+$, 865$[M\text{-}OH^-\text{-}SO_3+Na^+\text{-}H^+]^+$, 785$[M\text{-}OH^-\text{-}2SO_3+Na^+\text{-}H^+]^+$.

Fluorescence (DMF) λ: 680 nm.

6.2.24 Oxophosphorus(V) 4,11,18,25-tetrakis-(3-pyridyloxy)triaza-tetrabenzcorrole (**29**)

A mixture of metal-free 2,9,16,23-tetrakis-(3-pyridyloxy)phthalocyanine (**10**) (124 mg, 0.14 mmol) and dry pyridine (15 ml) was placed in a 50 ml three-necked round-bottomed flask, equipped with a reflux condenser and a magnetic stirrer. PCl_3 (1ml, 11.33 mmol) was added dropwise via syringe into the flask and the resulting mixture was heated at 120°C under argon for 1.5 h. After cooling to room temperature, the mixture was poured slowly into the water, and the resulting precipitate was filtered, and the collected solid was washed thoroughly with water. The crude product was dissolved in pyridine and purified by column chromatography on silica gel using initially a mixture of pyridine and hexane (1:1), which was changed later for a mixture of pyridine and hexane (1:0.5). The product was further purified by second column chromatography on silica gel with a mixture of CH_2Cl_2 and methanol (4:1) as eluent. The green band was collected and concentrated to dryness, affording 119 mg (96 %) of green solid. M = 917.84 g/mol, $C_{52}H_{28}N_{11}O_5P$.

IR (KBr): ν = 3064, 1618, 1574, 1510, 1472, 1423, 1341, 1235(C-O-C), 1125, 1100, 1062, 1021, 826, 727, 706, 591 cm^{-1}.

UV-Vis (DMF, 10^{-5} mol/l) λ nm (ε x 10^5): 659(0.65), 629(0.39), 600(0.2), 446(1.47), 416(0.53).

DCI-MS (negative, NH_3): *m/z* 917$[M]^-$.

6.2.25 Oxophosphorus(V) 4,11,18,25-tetrakis-[3-(N-methyl)pyridyloxy]-triazatetrabenzcorrole tetraiodide (**30**)

A quantity of 60 mg (0.065 mmol) of **29** was dissolved in DMF (5 ml). An excess of methyl iodide (2 ml, 32 mmol) was added and the solution was stirred for 14 h under nitrogen at 50°C. The methyl iodide was evaporated and the reaction product was precipitated with CH_2Cl_2, filtered off and washed with CH_2Cl_2. The compound was dissolved in water and after filtration isolated by freeze-drying, affording 90 mg (93 %) of green solid. M = 1485.60 g/mol, $C_{56}H_{40}N_{11}O_5PI_4$.

IR (KBr): ν = 3033, 1618, 1583, 1499, 1471, 1409, 1341, 1307, 1276(C-O-C), 1161, 1101, 1063, 968, 821, 724, 664 cm^{-1}.

UV-Vis (H_2O, pH 13, SDS 0.1 mol/l) λ nm (ε x 10^5): 659(0.96), 620(0.43), 595(0.3), 445(2.9), 437(1.08), 416(0.63).

UV-Vis (H_2O, pH 7, SDS 0.1 mol/l) λ nm (ε x 10^5): 658(0.84), 634, 601, 443(1.96), 413.

ESI-MS (positive ion mode) *m/z*: 248.6[M-4I^-+H_2O]$^{4+}$, 373.6[M-3I^-+H_2O]$^{3+}$, 623.9[M-2I^-+H_2O]$^{2+}$.

6.2.26 Oxophosphorus(V) 4,11,18,25-tetrakis-[3-(3-propanesulfonic acid)-pyridiniumoxy]triazatetrabenzcorrole (**31**)

A quantity of 60 mg (0.065 mmol) of **29** and 1,3-propanesultone (0.5 g, 4.09 mmol) were dissolved in DMF (5 ml) and kept at 50°C for 17 h under nitrogen with stirring. The product was precipitated with CH_2Cl_2 (250 ml), filtered off and washed with plenty of CH_2Cl_2 and acetone to remove an excess of 1,3-propanesultone. The compound was dried at 80°C to give 72 mg (78 %) of green solid product. M = 1406.42 g/mol, $C_{64}H_{52}N_{11}O_{17}PS_4$.

IR (KBr): ν = 3055, 1618, 1583, 1550, 1501 1473, 1416, 1340, 1279(C-O-C), 1185(S=O, ν_{as}), 1102, 1040(S=O, ν_{sym}), 986, 819, 726, 681, 600, 526 cm^{-1}.

UV-Vis (H_2O, pH 13, SDS 0.1 mol/l) λ nm (ε x 10^5): 659(0.84), 621(0.41), 596(0.27), 445(1.55), 416(0.57).

UV-Vis (H_2O, pH 7, SDS 0.1 mol/l) λ nm (ε x 10^5): 658(0.69), 636, 602, 443(1.6), 414.

ESI-MS (positive ion mode) *m/z*: 1284[M-122+H^+]$^+$, 1162[M-2x122+H^+]$^+$, 1040[M-3x122+H^+]$^+$, 1324[M-H_2SO_3+H^+]$^+$, 1202[M-H_2SO_3-122+H^+]$^+$, 1080[M-H_2SO_3-2x122+H^+]$^+$.

6.2.27 Phenoxy[2,9,16-triiodosubphthalocyaninato]boron(III) (**32**)

Dried 4-iodophthalonitrile (**6**) (1.5 g, 5.9 mmol) was placed in two-necked round-bottom flask equipped with a reflux condenser and magnetic stirring. A commercially available 1 M solution of BCl_3 (6 ml, 6 mmol) in p-xylene was transferred to the flask with the aid of syringe. The reaction mixture was refluxed under argon at 150°C for one hour. After cooling down to room temperature the unreacted BCl_3 and solvent was quickly removed. To the resulting dark purple crude product a mixture of phenol (0.8 g, 8.5 mmol) and dry toluene (10 ml) were added. The reaction mixture was warmed up to 120°C overnight under argon. The compound was easily purified by column chromatography on silica gel with toluene to give 0.41 g (24 %) of dark purple solid. M = 866.01 g/mol, $C_{30}H_{14}N_6OBI_3$.

IR (KBr): ν = 3082, 3059, 1639, 1602, 1547, 1492, 1461, 1442, 1428, 1387, 1306, 1291, 1259, 1231, 1178, 1141, 1087, 1064, 1041, 921, 881, 861, 812, 754, 705 cm^{-1}.

^{1}H-NMR (200 MHz, $CDCl_3$) δ (ppm): 9.21 (s, 3H), 8.56 (d, 3H), 8.22 (d, 3H), 6.81-6.66 (m, 3H), 5.36 (d, 2H).

UV-Vis (CH_2Cl_2) λ nm (ε x 10^5): 567(0.59), 316(0.31), 268(0.48), 240(0.31).

DCI-MS (NH_3) *m/z*: 866[M^-].

Fluorescence (CH_2Cl_2) λ: 582 nm.

6.2.28 Phenoxy[2,9,16-tris(2-(3-pyridynyl)ethynyl)subphthalocyaninato]-boron(III) (**34a**)

To a solution of subphthalocyanine **32** (0.4 g, 0.462 mmol), $Pd(PPh_3)_2Cl_2$ (25 mg, 0.0356 mmol), CuI (70 mg, 0.368 mmol) and 3-ethynylpyridine (**33**) (0.57 g, 5.53 mmol) freshly distilled and degassed TEA (6 ml) was added. All reactants were allowed to stir under nitrogen at room temperature. The reaction was monitored by TLC (with EtOAc/PE 1:1); after 20 h the starting material reacted. The solvent was gently removed under diminished pressure. The reaction mixture was purified on silica gel with CH_2Cl_2 to remove part of the impurities. Then the solvent was changed to CH_2Cl_2/MeOH 5:1 to collect all pink-coloured band. The TLC revealed that this fraction consisted of three compounds. The residue was further purified by a second silica gel column. The first band was eluted using EtOAc/PE 2:1 and identified as mono-substituted derivative. Next fraction was collected using EtOAc/PE 3:1 and identified as di-substituted derivative. The last fraction was collected using EtOAc/Acetone 1:2 and was identified as the desired product.

Phenoxy[2,9,16-tris(2-(3-pyridynyl)ethynyl)subphthalocyaninato]boron(III) (**34a**). Yield 206 mg (56 %). M = 791.64 g/mol, $C_{51}H_{26}N_9OB$.

IR (KBr): ν = 3053, 2213 (C ≡ C), 1613, 1560, 1481, 1468, 1451, 1434, 1406, 1384, 1289, 1258, 1231, 1182, 1150, 1117, 1057, 1022, 956, 893, 831, 805, 756, 709,629cm^{-1}.

^{1}H-NMR (200 MHz, $CDCl_3$) δ (ppm): 9.05 (s, 3H), 8.88 (d, 3H), 8.83 (dd, 3H), 8.63 (dd, 3H), 8.07 (dd, 3H), 7.93 (d, 3H), 7.37 (m, 3H), 6.84-6.67 (m, 3H), 5.43 (d, 2 H).

UV-Vis (CH_2Cl_2) λ nm (ε x 10^5): 581(0.71), 352(0.37), 294(0.64).

DCI-MS (NH_3) *m/z*: 791[M^-].

R_f (CH_2Cl_2:Acetone 1:1) = 0.38.

Phenoxy[2-iodo-9,16-bis(2-(3-pyridynyl)ethynyl)subphthalocyaninato]boron(III) (**34b**). Yield 53 mg (14 %). M = 816.43 g/mol, $C_{44}H_{22}N_8OBI$.

IR (KBr): ν = 3081, 3058, 2212 (C ≡ C), 1728, 1612, 1579, 1559, 1474, 1448, 1434, 1412, 1384, 1290, 1259, 1230, 1183, 1120, 1062, 1022, 956, 895, 827, 804, 756, 699, 625 cm^{-1}.

UV-Vis (CH_2Cl_2) λ nm (ε x 10^5): 574(0.37), 301(0.48).

DCI-MS (NH_3) *m/z*: 724[M^- - C_6H_5O + H]$^-$.

Phenoxy[2,9-diiodo-16-(2-(3-pyridynyl)ethynyl)subphthalocyaninato]boron(III) (**34c**). Yield 5 mg (1.3 %). M = 846.22 g/mol, $C_{37}H_{18}N_7OBI_2$.

IR (KBr): ν = 1723, 1655, 1609, 1546, 1477, 1409, 1379, 1260, 1184, 1121, 1096, 1066, 1023, 804, 755, 704 cm^{-1}.

UV-Vis (CH_2Cl_2) λ nm (ε x 10^5): 570(0.48), 305(0.33), 271(0.38).

DCI-MS (NH_3) *m/z*: 841[M + H^+]$^+$.

R_f (CH_2Cl_2:EtOAc 1:1) = 0.61.

6.2.29 Phenoxy[2,9,16-tris{2-(3-(N-methyl)pyridynyl)ethynyl}subphthalo-cyaninato]boron(III) triiodide (**35**)

A quantity of 50 mg (0.063 mmol) of subphthalocyanine **34a** was dissolved in DMF (5 ml). An excess of methyl iodide (5 ml, 80 mmol) was added and the solution was stirred for 4 h at 50°C under nitrogen. The reaction mixture was protected from light. The methyl iodide was evaporated and the reaction product was precipitated with CH_2Cl_2, filtered off and washed with CH_2Cl_2. The compound was dissolved in water and after filtration isolated by freeze-drying. Yield 60 mg (78 %). M = 1217.46 g/mol, $C_{54}H_{35}N_9OBI_3$.

IR (KBr): ν = 3070, 2929, 2216(C ≡ C), 1720, 1626, 1583, 1505, 1454, 1289, 1264, 1230, 1193, 1166, 1122, 1057, 897, 809, 756, 709, 670, 619, 556 cm^{-1}.

UV-Vis (H_2O) λ nm (ε x 10^5): 585(0.75), 285(0.74), 216(0.81).

ESI-MS (positive ion mode) *m/z*: 278.4[M-3I^-]$^{3+}$.

6.2.30 Phenoxy[2,9,16-tris{2-(3-(3-propanesulfonic acid)pyridinium)-ethynyl}subphthalocyaninato]boron(III) (**36**)

50 mg (0.063 mmol) of subphthalocyanine **34a** and 1,3-propanesultone (0.4 g, 3.72 mmol) were dissolved in DMF (3 ml) and kept at 50°C for 4 h under nitrogen with stirring. The product was dissolved in 20 ml of DMF and precipitated with CH_2Cl_2, filtered off and washed with plenty of CH_2Cl_2 and acetone to remove excess of 1,3-propanesultone. The product was dried at 60°C overnight to give 60 mg (83 %) of dark red solid. M = 1158.07 g/mol, $C_{60}H_{44}N_9O_{10}S_3B$.

IR (KBr): ν = 3086, 2929, 2218(C ≡ C), 1720, 1627, 1580, 1502, 1451, 1292, 1191(SO_2, ν_{as}), 1121, 1043(SO_2, ν_{sym}), 990, 830, 813, 758, 710, 679, 623, 525 cm^{-1}.

UV-Vis (H_2O, 0.6 M KCl) λ nm (ε x 10^5): 579(0.20), 547(0.21), 286(0.46), 205(0.60).

ESI-MS (positive ion mode) *m/z*: 1180[M-Na^+]$^+$, 1058[M-122+Na^+]$^+$, 936[M-2x122+Na^+]$^+$.

ESI-MS (negative ion mode) *m/z*: 1156[M-H^+]$^-$, 1034[M-122-H^+]$^-$, 912[M-2x122-H^+]$^-$.

6.2.31 Phenoxy[2,9,16-tris(2-(2-pyridynyl)ethynyl)subphthalocyaninato]-boron(III) (37a)

To a solution of **32** (0.2 g, 0.23 mmol), $Pd(PPh_3)_2Cl_2$ (10 mg, 0.014 mmol), CuI (35 mg, 0.184 mmol) and 2-ethynylpyridine (**7**) (0.28 ml, 2.77 mmol), freshly distilled and deoxygenated TEA (3 ml) was added. All reactants were allowed to stir under nitrogen at room temperature. The reaction was monitored by TLC (with EtOAc/PE 1:1), and after 20 h the starting material had reacted. The solvent was gently removed under diminished pressure. The reaction mixture was purified on silica gel with CH_2Cl_2 to remove part of the impurities. The solvent was then changed to CH_2Cl_2/ MeOH (5:1) to collect all pink-coloured fractions. The TLC revealed that the fraction collected consisted of three compounds. To isolate all fractions second silica gel column chromatography was applied. The first band was eluted using CH_2Cl_2/PE/EtOAc (1:1:1) and identified as mono-substituted derivative. Next fraction was collected using CH_2Cl_2/EtOAc (1:1) and identified as di-substituted derivative. The last fraction collected using EtOAc/CH_2Cl_2 (3:1) was the desired product.

Phenoxy[2,9,16-tris(2-(2-pyridynyl)ethynyl)subphthalocyaninato]boron(III) (**37a**). Yield 78 mg (42 %). M = 791.64 g/mol, $C_{51}H_{26}N_9OB$.

IR (KBr): ν = 3053, 2213 (C ≡ C), 1720, 1613, 1579, 1560, 1474, 1461, 1428, 1383, 1260, 1231, 1186, 1152, 1120, 1084,1058, 990, 891, 825, 808, 776, 755, 735, 710, 621 cm^{-1}.

UV-Vis (CH_2Cl_2) λ nm (ε x 10^5): 582(0.74), 352(0.39), 294(0.65).

EI-MS (positive ion mode) *m/z*: 791[M^+], 698[M – $C_6H_5O^-$]$^+$.

DCI-MS (NH_3) *m/z*: 791[M^-], 715[M^- - OPh + NH_3]$^-$.

R_f (CH_2Cl_2:EtOAc 1:1) = 0.36.

Phenoxy[2-iodo-9,16-bis(2-(2-pyridynyl)ethynyl)subphthalocyaninato]boron(III) (**37b**). Yield 38 mg (20 %). M = 816.43 g/mol, $C_{44}H_{22}N_8OBI$.

IR (KBr): ν = 3064, 2218 (C ≡ C), 1725, 1608, 1580, 1560, 1490, 1462, 1451, 1432, 1387, 1292, 1255, 1233, 1186, 1121, 1088, 1060, 1023, 892, 811, 780, 755, 704 cm^{-1}.

UV-Vis (CH_2Cl_2) λ nm (ε x 10^5): 576(0.39), 303(0.50).

DCI-MS (NH_3) *m/z*: 816[M^-], 724[M^- - OPh + H]$^-$.

R_f (CH_2Cl_2:EtOAc 1:1) = 0.60.

Phenoxy[2,9-diiodo-16-(2-(2-pyridynyl)ethynyl)subphthalocyaninato]boron(III) (**37c**). Yield 10 mg (5 %). M = 846.22 g/mol, $C_{37}H_{18}N_7OBI_2$.

IR (KBr): ν = 3047, 2212 (C ≡ C), 1710, 1720, 1613, 1578, 1560, 1460, 1426, 1381, 1289, 1259, 1184, 1149, 1119, 1090, 1056, 984, 827, 811, 776, 755, 709, 696, 540 cm^{-1}.

UV-Vis (CH_2Cl_2) λ nm (ε x 10^5): 570(0.46), 300(0.31), 272(0.37).

DCI-MS (NH_3) *m/z*: 841[M^-], 749[M^- - OPh + H]$^-$.

DCI-MS (NH_3) *m/z*: 841[M + H^+]$^+$.

R_f (CH_2Cl_2:EtOAc 1:1) = 0.77.

6.2.32 Phenoxy[2,9,16-tris(2-(2-pyridynyl)ethyl)subphthalocyaninato]-boron(III) (38)

A mixture of subphthalocyanine **37a** (80 mg, 0.101 mmol) and 10% palladium on charcoal (80 mg) in AcCN/CH_2Cl_2 (30ml:10ml) was placed in 100 ml two-necked round-bottomed flask equipped with a reflux and magnetic stirrer. A stream of dry hydrogen was bubbled through a suspension for 7 h. The solution was filtered from the catalyst and concentrated. The compound was purified by column chromatography on silica gel using a mixture of CH_2Cl_2 and EtOH (3:2) to give 50 mg (61 % yield) of product. M = 803.73 g/mol, $C_{51}H_{38}N_9OB$.

IR (KBr): ν = 3053, 3008, 2963, 2924, 2857, 1762, 1718, 1667, 1618, 1591, 1568, 1474, 1455, 1433, 1385, 1291, 1261, 1233, 1165, 1125, 1093, 1052, 889, 805, 754, 712, 693 cm^{-1}.

UV-Vis (CH_2Cl_2) λ nm (ε x 10^5): 564(0.47), 309(0.26), 258(0.36), 230(0.36).

DCI-MS (NH_3) *m/z*: 804[M + H^+]$^+$.

Fluorescence (CH_2Cl_2) λ: 578 nm.

6.2.33 Phenoxy[2,9,16-tris{2-(2-(N-methyl)pyridynyl)ethyl}subphthalo-cyaninato]boron(III) triiodide (39)

A quantity of 20 mg (0.0248 mmol) of subphthalocyanine **39** was dissolved in DMF (3 ml). An excess of methyl iodide (5 ml, 80 mmol) was added and the solution was stirred 4 h at room temperature under nitrogen. The methyl iodide was evaporated and the reaction product was precipitated with a mixture CH_2Cl_2/PE, filtered off and washed with CH_2Cl_2 to remove yellow impurities. The compound was dissolved in water and

after filtration isolated by freeze-drying. The product was dried at 80°C for 24 h to give 26 mg (87 %) of solid product. M = 1229.55 g/mol, $C_{54}H_{47}N_9OBI_3$.

IR (KBr): ν = 3020, 3000, 2975, 2959, 1764, 1718, 1630, 1578, 1513, 1460, 1438, 1404, 1385, 1289, 1256, 1233, 1166, 1129, 1094, 1051, 1017, 880, 832, 756, 713, 696, 621 cm^{-1}.

UV-Vis (H_2O) λ nm (ε x 10^5): 567(0.31), 309(0.17).

ESI-MS (positive ion mode) *m/z*: 282.8$[M-3I^-]^{3+}$.

Fluorescence (H_2O) λ: 582 nm.

6.2.34 Phenoxy[2,9,16-tris-(3-pyridyloxy)subphthalocyaninato]boron(III) (40)

Dry 4-(3-pyridyloxy)phthalonitrile (**3**) (0.5 g, 2.3 mmol) was placed in two-necked round-bottom flask equipped with a reflux condenser and magnetic stirring. A commercially available 1 M solution of BCl_3 (4.6 ml, 4.6 mmol) in p-xylene was transferred to the flask with the aid of syringe (phthalonitrile to BCl_3 molar ratio: 1:2). The reaction mixture was brought quickly to reflux and kept at 160°C for 15 min. The reaction time and temperature should not be exceeded to avoid fast decomposition of the subphthalocyanine, which appears to be a very sensitive compound. After cooling down to room temperature the remaining unreacted BCl_3 and solvent was quickly removed. To the resulting dark purple crude product a mixture of phenol (0.6 g, 6.4 mmol) and DMF (2 ml) was added. The reaction mixture was kept at 120°C for 2 h under argon. A mixture of desired product and impurities sticks firmly to the silica gel. Hence, a combination of $CHCl_3$ and DMF was used to get rid of impurities. The compound was initially purified by column chromatography on silica gel with $CHCl_3$/DMF 10:2 to remove green impurities and then $CHCl_3$/DMF 10:4 to give pink colour fraction. The rest of subphthalocyanine was removed from silica gel with DMF. The pink colour fractions were collected and the solvent was evaporated. The compound was finally purified by second column chromatography on silica gel with CH_2Cl_2/EtOAc 10:4 to remove green and blue impurities and then the eluent was changed into CH_2Cl_2/MeOH 10:1 to give 71mg (12 %) of dark purple solid. M = 767.57 g/mol, $C_{45}H_{26}N_9O_4B$.

IR (KBr): ν = 3046, 1618, 1584, 1495, 1472, 1430, 1384, 1272 (Ar-O-Ar), 1166, 1124, 805, 665, 604 cm^{-1}.

UV-Vis (DMF) λ nm (ε x 10^5): 565(0.22).

ESI-MS (positive ion mode) *m/z*: 768$[M + H^+]^+$.

R_f (Toluene:MeOH 1:1): 0.6.

6.2.35 Phenoxy[2,9,16-tris-(3-(N-methyl)pyridyloxy)subphthalocyaninato]-boron(III) triiodide (41)

A quantity of 50 mg (0.07 mmol) of subphthalocyanine **40** was dissolved in DMF (1.5 ml). An excess of methyl iodide (2 ml, 32 mmol) was added and the solution was stirred for 2 h at 50°C under nitrogen. The reaction mixture was protected from light. The methyl iodide was evaporated and the reaction product was precipitated with CH_2Cl_2, filtered off and washed with CH_2Cl_2. The compound was dissolved in water and after filtration isolated by freeze-drying. Yield 83 mg (98 %). M = 1193.39 g/mol, $C_{48}H_{35}N_9O_4BI_3$.

IR (KBr): ν = 3047, 1714, 1619, 1586, 1499, 1474, 1432, 1384, 1303, 1275 (Ar-O-Ar), 1211, 1166, 1124, 962, 886, 805, 752, 665, 604 cm^{-1}.

UV-Vis (H_2O) λ nm (ε x 10^5): 562(0.21).

ESI-MS (positive ion mode) *m/z*: 270.4$[M-3I^-]^{3+}$, 282$[M^{3+}-OPh-2I^-+H^+]^{3+}$, 1066$[M-I^-]^+$, 924$[M-CH_3^+-2I^-]^+$, 990$[M-C_6H_5^+-I^-+H^+]^+$, 469$[M-2I^-]^{2+}$, 360.7$[M-3I^--C_6H_5^+-CH_3^++H^+]^{2+}$, 431.1$[M-C_6H_5^+-2I^-+H^+]^{2+}$, 398.2$[M-3I^--CH_3^+]^{2+}$.

ESI-MS (negative ion mode) *m/z*: 1320$[M+I^-]^-$, 1178$[M-CH_3^+]^-$, 1228$[M-PhO^-+I^-+H^+]^-$, 1244$[M-C_6H_5^++I^-+H^+]^-$.

6.2.36 3-Pyridyloxy[subphthalocyaninato]boron(III) (43)

In a round bottom flask the commercially available chloro[subphthalocyaninato]boron(III) (**42**) (0.45 g, 1.04 mmol), 3-hydroxypyridine (**1**) (0.5 g, 5.26 mmol) and a dry toluene (10 ml) were placed. The mixture was kept at 120°C under nitrogen for 12 h with vigorous stirring. The resulting reaction mixture was chromatographed on silica gel using CH_2Cl_2/EtOAc (5:3). The first band was discarded and solvent was changed to CH_2Cl_2/EtOAc (1:1). The read band was collected and the compound was additionally purified on silica gel with $CHCl_3$/EtOAc (25:5) to remove the traces of unreacted material. Than the eluent was changed to $CHCl_3$/EtOAc (1:1) and a bright read band was collected and the solvent was evaporated affording 322 mg (63 %) of read solid. M = 489.30 g/mol, $C_{29}H_{16}N_7OB$.

IR (KBr): ν = 3057, 1724, 1614, 1573, 1458, 1432, 1417, 1386, 1325, 1287, 1258, 1234, 1197, 1170, 1153, 1132, 1052, 1033, 911, 825, 765, 738, 709, 697, 582, 572 cm^{-1}.

^{1}H-NMR (200 MHz, D_6-acetone) δ (ppm): 8.86 (m, 6H, 1,4-ArH), 8.01 (m, 6H, 2,3-ArH), 7.83 (dd, 1H), 6.77 (m, 2H), 5.81 (m, 1H).

UV-Vis ($CHCl_3$) λ nm (ε x 10^5): 563(0.65).

ESI-MS (positive ion mode) *m/z*: 490$[M + H^+]^+$, 395$[M - C_5H_4NO^-]^+$.

6.2.37 3-(N-methyl)pyridyloxy[subphthalocyaninato]boron(III) iodide (44)

A quantity of 50 mg (0.102 mmol) of **43** was dissolved in DMF (5 ml). An excess of methyl iodide (5 ml, 80 mmol) was added and the solution was stirred for 2 h at 50°C under argon. The solvent was evaporated under diminished pressure and the product was washed with small volume of CH_2Cl_2 to give 60 mg (93%) as dark read solid. M = 631.24 g/mol, $C_{30}H_{19}N_7OBI$.

IR (KBr): ν = 3045, 1773, 1727, 1632, 1613, 1583, 1505, 1455, 1433, 1384, 1324, 1288, 1231, 1195, 1168, 1153, 1133, 1088, 1042, 1020, 956, 884, 751, 742, 731, 717, 696, 675, 646, 588, 572 cm^{-1}.

UV-Vis (DMF) λ nm (ε x 10^5): 565(0.64).

ESI-MS (positive ion mode) *m/z*: 504$[M–I^-]^+$, 395$[M–C_6H_7NOI^-]^+$.

Fluorescence (DMF) λ: 576 nm.

6.2.38 5,10,15,20-Teterakis-(N-methyl-4-pyridyl)-21H,23H-porphyrin tetraiodide (46)

A quantity of 100 mg (0.16 mmol) of commercially available (Aldrich Chem. Co.) 5,10,15,20-tetra(4-pyridyl)-21*H*,23*H*-porphine (**45**) was dissolved in DMF (20 ml). An excess of methyl iodide (5 ml, 80 mmol) was added and the solution was stirred for 18 h at 50°C under argon. The product was precipitated with CH_2Cl_2, washed thoroughly with CH_2Cl_2, acetone, dissolved in hot water and isolated by freeze-drying to give solid in 96% (183 mg) yield. M = 1186.44 g/mol, $C_{44}H_{38}I_4N_8$.

IR (KBr): ν = 3008, 1637, 1561, 1509, 1481, 1458, 1402, 1277, 1184, 971, 945, 887, 859, 799, 731, 712 cm^{-1}.

UV-Vis (H_2O) λ nm: 419, 515, 550, 581, 637.

UV-Vis (H_2O, pH 13, SDS 0.1 mol/l) λ nm: 421, 441, 580.

6.2.39 5,10,15,20-Tetrakis-[4-(3-propanesulfonic acid)pyridinium]-21H,23H-porphyrin (47)

100 mg (0.16 mmol) of of commercially available (Aldrich Chem. Co.) 5,10,15,20-tetra(4-pyridyl)-21*H*,23*H*-porphine (**45**) and 1,3-propanesultone (0.5 g, 4.09 mmol) were dissolved in DMF (15 ml) and kept at 80°C for 16 h under nitrogen with stirring. The product was precipitated with CH_2Cl_2, filtered off and washed with plenty of CH_2Cl_2 and acetone to remove excess of 1,3-propanesultone. The product was dissolved in hot water and after freeze-drying 163 mg (92 %) of porphyrin was obtained. M = 1107.26 g/mol, $C_{52}H_{50}N_8O_{12}S_4$.

IR (KBr): ν = 3100, 3051, 1637, 1560, 1511, 1462, 1406, 1356, 1293, 1195(SO_2, ν_{as}), 1040(SO_2, ν_{sym}), 970, 885, 864, 808, 730, 597, 526 cm^{-1}.

UV-Vis (H_2O) λ nm: 420, 516, 553, 581, 638.

UV-Vis (H_2O, pH 13, SDS 0.1 mol/l) λ nm: 426, 514, 578.

ESI-MS (positive ion mode) *m/z*: 576$[M+2Na^+]^{2+}$, 554$[M+2H^+]^{2+}$, 741$[M-3x122+H^+]^+$, 885$[M-2x122+Na^+]^+$, 1007$[M-122+Na^+]^+$, 619$[M-4x122+H^+]^+$, 432$[M-2x122+2xH^+]^{2+}$, 493$[M-122+2xH^+]^{2+}$, 370$[M+3H^+]^{3+}$, 247M-3x122+3$H^+]^{3+}$.

6.2.40 5,10,15,20-Teterakis-(4-pyridyl)-porphyrin-Zn(II) (48)

A sample of commercially available (Aldrich Chem. Co.) 5,10,15,20-tetra(4-pyridyl)-21*H*,23*H*-porphine (**45**) (210 mg, 0.339 mmol) was dissolved in 20 ml of DMF. An excess of $Zn(CH_3COO)_2$•2 H_2O (440 mg, 2 mmol) was added and the reaction mixture was stirred for 48 h at 100°C. The product was precipitated by water addition filtered off and washed with a plenty of water and acetone. After drying at 80°C overnight 226 mg (98 %) of **40** was obtained. The product was free of the starting material as confirmed by negative DCI mass spectrometry. M = 682.06 g/mol, $C_{40}H_{24}N_8Zn$.

IR (KBr): ν = 3042, 1635, 1561, 1528, 1460, 1276, 996, 799 cm^{-1}.

UV-Vis (DMF) λ nm (ε x 10^5): 423(3.01), 557(0.19), 597(0.05).

DCI-MS (NH_3) *m/z*: 680$[M^-]$.

6.2.41 5,10,15,20-Teterakis-(N-methyl-4-pyridyl)-porphyrin-Zn(II) tetraiodide (49)

A quantity of 90 mg (0.13 mmol) of 5,10,15,20-tetrakis-(4-pyridyl)-porphyrin-Zn(II) (**48**) was dissolved in DMF (20 ml). An excess of methyl iodide (5 ml, 80 mmol) was added and the solution was stirred for 18 h at 50°C under argon. The product was

precipitated with CH_2Cl_2, washed thoroughly with CH_2Cl_2, dissolved in hot water and isolated by freeze-drying to give 159 mg (98%).M = 1249.82 g/mol, $C_{44}H_{36}I_4N_8Zn$.

IR (KBr): ν = 3120, 3042, 1639, 1560, 1527, 1510, 1460, 1278, 1191, 1118, 995, 864, 800, 618 cm^{-1}.

UV-Vis (H_2O, pH 13, SDS 0.1 mol/l) λ nm (ε x 10^5): 452, 569, 609

UV-Vis (H_2O, pH 7, SDS 0.1 mol/l) λ nm (ε x 10^5): 446, 567, 609.

ESI-MS (positive ion mode) *m/z*: 184.8$[M\text{-}4I^-]^{4+}$, 169.3$[M\text{-}4I^-\text{-}Zn^{2+}\text{+}2H^+]^{4+}$, 241.4$[M\text{-}4I^-\text{-}CH_3^+]^{3+}$, 354.7$[M\text{-}4I^-\text{-}2CH_3^+]^{2+}$.

6.2.42 5,10,15,20-Tetrakis-[4-(3-propanesulfonic acid)pyridinium]-porphyrin-Zn(II) (50)

90 mg (0.13 mmol) of 5,10,15,20-tetrakis-(4-pyridyl)-porphyrin-Zn(II) (**48**) and 1,3-propanesultone (0.5 g, 4.09 mmol) were dissolved in DMF (15 ml) and kept at 80°C for 16 h under nitrogen with stirring. The product was precipitated with CH_2Cl_2, filtered off and washed with plenty of CH_2Cl_2 to remove excess of 1,3-propanesultone. The product was dissolved in hot water and after freeze-drying 146 mg (96 %) of porphyrin was obtained. M = 1170.64 g/mol, $C_{52}H_{48}N_8O_{12}S_4Zn$.

IR (KBr): ν = 3115, 3047,1634, 1529, 1496, 1459, 1420, 1202, 1184(SO_2, ν_{as}), 1041(SO_2, ν_{sym}), 994, 866, 799, 721, 599, 571, 528 cm^{-1}.

UV-Vis (H_2O, pH 13, SDS 0.1 mol/l) λ nm (ε x 10^5): 451, 569, 615.

UV-Vis (H_2O, pH 7, SDS 0.1 mol/l) λ nm (ε x 10^5): 455, 569, 615.

ESI-MS (positive ion mode) *m/z*: 1096$[M\text{-}122\text{+}Na^+]^+$, 947$[M\text{-}2x122\text{+}Na^+]^+$, 925$[M\text{-}2x122\text{+}H^+]^+$, 825$[M\text{-}3x122\text{+}Na^+]^+$, 803$[M\text{-}3x122\text{+}H^+]^+$.

6.2.43 5,10,15,20-Tetrakis-(4-sulfonatophenyl)-porphyrin-Zn(II) (52)

A sample of commercially available 5,10,15,20-tetrakis-(4-sulfonatophenyl)-21H,23H-porphyrin (**51**) (100 mg, 0.107mmol) and $Zn(CH_3COO)\bullet 2\ H_2O$ (200 mg, 0.91 mmol) was dissolved in 20 ml of DMF. The reaction mixture was stirred for 24 hours at 80°C. The product was precipitated with CH_2Cl_2, washed with CH_2Cl_2, dissolved in water, placed in dialysis tube and immersed into the distilled water. The dialysis was conducted for 48 hours with frequently changed of water. While the dialysis is finished water is removed by freeze-drying to give brown powder (101 mg, 94 %). M = 998.38 g/mol, $C_{44}H_{28}N_4S_4O_{12}Zn$.

IR (KBr): ν = 1626, 1405, 1338, 1186 (SO_2, ν_{as}), 1121, 1038 (SO_2, ν_{sym}), 996, 798, 739, 698, 622,553 cm^{-1}.

UV-Vis (H_2O, pH 13, CTAC 0.1 mol/l) λ nm (ε x 10^5): 429(1.26), 562, 598.

6.3 Photocatalytic measurements

6.3.1 Equipment for photocatalytic oxidation

The individual activities were measured volumetrically by oxygen consumption over time. The equipment utilized during these measurements is the commercially available micro-hydrogenation apparatus Marhan (NORMAG, Postfach 1269, 65719 Hofheim, Germany). The equipment consists of a two-necked 100 ml reaction vessel connected by a glass bridge to a 50 ml gas burette. All glass parts are double-walled and connected to thermostat filled with 25°C water (Fig. 6.1) [7].

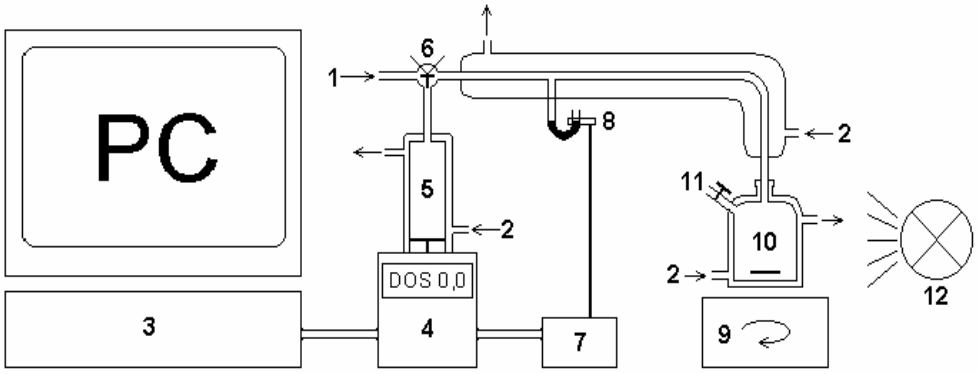

Figure 6.1. Laboratory equipment for the measurement of the oxygen consumption over time: 1 gas inlet, 2 termostated water inlet, 3 computer, 4 dosimat, 5 oxygen reservoir, 6 tap, 7, 8 Hg light barrier, 9 stirrer, 10 reaction vessel (100 ml), 11 reaction solution inlet, 12 light source (quartz-halogen lamp, light intensity at the reaction vessel: ~ 180 $mW \cdot cm^{-2}$) (by courtesy of Dr. Robert Gerdes).

It has to be pointed out that no additional filter to cut short and long wavelengths off was used. Water itself is a good filter for IR radiation and the optical glass cuts wavelengths below 300 nm. As irradiation source a 250 W slide projector with a quartz-halogen lamp was used. Quartz-halogen lamp emits photons between 300 and 2700 nm. In the visible region the light intensity is relatively continuous [3]. The slide projector lens was placed at a distance of 5 cm from the reaction vessel so that the light intensity was around 180 $mW \cdot cm^{-2}$ as determined with a bolometer.

6.3.2 Photo-oxidation of 2-mercaptoethanol

For measurements at pH 13, an aqueous solution of 50 ml of sodium hydroxide (0.12 M) solution containing 0.25 μmol photosensitizer was employed. For measurements at pH 10, a mixture of 25 ml of borate buffer, 25 ml of water and 0.25 μmol photosensitizer was used. For negatively charged photosensitizers cetytrimethylamonium chloride (CTAC) was employed; 5 mmol per 50 ml of the reaction solution (*i.e.* overall concentration 0.1 mol/l). For positively charged photosensitizer sodium dodecylsulfate (SDS) was employed; 5 mmol per 50 ml of the reaction solution (*i.e.* overall concentration 0.1 mol/l). After filling the reaction vessel with 50 ml of the reaction solution, the apparatus was flushed with oxygen for 10 min. Then 50 μl of 2-mercaptoethanol (0.7 mmol) was added. The reaction flask was irradiated under intensive magnetic stirring and the oxygen consumption over time was recorded (T = 298 K). The reaction was conducted for three hours. The reactions were mainly conducted at pH 13 (in some particular cases at pH 10 due to low stability at pH 13) to secure the high concentration of thiolate anions (pK_s 9.6) and, on the other hand, to make the reaction comparable with the industrial MEROX process (*i.e.* the catalytic oxidation of thiols) [10].

Photosensitizer: 5 μmol/l
Detergent (CTAC or SDS): 0.1 mol/l
Substrate: 14 mmol/l
pH 13: NaOH 0.12 mol/l
pH 10: borate buffer (diluted with water 1:1)

Around 25.7 ml of oxygen corresponds to the formation of 2-hydroxyethanesulfonic acid. Thus, the calculated molar ratio of consumed oxygen to employed substrate amounts to 1.5.

6.3.3 Photo-oxidation of phenol

For measurements at pH 13, an aqueous solution of 50 ml of sodium hydroxide (0.12 M) containing 0.25 μmol of photosensitizers was employed. For measurements at pH 10, 25 ml of borate buffer diluted with 25 ml of distilled water was prepared and 0.25 μmol of photosensitizer was added to a solution. An appropriate detergent, CTAC or SDS, was used for the reactions in a micellar solution (concentration 0.1 mol/l). After filling the reaction vessel with 50 ml of the solution, the apparatus was flushed with pure oxygen for 10 min. 72 mmol of phenol was dissolved in 50 ml of ethanol. Then 0.25 ml of this solution (0.36 mmol of phenol) was injected to the reaction vessel. The reaction system was closed immediately and the light source was switched on. The oxygen consumption was measured volumetrically at 298 K and the solution was stirred with a magnetic bar (1000 rpm). Reaction was conducted for three hours.

Photosensitizer: 5 μmol/l
Detergent (CTAC or SDS): 0.1 mol/l
Substrate: 7.2 mmol/l
pH 13: NaOH 0.12 mol/l
pH 10: borate buffer (diluted with water 1:1)

Around 8.81 ml of O_2 is required to convert the amount of phenol employed in the experiment to *p*-benzoquinone formed in the first step. Gerdes *et al.* [1] postulated that the oxidation proceeds further. Thus, further consumption of 1 mol of singlet oxygen and 1.5 mol of triplet oxygen results in simple carboxylic acids (maleic or fumaric acid) and carbonate formation (see chapter 5.3). Altogether, around 30.8 ml of O_2 is required.

6.3.4 Immobilization of photosensitizers on ion exchangers

The photocatalytic activities of the photosensitizers were investigated in a homogeneous manner, *i.e.* in water solution, as well as in a heterogeneous form, *i.e.* with photosensitizers bound ionically at ion exchangers. Ionically polymer bound photosensitizers were easily obtained by the reaction of negatively charged dyes with the basic anion exchanger or by the reaction of positively charged dyes with the acidic cation exchanger. Following, commercially available, ion exchangers were employed during this studies:

- **Amberlite IRA-402** is a strongly basic anion exchanger with quaternary ammonium functionality. This anion exchanger may operate at very broad pH range, *i.e.* 1-14 pH, with a total exchange capacity calculated for Cl^- anions 1.2 meq/ml of wet resin. Amberlite IRA-402 is a styrene/DVB resin (Fig. 6.2).

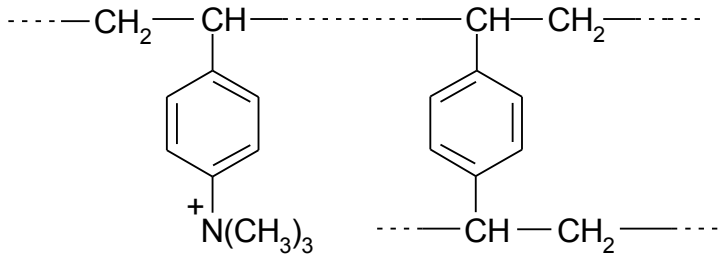

Amberlite IRA-402

Figure 6.2. The structure of anion exchanger Amberlite IRA-402.

- **Amberlite IRA-120** is a strongly acidic cation exchanger with sulfonic acid functionality. As Amberlite IRA-402 this resin may operate at very broad, *i.e.* 1-14, pH value range with a total exchange capacity 4.4 meq/g of dry polymer. Amberlite IRA-120 is based on a styrene/DVB backbone.

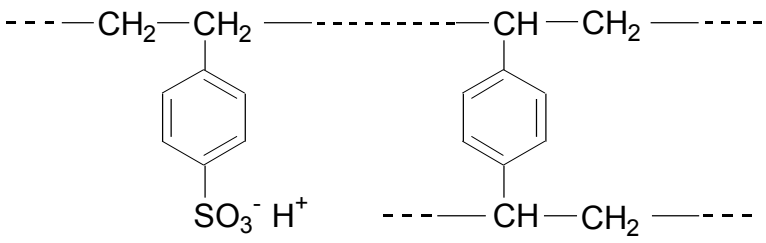

Amberlite IRA-120

Figure 6.3. The structure of cation exchanger Amberlite IRA-120.

- **Amberlite IRA-958** is a strongly basic anion exchanger with quaternary ammonium functionality. Amberlite IRA-958 is an acrylic-based resin operating at 0-14 pH value with a total exchange capacity 0.8 meq/ml of wet resin. It is characterized by an excellent stability and resistance to abrasion.

All ion exchangers but IRA-958 were dried overnight at 50°C prior to use. Then 10 g of dry Amberlite was suspended in 100 ml of distilled water. A photosensitizer (4 μmol) was dissolved in water (40 ml) and added dropwise during 30 min under gentle stirring. The immobilization was carried out till ion exchanger consumed all amount of dye. The reaction was usually completed after 3 h, although in some cases much longer reaction time was necessary. The solution became colorless and the Amberlite intensively coloured. The polymer was isolated by filtration, washed with water and then with ethanol and dried at 50°C overnight. The immobilization is irreversible and no desorption of the dyes could be observed under reaction condition. In this way a polymers containing photosensitizer (0.4 μmol/g) were obtained.

In the case of heterogeneous photo-oxidation 2.5 g polymer containing 0.4 μmol/g photosensitizer was added to the reaction vessel. For measurements at pH 13, the reaction vessel was filled with 50 ml of sodium hydroxide (0.12 M) solution. For measurements at pH 10, the reaction vessel was filled with a mixture of 25 ml of borate buffer and 25 ml of water. An appropriate substrate was added (50μl of 2-mercaptoethanol or 0.36 mmol of phenol) after the apparatus was flushed with oxygen for 10 min. The reaction flask was irradiated under intensive magnetic stirring and the oxygen consumption over time was recorded. The reaction was conducted for three hours. No detergent was applied in the case of heterogeneous photo-oxidation.

6.3.5 Turnover number calculation

The ratio of the number of photoinduced transformations for a given period of time to the number of photocatalytic sites (in heterogeneous photocatalysis) or to the number of photocatalyst molecules (in homogeneous photocatalysis) is referred to as **turnover number** (**TON**) [9]. The photocatalytic activity of different photocatalysts was estimated from the initial rate of the oxygen consumption (RR_i) and the turnover number (TON) was calculated from mol O_2 consumption per time unit (min) per mol of the photocatalyst.

6.3.6 Action spectra measurements

Action spectrum has been defined as *"A plot of a (...) chemical photoresponse per number of incident photons, against wavelength (...) of light. (...)."* [9]. Action spectrum provides an important piece of chemical information, *i.e.* gives an insight into the photocatalytic activity of the molecule of interest at a particular wavelength of irradiation. To make the action spectrum correspond to the spectrum of photocatalyst activity, the experimental conditions for the linear dependence of the reaction rate on light intensity over the whole spectral range must be established. Action spectra of photosensitizers were obtained in the equipment used previously to determine the photocatalytic activity (Fig. 6.1). Reaction conditions and concentrations of photosensitizer, substrate and detergent were employed as those during photocatalytic activity determination with the exception being the use of interference filters (Oriel, 420-680 nm, bandwidth at 0.5 peak amounts to 10 nm), which were placed into the light beam and constantly cooled by air during the course of the reaction. The light intensity was measured with the aid of calibrated silicon PIN photodiode (BPX 65). The photon number was evaluated for every wavelength. The TON was calculated as described before then normalized to the number of photons and plotted against the wavelength of irradiation. Results are collected in Table 6.1 and Table 6.2.

Table 6.1. Action spectrum data obtained for PO(tbc)OPM **30**.

Wavelength [nm]	**Number of photons [x $10^{15}s^{-1}cm^{-2}$]**	**TON [min^{-1}]**	**TON$^{norm\ a)}$ [min^{-1}]**
420	2.6	3.89	14.9
430	2.4	3.73	15.5
440	4.4	4.88	11.1
460	5.2	3.75	7.21
520	23.66	0.47	0.2
580	31.37	2.01	0.64
600	33.98	7.61	2.24
610	32.47	4.61	1.42
620	34.8	11.75	3.37
640	28.0	8.45	3.02
660	23.75	13.02	5.48
670	24.62	8.28	3.36
680	16.36	4.35	2.66

a) x 10^{-16}

Table 6.2. Action spectrum data obtained for ZnPoOPM **49**.

Wavelength [nm]	**Number of photons [x $10^{15}s^{-1}cm^{-2}$]**	**TON [min^{-1}]**	**TON$^{norm\ a)}$ [min^{-1}]**
430	2.4	5.54	23.1
440	4.4	10.08	22.9
450	4.9	11.12	22.7
460	5.2	10.14	19.5
470	8.76	12.44	14.2
500	19.82	4.16	2.1
540	26.36	11.33	4.3
560	28.89	23.11	8.0
570	29.10	25.90	8.9
580	31.37	19.76	6.3
600	33.98	14.27	4.2
610	32.47	15.91	4.9
620	34.8	13.22	3.8

a) x 10^{-16}

6.3.7 Measurement of photodegradation

Photodegradation (**PD**) of photosensitizers was simple measured spectrophotometrically. The absorption intensity at maximum absorption wavelength (*i.e.* Q-band in the case of phthalocyanines) prior to ($\mathbf{A_0}$) and after (**A**) 3 hours of reaction was measured. The loss of absorption intensity of the reaction solution indicates the extent of photobleaching.

$$PD = \frac{A_O - A}{A_O} \cdot 100$$

However, this method of determination of the degree of photodegradation is useless in the case of porphyrins and photo-oxidation of phenol since the reaction intermediate itself absorbs in the region of Soret band, which is the most intensive one. Hence, another approach was applied. The photo-oxidation of phenol was conducted for three hours and after the reaction was stopped the RR_i was calculated. Another portion of substrate to be photooxidized was injected to the reaction vessel. The apparatus was flushed with pure oxygen, the reaction system was closed immediately and the light source was switched on. After the reaction was finished the RR_i was calculated again. The difference between the RR_i recorded during the first reaction ($\mathbf{RR_i^o}$) and during the second run ($\mathbf{RR_i}$) allows calculating the degree of photodegradation (**PD**) of photosensitizer.

$$PD = \frac{RR_i^o - RR_i}{RR_i^o} \, 100\%$$

This approach was used to determine the photodegradation of triazatetrabenzcorroles as well as in all these cases where the first method gave poor results.

6.3.8 Sodium azide and D_2O test

In order to determine the relative contribution of the Type I radical pathway for investigated photosensitizers, experiments were carried out in a solution containing the

singlet oxygen quencher, i.e. sodium azide NaN_3. The influence of addition of NaN_3 on the initial reaction rate (**RR_i**) was studied for the solutions containing photosensitizer, detergent, and substrate at the concentrations and pH value as described in subchapter 6.3.2 and 6.3.3. The concentration of sodium azide in solution was 2.5 x 10^{-3} mol l^{-1}. Indirect tests for singlet oxygen are based on the inhibiting effect of an additive on the rate of a photochemical reaction. Azide ion (N_3^-) is a useful water-soluble agent, the inhibiting effect of which is attributed to physical quenching:

$$^1O_2 + N_3^- = {}^3O_2 + N_3^\bullet$$

D_2O can be used for indirect detection of $^1O_2$ presence because the lifetime of $^1O_2$ is more than 10-fold longer in D_2O than in H_2O. Thus, if a reaction in aqueous solution is dependent on singlet oxygen, carrying it out in D_2O instead should greatly improve the reaction rate.

6.3.9 Determination of hydrogen peroxide

The experiments were carried out to determine the participation of hydrogen peroxide in the photo-oxidation reactions investigated during these studies. The method reported earlier by Egerton et al. was employed [11]. 1 g of $TiOSO_4$ was dissolved in 10 ml of distilled water. After filtration 4 ml of this solution was diluted with 40 ml of concentrated sulphuric acid. Then the solution was diluted with distilled water in 100 ml flask. 5 ml of the reaction solution and 3 ml of the previously prepared titanium reagent were mixed together and then diluted with distilled water in 25 ml flask. A yellow colour indicates the presence of H_2O_2 in the reaction solution due to formation of peroxotitanium cation $[TiO_2]^{2+}$ with maximum absorption at 410 nm:

$$(TiO)SO_4 + 2\ H_2SO_4 \rightarrow H_2[Ti(SO_4)_3] + H_2O$$
$$H_2[Ti(SO_4)_3] + H_2O_2 \rightarrow H_2[TiO_2(SO_4)_2]\ (\lambda_{max}\ 410\ nm) + H_2SO_4$$

6.4 References

[1] R. Gerdes, *Niedermoleculare und immobilisierte Phthalocyaninetetrasulfonsäuren als Photosensibilisatoren für die Photooxidation von Phenol und Chlorophenolen,* Doctoral Dissertation, Universität Bremen **2000**.

[2] Wöhrle, D.; Iskander, N.; Graschew, G.; Sinn, H.; Friedrich, E.; Maier-Borst, W.; Stern, J.; Schlag, P. *Photochem. Photobiol.* **1990**, 51, 351-356.

[3] Oliver, S. W.; Smith, T. D.; *Heterocycles,* **1984**, Vol 22, 9, 2047-2052.

[4] Leznoff, C. C.; Terekhov, D. S.; McArthur, C. R.; Vigh, S.; Li, J.; *Can J. Chem.* **1995**, 73,435.

[5] Joyner, R. D.; Kenney, M. E.; *Inorg. Chem,* **1962**, Vol. 1, 236-237.

[6] Joyner, R. D.; Kenney, M. E.; *Inorg. Chem,* **1960**, 82, 5790-5791.

[7] Gerdes, R.; Bartels, O.; Schneider, G.; Wöhrle, D.; Schultz-Ekloff, G.; *Intern. J. Photoenergy*, **1999**, 1, 41-47.

[8] Oriel Corporation, P.O. Box 872, Stratford, CT, 06497-0872, USA; Catalog Vol. II, Light Sources etc.

[9] Parmon, V.; Emeline, A.; V.; Serpone, N.; "Glossary of Terms in Photocatalysis and Radiocatalysis" in: *Intern. J. Photoenergy,* **2002**.

[10] Wöhrle, D. et al. *Processes of petrochemistry and oil refining* **2002**, 10, p 30-46.

[11] Egerton, A. C.; Everett, A. J.; Minkoff, G. J.; Rudrakanchana, S.; Salooja, K. C.; *Anal. Chim. Acta.* **1954**, 10, 422.

[12] Wöhrle, D.; Iskander, N.; Graschew, G.; Sinn, H.; Friedrich, E.; Maier-Borst, W.; Stern, J.; Schlag, P. *Photochem. Photobiol.* **1990**, 51, 351-356.

[13] Schneider, G.; Wöhrle, D.; Spiller, W.; Stark, J.; Schulz-Ekloff, G.; *Photochem. Photobiol.*, **1994**, 60, pp. 333-342.

7. Conclusions & Outlook

Investigations were carried out, aiming to prepare a set of differently charged, water-soluble compounds, potentially applicable as photocatalysts. The following synthetic tetrapyrrolic macrocycles were investigated:

- metal-free, silicon and germanium phthalocyanines,
- oxophosphorus(V) and hydroxysilicon triazatetrabenzcorroles,
- subphthalocyanines,
- metal-free and zinc porphyrins.

Synthesis of all these dyes was undertaken purposely, *i.e.* to find possibly stable and efficient new photocatalysts useful in the photo-oxidation of severe pollutants present in the environment to nonhazardous products. Besides, of interest were multicomponent systems absorbing at different wavelengths of ultraviolet and visible irradiation. Since the photo-oxidation reactions of 2-mercaptoethanol and phenol were conducted in aqueous solution, the essential feature of all obtained photosensitizers is their water solubility (see chapter 2.1). In order to induce water-solubility two functional groups have been added to the macrocycle framework, *i.e.* sulfonate and quaternized aromatic amines.

In order to make the synthesis of water-soluble phthalocyanines available four precursor compounds were synthesized, purified and characterized (see chapter 2.2). A common feature of these compounds is the “pyridyl motif” attached to the molecule that allows N-methylation or quaternization with 1,3-propanesultone to give excellent water-soluble cationic and zwitterionic phthalocyanines and related compounds.

The synthesis of nine water-soluble phthalocyanines has been worked out in the present study. Both silicon and germanium sulfophthalocyanines – two precious photocatalysts - have been already reported in chemical literature, however, procedures described there lack many important details and proved to be irreproducible in our hands. Hence, the synthesis of silicon and germanium sulfophthalocyanines (**25**, **28**) was thoroughly reinvestigated (see chapter 2.3.2). As a result new methods were proposed. It was demonstrated that the method described previously, that is sulfonation of unsubstituted

silicon phthalocyanine **22** with oleum at 75°C yields sulfonated hydroxysilicon(IV) triazatetrabenzcorroles (**23**), instead of expected silicon sulfophthalocyanine. The UV-Vis spectrum of the unexpected product (in water) displays a very sharp Soret band at 452 nm and a Q-band at 670 nm with intensity ca. half that of the Soret band. The spectrum closely resembles that of the hydroxysilicon triazatetrabenzcorrole - the compound reported by Hanack *et al*. and found to be the contracted phthalocyanine with one *meso*-nitrogen missing in the macrocycle framework. Apparently, the dichlorosilicon phthalocyanine (**22**) was not only sulfonated but also underwent reduction to hydroxysilicon sulfotriazatetrabenzcorrole (**23**). The chlorosulfonation of $SiCl_2Pc$ (**22**) followed by hydrolysis of the chlorosulfonated derivative **24** was found to be considerably better method compared to sulfonation of $SiCl_2Pc$ (**22**) with oleum. Water-soluble germanium sulfophthalocyanine (**28**) has been successfully obtained by chlorosulfonation and hydrolysis of the sulfochloride derivative **27**. Unlike $SiCl_2Pc$ (**22**), sulfonation of $Ge(OH)_2Pc$ (**26**) with oleum gives exclusively germanium sulfophthalocyanine (**28**). Apparently, $Ge(OH)_2Pc$ (**26**) is much less susceptible to reduction and ring contraction compared to $SiCl_2Pc$ (**22**). Metal-free sulfophthalocyanine (**20**) was obtained by the cyclotetramerization of 4-sulfophthalate in melted urea. Moreover, the synthesis of positively charged and zwitterionic silicon and germanium phthalocyanines (**14**, **15**, **17**, **18**) was investigated. Besides, sulfonated, cationic and zwitterionic metal-free phthalocyanines were obtained (**11**, **12**, **20**).

The reaction of metal-free phthalocyanine **10** with PCl_3 in pyridine resulted in ring-contracted compound, namely, oxophosphorus(V) triazatetrabenzcorrole (see chapter 2.4). This compound after reacting it with methyl iodide and 1,3-propanesultone gave two water-soluble dyes (**30**,**31**). Their water solutions are bright green and show two strong absorptions at ca. 446 nm and 658 nm. Thereby, for the first time the photocatalytic activity of oxophosphorus(V) triazatetrabenzcorroles has been studied. They proved to be useful photosensitizers in the oxygen activation.

The synthesis of water-soluble subphthalocyanines is particularly challenging and difficult as many phthalonitriles successfully utilized during phthalocyanines synthesis are useless for the subphthalocyanines. This is due to incompatibility of many functional groups and very reactive boron trichloride used for subphthalocyanines preparation (see chapter 1.3). The synthesis of five novel water-soluble SubPcs has been achieved (see chapter 2.5).

Additionally, several tatraanionic, tetracationic and zwitterionic porphyrins were synthesized aiming to reveal their photocatalytic properties (see chapter 2.6). They proved to be precious photocatalysts exhibiting high activity along with extraordinary photostability (see chapters 5.10 and 5.11).

A very strong aggregation may effectively hamper photocatalytic process by dissipation of the energy of the excited state of the photosensitizer. The singlet oxygen generation requires that the photosensitizer be in the monomeric state otherwise in aggregates the oxygen is not activated. A very effective approach to avoid aggregates is to employ surfactants, which form micelles in which photosensitizer molecule exists as a monomer (see chapter 4.4). All the water-soluble compounds prepared during this work have charged groups at their periphery, such as a sulfonate or quaternary aromatic amine. The nature of the charge determines choice of detergent as the ionic photosensitizers disaggregate better in micelles formed from surfactants with opposite charge. The UV-Vis spectra of investigated compounds were recorded both in micellar and non-micellar solution. Comparison of such spectra gives an important piece of chemical information, *i.e.* the extent of aggregation process can be followed. Thus, no aggregation is seen for subphthalocyanines due to their nonplanar cone-shaped structure. Also no aggregation is discernible for two sulfophthalocyanines SiPcTS **25** and GePcTS **28**, while metal-free sulfophthalocyanine H_2PcTS **20** occurs in a highly aggregated state. The triazatetrabenzcorroles studied in this work, *i.e.* PO(tbc)OPM **30** and Si(tbc)TS **23**, exist mainly in a disaggregated form. On the other hand, positively charged phthalocyanines GePcOPM **17**, SiPcOPM **14** and H_2PcOPM **11** exhibit very strong aggregation. All zwitterionic compounds show enormously strong aggregation. This feature can be most probably explained on the basis of strong intermolecular interaction, caused by attractive forces between negative and positive functionalities. This undesirable interaction leads to low solubility as well as to decrease of the photocatalytic activity since an essential prerequisite during photocatalytic measurements is monomerization of the photosensitizer in solution. The results that were discussed in this dissertation explicitly show that aggregation is a very complex phenomenon. On the one hand, it depends on the structure of the molecule, especially on the bulkiness of the substituents, and, on the other hand, it is complicated by coulombic, hydrophobic and strong π-electron interaction. The positively charged compounds investigated during this work have “electron rich” peripheral substituents that could presumably increase the π-π

interaction between molecules and additionally enhance aggregation in water solution. Moreover, there is a noticeable response of the state of aggregation to the varying physical environment, *i.e.* solvent, presence of electrolytes, pH and addition of surfactants.

Part of this work was devoted to studies towards photocatalytic properties of phthalocyanines and related compounds (see chapter 5). Tetrapyrrolic dyes were used to activate oxygen to rapidly convert 2-mercaptoethanol and phenol, two severe pollutants present in the environment, to nonhazardous products, using three inexhaustible natural resources: oxygen (present in the air), photons (from sunlight), water (as environmentally friendly solvent). The results included within this dissertation are part of ongoing worldwide investigation dedicated to new possibly economic green approach for the treatment of hazardous organic contaminations in wastewater. An extraordinary photocatalytic activity of positively charged and zwitterionic porphyrins has been found (see chapters 5.10 and 5.11). In turn, the tetraanionic zinc porphyrin proved to be very poor photocatalyst. For the first time the photocatalytic activity of triazatetrabenzcorroles has been studied (see chapter 5.4). In general, positively charged **30** and zwitterionic **31** oxophosphorus(V) triazatetrabenzcorroles exhibit good photocatalytic activity in a micellar solution. The activities of PO(tbc)OPM **30** and PO(tbc)OPPS **31** in a non-micellar solution are lower. The photocatalytic activities of three different sulfophthalocyanines (Si(IV), Ge(IV) and metal-free) were investigated (see chapter 5.5). The silicon **25** and germanium **28** sulfophthalocyanines are examples of dyes, which are fully disaggregated in aqueous solution, which is a fundamental prerequisite for good photosensitizer. Thus, presence of detergent is not required in that case. SiPcTS **25** was used to photo-oxidize 2-mercaptoethanol. It was rather stable but low oxygen consumption was found, indicating that the thiol was not fully oxidized. In 2001 Gerdes et al. described results concerning photocatalytic activity of SiPcTS **25** in the photo-oxidation of phenol, cyclopentadiene and (S)-(-)-citronellol. High activity along with extraordinary stability of the SiPcTS **25** immobilized on anion exchanger IRA-400 enabling repeated use of such photosensitizer was claimed. The results obtained during this study, with 2-mercaptoethanol as substrate, contrast sharply with those reported by Gerdes et al. The polymer bound SiPcTS **25** demonstrated fairly low photostability during photo-oxidation of thiol. The GePcTS **28** is somewhat more active in a solution compared to SiPcTS **25**. A very low photocatalytic activity was found for metal-free sulfophthalocyanine **20**. Because of pronounced tendency to aggregate in

aqueous solution along with poor photostability, metal-free sulfophthalocyanine **20** is a very bad candidate for photosensitizer. The water-soluble SiPcOPM **14** and SiPcOPPS **15** are examples of compounds exhibiting pronounced tendency towards aggregates formation in aqueous solution resulting in negligible activity (see chapter 5.7). Even at pH 13 upon addition of surfactant SDS to the water solution of SiPcOPM **14** and SiPcOPPS **15** the activities (RR_i, final oxygen consumption) are not increased. The photocatalytic activities of GePcOPM **17** and GePcOPPS **18** are vastly superior to the activities of their silicon-containing counterparts (see chapter 5.8). The homogeneous reaction could be conducted at pH 13 since both germanium phthalocyanines proved to be stable at high pH. Both GePcOPM **17** and GePcOPPS **18** turned out to be efficient photosensitizers for the photo-oxidation of 2-mercaptoethanol. However, the presence of anionic detergent (SDS) was essential for good photocatalytic activity. Addition of surfactant SDS to the water solution of metal-free phthalocyanines H_2PcOPM **11** and H_2PcOPPS **12** results in a strong increase of the photocatalytic activity. Obviously, without detergent the phthalocyanines were highly aggregated and dissipation of energy of the excited state occurs. Both metal-free phthalocyanines remain virtually inactive as photocatalysts in the absence of appropriate detergent (see chapter 5.9).

During the photo-oxidation of 2-mercaptoethanol and phenol the photosensitizers may oxidatively decompose. The degradation of photosensitizers investigated during this work was followed by measuring the UV-Vis absorption intensity at the beginning and at the conclusion of the photo-oxidation (usually after 3 hours). Of special interest are photosensitizers that exhibit increased stability towards intense light and oxygen. By far the most stable are ZnPoOPM **49** and ZnPoOPPS **50** (see chapter 5.10). A very insignificant photodegradation was measured for these two compounds, *i.e.* between 0 and 2 %. Good stability was found for two sulfophthalocyanines, *i.e.* SiPcTS **25** and GePcTS **28**, and zwitterionic phthalocyanine GePcOPPS **18** (see chapters 5.5 and 5.8). Moderately stable are triazatetrabenzcorroles PO(tbc)OPM **30** and PO(tbc)OPPS **31** (see chapter 5.4). A notorious disadvantage of all subphthalocyanines obtained during this study is their extreme instability upon irradiation with intense light. This hinders entirely their utility as photocatalysts. It has been demonstrated that the reaction conditions, presence of detergent, pH as well as the choice of substrate to be photo-oxidized have strong influence on the photostability and activity of the sensitizer. Thus, photo-oxidation of 2-mercaptoethanol was compared with photo-oxidation of phenol. For example, metal-free porphyrin H_2PoOPPS **47** was employed in the photo-oxidation

of thiol resulting in 67% degradation of dye. Then H_2PoOPPS **47** was utilized under the same reaction conditions in the photo-oxidation of phenol. Surprisingly, no degradation was observed in this case (see chapter 5.11).

Action spectra, that are a plot of a photocatalytic activity per number of incident photons, against wavelength of light, were obtained during this work. The action spectra show that each photosensitizer is photocatalytically active solely in the area of absorption (Q-band and Soret band). In principle, there is no activity in the region between absorption maxima. The idea of panchromatically absorbing systems rests on the assumption that phthalocyanines, porphyrins, triazatetrabenzcorroles and other dye molecules coupled together would be capable of collecting a considerable fraction of the solar spectrum, much more than each of these compounds would be able being used separately. In the photocatalytic experiments the incident beam of light consists of photons of different energies. Using one photosensitizer only small fraction of the spectrum of light is effectively utilized to drive the photochemical process. It was shown that combination of a few photosensitizers, absorbing at different wavelengths, greatly improve the reaction efficiency leading to rapid photo-oxidation of 2-mercaptoethanol (see chapter 5.12). For instance, it has been demonstrated that combination of three photosensitizers, *i.e.* PO(tbc)OPM **30**, GePcOPM **17** and ZnPoOPM **49**, gives rise to around 3-fold enhancement of the reaction rate of the oxidation of thiol in water solution at pH 13. That is because three-component system harvests considerably fraction of light, more that single compound. The UV-Vis spectrum of the solution containing combined dyes exhibits absorption in the regions of 416-452 nm and 569–768 nm. Since it has been unambiguously shown that the multi-component system is superior to the photocatalytic system that consists of single photosensitizer, it would be of great value to continue this study using also polymer-immobilized photosensitizers. It would be also very interesting to apply more than three different dyes harnessing as much of the solar spectrum as possible to improve the photocatalytic efficiency.

The present study, after collecting substantial data on the photocatalytic activity of different tetrapyrrolic macrocycles, demonstrated that these compounds are prone to activate oxygen in the presence of light leading to highly reactive singlet oxygen ($^1O_2$) which then can be utilize to oxidize toxic compounds or for the synthesis of some fine chemicals. The influence of peripheral substituents as well as central metal on the photostability and efficiency of the singlet oxygen formation needs more detailed

studies. Understanding of the effect of the substituents and central metal would be of great importance for the reasonable design of new efficient photocatalysts.

At the very beginning of my work in the group of Professor Dieter Wöhrle my desire was to develop a truly efficient, universal photocatalyst that would have a wide scope of applications. However, now I think that my belief that such universal photocatalyst can be developed was nothing more but a naivety. The experimental results presented in this dissertation suffice to show that the photocatalysis (with phthalocyanines and related tetrapyrrolic macrocycles) continues to be a very sensitive function of sensitizer structure (central metal, peripheral substituents) and reaction condition (presence of detergent, additives, pH). Moreover, even choice of substrate is of crucial importance for the photochemical and photophysical processes that take place during reaction. Thus, our ability to predict the course of the photocatalytic process in a rational manner is severely limited. Therefor, it is always necessary to find proper photosensitizer and establish appropriate reaction conditions for a particular substrate and purpose.